# Environmental processes transforming inorganic nanoparticles: implications on aquatic invertebrates

# Umweltprozesse transformieren anorganische Nanopartikel: Auswirkungen auf aquatische Invertebraten

by

Simon Lüderwald

Mannheim, Germany

Accepted dissertation thesis for the partial fulfillment of the requirements for a

Doctor of Natural Sciences

Faculty 7: Natural and environmental sciences,

University of Koblenz-Landau

Thesis examiners:

Jun.-Prof. Dr. Mirco Bundschuh, University of Koblenz-Landau

Prof. Dr. Ralf Schulz, University of Koblenz-Landau

Date of oral examination: January 23$^{rd}$, 2020

## DECLARATION

I hereby declare that I independently conducted the work presented in this thesis entitled **"Environmental processes transforming inorganic nanoparticles: implications on aquatic invertebrates"**. All used assistances are mentioned and involved contributors are either co-authors of or are acknowledged in the respective publications. For the literature review resulting in publication 1 (Appendix A. 1), and the microcosm experiment resulting in publication 5, I was co-author with substantial involvement in manuscript discussions and preparations, as well as implementation of the experiment, respectively. For publications 2–4 (Appendix A. 2–4), I designed and planned the studies, conducted the experiments, performed the associated analyses, evaluated the data, and wrote the respective publications – with support of the named persons. Publication 4 contains data that was collected preceding this PhD thesis. In detail, this concerns the data of the bioassay that addressed exposure pathway dependent effects of $TiO_2$ nanoparticles on *Gammarus fossarum*. One task of the current thesis was to assess, if potential (adverse) effects on aquatic organisms observed for one type of nanoparticle, can be transferred to another type. Consequently, the experimental setup of the $TiO_2$ bioassay served as basis for the setup of the Ag bioassay. The two bioassays were independent studies and the data of both studies were merged for the purpose of answering the question of a potential transferability among two types of nanoparticles. Therefore, the Ag bioassay conducted within this thesis, comparing waterborne and dietary effects on *G. fossarum* was supplemented by the $TiO_2$ data, allowing the development of a comprehensive discussion comparing the results of the two studies. Thus, the contribution of the $TiO_2$ data on publication 4 is estimated to be approx. 25%. This thesis has never been submitted elsewhere for an examination, as a thesis or for evaluation in a similar context to any department of this University or any scientific institution. I am aware that a violation of the aforementioned conditions can have legal consequences.

Mannheim, December 20, 2019

Place, Date                                                                 Simon Lüderwald

**The present thesis is a cumulative dissertation based on the following peer-reviewed publications:**

I.  **Appendix A. 1:** Bundschuh, M., Filser, J., **Lüderwald, S.**, McKee, M., Metreveli, G., Schaumann, G.E., Schulz, R., Wagner, S. (2018) Nanoparticles in the environment – where do we come from, where do we go to? Environ. Sci. Eur. 30. https://doi.org/10. 1186/ s12302-018-0132-6.

II.  **Appendix A. 2: Lüderwald, S.**, Dackermann, V., Seitz, F., Adams, E., Feckler, A., Schilde, C., Schulz, R., Bundschuh, M. (2019). A blessing in disguise? Natural organic matter reduces the UV light-induced toxicity of nanoparticulate titanium dioxide. Sci. Total Environ. 663:518-526. https://doi.org/10.1016 /j.scitotenv.2019.01.282.

III.  **Appendix A. 3: Lüderwald, S.**, Meyer, F., Gerstle, V., Friedrichs, L., Rolfing, K., Bakanov, N., Schulz, R., Bundschuh, M. (submitted, revisions received). Reduction of pesticide toxicity under field relevant conditions? The interaction of titanium dioxide nanoparticles, UV, and NOM.

IV.  **Appendix A. 4: Lüderwald, S.**, Schell, T., Newton, K., Salau, R., Seitz, F., Rosenfeldt, R., Dackermann, V., Metreveli, G., Schulz, R., Bundschuh, M. (2019). Exposure pathway dependent effects of titanium dioxide and silver nanoparticles on the benthic amphipod *Gammarus fossarum*. Aquat. Toxicol. 212. https://doi.org/10.1016/j. aquatox.2019.04.016.

V.  **Appendix A. 5:** Bundschuh, M., Englert, D., Rosenfeldt, R.R., Bundschuh, R., Feckler, A., **Lüderwald, S.**, Seitz, F., Zubrod, J.P., Schulz, R. (2019). Nanoparticles transported from aquatic to terrestrial ecosystems via emerging aquatic insects compromise subsidy quality. Sci. Rep. 9. https://doi.org /10.1038/s41598-019-52096-7.

**TABLE OF CONTENTS**

# ABSTRACT

Engineered inorganic nanoparticles (EINPs) are produced and utilized on a large scale and will end up in surface waters. Once in surface waters, EINPs are subjected to transformations induced by environmental processes altering the particles' fate and inherent toxicity. UV irradiation of photoactive EINPs is defined as one effect-inducing pathway, leading to the formation of reactive oxygen species (ROS), increasing EINP toxicity by exerting oxidative stress in aquatic life. Simultaneously, UV irradiation of photoactive EINP alters the toxicity of co-occurring micropollutants (e.g. pesticides) by affecting their degradation. The presence of natural organic matter (NOM) reduces the agglomeration and sedimentation of EINPs, extending the exposure of pelagic species, while delaying the exposure of benthic species living in and on the sediment, which is suggested as final sink for EINPs. However, the joint impact of NOM and UV irradiation on EINP-induced toxicity, but also EINP-induced degradation of micropollutants, and the resulting risk for aquatic biota, is poorly understood. Although potential effects of EINPs on benthic species are increasingly investigated, the importance of exposure pathways (waterborne or dietary) is unclear, along with the reciprocal pathway of EINPs, i.e. the transport back from aquatic to terrestrial ecosystems. Therefore, this thesis investigates: (i) how the presence of NOM affects the UV-induced toxicity of the model EINP titanium dioxide ($nTiO_2$) on the pelagic organism *Daphnia magna*, (ii) to which extent UV irradiation of $nTiO_2$ in the presence and absence of NOM modifies the toxicity of six selected pesticides in *D. magna*, (iii) potential exposure pathway dependent effects of $nTiO_2$ and silver (nAg) EINPs on the benthic organism *Gammarus fossarum,* and (iv) the transport of $nTiO_2$ and gold EINPs (nAu) via the merolimnic aquatic insect *Chaetopteryx villosa* back to terrestrial ecosystems. $nTiO_2$ toxicity in *D. magna* increased up to 280-fold in the presence of UV light, and was mitigated by NOM up to 12-fold. Depending on the pesticide, UV irradiation of $nTiO_2$ reduced but also enhanced pesticide toxicity, by (i) more efficient pesticide degradation, and presumably (ii) formation of toxic by-products, respectively. Likewise, NOM reduced and increased pesticide toxicity, induced by (i) protection of *D. magna* against locally acting ROS, and (ii) mitigation of pesticide degradation, respectively. *Gammarus'* energy assimilation was significantly affected by both EINPs, however, with distinct variation in direction and pathway dependence between $nTiO_2$ and nAg. EINP presence delayed *C. villosa* emergence by up to 30 days, and revealed up to 40% reduced lipid reserves, while the organisms carried substantial amounts of nAu (~1.5 ng/mg), and $nTiO_2$ (up to 2.7 ng/mg). This thesis shows, that moving test conditions of EINPs towards a more field-relevant approach, meaningfully modifies the risk of EINPs for aquatic organisms. Thereby, more efforts need to be made to understand the relative importance of EINP exposure pathways, especially since a transferability between different types of EINPs may not be given. When considering typically applied risk assessment factors, adverse effects on aquatic systems might already be expected at currently predicted environmental EINP concentrations in the low ng-µg/L range.

# 1. INTRODUCTION

## 1.1 Engineered inorganic nanoparticles in the environment

During the last years nanotechnology has evolved to one of the major technologies of the 21st century and took over a significant position at the cutting edge of today's engineering (Forster et al., 2011; Rao et al., 2015). Engineered inorganic nanoparticles (EINPs) possess unique properties relative to their bulk or dissolved counterparts (e.g. particle size, shape, surface area, and reactivity; Bundschuh et al., 2018), enabling a growing application field, for instance as part of consumer products or for industrial purposes (e.g. cosmetics, nourishment, medicine; Farre et al., 2009; Keller and Lazareva, 2014; Scheringer, 2008).

As a consequence of their continual utilization, EINPs are emitted into surface waters (Gondikas et al., 2014; Klaine et al., 2011). Thereby, facade paint runoff or effluents of wastewater treatment plants are considered as major entry pathways of EINPs into aquatic ecosystems (Kaegi et al., 2010; Kiser et al., 2009; Westerhoff et al., 2011). Recent modeling approaches, predicting EINP concentrations in natural ecosystems, projected EINPs to be found in surface waters in the low ng/L–µg/L range, depending on the EINP type (Gottschalk et al., 2013; Sun et al., 2014).

Typical representatives of EINPs are metals and metal oxides (Nowack and Bucheli, 2007). Among metal-based EINPs, nano-sized titanium dioxide ($nTiO_2$) and silver (nAg) are frequently manufactured and used (Aitken et al., 2006; Piccinno et al., 2012). The ecotoxicological potential of $nTiO_2$ and nAg is determined by their intrinsic properties. Whereas the toxicity of nAg for aquatic biota is mainly driven by the release of $Ag^+$ ions, the toxicity of $nTiO_2$ is predominantly induced by (i) an attachment of the particles to the organisms' outer surface or (ii) its photocatalytic activity leading to the formation of reactive oxygen species (ROS; Bundschuh et al., 2018; Mansfield et al., 2015; Völker et al., 2013).

However, after their release into surface waters EINPs are subjected to several environmental processes, including chemical transformation (e.g. photoactivation, dissolution, or sulfidation), agglomeration (e.g. homo- and/or hetero-agglomeration), or interactions with co-occurring substances such as natural organic matter (e.g. adsorption), which unavoidably alter the fate and effects of EINPs on aquatic life (Bundschuh et al., 2018; Bundschuh et al., 2016; Seitz et al., 2015a; Wormington et al., 2017; Zhang et al., 2018; Fig. 1 a).

## 1.2 Chemical transformation

The presence of UV radiation is known to trigger the photocatalytic properties of photoactive EINPs like $nTiO_2$ and results in the formation of ROS (Bhatkhande et al., 2002), leading to a considerably enhanced ecotoxicological potential of $nTiO_2$ already at ambient UV intensities (Bar-Ilan et al., 2013; Marcone et al., 2012). Following, the latter process will be defined as "triggering". ROS induce oxidative stress in organisms resulting in a damage of lipids, carbohydrates, proteins and DNA (Fan et al., 2012; Kim et al., 2010). Contrasting, excessive amounts of ROS can simultaneously affect the implications of co-occurring micropollutants, such as pesticides (e.g. Chen et al., 2007; Wu and Linden, 2008). For instance, the toxicity of the insecticide pirimicarb to *Daphnia magna* was partly significantly reduced, when combining the presence of 2, 0.2, and 0.02 mg $nTiO_2$/L (acting as photocatalyst) with UV radiation (40 W/m$^2$), as result of an enhanced degradation of the insecticide (Seitz et al., 2012).

In particular, the study of Seitz and colleagues (2012) was characterized by pre-treating a pirimicarb solution in the presence or absence of UV radiation and $nTiO_2$, before assessing the treated solutions' toxicity towards *D. magna* over 72 hours. It was shown, that a pre-treatment with UV radiation alone, only slightly decreased the measured pirimicarb concentration after a period of 72 hours. If the pre-treatment was realized in the presence of UV and 0.2 mg $nTiO_2$/L, approx. 50% of the initial pirimicarb concentration was decreased over 72 hours, which was even more pronounced in the presence of 2 mg $nTiO_2$/L, revealing a pirimicarb decrease below the limit of quantification after 72 hours. Furthermore, treating the pirimicarb solution with UV and 2 mg $nTiO_2$/L almost completely reduced any observed adverse effects in *Daphnia*. Mapping a more environmentally relevant exposure scenario, however, would require a systematic approach where tested scenarios would also include a simultaneous exposure of the tested organism to the relevant factors, while quantifying the degradation of a certain pesticide under those conditions.

## 1.3 Interactions with natural organic matter

In the environment, interactions between EINPs and natural organic matter (NOM) is a process that will alter the fate and ecotoxicological potential of EINPs (Bundschuh et al., 2018; Collin et al., 2014; Seitz et al., 2016). Molecules of dissolved organic matter (DOM), for instance, form a coating around the EINPs' surface, leading to an increased stability of the EINPs in the surrounding medium by exerting electrostatic repulsion

between the single particles (Domingos et al., 2009; Erhayem and Sohn, 2014). EINPs coated with NOM are considered to be less susceptible towards agglomeration and sedimentation, but might also be less photoactive or susceptible to ion release, which in turn decreases the EINPs' ecotoxicological potential. Consequently, reducing the EINPs' reactivity will inevitably lead to a decreased formation of ROS (Wormington et al., 2017), which on the one hand will reduce the EINPs ecotoxicological potential, but also the quality to degrade co-occurring micropollutants.

## 1.4 Homo- and hetero-agglomeration

In surface waters EINPs are subjected to homo-aggregation (interactions between the same EINP type), but also hetero-agglomeration (interactions between different EINP types, e.g. microorganisms, or adsorption to biological surfaces like algae; Adam et al., 2016; Bundschuh et al., 2018; Bundschuh et al., 2016; Petosa et al., 2010; Sillanpää et al., 2011), ultimately altering their fate along with the risk of exposure for different types of aquatic organisms (Klaine et al., 2008). In particular, shortly after their release into an aquatic ecosystem EINPs might possess an ecotoxicological impact on pelagic species (Dabrunz et al., 2011; Lovern and Klaper, 2006; Rosenkranz et al., 2009; Seitz et al., 2013). Following, the formation of EINP homo- and/or hetero-agglomerates leads to a rapid precipitation suggesting sediments as a final sink, but increasing the exposure for benthic species (Baun et al., 2008; Rajala et al., 2018; Velzeboer et al., 2014; von der Kammer et al., 2010), which might be delayed by the stabilizing effect of co-occurring NOM (Seitz et al., 2016).

In and on the sediment, though, inhabiting organisms might be exposed via different exposure pathways, namely a direct exposure to either strong and/or less homo-agglomerated particles (waterborne pathway), or through hetero-agglomerates, potentially carrying co-contaminants attached to the EINP surface, and EINPs adsorbed to the organisms' food (dietary pathway). When following the aquatic life cycle of EINPs, the potential transport from the aquatic surrounding back to the terrestrial environment through merolimnic aquatic insects has been neglected so far. During the aquatic life stage of those insects, EINPs might be consumed via their food, resulting in a potentially increased EINP bioavailability for terrestrial predatory species (Bundschuh et al., 2019) after the insects' emergence. Moreover, EINP exposure might affect the emergence pattern and nutritional value (i.e. energy reserves) of those insects (Bundschuh et al., 2019).

## 2. OBJECTIVES AND THESIS STRUCTURE

The present thesis was integrated in the project IMPACT as part of the DFG funded project INTERNANO. IMPACT aimed at contributing to a systematic understanding of relevant environmental processes and central mechanisms defining biological effects of EINPs in macroinvertebrates (i.e. aquatic invertebrates). As such, the first approach of the current thesis comprised an involvement in a review paper, addressing recent achievements in the field of nano-ecotoxicology in aquatic and terrestrial systems, but also referred to existing gaps that require further attention in the future. This contribution was limited to the fate of EINPs, their effect mechanisms on aquatic biota, as well as EINP interactions in the aquatic environment, serving as basis for the objectives and tasks of the current thesis (Task 1; Fig. 1; Appendix A. 1).
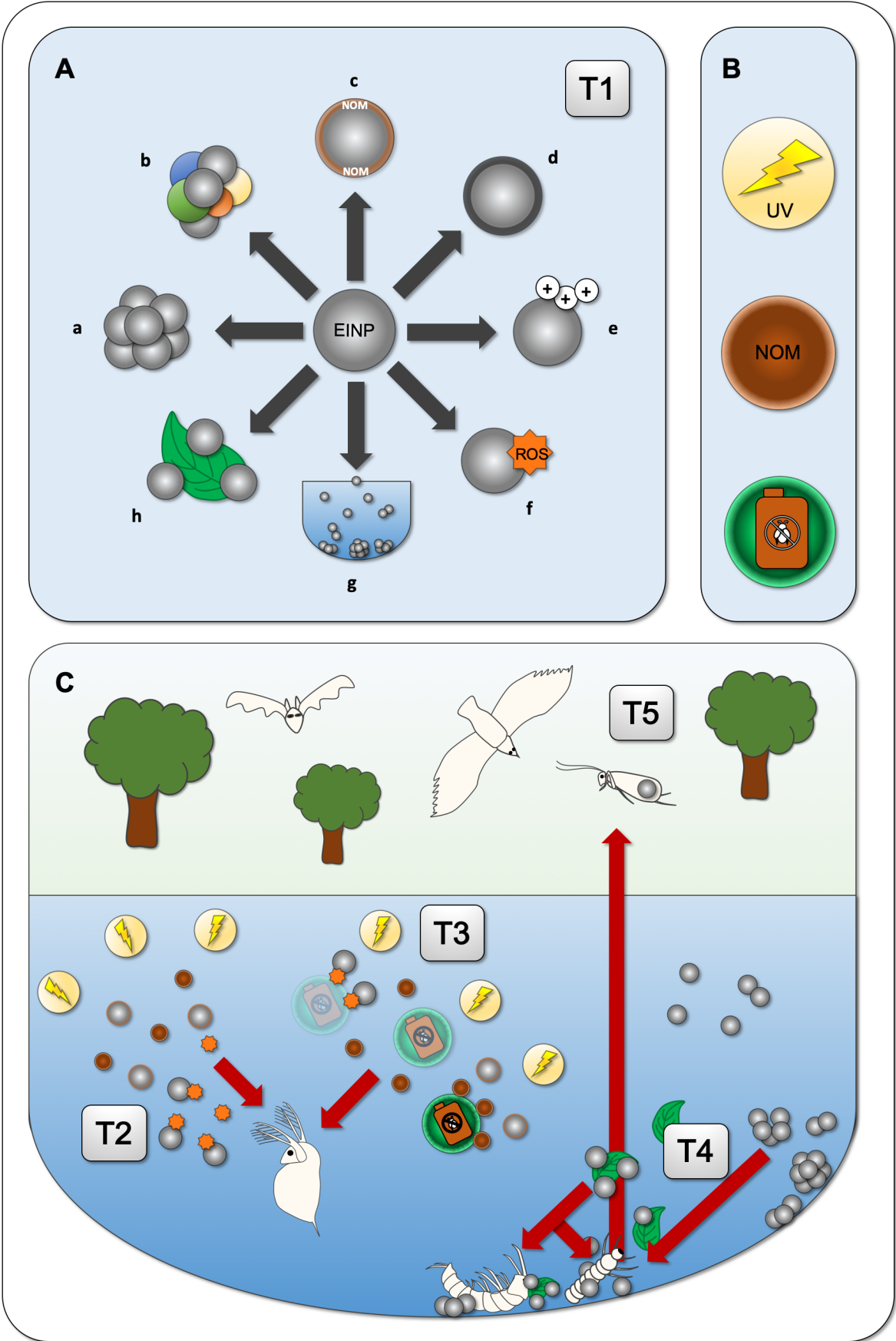
In a second step, this thesis focused on determining whether triggering (UV-induced alteration of photoactive EINPs) of masked (EINPs potentially coated with NOM; Fig. 2) and bare (unmasked) photoactive EINPs does alter their ecotoxicological potential in aquatic invertebrates (Task 2; Fig. 1; Appendix A. 2). For photoactive EINPs, triggering is besides physical effects (e.g. a coating of the organisms' outer surface; Dabrunz et al., 2011) suggested a considerable effect-inducing pathway. Thereby the impact of NOM on EINP-triggering is insufficiently understood, introducing the need for systematic assessments of this interplay.

The insights gathered in Task 2 served as basis for the third approach, where the impact that triggering of masked and unmasked photoactive EINPs has on the ecotoxicological potential of co-occurring micropollutants was assessed (Task 3; Fig. 1; Appendix A. 3). There are several studies addressing this issue, however, being mainly focused on environmentally irrelevant photocatalyst concentrations (e.g. mg– g/L) and relatively high UV intensities (e.g. 30 W/m$^2$). The motivation of Task 3 was to demonstrate, that a photocatalytic degradation (induced by the presence of $nTiO_2$) and potentially involved detoxification of pesticides, takes place even under conditions that can be considered very close to field relevant (in terms of UV: $\leqq 2.6$ W UVA/m$^2$, $nTiO_2$: 0.05 mg/L, and NOM: $\leqq 4$ mg TOC/L), including the application of a more realistic exposure scenario.

When following the aquatic life cycle of EINPs, sediments are suggested to act as final sink (Sun et al., 2016). Thereby, EINPs tend to leave the aqueous phase as homo-agglomerates, or hetero-agglomerates attached to other particulate materials, but also to algae or leaf litter, inter alia serving as food source for aquatic life. As a result,

sediment-inhabiting organisms could be exposed to EINPs by different pathways. Therefore, the fourth part of the current thesis investigated the relative importance of potential exposure pathway-dependent effects of EINPs towards a benthic aquatic invertebrate, differentiating between a waterborne and dietary exposure. Furthermore, this approach assessed a potential transferability of observed effects between two types of EINPs (nTiO$_2$ and nAg; Task 4; Fig. 1; Appendix A. 4).

Lastly, not much is known about the final destination of EINPs, especially when it comes to a potential transport of EINPs back from the aquatic to terrestrial ecosystems. Therefore, the last part of this thesis contains insights of a study that investigated the emergence of the merolimnic aquatic insect *Chaetopteryx villosa* while being exposed for 140 days of its' aquatic life to nTiO$_2$ or nanoparticulate gold (nAu; Task 5; Fig. 1; Appendix A. 5).

**T1** **EINPS IN THE ENVIRONMENT**

**TASK 1:** What were the recent achievements in the field of nano-ecotoxicology and what are substantial gaps that need further attention in the future?

[Publication 1 – Appendix A. 1]

**T2** **NOM AFFECTS UV-INDUCED EINP TOXICITY**

**TASK 2:** How does the presence of NOM affect UV-induced EINP toxicity in aquatic invertebrates?

[Publication 2 – Appendix A. 2]

**T3** **UV-ILLUMINATION OF EINPS MODIFIES PESTICIDE TOXICITY**

**TASK 3:** To which extent do UV-illuminated EINPs modify the ecotoxicological potential of pesticides on a pelagic model invertebrate? In which way does the presence of natural organic matter affect the outcome?

[Publication 3 – Appendix A. 3]

**T4** **EINP EFFECTS IN BENTHIC AQUATIC INVERTEBRATES**

**TASK 4:** Are there exposure pathway dependent effects of EINPS on a benthic model invertebrate? Is there a similarity of observed effect patterns between two EINP types?

[Publication 4 – Appendix A. 4]

**T5** **EINP TRANSPORT FROM AQUATIC TO TERRESTRIAL SYSTEMS**

**TASK 5:** Is there a reciprocal transport of EINPs via an emerging aquatic model insect from the aquatic environment back to terrestrial ecosystems?
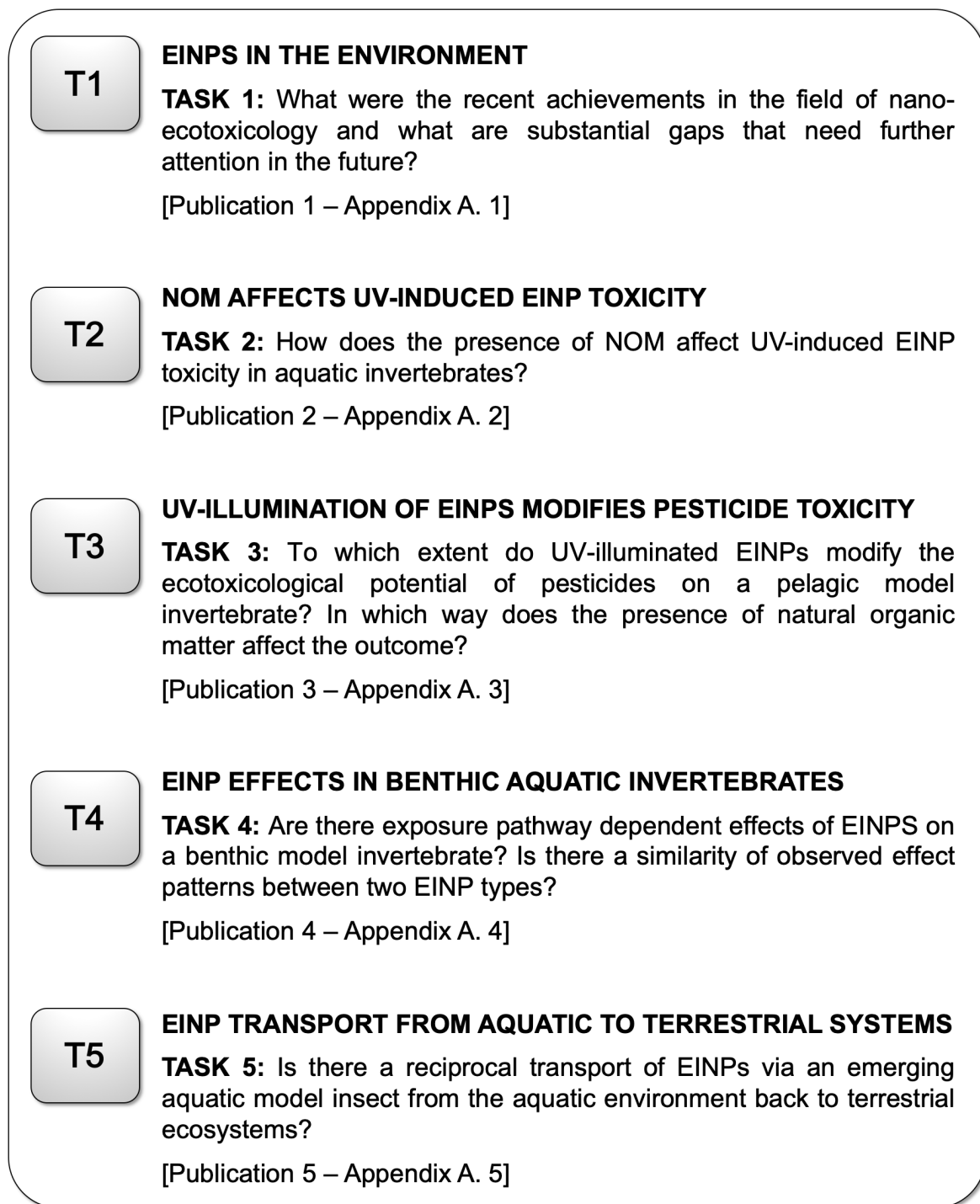
[Publication 5 – Appendix A. 5]

**Fig. 1.** Outline of the main tasks (T1–T5) of the present thesis, and the corresponding scientific publications. **A:** Interactions and fate of EINPs in the environment considering homo-agglomeration (a), hetero-agglomeration (b), surface coating with NOM (c), sulfidation (d), dissolution (e), photoactivation (f), sedimentation/deposition (g), adsorption on biological surfaces (h); modified after Bundschuh et al. (2018). **B:** UV irradiation and NOM as environmental factors, and pesticides as co-occurring micropollutant, selected as key-factors for the experiments of task 2 and 3. **C:** Schematic visualization of the tasks 2–5. **[Appendix A. 1–A. 5]**

## 3. METHOD OVERVIEW

### 3.1 NOM affects UV-induced EINP toxicity

This part assessed the individual and combined effects of varying NOM levels and UV intensities on the ecotoxicological potential of $nTiO_2$. To do so, a series of acute toxicity studies was conducted using the immobility of the water flea *Daphnia magna* as response variable. With the collected data 96-h $EC_{50}$ values (half maximal effect concentrations) were calculated for the different exposure scenarios. The experimental setup predominantly followed the OECD guideline 202 (OECD, 2004), while adopting the exposure duration from 48 hours to 96 hours, as recommended for nanoparticle testing (Dabrunz et al., 2011). Moreover, the illumination conditions were changed from laboratory light to comparably low but field relevant UV intensities (0.00–5.20 W $UVA/m^2$; wavelength: 315–380 nm; exposure period: 8 hours/day; Amiano et al., 2012; Häder et al., 2007; Fig. 2). Additionally, the test medium was enriched with varying ambient levels of NOM (seaweed extract; 0.00–4.00 mg TOC/L; Marinure®, Glenside, Scotland; Ryan et al., 2009; Fig. 2).

In order to relate the photocatalytic activity of $nTiO_2$ under the different exposure scenarios to the respective ecotoxicological impact, the formation of ROS (using •OH radicals as a proxy) was measured during the course of the experiments. Glutathione-S-transferase (GST) activity, glutathione (GSH) content, and acetylcholinesterase (AChE) activity in *Daphnia* was determined, as biomarkers that are involved in the defense towards oxidative and neurotoxic stress (Barata et al., 2005; Kim et al., 2010; Ulm et al., 2015). It was hypothesized that the presence of NOM reduces the toxicity of UV-illuminated $nTiO_2$ towards *D. magna*, which can be explained by (i) suppression of ROS formation through EINP masking, and (ii) reduced biomarker responses within the respective treatments. **[Appendix A. 2]**
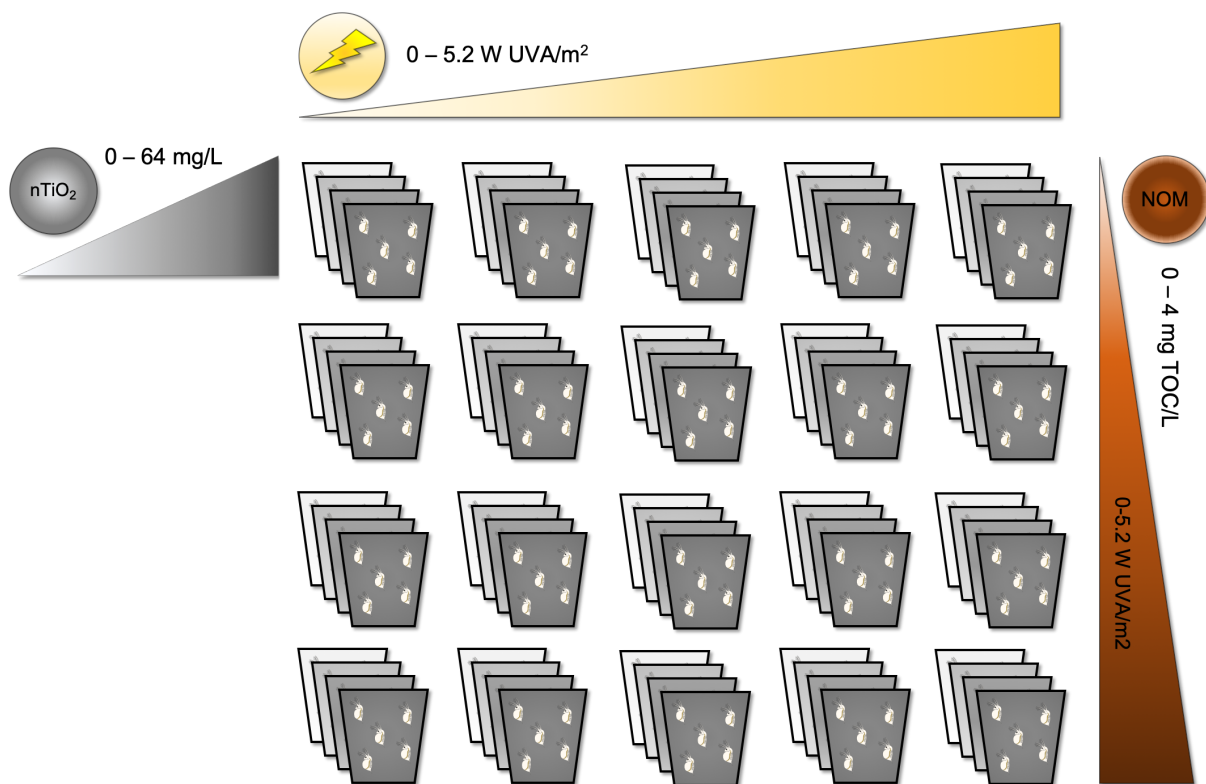
**Fig. 2.** Illustration of the experimental setup: increasing levels of $nTiO_2$ (0, 0.1, 0.2, 1, 2, 4, 8, 16, 32, and 64 mg/L), combined with increasing UVA intensities (0, 0.4-0.6, 1-1.4, 2.2-2.6, and 4.8-5.2 W $UVA/m^2$), and NOM levels (0, 0.04, 0.4, and 4 mg TOC/L). Each UVA intensity was combined with each NOM level and used as testing environment to assess the acute toxicity of $nTiO_2$. **[Appendix A. 2]**

### 3.2 UV illumination of EINPs modifies pesticide toxicity

This objective was aiming to assess the influence of the three factors, presence and absence of $nTiO_2$ (P25; ~80 nm; 0.05 mg/L), NOM (4 mg TOC/L), and varying UV-intensities (0.0–2.6 W $UVA/m^2$) on the acute toxicity of six model pesticides (azoxystrobin (AZO), dimethoate (DIM), malathion (MAL), parathion (PAR), permethrin (PER), and pirimicarb (PIR)) towards *D. magna.* The pesticides were selected based on varying photostability ($DT_{50}$), ranging between 0.5–175 days. The tested $nTiO_2$ concentrations and UV intensities were set at low levels in order to prevent adverse effects on the organisms exclusively induced by these factors, enabling the application of closer-to-field ($nTiO_2$; Gottschalk et al., 2013; Sun et al., 2014) and field-relevant levels (UV and NOM; Häder et al., 2007; Ryan et al., 2009) of the applied factors. This allowed a systematic assessment of the altered ecotoxicological potential of the selected pesticides depending on the different factor and factor level combinations (Fig. 3).

This assessment was realized by implementing acute toxicity tests largely following the OECD guideline 202 (OECD, 2004), with an elongated exposure duration of 96 hours (Dabrunz et al., 2011). The illumination conditions were adapted from laboratory light to field relevant UV intensities (0.0–2.6 W UVA $m^2$; wavelength: 315–380 nm; exposure period: 8 h/day; Amiano et al., 2012; Häder et al., 2007). For each pesticide a series of 16 individual toxicity tests, i.e. varying combinations of the factors $nTiO_2$, NOM, increasing UV light, and pesticide concentrations was established (Fig. 3). With the collected data 96-h $EC_{50}$ values (half maximal effect concentrations) were calculated for the different pesticides and exposure scenarios.

It was hypothesized that the presence of $nTiO_2$ and increasing UV intensities will induce increasing ROS formation, leading to a photocatalytic degradation of the pesticides, ultimately reducing the acute toxicity towards *D. magna*. Thereby, the magnitude of effects will correlate with the photostability of the compounds. The presence of NOM was expected to act in two ways: (i) reduce the toxic potential of the applied pesticides, functioning as a food source for *D. magna* already increasing energy reserves in the organisms during the 96 h exposure, or acting as ligand reducing the pesticides bioavailability (Bergman Filho et al., 2011; Bouchnak and Steinberg, 2010; Seitz et al., 2015a), and (ii) reduce the photocatalytic degradation of the pesticides as a result of a reduced photoactivity of NOM masked $nTiO_2$. The potential impact of the three applied factors (presence and absence of $nTiO_2$, NOM and varying UV-intensities) on the photo(cata)lytic degradation of the pesticides was measured in each exposure scenario at the start (0 h), and the end (approx. after 96 h) of the experiments. **[Appendix A. 3]**
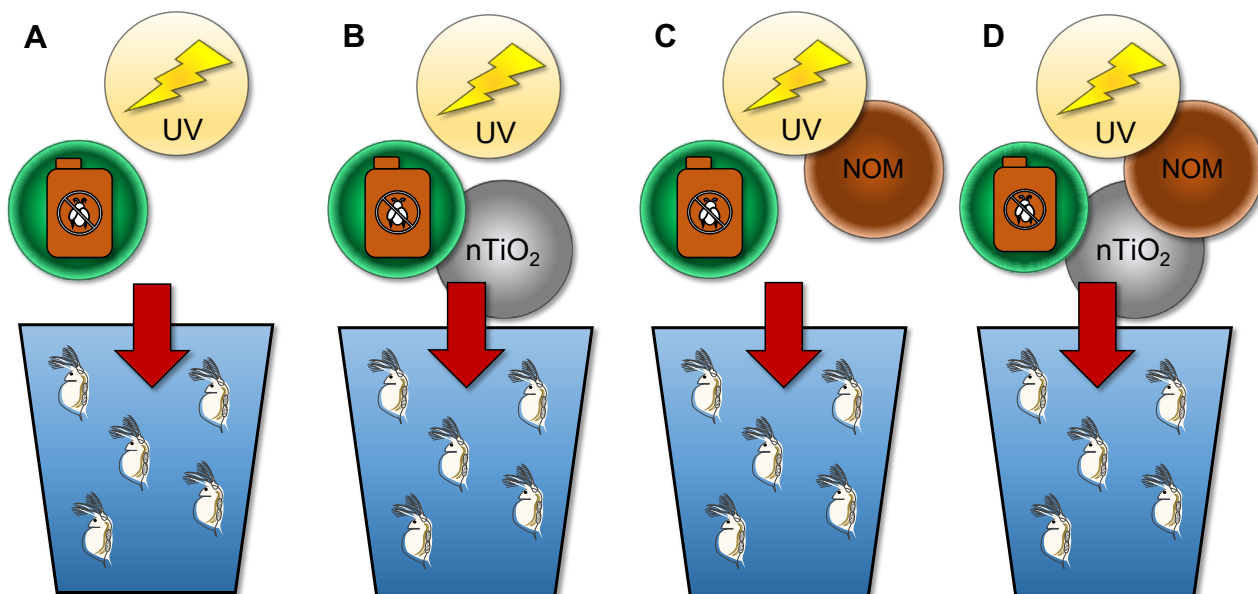
**Figure 3.** Applied factor combinations for the acute toxicity bioassays. Each scenario was applied to each of the six pesticides (AZO, DIM, MAL, PAR, PER, and PIR). **A:** impact of varying UVA intensities (0–2.6 W/m$^2$) on the pesticide toxicity; **B:** impact of varying UVA intensities (0–2.6 W/m$^2$) and nTiO$_2$ (0.05 mg/L) on the pesticide toxicity; **C:** Impact of varying UVA intensities (0–2.6 W/m$^2$) and NOM (4 mg TOC/L) on the pesticide toxicity; **D:** Impact of varying UVA intensities (0–2.6 W/m$^2$), nTiO$_2$ (0.05 mg/L), and NOM (4 mg TOC/L) on the pesticide toxicity. **[Appendix A. 3]**

### 3.3 EINP effects in benthic aquatic invertebrates

This part investigated potential effects provoked by two exposure pathways (waterborne or diet-related) for two types on EINPs, namely nTiO$_2$ and nAg. Therefore, two 30-d long bioassays were conducted. Following the fate of EINPs they are likely to leave the water phase and will end up in sediments, why *Gammarus fossarum* was selected as test species, representing a benthic model organism. The two exposure pathways were differentiated by applying a 2x2 factorial test design. The experiments were performed with nTiO$_2$ (P25; ~80 nm; 4 mg/L), and nAg (citrate-coated; ~30 nm; 0.125 mg/L) as representatives for chemically stable (non-dissolving) and ion-releasing (dissolving) EINPs, respectively (Bundschuh et al., 2018).

The first factor was characterized by the EINPs being applied to the water phase during the course of the experiment (waterborne exposure pathway; Fig. 4B). The second factor was accomplished by the EINPs being adsorbed to the diet of *Gammarus* (black alder leaf material), which was realized by a 6-d long aging of the leaf material in the

presence or absence (control) of the EINPs, before it was offered to the organism (dietary exposure pathway; Fig. 4 C, 4 D). Mortality (as evidence for possible acute effects), food consumption, feces production, and energy assimilation (as sensitive and robust sub-lethal response variables; see Maltby et al., 2002) were measured during the 30-d exposure. After the termination of the experiments, the physiological fitness of the animals in terms of lipid content and dry weight was determined. EINP exposure via the waterborne pathway was expected to be higher relative to a dietary exposure, and consequently the effects on gammarids to be less pronounced for the dietary pathway. Combining both exposure pathways was suggested to reveal additive effects on the test organism. **[Appendix A. 4]**
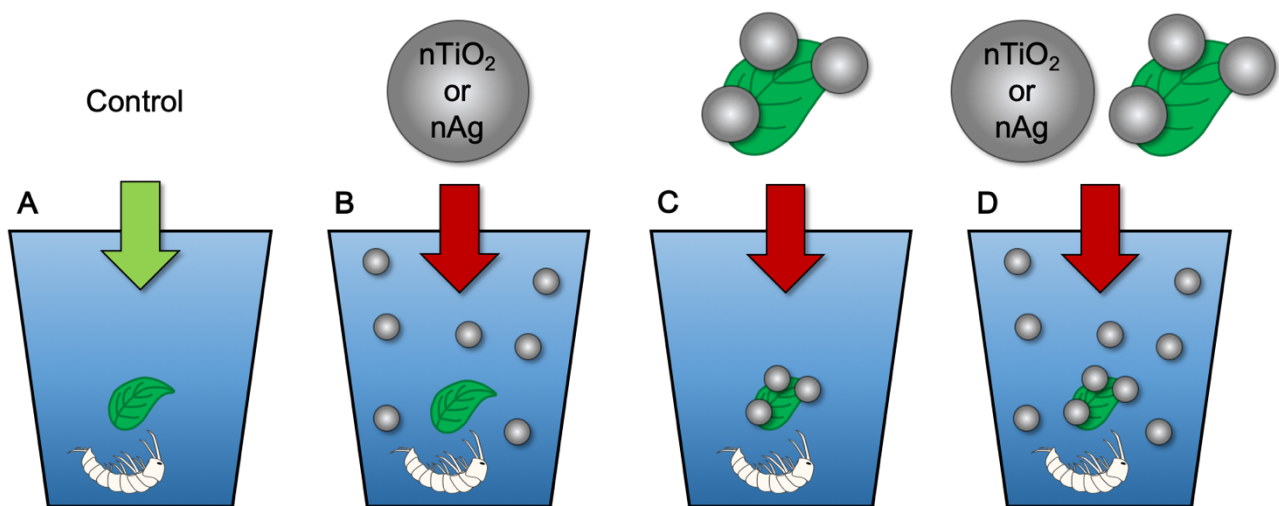


**Fig. 4.** Visualization of the experimental treatments. **A:** EINP-free control, **B:** waterborne exposure pathway, **C:** dietary exposure pathway, **D:** waterborne combined with dietary exposure. **[Appendix A. 4]**

## 3.4 EINP transport from aquatic to terrestrial systems

For the experiment 24 independent artificial stream channels made of stainless steel (120x30x20 cm; approx. 50 liters water volume) were used (Fig. 5). In total six control units (Pequitec, Switzerland) regulated the supply with test medium (SAM-5S; Borgmann, 1996), while each unit provided the medium for four streams, enabling a complete medium exchange within 24 hours, and respective dosing of the EINPs. The test organisms (*C. villosa*, 4th instar) were acclimatized in the stream channels for 14 days at 14±1°C before dosing with EINPs started.

In each stream, *C. villosa* larvae (length >10 mm) were held in groups of 40 in stainless steel cages which were additionally enriched with artificial sediment comprised of glass spheres with diameters ranging between 105–1200 μm (Worf Glaskugeln GmbH). The cages were positioned in front of a paddle wheel inside of the stream channels in order to simulate running water conditions with a velocity of 0.1 m/s (Fig. 5). Daylight was simulated in a 12:12 hours (light:dark) rhythm with a system emitting UVA and UVB irradiation at 9.7 and 0.35 W/m$^2$ (at the water surface), respectively. The study design allowed the establishment of six different treatments (n=4; Fig. 5):

**(a)**    EINP-free control in the absence of UV

**(b)**    EINP-free control in the presence UV

**(c)**    4 μg $nTiO_2$/L in the absence of UV

**(d)**    4 μg $nTiO_2$/L in the presence of UV

**(e)**    400 μg $nTiO_2$/L in the presence of UV

**(f)**    6.5 μg nAu/L in the absence of UV

Depending on the treatment, either a UV-transparent or -filtering film (LLumar® UV CL-SR PS, SUNPOINT, Germany) was used to cover the individual stream channels. Additionally, this cover served as a barrier to emerging insects. The study lasted for 140 days. Over the course of the study, every other week the test organisms received ~10 g (dry weight) of preconditioned leaf material (black alder) as food source, while the remaining food was removed each food exchange in order to determine the consumed leaf material. At the same time, dead larvae were removed from the system. Every day each stream channel was checked for emerging caddisflies, which were stored frozen until used for the measurement of energy reserves (i.e. lipid content). **[Appendix A. 5]**
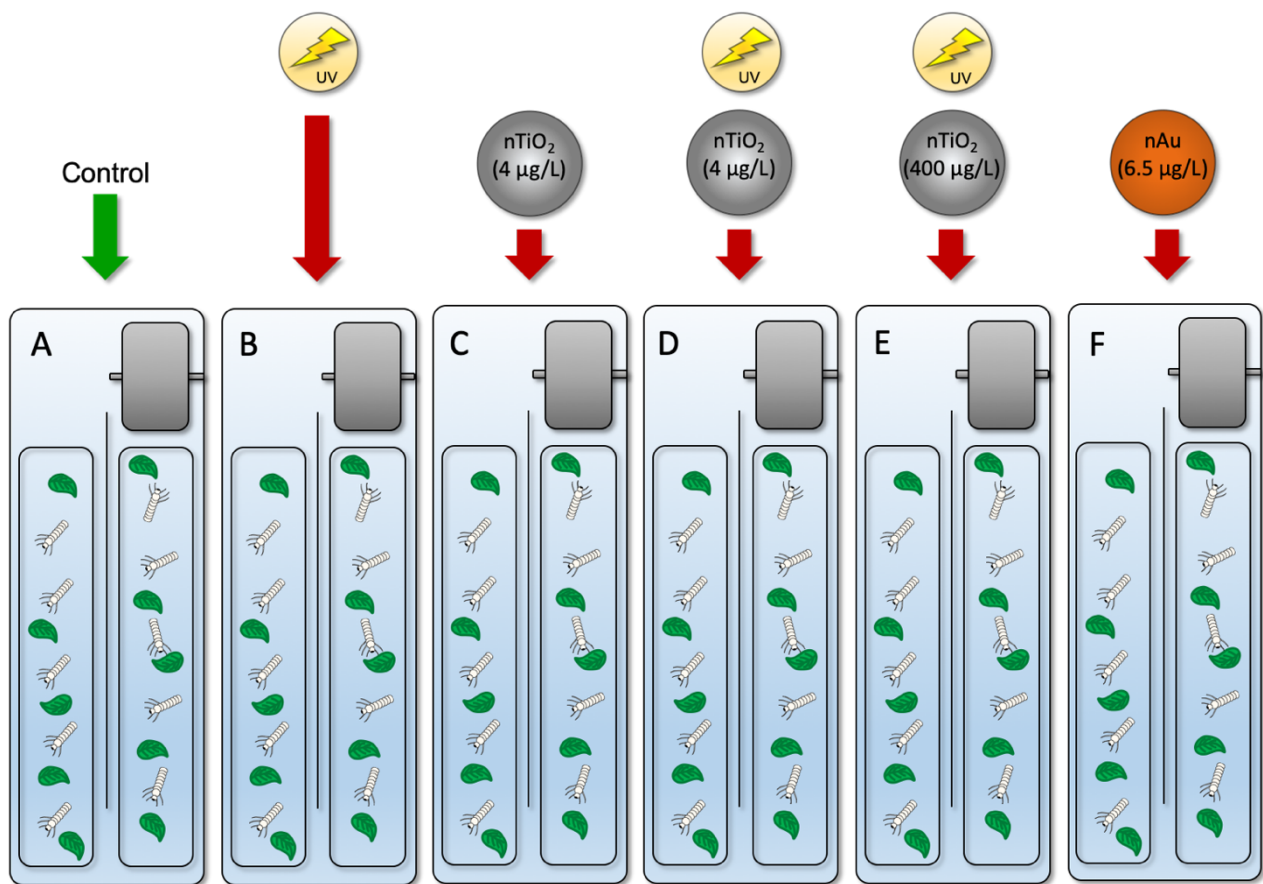
**Figure 5.** Visualization of the experimental treatments. **A:** EINP-free control, absence of UV, **B:** EINP-free control, presence UV, **C:** 4 µg $nTiO_2$/L, absence of UV, **D:** 4 µg $nTiO_2$/L, presence of UV, **E:** 400 µg $nTiO_2$/L, presence of UV, and **F:** 6.5 µg nAu/L, absence of UV. Each stream channel was equipped with cages containing caddisflies in groups of 40, artificial glass-sphere sediment, as well as black alder leaf material as food source. Velocity (0.1 m/s) was generated by a paddle wheel above the cages. Each treatment was replicated four times. **[Appendix A. 5]**

# 4. RESULTS

## 4.1 NOM affects UV-induced EINP toxicity

With increasing UV radiation, the ecotoxicological potential of $nTiO_2$ was up to 280-fold enhanced, whereas higher NOM levels mitigated the observed effects up to 12-fold, relative to an $nTiO_2$ and NOM absence (Fig. 6). This observation was attributed to reduced reactive oxygen species (ROS; measured as $\cdot OH$ radicals) formation at lower UV intensities (Fig. 7). The $nTiO_2$-mediated ROS formation was not proportional to increasing NOM levels. In particular, lower concentrations (0.04–0.4 mg TOC/L) marginally reduced, whereas the highest applied concentration (4 mg TOC/L) amplified the formation of ROS quantity in the presence of $nTiO_2$, regardless of the applied UV intensity (Fig. 7). Increasing AChE and GST activities in daphnids (in presence of 8 mg/L $nTiO_2$ and elevated UV intensity) point towards neurotoxic and oxidative stress as a driver for the observed effect patterns (Fig. 8).
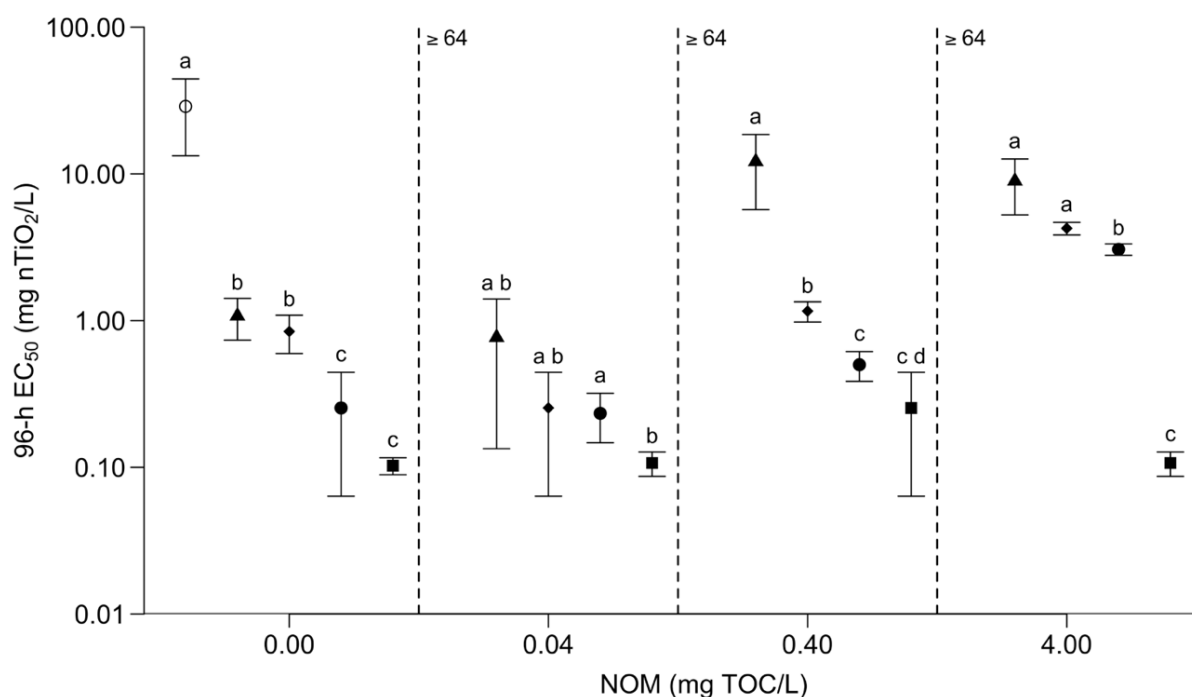


**Figure 6.** 96-h $EC_{50}$ (±95% CI) of *D. magna*, exposed to $nTiO_2$ (0–64 mg/L) in ASTM +NOM (0–4 mg TOC/L), in the presence of UV light (0–5 W UVA/ $m^2$). ○ = 0 W UVA/$m^2$, ▲ = 0.4–0.6 W UVA/$m^2$, ◆ = 1–1.4 W UVA/$m^2$), ● = 2.2–2.6 W UVA/$m^2$, and ■ = 4.8–5.2 W UVA/$m^2$. Different letters denote statistically significant difference between individual TS but within one NOM level. ≥64 represents the treatments where a 96-h $EC_{50}$ calculation was not possible due to less than 50% observed immobility of the test organism at the highest applied $nTiO_2$ concentration (64 mg/L). **[Appendix A. 2]**
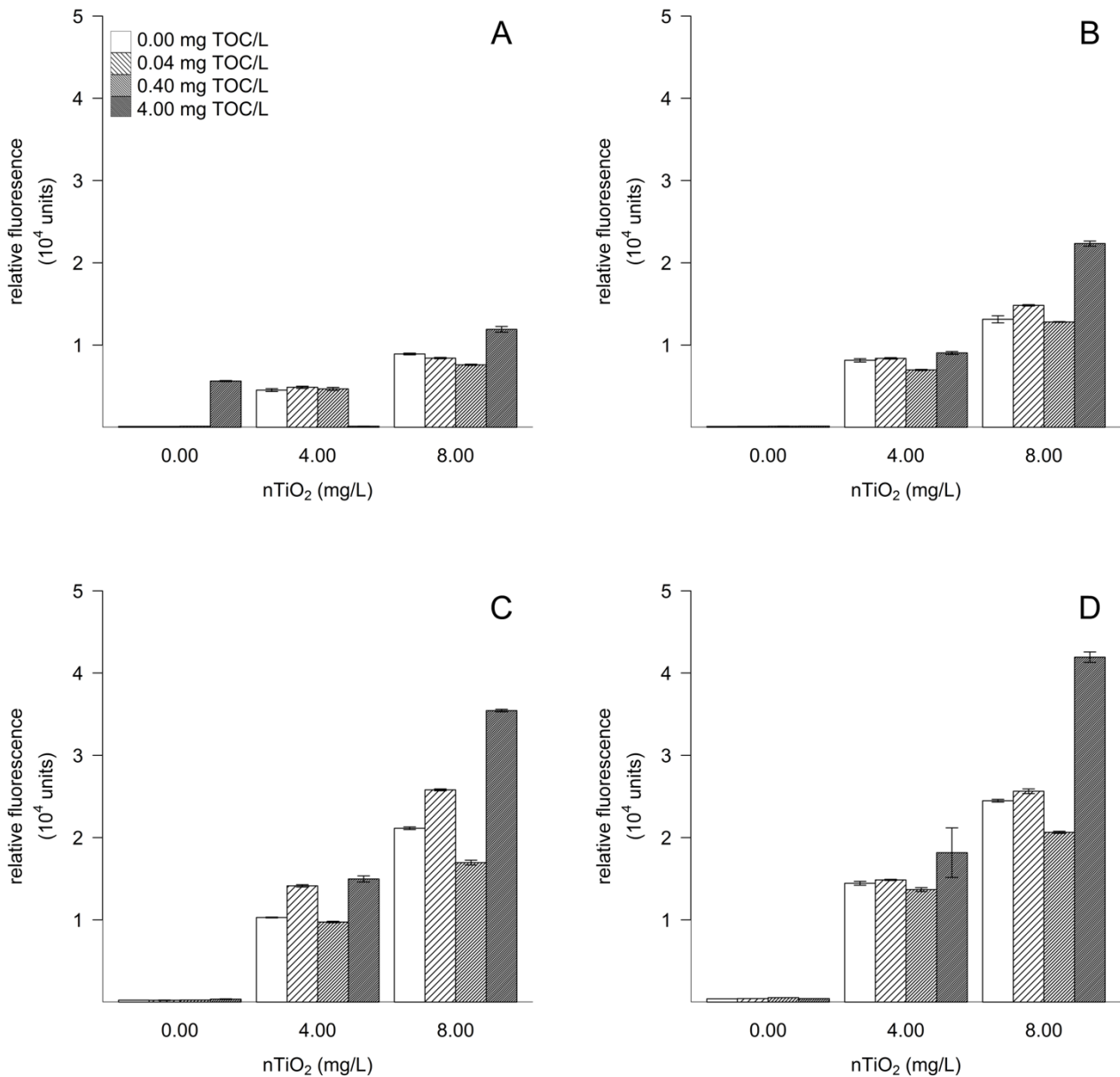
**Figure 7.** Mean relative fluorescence ($10^4$ units ±SD, n=3), representative for ROS formation of $nTiO_2$ (0, 4, and 8 mg/L), measured in ASTM +NOM (0, 0.04, 0.40, and 4 mg TOC/L) after 96 h in the presence of different UV light intensities (A: 0.4–0.6 W $UVA/m^2$; B: 1–1.4 W $UVA/m^2$; C: 2.2–2.4 W $UVA/m^2$; D: 4.8–5.2 W $UVA/m^2$). Mean relative fluorescence of approx. 70 fluorescence units in the absence of UV is not shown. **[Appendix A. 2]**
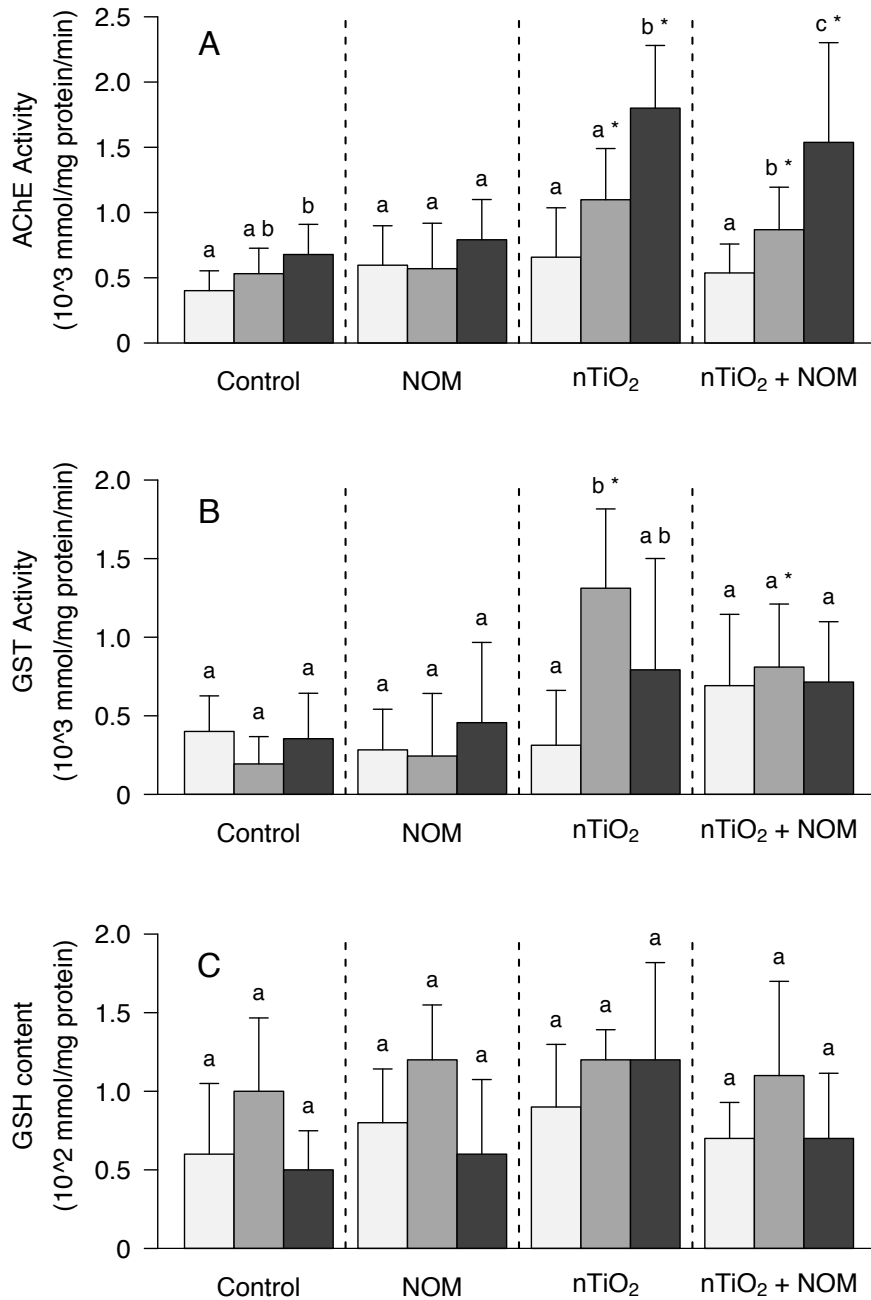
**Figure 8.** Median **A:** AChE activity (±SD; mmol/mg protein/min), **B:** GST activity (±SD; mmol/mg protein/min), and **C:** GSH content (±SD; mmol/mg protein) in *D. magna* after being exposed for 48 hours to the control, NOM (SW; 4 mg TOC/L), $nTiO_2$ (P25; 8 mg/L), as well as the combination of $nTiO_2$ +NOM (P25, 8 mg/L; SW, 4 mg TOC/L). The shading of the bars indicates the applied UVA intensities (light grey: 0 $W/m^2$, medium grey: 0.4–0.6 $W/m^2$, and dark grey: 2.2–2.6 $W/m^2$). Different letters denote statistically significant difference between increasing UVA intensities within one treatment. Asterisks denote statistically significant difference to the control treatment at the respective applied UVA intensity. **[Appendix A. 2]**

**4.2 UV illumination of EINPs modifies pesticide toxicity**

Increasing UV radiation alone partially reduced pesticide toxicity due to enhanced degradation (Fig. 9; Tab. 1). Particularly, DIM and PIR toxicity was reduced up to 3-fold and 2-fold, along with a degradation of 13% and 79% at the highest applied UV radiation (UVA-IV; Tab. 1; Tab. 2), respectively. PAR showed a trend to a reduced toxicity by up to 70%, comparing the UVA-I with UVA-IV (Fig. 9; Tab. 1), though not statistically significant. As PAR samples were not analytically measured, the decrease in toxicity cannot definitely be attributed to an increased degradation. $DT_{50}$s of 175 d (DIM), 30 d (PAR), and 0.5–6 d (PIR) point towards an enhanced UV-induced degradation efficiency with decreasing photostability.

The application of $nTiO_2$ (50 µg/L) reduced but also increased pesticide toxicity in the presence of UV radiation relative to an $nTiO_2$ absence, which was attributed to (i) more efficient pesticide degradation, and probably (ii) photocatalytic-induced formation of toxic byproducts, respectively. More efficient degradation was observed for AZO (PEST: -23% vs. PEST+$nTiO_2$: 18%; UVA-IV), DIM (PEST: 13% vs. PEST+$nTiO_2$: 31%; UVA-IV), and PIR (PEST: 79% vs. PEST+$nTiO_2$: <LOQ; UVA-IV; Tab 1; Tab 2). For PAR and MAL, it was assumed that the additional $nTiO_2$-induced photocatalytic degradation promoted the formation of metabolites that were more toxic than the parent compound, explaining the partly increasing toxicity in $nTiO_2$ presence (Fig. 9; Tab. 1).

The presence of NOM partly mitigated pesticide toxicity, which was not evidently accompanied by an enhanced pesticide degradation, observed for DIM, PAR, and PIR (relative to PEST, and PEST+$nTiO_2$; Fig. 9; Tab 1; Tab. 2). This mitigated pesticide toxicity was seemingly driven by the potential of NOM to serve as energy source with a positive effect on the fitness of *D. magna*. On the other side, NOM presence also inhibited the pesticide degradation (Tab. 1), leading to an increased pesticide toxicity, which was assumed for MAL. All in all, conclusions on the reduction of the ecotoxicological potential of pesticides based on their hydro- and photo(cata)lysis or interaction with NOM were hardly possible.

**Table 1.** Measured concentrations of azoxystrobin (AZO), dimethoate (DIM), malathion (MAL), and pirimicarb (PIR) in the different test series (TS), at varying UVA radiations (UVA-I-IV), approx. 10 min (0 h) after pesticide application to the respective test medium and exposure scenario, as well as after the termination of the experiments (96 h). Due to a malfunctioning freezer PAR and PER samples were not suitable for chemical analysis and are therefore not listed. ∆ illustrates the relative degradation in % after 96 h referring to the 0-h concentrations of the respective test series, whereas negative values indicate pesticide degradation. NA=not assessable. **[Appendix A. 3]**

| TS | UVA (W/m$^2$) | UVA (level) | Time (h) | AZO (µg/L) | ∆ (%) | DIM (µg/L) | ∆ (%) | MAL (µg/L) | ∆ (%) | PIR (µg/L) | ∆ (%) |
|---|---|---|---|---|---|---|---|---|---|---|---|
| PEST | - | | 0 | 1396 | - | 2900 | - | 6.3 | - | 69.6 | - |
| | 0 | UVA-I | 96 | 1817 | 30 | 2862 | -1 | 2.0 | -68 | 80.7 | 16 |
| | 0.4-0.6 | UVA-II | 96 | 1867 | 34 | 2633 | -9 | 2.7 | -58 | 67.6 | -3 |
| | 1-1.4 | UVA-III | 96 | 1476 | 6 | 2688 | -7 | 2.1 | -66 | 30.0 | -57 |
| | 2.2-2.6 | UVA-IV | 96 | 1713 | 23 | 2532 | -13 | 2.0 | -68 | 14.6 | -79 |
| PEST | - | | 0 | 1443 | - | 2856 | - | 2.6 | - | 64.7 | - |
| + | 0 | UVA-I | 96 | 1693 | 17 | 2827 | -1 | 1.3 | -48 | 91.9 | 42 |
| nTiO$_2$ | 0.4-0.6 | UVA-II | 96 | 1648 | 14 | 2804 | -2 | 2.2 | -14 | 7.0 | -89 |
| | 1-1.4 | UVA-III | 96 | 1441 | 0 | 2946 | 3 | 1.1 | -58 | <LOD | NA |
| | 2.2-2.6 | UVA-IV | 96 | 1186 | -18 | 1983 | -31 | 0.9 | -65 | <LOD | NA |
| PEST | - | | 0 | 1533 | - | 2989 | - | 4.4 | - | 35.6 | - |
| + | 0 | UVA-I | 96 | 1575 | 3 | 2798 | -6 | 3.2 | -29 | 43.0 | 21 |
| NOM | 0.4-0.6 | UVA-II | 96 | 1431 | -7 | 2887 | -3 | 3.1 | -29 | 22.7 | -36 |
| | 1-1.4 | UVA-III | 96 | 1200 | -22 | 2652 | -11 | 2.9 | -35 | 17.5 | -51 |
| | 2.2-2.6 | UVA-IV | 96 | 1066 | -30 | 2150 | -28 | 3.2 | -29 | 9.2 | -74 |
| PEST | - | | 0 | 1496 | - | 2981 | - | 2.9 | - | 37.0 | - |
| + | 0 | UVA-I | 96 | 1520 | 2 | 2837 | -5 | 2.1 | -30 | 38.8 | 5 |
| nTiO$_2$ | 0.4-0.6 | UVA-II | 96 | 1275 | -15 | 2841 | -5 | 2.0 | -31 | 29.4 | -20 |
| + | 1-1.4 | UVA-III | 96 | 1356 | -9 | 2700 | -9 | 2.2 | -25 | 13.8 | -63 |
| NOM | 2.2-2.6 | UVA-IV | 96 | 1228 | -18 | 2028 | -32 | 0.9 | -71 | 4.4 | -88 |

**Table 2.** Applied exposure scenarios for the acute toxicity bioassays. Each scenario was applied to each of the six pesticides (AZO, DIM, MAL, PAR, PER, and PIR). *Before the start of the experiments, UVA radiation was measured at the water-surface of the test vessels, which were randomly placed in the areas that were in the UV-range respectively listed. **[Appendix A. 3]**

| Test series | UV radiation* (W UVA/ m$^2$) | nTiO$_2$ (mg/L) | NOM (mg TOC/L) |
|---|---|---|---|
| PEST | 0 | 0 | 0 |
| | 0.4–0.6 | 0 | 0 |
| | 1–1.4 | 0 | 0 |
| | 2.2–2.6 | 0 | 0 |
| PEST+nTiO$_2$ | 0 | 0.05 | 0 |
| | 0.4–0.6 | 0.05 | 0 |
| | 1–1.4 | 0.05 | 0 |
| | 2.2–2.6 | 0.05 | 0 |
| PEST+NOM | 0 | 0 | 4 |
| | 0.4–0.6 | 0 | 4 |
| | 1–1.4 | 0 | 4 |
| | 2.2–2.6 | 0 | 4 |
| PEST+nTiO$_2$+NOM | 0 | 0.05 | 4 |
| | 0.4–0.6 | 0.05 | 4 |
| | 1–1.4 | 0.05 | 4 |
| | 2.2–2.6 | 0.05 | 4 |
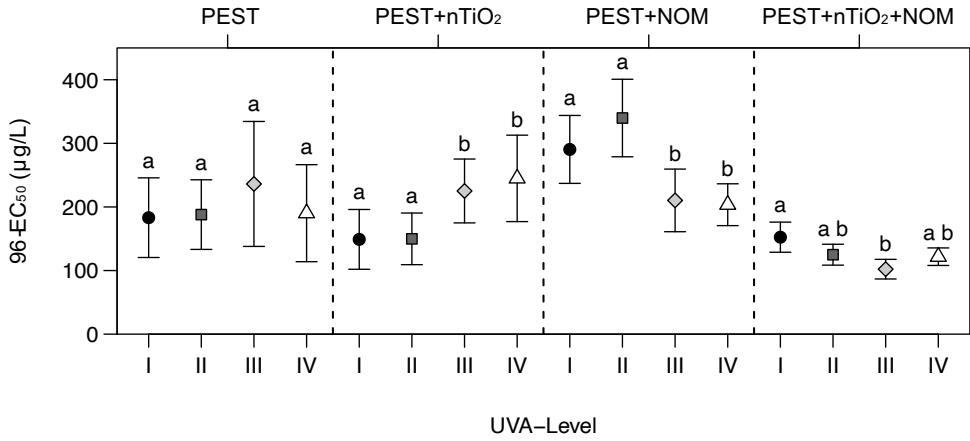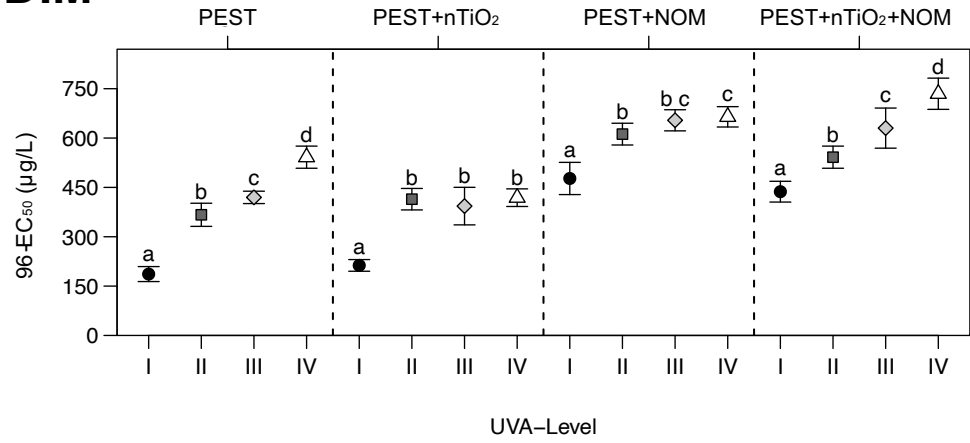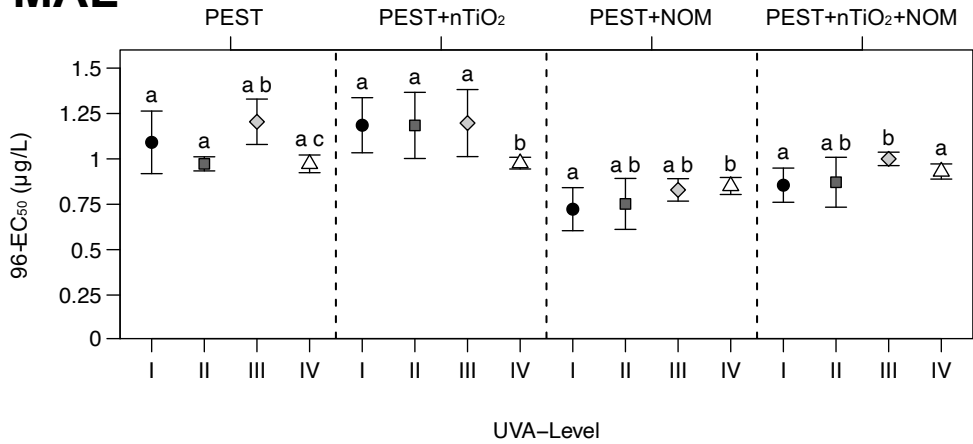
# PAR
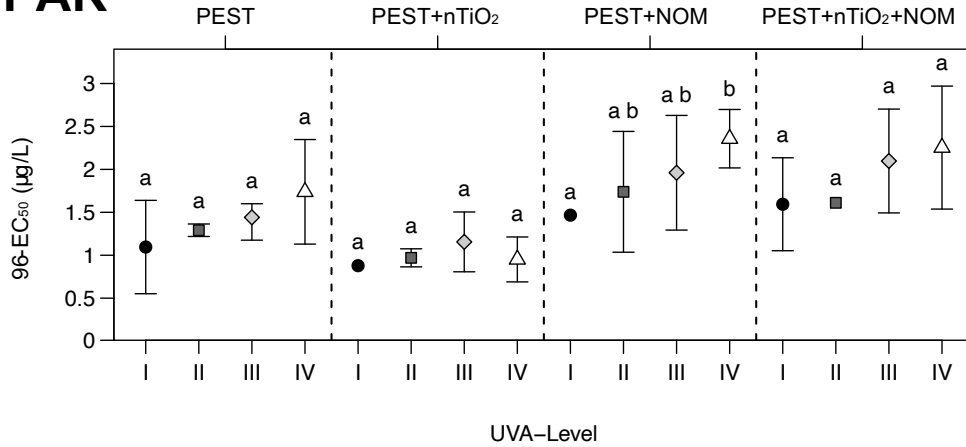


# PER
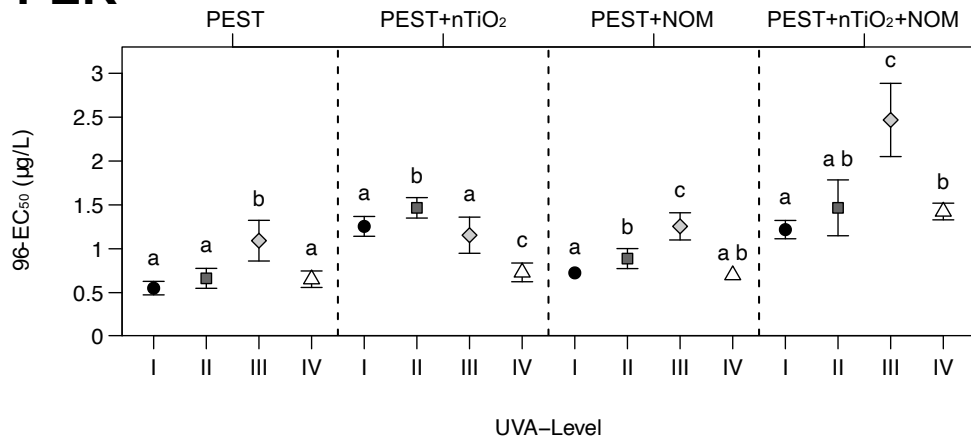


# PIR
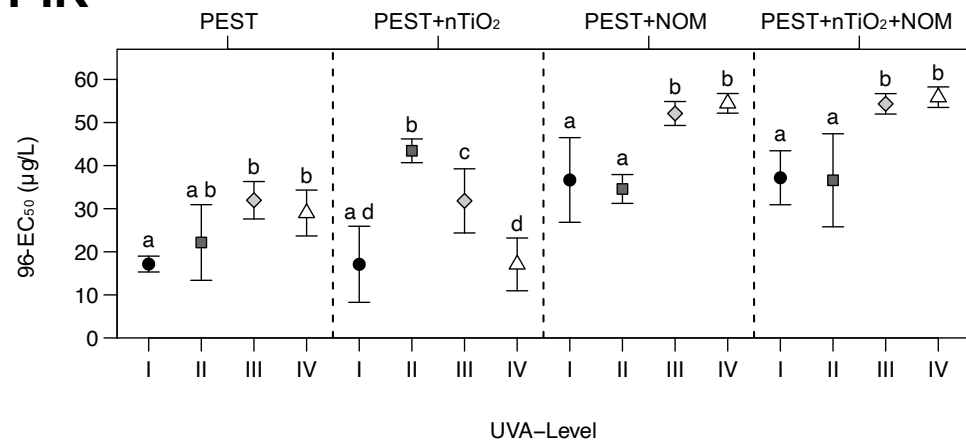


**Figure 9.** 96-h EC$_{50}$s (µg/L ±95% CI) of *D. magna* for the six pesticides azoxystrobin (AZO), dimethoate (DIM), malathion (MAL), parathion (PAR), permethrin (PER), and pirimicarb (PIR) based on nominal concentrations, under varying UVA radiation (I: 0 W UVA/m$^2$, II: 0.4–0.6 W UVA/m$^2$, III: 1–1.4W UVA/m$^2$, and IV: 2.2–2.6 W UVA/m$^2$), and TS (PEST, PEST+nTiO$_2$, PEST+NOM, and PEST+nTiO$_2$+NOM; Tab. 2). **[Appendix A. 3]**

## 4.3 EINP effects in benthic aquatic invertebrates

This study revealed a significantly reduced energy assimilation (up to ~30%) in *G. fossarum* induced by waterborne exposure towards nTiO₂. In contrast, the dietary exposure towards nAg significantly increased the organisms' energy assimilation (up to ~50%; Fig. 10).
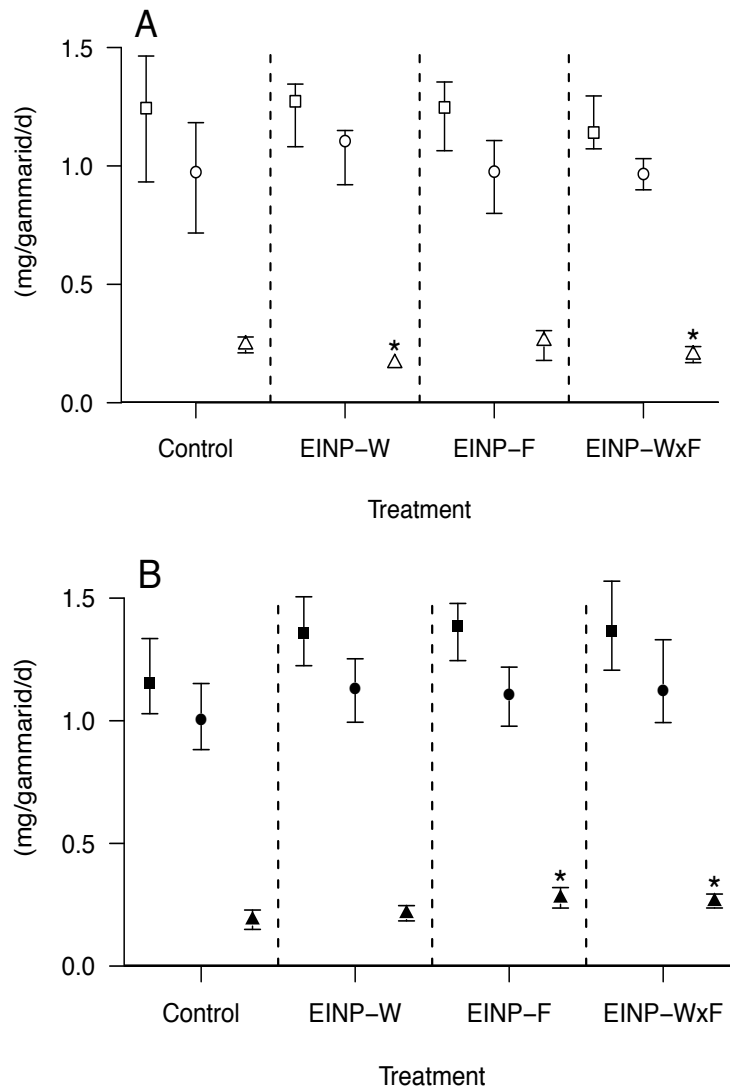


**Figure 10.** Median leaf consumption (squares), feces production (circles), and energy assimilation (triangles; ±95% CI) of *G. fossarum* in mg/gammarid/day after the 30-day exposure to the control, EINPs applied to the water phase (waterborne; EINP-W), EINPs adsorbed to the provided food (dietary; EINP-F), and the combination of both pathways (EINP-WxF). nTiO₂ exposure is represented in (A), whereas nAg exposure is illustrated in (B). Asterisks denote statistically significant difference to the respective control treatment. **[Appendix A. 4]**

24

Furthermore, the exposure towards $nTiO_2$ did not significantly affect the mortality of *Gammarus*, regardless of the exposure pathway (Tab. 3). The highest mortality rate was observed for the control (10%), followed by EINP-F (3.3%), EINP-W and $nTiO_2$ EINP-WxF (6.7%). In contrast, the nAg bioassay revealed a significant impact on *Gammarus* survival in the combined exposure scenario (EINP-WxF; $p$ = 0.008) with a mortality rate of 27%, relative the control (0%; Tab. 3). Exposure pathway dependent effects of EINPs cannot be generalized and remain particle specific resting upon their intrinsic properties (Lüderwald et al., 2019).

**Table 3.** Observed mortality after the 30-day exposure towards $nTiO_2$ and nAg, within the different treatments as absolute and relative values. **[Appendix A. 4]**

|  | Control | | EINP-W | | EINP-F | | EINP-WxF | |
| --- | --- | --- | --- | --- | --- | --- | --- | --- |
|  | $nTiO_2$ | nAg | $nTiO_2$ | nAg | $nTiO_2$ | nAg | $nTiO_2$ | nAg |
| Mortality (absolute) | 3 | 0 | 2 | 2 | 1 | 0 | 2 | 8 |
| Mortality (%) | 10 | 0 | 6.7 | 6.7 | 3.3 | 0 | 6.7 | 27 |

## 4.4 EINP transport from aquatic to terrestrial systems

Relative to the EINP-free controls, none of the treatments had an impact on the overall leaf consumption, survival, and emergence rate of *C. villosa* (Tab. 4). However, the temporal emergence pattern, energy reserves (measured as lipid content), as well as the EINP concentrations in the emerged caddisflies was considerably affected (Fig. 11). In particular, in the presence of nAu, the time until 50% of the organisms have emerged (median emergence) was delayed by up to one month, along with up to 25% reduced energy reserves in the adult caddisflies (Fig. 11). Whereas UV irradiation alone delayed the time to median emergence by 11 days relative to the control, the addition of 4 and 400 µg $nTiO_2$/L promoted this delay to 16 and 20 days, respectively. Moreover, adult caddisflies in the $UVxnTiO_2$ treatments showed significantly reduced energy reserves (Fig. 11). In the treatments that received EINP, emerging *C. villosa* carried median concentrations of approx. 1.5 and up to 2.7 ng/mg for either Au or $TiO_2$, respectively (Tab. 5).

**Table 4.** Impact of EINPs on the emergence rate, survival and feeding. Mean (±standard deviation) number of emerged and dead *C. villosa* larvae together with cumulative leaf mass loss over the study duration of 140 days. (n=4) **[Appendix A. 5]**

| Treatment | Mean emergence (No.) | Mean death (No.) | Cumulative leaf mass loss (mg) |
|---|---|---|---|
| Control | 19.0 (±6.6) | 21.0 (±6.6) | 773.4 (±36.5) |
| UV | 18.8 (±4.9) | 21.2 (±4.9) | 754.0 (±30.7) |
| 4 µg $nTiO_2$/L | 17.8 (±4.2) | 22.2 (±4.2) | 710.8 (±89.9) |
| UVx4 µg $nTiO_2$/L | 16.3 (±4.3) | 23.7 (±4.3) | 716.1 (±24.5) |
| UVx400 µg $nTiO_2$/L | 19.5 (±3.1) | 20.5 (±3.1) | 738.0 (±74.0) |
| 6.5 µg nAu/L | 21.0 (±1.8) | 19.0 (±1.8) | 783.8 (±73.1) |

**Figure 11.** Days to median emergence (a), and mean lipid concentrations (b) in adult *C. villosa* exposed as larvae to nAu and $nTiO_2$ for 140 days in stream microcosms. Letters A and B refer to a statistically significant difference relative to the control or the UV treatment, respectively. **[Appendix A. 5]**

**Table 5.** Concentrations of Au and TiO$_2$ in adult caddisflies exposed as larvae for 140 days in stream microcosms to nanoparticles. **[Appendix A. 5].**

| Treatment | Median Au concentration (ng/mg; range) | Median TiO$_2$ concentration (ng/mg; range) |
|---|---|---|
| Control | | |
| | <LOQ | 0.43 (0.25–1.09)[a] |
| UV | | |
| 4 µg nTiO$_2$/L | NA | |
| | | 0.93 (0.54–18.40)* |
| UVx4 µg nTiO$_2$/L | NA | |
| UVx400 µg nTiO$_2$/L | NA | 2.68 (0.47–9.44)* |
| 6.5 µg nAu/L | 1.51 (<LOQ–15.33)* | NA |

*Statistically significant compared to the control (p<0.05)

[a]As titanium is among the ten most common elements of the earth crust, the detection of trace levels in organisms are expected even when they were not exposed to nTiO$_2$, e.g. shown by (Rosenfeldt et al., 2014).

NA=not assessed

LOQ=Limit of quantification (3.6 ng for Au)

## 5. DISCUSSION

### 5.1 NOM affects UV-induced EINP toxicity

Within this thesis it has been demonstrated that NOM in sufficient quantities (i.e. ≥ 0.40 mg TOC/L) reduces the ecotoxicological potential of $nTiO_2$ (Appendix A. 2). Thereby, the masking of $nTiO_2$ with NOM is suggested to play a major role, resulting in enhanced steric repulsion forces between the $nTiO_2$ particles, leading an increased energy barrier to agglomeration (Erhayem and Sohn, 2014). This assumption was indirectly supported by zeta potential measurements, showing a more negative zeta potential of $nTiO_2$ with increasing NOM concentrations, indicating an increased adsorption of NOM to the particles' surface (as detailed in Seitz et al., 2016; Appendix A. 2). Consequently, this increased adsorption might have reduced the bioavailability of $nTiO_2$ for *D. magna* (Hall et al., 2009) in two ways: (i) reduced interactions, i.e. suppressed $nTiO_2$ coating of the organisms' outer surface (Dabrunz et al., 2011; Wang et al., 2016), and (ii) inhibition of ROS driven adverse effects (Lin et al., 2012).

At the same time, UV radiation enhanced the ecotoxicological potential of $nTiO_2$ towards *D. magna* distinctively, already at intensities as low as 5.2 W UVA/m² (Fig. 6). This impact was attributed to $nTiO_2$s' photocatalytic properties, inducing the formation of ROS when illuminated by UV radiation (Johnston et al., 2009; Ma et al., 2012). Excessive amounts of ROS are, in turn, causing oxidative stress in aquatic organisms, for instance trough lipid peroxidation within cell membranes, oxidative damage of proteins or mutation of DNA (Buonocore et al., 2010; Cabiscol et al., 2000). The conducted ROS measurements (measured as $^{\bullet}$OH radicals) in the presence of 8 mg $nTiO_2$/L confirmed this assumption by revealing higher quantities of ROS at a UV radiation of 4.8–5.2 W UVA/m², relative to lower UV intensities (Appendix A. 2).

Surprisingly, in the presence of 4.8–5.2 W UVA/m², the combination of the highest applied NOM level (4 mg TOC/L) and $nTiO_2$ (8 mg/L) revealed the highest amount of ROS, which partly contradicts the outcome of the bioassays.

The latter demonstrated a decreasing toxicity of $nTiO_2$ with increasing NOM quantity. This phenomenon was explained by a considerably reduced interaction of ROS with *Daphnia* when NOM is present in sufficient quantities (Brame et al., 2014). More specifically, NOM could (i) coat daphnids' surface and thereby act as barrier for mostly locally acting ROS (Feckler et al., 2015), and (ii) function as an antioxidant (Fabrega

et al., 2009) by interacting with ROS, partly preserving *Daphnia* against harmful radicals (Brame et al., 2014).

## 5.2 UV illumination of EINPs modifies pesticide toxicity

***Applying UV radiation to pesticides over 96 hours revealed two effect patterns:***

(i)     pesticide toxicity was decreased with increasing UV radiation (0–2.6 W UV-A/m$^2$).

(ii)    the pesticide toxicity remained constant, independent of the applied UV radiation.

Pattern (i) was observed for DIM, PAR and PIR. For DIM and PIR chemical analyses confirmed the assumption of an increasing pesticide degradation when illuminated with UV, by up to 15% and 80% reduced concentrations, respectively. This effect pattern is in line with existing studies (c.f. Evgenidou et al., 2007; Romero et al., 1994; Schwack and Kopf, 1993; Seitz et al., 2012). Although not confirmable by chemical analyses in this study (no usable samples due to a malfunctioning freezer), it is suggested that also PAR was photolytically degraded, given the observed reduced toxicity (by up to ~65%) under UV irradiation alone (comparing 0 vs. 2.2–2.6 W UVA/m$^2$; Fig. 9). Likewise, Zoh et al. (2006) reported a degradation of PAR under solar radiation, although at average intensities beyond the ones applied in this thesis (average intensity Zo et al. (2006): 6.4–19 W/m$^2$).

Regardless of the applied UV radiation AZO, MAL and PER showed a steady acute toxicity in *D. magna* (pattern (ii)), suggesting no degradation. This was confirmed for AZO, where a degradation under solar radiation was negligible (Tab. 1). Theoretically, the UV-visible absorption spectrum of AZO slightly overlaps with the solar light spectrum, allowing a photodegradation of AZO, however, this process was also not observed in the study of (Boudina et al., 2007). Against the stable retention of AZO, MAL was already degraded by up to approx. 70%, independent of the applied UV radiation (Tab. 1), suggesting hydrolysis as driving force behind the observed degradation. This degradation ranged approx. 60–70% for all applied UV intensities, explaining the largely constant MAL toxicity under UV alone. The mainly steady 96-h EC$_{50}$ of PER with increasing UV radiation (Fig. 9) could point towards the possibility of a "knock down" effect induced by the substance, as result of a fast *Daphnia* interference resulting in death of the organism, as a typical mode of action for

pyrethroids (Ensley, 2007; EPA, 2006). Ultimately, the immobilization of the test organism induced by the PER exposure might have occurred faster than a potential degradation.

### The combination of UV radiation and nTiO$_2$ (50 µg/L) resulted in three patterns:

(i)     a more effective pesticide degradation relative to nTiO$_2$ absence.

(ii)    enhanced pesticide toxicity at higher UV radiation.

(iii)   steady 96-h EC$_{50}$s throughout the applied UV intensities, while observing a generally higher toxicity relative to nTiO$_2$-absence.

Pattern (i) was observed for AZO, DIM and PIR. This amplified degradation was attributed to occurring redox reactions when nTiO$_2$ is UV illuminated, which leads to the formation of ROS that have the potential to mineralize and detoxify organic compounds like pesticides (Hoffmann et al., 1995; Konstantinou and Albanis, 2003; Low et al., 1991; Pelizzetti and Minero, 1999; Robert and Malato, 2002; Turchi and Ollis, 1989).

Following pattern (ii) when looking at higher UV radiation in the presence of nTiO$_2$, MAL, PER and PIR demonstrated an increased toxicity in *D. magna* despite elevated degradation (Fig. 9, Tab. 1). This can probably be explained by these pesticides' mode of action. MAL, PER, and PIR are acting as acetylcholinesterase inhibitor, a knowingly fast-acting mode of action (Cambon et al., 1979; Xuereb et al., 2009). In combination with the presence of nTiO$_2$ and UV radiation this might have favored synergistic stress causing the here observed effects outweighing the degradation-induced detoxification. Higher pesticide toxicity in the presence of nTiO$_2$ independent of the applied UV intensity (pattern (iii)) could be induced by the formation of metabolites having a higher toxicity towards *D. magna* than the parent substance. Evgenidou et al. (2006) showed that during photocatalytic degradation with nTiO$_2$, DIM is degraded into several by-products, including omethoate, which is considered 90-fold more toxic than DIM (Lewis et al., 2016; Van Scoy et al., 2016). Likewise, a photocatalytic degradation of MAL and PAR increased the toxicity relative to a photolytic degradation (Evgenidou et al., 2007; Li et al., 2019). For instance, the photocatalytic transformation of PAR can result in the formation of paraoxon, whose acute toxicity in *D. magna* is ~10-times higher than PAR, potentially explaining the increased PAR toxicity in presence of nTiO$_2$ (Guilhermino et al., 1996).

**The application of NOM revealed two different patterns:**

(i)      reduced pesticide toxicity, not accompanied by enhanced pesticide degradation

(ii)     NOM-induced inhibition in pesticide degradation, increasing pesticide toxicity

A detoxifying effect of NOM presence was shown for DIM, PAR, and PIR, which, however, was not linked to a more efficient degradation of the pesticides (pattern (i); Fig. 9; Tab. 1). This seems to be driven by the potential of NOM to act as energy source having a positive effect on the fitness of *D. magna*, by increasing the tolerance towards stressors (Bergman Filho et al., 2011; Bouchnak and Steinberg, 2010). Moreover, NOM could have also adsorbed to the pesticides, which can reduce the bioavailable fraction of the dissolved pesticide (Yang et al., 2006).

Contrastingly, pattern (ii) could be explained by NOMs' light absorbing potential, leading to a UV-attenuating shading effect (Albrektienė et al., 2012), indirectly mitigating the photo(cata)lysis potential of certain pesticides (Garbin et al., 2007). Thus, the increased toxicity of MAL in presence of NOM might be a result of a shading decreased availability of UV radiation lowering the potential for pesticide degradation or the formation of less toxic metabolites. For AZO and PER no clear patterns were observable.

### 5.3 EINP effects in benthic aquatic invertebrates

### 5.3.1 nTiO$_2$ bioassay

Neither gammarids' leaf consumption nor feces production was affected by the waterborne exposure, dietary exposure, or the combination of both exposure pathways (Fig. 10). These results are in line with former studies (Rosenfeldt et al., 2015) where waterborne exposure towards 5 mg nTiO$_2$/L did not have an effect of the food consumption of *G. fossarum*, however did cause a nearly significant increased feces production. Likewise, the results of the current study showed a tendency of an increased feces production under waterborne nTiO$_2$ exposure.

This trend is underpinned by a significantly decreased energy assimilation via the waterborne exposure pathway (Fig. 10). One explanation could be the increased ingestion of nTiO$_2$ by the test organism after applying the particles to the water phase, compared to the dietary exposure pathway, where most likely not all nTiO$_2$ applied during the aging phase of this experiment were associated with leaf discs. Additionally, the recurring medium renewal, followed by a new application of nTiO$_2$ every 3$^{rd}$ day of

the experiment in the waterborne exposure scenarios, may have also driven the comparably increased ingestion. It is suggested that, as a consequence, the gammarids prioritized the excretion of the ingested NPs, which ultimately lead to the comparably higher production of feces, causing the significantly reduced assimilation (Rosenfeldt et al., 2015; Schaller et al., 2011).

### 5.3.2 nAg bioassay

Exposure to nAg tendentially increased the leaf consumption of *Gammarus* by approx. 20%, relative to the EINP-free control (Fig. 10). Furthermore, in the treatments that received the dietary nAg exposure the ratio between leaf consumption and feces production accounted for approx. 80%, excretion of the consumed food, which lead to a significantly increased assimilation in the respective treatments (up to 40%), compared to the control (Fig. 10). Opposing to the assumptions for $nTiO_2$ the ingestion of nAg via the provided food seems to be the relevant pathway possibly due to the different mechanisms of toxic action of these two EINP types.

In particular, effects caused by nAg are suggested to be mainly driven by the release of Ag ions ($Ag^+$; Kennedy et al., 2010; Seitz et al., 2015b), which classifies Ag besides its antimicrobial properties as one of the most toxic metals in natural waters (Ribeiro et al., 2017; Salomoni et al., 2017; Zhai et al., 2018). A study by Croteau et al. (2011) supports this theory, suggesting that for all forms of silver including citrate coated nAg (same type of EINP used in this thesis), a dietary uptake will result in high Ag body levels of freshwater invertebrates. Especially for Ag adsorbed to particulate matter, ingestion appears to be a prominent path of uptake, inducing potential adverse effects more distinct relative to a waterborne Ag exposure (Croteau et al., 2011). The latter seems to be most likely caused by subsequent dissolution of Ag ions after ingestion, leading to high concentrations of biologically active ions in the body of the organisms (Reidy et al., 2013). Thereby, adverse effects may comprise, for instance, oxidative stress, apoptosis or cytotoxic effects on intestinal cells (Fröhlich and Fröhlich, 2016; Völker et al., 2013). This may have favored an energetic reallocation in *Gammarus*, while prioritizing detoxification in order to ensure maintenance (Vellinger et al., 2012). It was suggested by Zubrod et al. (2010) that oxidative stress in *Gammarus* can have an impact on the organisms' energy assimilation, which in turn might alter its feeding behavior. Finally, coping with stress, e.g. induced by an exposure to nAg, may require

more energy, which in turn could translate in an increased feeding rate of *Gammarus* (Andreï et al., 2016; Maltby, 1999).


## 5.4 EINP transport from aquatic to terrestrial systems

The outcome of this study is of environmentally relevance, when considering the delay in emergence of *C. villosa* at ambient UV irradiation and 4 µg $nTiO_2$/L, a concentration that is approx. seven times lower than concentrations that have already been measured in the field (Gondikas et al., 2014; Kiser et al., 2009). More importantly, exposure to nAu revealed an even more distinct emergence delay and reduction of energy reserves than observed for $nTiO_2$. This is of concern, given that effects for nAu were observed at concentrations that are regarded as environmentally safe for aquatic ecosystems, at least in terms of Au ions (Nam et al., 2014). That requires even more attention when looking at potential adverse effects, which shifts in temporal emergence patterns and energy reserves (i.e. nutritional values) of emerging adult aquatic insects, might induce in terrestrial predators such as spiders, birds, bats, and birds (Baxter et al., 2005). As one result, those predators could experience a negatively affected reproductive success (Jackson and Fisher, 1986; Strasevicius et al., 2013). Moreover, migratory bird species may not sufficiently be able to fill their energy reserves before or following a seasonal movement, consequently inducing substantial implications on the life cycle of the birds (Uesugi and Murakami, 2007).

EINPs being transported from the aquatic system to the terrestrial food web, therefore, represents a novel route in the environment, that has been rather disregarded so far.

As already suggested for aquatic invertebrates (Campos et al., 2013; Fouqueray et al., 2012) an EINP uptake into the gut of a terrestrial predator might affect its digestive system (Mahler et al., 2012), and hence the predators' physiological condition. Estimating a daily consumption of approx. 6 g of insects of little brown bats (*Myotis lucifugus*; Kurta et al., 1989), containing as much nAu as the median detected concentrations in the current study, extrapolations suggest a theoretical ingestion that is 1000-times higher than the considered maximum intake for humans of Au from usage in food additives (EFSA ANS Panel, 2016).

# 6. CONCLUSION AND OUTLOOK

The present thesis clearly demonstrates that shifting existing test methods for EINPs to a more field-relevant approach by considering environmental factors such as NOM and UV-radiation, the risk of EINPs for aquatic life is substantially modified. Such modifications lead to effect concentrations (e.g. 0.1 mg $nTiO_2$/L as 96-h $EC_{50}$ in *D. magna* or 4 µg $nTiO_2$/L in *C. villosa*; Appendix A. 2, A. 5) no longer far from currently predicted environmental concentrations (Gondikas et al., 2014). When expecting a continuously growing demand of EINPs in the upcoming years (Farre et al., 2009; Scheringer, 2008), the predicted release into aquatic ecosystems might increase further, along with the risk for inhabiting biota.

This thesis also shows that $nTiO_2$ even at concentrations as low as 50 µg/L, interacting with NOM and UV radiation at field-relevant levels, will modify the ecotoxicological potential of co-occurring stressors, such as pesticides. This modification seems rather controlled by the underlying transformation process, i.e. photo(cata)lysis (Li et al., 2019), than by the pesticides' physico-chemical properties, such as hydrolytic and photolytic $DT_{50}$ or $K_{OC}$ (Appendix A. 3). Whereas in nature the presence of NOM and UV potentially facilitates the detoxification of such micropollutants, their photocatalytic degradation in the presence of $nTiO_2$ partially even increased the pollutants' ecotoxicological potential. This might be attributed to the formation of by-products that are more toxic than the parent compound (Guilhermino et al., 1996; Lewis et al., 2016; Van Scoy et al., 2016).

Following the aquatic life cycle of EINPs, an exposure of benthic organisms will most likely be induced by sedimented EINP agglomerates, either in homo- or hetero-agglomerated form. Thereby, it is crucial to consider EINPs that are settled on or adsorbed to food sources, biofilms, leaf material, or sediment (Selck et al., 2016; Appendix A. 1). The partly opposing effects on *Gammarus* for the two types of EINPs tested in this thesis, indicate that the importance of the exposure pathway seemingly rests upon the physical and chemical properties of the respective EINP (Sukhanova et al., 2018), i.e. chemically stable vs. iron releasing, rather denying the question of a potential transferability of observed effects among different types of EINPs (Appendix A. 4). This calls for a categorization of EINPs divided into their characteristics, such as morphology, shape, reactivity, or solubility (Lamon et al., 2018) for a more accurate risk assessment for aquatic ecosystems. The latter process has partly been covered as stepwise grouping approach supporting the hazard and fate identification of

nanoforms (ECHA, 2017). The insights that have been gathered on the transport of EINPs from aquatic to terrestrial systems raise concern about potential implications for higher trophic levels, especially in riparian areas. More importantly, potential implications can be expected at concentrations that are below the ones that have already been measured and modeled in and for the aquatic environment (Appendix A. 5; Gondikas et al., 2014; Gottschalk et al., 2013). Lastly, the impact of EINP coating, either deliberately as functionalization of EINPs or based on natural processes, for instance through NOM, on the fate and effects of EINPs is underrepresented in literature and requires more attention in the future (Appendix A. 1). As the number of environmental factors in nature is not only limited to NOM and/or UV radiation, a systematic assessment is needed, considering the individual and combined impact of other factors to safeguard a more reliable EINP risk assessment.

## 7. REFERENCES

Adam, V., Loyaux-Lawniczak, S., Labille, J., Galindo, C., del Nero, M., Gangloff, S., Weber, T., Quaranta, G., 2016. Aggregation behavior of $TiO_2$ nanoparticles in natural river water. J. Nanopart. Res. 18, 13. https://doi.org /10.1007/s11051-015-3319-4

Aitken, R.J., Chaudhry, M.Q., Boxall, A.B.A., Hull, M., 2006. Manufacture and use of nanomaterials: current status in the UK and global trends. Occup. Med. 56, 300–306. https://doi.org/10.1093/occmed/kql051

Albrektienė, R., Rimeika, M., Zalieckienė, E., Šaulys, V., Zagorskis, A., 2012. Determination of organic matter by UV absorption in the ground water. J. Environ. Eng. Landsc. 20, 163–167. https://doi.org/10.3846/16486897. 2012.674039

Amiano, I., Olabarrieta, J., Vitorica, J., Zorita, S., 2012. Acute toxicity of nanosized $TiO_2$ to *Daphnia magna* under UVA irradiation. Environ. Toxicol. Chem. 31, 2564–2566. https://doi.org/10.1002/etc.1981

Andreï, J., Pain-Devin, S., Felten, V., Devin, S., Giambérini, L., Mehennaoui, K., Cambier, S., Gutleb, A.C., Guérold, F., 2016. Silver nanoparticles impact the functional role of *Gammarus roeseli* (Crustacea Amphipoda). Environ. Pollut. 208, 608–618. https://doi.org/10.1016/j.envpol.2015.10.036

Barata, C., Varo, I., Navarro, J.C., Arun, S., Porte, C., 2005. Antioxidant enzyme activities and lipid peroxidation in the freshwater cladoceran *Daphnia magna* exposed to redox cycling compounds. Comp. Biochem. Phys. C 140, 175–186. https://doi.org/10.1016/j.cca.2005.01.013

Bar-Ilan, O., Chuang, C.C., Schwahn, D.J., Yang, S., Joshi, S., Pedersen, J.A., Hamers, R.J., Peterson, R.E., Heideman, W., 2013. $TiO_2$ Nanoparticle exposure and illumination during zebrafish development: mortality at parts per billion concentrations. Environ. Sci. Technol. 47, 4726–4733. https://doi.org/10.1021/es304514r

Baun, A., Hartmann, N.B., Grieger, K., Kusk, K.O., 2008. Ecotoxicity of engineered nanoparticles to aquatic invertebrates: a brief review and recommendations for future toxicity testing. Ecotoxicology 17, 387–395. https://doi.org/10.1007/s 10646 -008-0208-y

Baxter, C.V., Fausch, K.D., Saunders, W.C., 2005. Tangled webs: reciprocal flows of invertebrate prey link streams and riparian zones. Freshw. Bio. 50, 201–220. https://doi.org/10.1111/j.1365-2427.2004.01328.x

Bergman Filho, T., Soares, A., Loureiro, S., 2011. Energy budget in *Daphnia magna* exposed to natural stressors. Environ. Sci. Pollut. Res. 18, 655–662. https://doi.org/10.1007/s11356-010-0413-0

Bhatkhande, D.S., Pangarkar, V.G., Beenackers, A., 2002. Photocatalytic degradation for environmental applications - a review. J. Chem. Technol. Biotechnol. 77, 102–116. https://doi.org/10.1002/jctb.532

Borgmann, U., 1996. Systematic analysis of aqueous ion requirements of *Hyalella azteca*: a standard artificial medium including the essential bromide ion. Arch. Environ. Contam. Toxicol. 30, 356–363. https://doi.org/10.1007/BF00212294

Bouchnak, R., Steinberg, C.E.W., 2010. Modulation of longevity in *Daphnia magna* by food quality and simultaneous exposure to dissolved humic substances. Limnologica 40, 86–91. http://dx.doi.org/10.1016/j.limno.2009.11.010

Boudina, A., Emmelin, C., Baaliouamer, A., Païssé, O., Chovelon, J.M., 2007. Photochemical transformation of azoxystrobin in aqueous solutions. Chemosphere 68, 1280–1288. https://doi.org/10.1016/j.chemosphere.2007.01.051

Brame, J., Long, M., Li, Q., Alvarez, P., 2014. Trading oxidation power for efficiency: differential inhibition of photo-generated hydroxyl radicals versus singlet oxygen. Water Res. 60, 259–266. http://dx.doi.org/10.1016/j.watres.2014.05.005

Bundschuh, M., Englert, D., Rosenfeldt, R.R., Bundschuh, R., Feckler, A., Lüderwald, S., Seitz, F., Zubrod, J.P., Schulz, R., 2019. Nanoparticles transported from aquatic to terrestrial ecosystems via emerging aquatic insects compromise subsidy quality. Sci. Rep. 9, 1–8. https://doi.org/10.1038/s41598-019-52096-7

Bundschuh, M., Filser, J., Lüderwald, S., McKee, M.S., Metreveli, G., Schaumann, G.E., Schulz, R., Wagner, S., 2018. Nanoparticles in the environment: where do we come from, where do we go to? Environ. Sci. Eur. 30, 6. https://doi.org/10. 11 86 /s12302-018-0132-6

Bundschuh, M., Vogt, R., Seitz, F., Rosenfeldt, R.R., Schulz, R., 2016. Do titanium dioxide nanoparticles induce food depletion for filter feeding organisms? a case study with *Daphnia magna.* Environ. Pollut. 214, 840–846. https://doi.org/10 .1016 /j.envpol.2016.04.092

Buonocore, G., Perrone, S., Tataranno, M.L., 2010. Oxygen toxicity: chemistry and biology of reactive oxygen species. Semin. Fetal. Neonat. M. 15, 186–190. http://dx.doi.org/10.1016/j.siny.2010.04.003

Cabiscol, E., Tamarit, J., Ros, J., 2000. Oxidative stress in bacteria and protein damage by reactive oxygen species. Int. Microbiol. 3, 3–8. http://hdl.handle.net/ 10459.1/56751

Cambon, C., Declume, C., Derache, R., 1979. Effect of the insecticidal carbamate derivatives (carbofuran, pirimicarb, aldicarb) on the activity of acetylcholinesterase in tissues from pregnant rats and fetuses. Toxicol. Appl. Pharmacol. 49, 203–208. https://doi.org/10.1016/0041-008X(79)90242-4

Campos, B., Rivetti, C., Rosenkranz, P., Navas, J.M., Barata, C., 2013. Effects of nanoparticles of $TiO_2$ on food depletion and life-history responses of *Daphnia magna*. Aquat. Toxicol. 130–131, 174–183. http://dx.doi.org/10.1016/j.aquatox.2013.01.005

Chen, J.Q., Wang, D., Zhu, M.X., Gao, C.J., 2007. Photocatalytic degradation of dimethoate using nanosized $TiO_2$ powder. Desalination 207, 87–94. https://doi.org/10.1016/j.desal.2006.06.012

Collin, B., Oostveen, E., Tsyusko, O.V., Unrine, J.M., 2014. Influence of natural organic matter and surface charge on the toxicity and bioaccumulation of functionalized ceria nanoparticles in *Caenorhabditis elegans*. Environ. Sci. Technol. 48, 1280–1289. https://doi.org/10.1021/es404503c

Croteau, M.-N., Misra, S.K., Luoma, S.N., Valsami-Jones, E., 2011. Silver bioaccumulation dynamics in a freshwater invertebrate after aqueous and dietary exposures to nanosized and ionic Ag. Environ. Sci. Technol. 45, 6600–6607. https://doi.org/10.1021/es200880c

Dabrunz, A., Duester, L., Prasse, C., Seitz, F., Rosenfeldt, R., Schilde, C., Schaumann, G.E., Schulz, R., 2011. Biological surface coating and molting inhibition as mechanisms of $TiO_2$ nanoparticle toxicity in *Daphnia magna*. PLoS ONE 6, e20112. https://doi.org/doi:10.1371/journal.pone.0020112

Domingos, R.F., Tufenkji, N., Wilkinson, K.J., 2009. Aggregation of titanium dioxide nanoparticles: role of a fulvic acid. Environ. Sci. Technol. 43, 1282–1286. https://doi.org/10.1021/es8023594

ECHA, 2017. Appendix R.6-1 for nanomaterials applicable to the guidance on QSARs and grouping of chemicals. [electronic resource]. https://echa.europa.eu/documents/10162/23036412/appendix_r6_nanomat erials_en.pdf.

EFSA ANS Panel, 2016. Scientific Opinion on the re-evaluation of gold (E 175) as a food additive. EFSA J. 14, 4362. https://doi.org/10.2903/j.efsa.2016.4362

Ensley, S., 2007. Chapter 41 - pyrethrins and pyrethroids, in: Gupta, R.C. (ed.), Veterinary Toxicology. Academic Press, Oxford, 494-498. https://doi.org/10.1016/B978-012370467-2/50138-3

EPA, U., 2006. Reregistration eligibility decision (RED) for permethrin [electronic resource]. U.S. Environmental Protection Agency, Prevention, Pesticides and Toxic Substances, Washington, DC. https://nepis.epa.gov/Exe/ZyPURL.cgi?Dockey=P10013E0.txt

Erhayem, M., Sohn, M., 2014. Effect of humic acid source on humic acid adsorption onto titanium dioxide nanoparticles. Sci. Total Environ. 470–471, 92–98. http://dx.doi.org/10.1016/j.scitotenv.2013.09.063

Evgenidou, E., Konstantinou, I., Fytianos, K., Albanis, T., 2006. Study of the removal of dichlorvos and dimethoate in a titanium dioxide mediated photocatalytic process through the examination of intermediates and the reaction mechanism. J. Hazard. Mater. 137, 1056–1064. https://doi.org/10.1016/j.jhazmat.2006.03.042

Evgenidou, E., Konstantinou, I., Fytianos, K., Poulios, I., Albanis, T., 2007. Photocatalytic oxidation of methyl parathion over $TiO_2$ and ZnO suspensions. Catal. Today 124, 156–162. https://doi.org/10.1016/j.cattod.2007.03.033

Fabrega, J., Fawcett, S.R., Renshaw, J.C., Lead, J.R., 2009. Silver nanoparticle impact on bacterial growth: effect of pH, concentration, and organic matter. Environ. Sci. Technol. 43, 7285–7290. https://doi.org/10.1021/es803259g

Fan, W.H., Cui, M.M., Shi, Z.W., Tan, C., Yang, X.P., 2012. Enhanced oxidative stress and physiological damage in *Daphnia magna* by copper in the presence of nano-$TiO_2$. J. Nanomate. 2012, 398720. https://doi.org/10.1155/2012/398720

Farre, M., Gajda-Schrantz, K., Kantiani, L., Barcelo, D., 2009. Ecotoxicity and analysis of nanomaterials in the aquatic environment. Anal. Bioanal. Chem. 393, 81–95. https://doi.org/10.1007/s00216-008-2458-1

Feckler, A., Goedkoop, W., Zubrod, J.P., Schulz, R., Bundschuh, M., 2016. Exposure pathway-dependent effects of the fungicide epoxiconazole on a decomposer-detritivore system. Sci. Total Environ. 571, 992–1000. https://doi.org/10.1016/j.scitotenv.2016.07.088

Feckler, A., Rosenfeldt, R.R., Seitz, F., Schulz, R., Bundschuh, M., 2015. Photocatalytic properties of titanium dioxide nanoparticles affect habitat selection of and food quality for a key species in the leaf litter decomposition process. Environ. Pollut. 196, 276–283. http://dx.doi.org/10.1016/j.envpol.2014.09.022

Forster, S.P., Olveira, S., Seeger, S., 2011. Nanotechnology in the market: promises and realities. Int. J. Nanotechnol. 8, 592–613. https://doi.org/doi:10.1504/IJNT.2011.040193

Fouqueray, M., Dufils, B., Vollat, B., Chaurand, P., Botta, C., Abacci, K., Labille, J., Rose, J., Garric, J., 2012. Effects of aged $TiO_2$ nanomaterial from sunscreen on *Daphnia magna* exposed by dietary route. Environ. Pollut. 163, 55–61. https://doi.org/10.1016/j.envpol.2011.11.035

Fröhlich, E.E., Fröhlich, E., 2016. Cytotoxicity of nanoparticles contained in food on intestinal cells and the gut microbiota. Int. J. Mol. Sci. 17, 509–509. https://doi.org/10.3390/ijms17040509

Garbin, J.R., Milori, D.M.B.P., Simões, M.L., da Silva, W.T.L., Neto, L.M., 2007. Influence of humic substances on the photolysis of aqueous pesticide residues. Chemosphere 66, 1692–1698. https://doi.org/10.1016/j.chemosphere.2006.07.017

Gondikas, A.P., von der Kammer, F., Reed, R.B., Wagner, S., Ranville, J.F., Hofmann, T., 2014. Release of $TiO_2$ nanoparticles from sunscreens into surface waters: a one-year survey at the old Danube recreational lake. Environ. Sci. Technol. 48, 5414–5411. https://doi.org/10.1021/es405596y

Gottschalk, F., Sun, T., Nowack, B., 2013. Environmental concentrations of engineered nanomaterials: review of modeling and analytical studies. Environ. Pollut. 181, 287–300. http://dx.doi.org/10.1016/j.envpol.2013.06.003

Guilhermino, L., Lopes, M.C., Carvalho, A.P., Soared, A.M.V.M., 1996. Inhibition of acetylcholinesterase activity as effect criterion in acute tests with juvenile *Daphnia Magna*. Chemosphere 32, 727–738. https://doi.org/10.1016/0045-6535(95)00360-6

Häder, D.P., Lebert, M., Schuster, M., del Campo, L., Helbling, E.W., McKenzie, R., 2007. ELDONET - a decade of monitoring solar radiation on five continents. Photochem. Photobiol. 83, 1348–1357. https://doi.org/10.1111/j.1751-1097.2007.00168.x

Hall, S., Bradley, T., Moore, J.T., Kuykindall, T., Minella, L., 2009. Acute and chronic toxicity of nano-scale $TiO_2$ particles to freshwater fish, cladocerans, and green algae, and effects of organic and inorganic substrate on $TiO_2$ toxicity. Nanotoxicology 3, 91–97. https://doi.org/10.1080/17435390902788078

Hoffmann, M.R., Martin, S.T., Choi, W., Bahnemann, D.W., 1995. Environmental applications of semiconductor photocatalysis. Chem. Rev. 95, 69–96. https://doi.org/10.1021/cr00033a004

Jackson, J.K., Fisher, S.G., 1986. Secondary production, emergence, and export of aquatic insects of a sonoran desert stream. Ecology 67, 629–638. https://doi.org/10.2307/1937686

Johnston, H.J., Hutchison, G.R., Christensen, F.M., Peters, S., Hankin, S., Stone, V., 2009. Identification of the mechanisms that drive the toxicity of $TiO_{(2)}$ particulates: the contribution of physicochemical characteristics. Part. Fibre Toxicol. 6, 33–33. https://doi.org/10.1186/1743-8977-6-33

Kaegi, R., Sinnet, B., Zuleeg, S., Hagendorfer, H., Mueller, E., Vonbank, R., Boller, M., Burkhardt, M., 2010. Release of silver nanoparticles from outdoor facades. Environ. Pollut. 158, 2900–2905. https://doi.org/10.1016/j.envpol.2010.06.009

Keller, A.A., Lazareva, A., 2014. Predicted releases of engineered nanomaterials: from global to regional to local. Environ. Sci. Tech. Let. 1, 65–70. https://doi.org/10.1021/ez400106t

Kennedy, A.J., Hull, M.S., Bednar, A.J., Goss, J.D., Gunter, J.C., Bouldin, J.L., Vikesland, P.J., Steevens, J.A., 2010. Fractionating nanosilver: importance for determining toxicity to aquatic test organisms. Environ. Sci. Technol. 44, 9571–9577. https://doi.org/10.1021/es1025382

Kim, K.T., Klaine, S.J., Cho, J., Kim, S.H., Kim, S.D., 2010. Oxidative stress responses of *Daphnia magna* exposed to $TiO_2$ nanoparticles according to size fraction. Sci. Total Environ. 408, 2268–2272. https://doi.org/10.1016/j.scitotenv.2010.01.041

Kiser, M.A., Westerhoff, P., Benn, T., Wang, Y., Perez-Rivera, J., Hristovski, K., 2009. Titanium nanomaterial removal and release from wastewater treatment plants. Environ. Sci. Technol. 43, 6757–6763. https://doi.org/10.1021/es901102n

Klaine, S.J., Alvarez, P.J.J., Batley, G.E., Fernandes, T.F., Handy, R.D., Lyon, D.Y., Mahendra, S., McLaughlin, M.J., Lead, J.R., 2008. Nanomaterials in the environment: behavior, fate, bioavailability, and effects. Environ. Toxicol. Chem. 27, 1825–1851.

Klaine, S.J., Koelmans, A.A., Horne, N., Carley, S., Handy, R.D., Kapustka, L., Nowack, B., von der Kammer, F., 2011. Paradigms to assess the environmental impact of manufactured nanomaterials. Environ. Toxicol. Chem. 31, 3–14. https://doi.org/10.1002/etc.733

Konstantinou, I.K., Albanis, T.A., 2003. Photocatalytic transformation of pesticides in aqueous titanium dioxide suspensions using artificial and solar light: intermediates and degradation pathways. Appl. Catal. B-Environ 42, 319–335. https://doi.org/10.1016/S0926-3373(02)00266-7

Kurta, A., Bell, G.P., Nagy, K.A., Kunz, T.H., 1989. Energetics of pregnancy and lactation in freeranging little brown bats (*Myotis lucifugus*). Physiol. Zool. 62, 804–818. https://www.jstor.org/stable/30157928

Lamon, L., Aschberger, K., Asturiol, D., Richarz, A., Worth, A., 2018. Grouping of nanomaterials to read-across hazard endpoints: a review. Nanotoxicology 13:1, 100–118. https://doi.org/10.1080/17435390.2018.1506060

Lewis, K.A., Tzilivakis, J., Warner, D.J., Green, A., 2016. An international database for pesticide risk assessments and management. Hum. Ecol. Risk Assess. 22, 1050–1064. https://doi.org/10.1080/10807039.2015.1133242

Li, W., Zhao, Y., Yan, X., Duan, J., Saint, C.P., Beecham, S., 2019. Transformation pathway and toxicity assessment of malathion in aqueous solution during UV photolysis and photocatalysis. Chemosphere 234, 204–214. https://doi.org/10.1016/j.chemosphere.2019.06.058

Lin, D., Ji, J., Long, Z., Yang, K., Wu, F., 2012. The influence of dissolved and surface-bound humic acid on the toxicity of $TiO_2$ nanoparticles to *Chlorella* sp. Water Res. 46, 4477–4487. http://dx.doi.org/10.1016/j.watres.2012.05.035

Lovern, S.B., Klaper, R., 2006. *Daphnia magna* mortality when exposed to titanium dioxide and fullerene ($C_{60}$) nanoparticles. Environ. Toxicol. Chem. 25, 1132–1137. 10.1897/05-278r.1

Low, G.K.C., McEvoy, S.R., Matthews, R.W., 1991. Formation of nitrate and ammonium ions in titanium dioxide mediated photocatalytic degradation of organic compounds containing nitrogen atoms. Environ. Sci. Technol. 25, 460–467. https://doi.org/10.1021/es00015a013

Lüderwald, S., Schell, T., Newton, K., Salau, R., Seitz, F., Rosenfeldt, R.R., Dackermann, V., Metreveli, G., Schulz, R., Bundschuh, M., 2019. Exposure pathway dependent effects of titanium dioxide and silver nanoparticles on the benthic amphipod *Gammarus fossarum*. Aquat. Toxicol. 212, 47–53. https://doi.org/10.1016/j.aquatox.2019.04.016

Ma, H., Brennan, A., Diamond, S.A., 2012. Photocatalytic reactive oxygen species production and phototoxicity of titanium dioxide nanoparticles are dependent on the solar ultraviolet radiation spectrum. Environ. Toxicol. Chem. 31, 2099–2107. https://doi.org/10.1002/etc.1916

Mahler, G.J., Esch, M.B., Tako, E., Southard, T.L., Archer, S.D., Glahn, R.P., Shuler, M.L., 2012. Oral exposure to polystyrene nanoparticles affects iron absorption. Nat. Nanotech. 7, 264–271. https://doi.org/10.1038/nnano.2012.3

Maltby, L., 1999. Studying stress: the importance of organism-level responses. Ecol. Appl. 9, 431–440. https://doi.org/10.1890/1051-0761(1999)009[0431:SSTIOO]2.0.CO;2

Maltby, L., Clayton, S.A., Wood, R.M., McLoughlin, N., 2002. Evaluation of the *Gammarus pulex* in situ feeding assay as a biomonitor of water quality: robustness, responsiveness, and relevance. Environ. Toxicol. Chem. 21, 361–368. https://doi.org/10.1002/etc.5620210219

Mansfield, C.M., Alloy, M.M., Hamilton, J., Verbeck, G.F., Newton, K., Klaine, S.J., Roberts, A.P., 2015. Photo-induced toxicity of titanium dioxide nanoparticles to *Daphnia magna* under natural sunlight. Chemosphere 120, 206–210. http://dx.doi.org/10.1016/j.chemosphere.2014.06.075

Marcone, G.P.S., Oliveira, A.C., Almeida, G., Umbuzeiro, G.A., Jardim, W.F., 2012. Ecotoxicity of $TiO_2$ to *Daphnia similis* under irradiation. J. Hazard. Mater. 211, 436–442. https://doi.org/10.1016/j.jhazmat.2011.12.075

Nam, S.-H., Lee, W.-M., Shin, Y.-J., Yoon, S.-J., Kim, S.W., Kwak, J.I., An, Y.-J., 2014. Derivation of guideline values for gold (III) ion toxicity limits to protect aquatic ecosystems. Water Res. 48, 126–136. https://doi.org/10.1016/j.watres.2013.09.019

Nowack, B., Bucheli, T.D., 2007. Occurrence, behavior and effects of nanoparticles in the environment. Environ. Pollut. 150, 5–22. https://doi.org/10.1016/j.envpol.2007.06.006

OECD, 2004. Test no. 202: *Daphnia* sp. acute immobilization test. OECD Guideline for Testing of Chemicals. OECD Publishing, Paris, 1–12. https://doi.org/10.1787/9789264069947-en

Pelizzetti, E., Minero, C., 1999. Role of oxidative and reductive pathways in the photocatalytic degradation of organic compounds. Colloids Surf., A 151, 321–327. https://doi.org/10.1016/S0927-7757(98)00580-9

Petosa, A.R., Jaisi, D.P., Quevedo, I.R., Elimelech, M., Tufenkji, N., 2010. Aggregation and deposition of engineered nanomaterials in aquatic environments: role of physicochemical interactions. Environ. Sci. Technol. 44, 6532–6549. https://doi.org/10.1021/es100598h

Piccinno, F., Gottschalk, F., Seeger, S., Nowack, B., 2012. Industrial production quantities and uses of ten engineered nanomaterials in Europe and the world. J. Nanopart. Res. 14, 1–11. https://doi.org/10.1007/s11051-012-1109-9

Rajala, J.E., Vehniäinen, E.-R., Väisänen, A., Kukkonen, J.V.K., 2018. Toxicity of silver nanoparticles to *Lumbriculus variegatus* is a function of dissolved silver and promoted by low sediment pH. Environ. Toxicol. Chem. 37, 1889–1897. https://doi.org/doi:10.1002/etc.4136

Rao, N.V., Rajasekhar, M., Vijayalakshmi, K., Vamshykrishna, M., 2015. The future of civil engineering with the influence and impact of nanotechnology on properties of materials. Proc. Mat. Sci. 10, 111–115. http://dx.doi.org/10.1016/j.mspro.2015.06.032

Reidy, B., Haase, A., Luch, A., Dawson, K.A., Lynch, I., 2013. Mechanisms of silver nanoparticle release, transformation and toxicity: a critical review of current knowledge and recommendations for future studies and applications. Materials 6, 2295–2350. https://doi.org/10.3390/ma6062295

Ribeiro, F., Van Gestel, C.A.M., Pavlaki, M.D., Azevedo, S., Soares, A.M.V.M., Loureiro, S., 2017. Bioaccumulation of silver in *Daphnia magna*: waterborne and dietary exposure to nanoparticles and dissolved silver. Sci. Total Environ. 574, 1633–1639. https://doi.org/10.1016/j.scitotenv.2016.08.204

Robert, D., Malato, S., 2002. Solar photocatalysis: a clean process for water detoxification. Sci. Total Environ. 291, 85–97. https://doi.org/10.1016/S0048-9697(01)01094-4

Romero, E., Schmitt, P., Mansour, M., 1994. Photolysis of pirimicarb in water under natural and simulated sunlight conditions. Pestic. Sci. 41, 21–26. https://doi.org/10.1002/ps.2780410105

Rosenfeldt, R.R., Seitz, F., Schulz, R., Bundschuh, M., 2014. Heavy metal uptake and toxicity in the presence of titanium dioxide nanoparticles: a factorial approach using *Daphnia magna*. Environ. Sci. Technol. 48, 6965–6972. https://doi.org /10.1021/es405396a

Rosenfeldt, R.R., Seitz, F., Zubrod, J.P., Feckler, A., Merkel, T., Lüderwald, S., Bundschuh, R., Schulz, R., Bundschuh, M., 2015. Does the presence of titanium dioxide nanoparticles reduce copper toxicity? a factorial approach with the benthic amphipod *Gammarus fossarum*. Aquat. Toxicol. 165, 154–159. http://dx.doi.org/10.1016/j.aquatox.2015.05.011

Rosenkranz, P., Chaudhry, Q., Stone, V., Fernandes, T.F., 2009. A comparison of nanoparticle and fine particle uptake by *Daphnia magna*. Environ. Toxicol. Chem. 28, 2142–2149. https://doi.org/10.1897/08-559.1.

Ryan, A.C., Tomasso, J.R., Klaine, S.J., 2009. Influence of pH, hardness, dissolved organic carbon concentration, and dissolved organic matter source on the acute toxicity of copper to *Daphnia magna* in soft waters: implications for the biotic ligand model. Environ. Toxicol. Chem. 28, 1663–1670. https://doi.org/10.1897/08-361.1

Salomoni, R., Léo, P., Montemor, A.F., Rinaldi, B.G., Rodrigues, M., 2017. Antibacterial effect of silver nanoparticles in *Pseudomonas aeruginosa*. Nanotechnol. Sci. Appl. 10, 115–121. https://doi.org/10.2147/NSA.S133415

Schaller, J., Brackhage, C., Mkandawire, M., Dudel, E.G., 2011. Metal/metalloid accumulation/remobilization during aquatic litter decomposition in freshwater: a review. Sci. Total Environ. 409, 4891–4898. https://doi.org/10.1016/j.scitotenv.2011.08.006

Scheringer, M., 2008. Nanoecotoxicology: environmental risks of nanomaterials. Nature Nanotech. 3, 322–323. https://doi.org/10.1038/nnano.2008.145

Schwack, W., Kopf, G., 1993. Photodegradation of the carbamate insecticide pirimicarb. Z. Lebensm Unters Forch 197, 264–268. https://doi.org/10.1007/BF01185283

Seitz, F., Bundschuh, M., Dabrunz, A., Bandow, N., Schaumann, G.E., Schulz, R., 2012. Titanium dioxide nanoparticles detoxify pirimicarb under UV irradiation at ambient intensities. Environ. Toxicol. Chem. 31, 518–523. https://doi.org/10.1002/etc.1715

Seitz, F., Bundschuh, M., Rosenfeldt, R.R., Schulz, R., 2013. Nanoparticle toxicity in *Daphnia magna* reproduction studies: the importance of test design. Aquat. Toxicol. 126, 163–168. https://doi.org/10.1016/j.aquatox.2012.10.015

Seitz, F., Lüderwald, S., Rosenfeldt, R.R., Schulz, R., Bundschuh, M., 2015a. Aging of TiO$_2$ nanoparticles transiently increases their toxicity to the pelagic microcrustacean *Daphnia magna*. PLoS ONE 10, e0126021. https://doi.org/10.1371/journal.pone.0126021

Seitz, F., Rosenfeldt, R.R., Müller, M., Lüderwald, S., Schulz, R., Bundschuh, M., 2016. Quantity and quality of natural organic matter influence the ecotoxicity of titanium dioxide nanoparticles. Nanotoxicology 10, 415–1421. https://doi.org/10.1080/17435390.2016.1222458

Seitz, F., Rosenfeldt, R.R., Storm, K., Metreveli, G., Schaumann, G.E., Schulz, R., Bundschuh, M., 2015b. Effects of silver nanoparticle properties, media pH and dissolved organic matter on toxicity to *Daphnia magna*. Ecotoxicol. Environ. Saf. 111, 263–270. http://dx.doi.org/10.1016/j.ecoenv.2014.09.031

Selck, H., Handy, R.D., Fernandes, T.F., Klaine, S.J., Petersen, E.J., 2016. Nanomaterials in the aquatic environment: a European Union–United States perspective on the status of ecotoxicity testing, research priorities, and challenges ahead. Environ. Toxicol. Chem. 35, 1055–1067. https://doi.org/10.1002/etc.3385

Sillanpää, M., Paunu, T.-M., Sainio, P., 2011. Aggregation and deposition of engineered TiO$_2$ nanoparticles in natural fresh and brackish waters. J. Phys. Conf. 304, 012018. https://doi.org/10.1088/1742-6596/304/1/012018

Strasevicius, D., Jonsson, M., Nyholm, N.E.I., Malmqvist, B., 2013. Reduced breeding success of pied flycatchers *Ficedula hypoleuca* along regulated rivers. Ibis 155, 348–356. https://doi.org/10.1111/ibi.12024

Sukhanova, A., Bozrova, S., Sokolov, P., Berestovoy, M., Karaulov, A., Nabiev, I., 2018. Dependence of nanoparticle toxicity on their physical and chemical properties. Nanoscale Res. Lett. 13, 44. https://doi.org/10.1186/s11671-018-2457-x

Sun, T. Y., Bornhoft, N.A., Hungerbuhler, K., Nowack, B., 2016 Dynamic probabilistic modeling of environmental emissions of engineered nanomaterials. Environ. Sci. Technol. 50, 4701–4711. https://doi.org/10.1021/acs.est.5b05828

Sun, T.Y., Gottschalk, F., Hungerbühler, K., Nowack, B., 2014. Comprehensive probabilistic modelling of environmental emissions of engineered nanomaterials. Environ. Pollut. 185, 69–76. http://dx.doi.org/10.1016/j .envpol.2013.10.004

Turchi, C.S., Ollis, D.F., 1989. Mixed reactant photocatalysis: Intermediates and mutual rate inhibition. J. Catal. 119, 483–496. https://doi.org/10.1016/0021-9517(89)90176-0

Uesugi, A., Murakami, M., 2007. Do seasonally fluctuating aquatic subsidies influence the distribution pattern of birds between riparian and upland forests? Ecol. Res. 22, 274–281. https://doi.org/10.1007/s11284-006-0028-6

Ulm, L., Krivohlavek, A., Jurašin, D., Ljubojević, M., Šinko, G., Crnković, T., Žuntar, I., Šikić, S., Vinković Vrček, I., 2015. Response of biochemical biomarkers in the aquatic crustacean *Daphnia magna* exposed to silver nanoparticles. Environ. Sci. Pollut. Res. 22, 19990–19999. https://doi.org/10.1007/s11356-015-5201-4

Van Scoy, A., Pennell, A., Zhang, X., 2016. Environmental fate and toxicology of dimethoate, in: de Voogt, W.P. (Ed.), Reviews of environmental contamination and toxicology 237, 53–70. Springer International Publishing. https://doi.org/10.1007/978-3-319-23573-8

Vellinger, C., Felten, V., Sornom, P., Rousselle, P., Beisel, J.-N., Usseglio-Polatera, P., 2012. Behavioural and physiological responses of *Gammarus pulex* exposed to cadmium and arsenate at three temperatures: individual and combined effects. PLoS ONE 7, e39153. https://doi.org/10.1371/journal .pone.0039153

Velzeboer, I., Quik, J.T.K., van de Meent, D., Koelmans, A.A., 2014. Rapid settling of nanoparticles due to heteroaggregation with suspended sediment. Environ. Toxicol. Chem. 33, 1766–1773. https://doi.org/doi:10.1002/etc.2611

Völker, C., Oetken, M., Oehlmann, J., 2013. The biological effects and possible modes of action of nanosilver, in: Whitacre, D.M. (Ed.), Reviews of Environmental Contamination and Toxicology 223, 81–106. Springer, New York. https://doi.org /10 .1007/978-1-4614-5577-6_4

von der Kammer, F., Ottofuelling, S., Hofmann, T., 2010. Assessment of the physico-chemical behavior of titanium dioxide nanoparticles in aquatic environments using multi-dimensional parameter testing. Environ. Pollut. 158, 3472–3481. https://doi.org/10.1016/j.envpol.2010.05.007

Wang, Z., Zhang, L., Zhao, J., Xing, B., 2016. Environmental processes and toxicity of metallic nanoparticles in aquatic systems as affected by natural organic matter. Environ. Sci.: Nano 3, 240–255. https://doi.org/10.1039/C5EN00230C

Westerhoff, P., Song, G., Hristovski, K., Kiser, M.A., 2011. Occurrence and removal of titanium at full scale wastewater treatment plants: implications for $TiO_2$ nanomaterials. J. Environ. Monit. 13, 1195–203. https://doi .org/10.1039/c1em10017c

Wormington, A.M., Coral, J., Alloy, M.M., Delmarè, C.L., Mansfield, C.M., Klaine, S.J., Bisesi, J.H., Roberts, A.P., 2017. Effect of natural organic matter on the photo-induced toxicity of titanium dioxide nanoparticles. Environ. Toxicol. Chem. 36, 1661–1666. https://doi.org/doi:10.1002/etc.3702

Wu, C., Linden, K.G., 2008. Degradation and byproduct formation of parathion in aqueous solutions by UV and $UV/H_2O_2$ treatment. Water Res. 42, 4780–4790. https://doi.org/10.1016/j.watres.2008.08.023

Xuereb, B., Lefevre, E., Garric, J., Geffard, O., 2009. Acetylcholinesterase activity in *Gammarus fossarum* (Crustacea Amphipoda): linking AChE inhibition and behavioural alteration. Aquat. Toxicol. 94, 114–122. https://doi.org/10.1016/j.aquatox.2009.06.010

Yang, W., Gan, J., Hunter, W., Spurlock, F., 2006. Effect of suspended solids on bioavailability of pyrethroid insecticides. Environ. Toxicol. Chem. 25, 1585–1591. https://doi.org/10.1897/05-448R.1

Zhai, Y., Brun, N.R., Bundschuh, M., Schrama, M., Hin, E., Vijver, M.G., Hunting, E.R., 2018. Microbially-mediated indirect effects of silver nanoparticles on aquatic invertebrates. Aquatic Sciences 80:44. https://doi.org/10.1007/s00027-018-0594-z

Zhang, W., Xiao, B., Fang, T., 2018. Chemical transformation of silver nanoparticles in aquatic environments: mechanism, morphology and toxicity. Chemosphere 191, 324–334. https://doi.org/10.1016/j.chemosphere.2017.10.016

Zoh, K.D., Kim, T.S., Kim, J.G., Choi, K., Yi, S.M., 2006. Parathion degradation and toxicity reduction in solar photocatalysis and photolysis. Water Sci. Technol. 53, 1–8. https://doi.org/10.2166/wst.2006.069

Zubrod, J.P., Bundschuh, M., Schulz, R., 2010. Effects of subchronic fungicide exposure on the energy processing of *Gammarus fossarum* (Crustacea; Amphipoda). Ecotoxicol. Environ. Saf. 73, 1674-1680. https://doi.org/10.1016/j.ecoenv.2010.07.046

## APPENDIX

**Appendix A. 1:** Bundschuh, M., Filser, J., **Lüderwald, S.**, McKee, M., Metreveli, G., Schaumann, G.E., Schulz, R., Wagner, S. (2018) Nanoparticles in the environment – where do we come from, where do we go to? Environ. Sci. Eur. 30. https://doi.org/10. 1186/ s12302-018-0132-6.

**Appendix A. 2: Lüderwald, S.**, Dackermann, V., Seitz, F., Adams, E., Feckler, A., Schilde, C., Schulz, R., Bundschuh, M. (2019). A blessing in disguise? Natural organic matter reduces the UV light-induced toxicity of nanoparticulate titanium dioxide. Sci. Total Environ. 663:518-526. https://doi.org/10.1016/j.scitotenv.2019.01.282.

**Appendix A. 3: Lüderwald, S.**, Meyer, F., Gerstle, V., Friedrichs, L., Rolfing, K., Bakanov, N., Schulz, R., Bundschuh, M. (submitted, revisions received). Reduction of pesticide toxicity under field relevant conditions? The interaction of titanium dioxide nanoparticles, UV, and NOM.

**Appendix A. 4: Lüderwald, S.**, Schell, T., Newton, K., Salau, R., Seitz, F., Rosenfeldt, R., Dackermann, V., Metreveli, G., Schulz, R., Bundschuh, M. (2019). Exposure pathway dependent effects of titanium dioxide and silver nanoparticles on the benthic amphipod *Gammarus fossarum*. Aquat. Toxicol. 212. https://doi.org/10.1016/j. aquatox.2019.04.016.

**Appendix A. 5:** Bundschuh, M., Englert, D., Rosenfeldt, R.R., Bundschuh, R., Feckler, A., Lüderwald, S., Seitz, F., Zubrod, J.P., Schulz, R. (2019). Nanoparticles transported from aquatic to terrestrial ecosystems via emerging aquatic insects compromise subsidy quality. Sci. Rep. 9. https://doi.org/10.1038/s41598-019-52096-7.

**Appendix A. 6:** Curriculum vitae,

**Appendix A. 1**

**Nanoparticles in the environment – where do we come from, where do we go to?**

Bundschuh, M., Filser, J., Lüderwald, S.,  McKee, M., Metreveli, G., Schaumann, G. E., Schulz, R., Wagner, S.

Environmental Sciences Europe

February 2018, Volume 30, Article 6

**ABSTRACT**

Nanoparticles serve various industrial and domestic purposes which is reflected in their steadily increasing production volume. This economic success comes along with their presence in the environment and the risk of potentially adverse effects in natural systems. Over the last decade, substantial progress regarding the understanding of sources, fate and effects of nanoparticles have been made. Predictions of environmental concentrations based on modelling approaches could recently be confirmed by measured concentrations in the field. Nonetheless, analytical techniques are, as covered elsewhere, still under development to more efficiently and reliably characterize and quantify nanoparticles, as well as to detect them in complex environmental matrixes. Simultaneously, the effects of nanoparticles on aquatic and terrestrial systems have received increasing attention. While the debate on the relevance of nanoparticle-released metal ions for their toxicity is still ongoing, it is a re-occurring phenomenon that inert nanoparticles are able to interact with biota through physical pathways such as biological surface coating. This amongst others interferes with the growth and behavior of exposed organisms. Moreover, co-occurring contaminants interact with nanoparticles. There is multiple evidence suggesting nanoparticles as a sink for organic and inorganic co-contaminants. On the other hand, in the presence of nanoparticles repeatedly an elevated effect on the test species induced by the co-contaminants has been reported. In this paper, we highlight recent achievements in the field of nano-ecotoxicology in both aquatic and terrestrial systems but also refer to substantial gaps that require further attention in the future.

**KEYWORDS**

Nanomaterials, Co-contaminants, Environmental parameters, Review, Fate

## INTRODUCTION

Nano-based technology has made enormous progress over the last decades, which is underpinned by a 25-fold increase between 2005 to 2010 in the numbers of products that either contain or require nanoparticles (NP) for their production [1]. This development is likely facilitated by their unique general properties (in particular particle size, surface area, surface reactivity, charge, and shape) relative to their bulk or dissolved counterparts. This enables a broad range of possible applications, including cosmetic, pharmaceutical, and medical utilization [2,3]. Engineered NP consist of carbon-based and inorganic forms, partly with functionalized surfaces [4].

Along with their unique general properties, the high diversity of NPs' elemental and structural composition have, however, challenged environmental scientists in multiple ways, ranging from NP characterisation and fate in complex matrixes [e.g., 5] to individual and combined NP effects in aquatic and terrestrial (eco)systems [e.g., 6]. The crystalline composition of titanium dioxide NP ($TiO_2$ NP), for instance, influences their toxicity for the water flea *Daphnia magna* when based on the mass concentration – a pattern independent of the initial particle size [7]. Such observations suggest that other or additional dose measures, such as particle number, surface area, or body burden, are needed to adequately reflect the exposure situation [8]. In fact, NPs' surface area explained a large share of variability in the resulting toxicity among crystalline structures [7].

In this paper, we give a brief overview of recent scientific advances enhancing the understanding of the (i) sources and (ii) fate of NP, (iii) the effects of NP in simplified studies, and (iv) how NP interact with biota in a more complex environment. We consider both aquatic and terrestrial systems but mainly focus on metal based NPs as carbon based NPs are covered elsewhere [9,10] . We will, however, not specifically cover the methodological developments in the context of NP quantification and properties as this has been covered elsewhere [see for instance, 11,12,13]. On this basis, we develop recommendations for future research directions in nano-ecotoxicology.

## Pathways of Nanoparticles into Natural Ecosystems

It has been anticipated that the increasing application of NP both quantitatively but also in terms of product diversity will lead to a diversification in emission sources into the environment [4]. Key products containing NP are amongst other coatings, paints and pigments, catalytic additives, and cosmetics [14]. This chapter will discuss NP emissions from such products whereas the release process is beyond our scope.

NP can enter the environment a long their life cycle and three emission scenarios are generally considered: (i) Release during production of raw material and nano-enabled products; (ii) Release during use; and (iii) Release after disposal of NP-containing products (waste handling) [15-17]. NP emissions can be either directly to the environment or indirectly via a technical system such as wastewater treatment plants (WWTPs) or landfills. Indirect emissions are likely occurring either via the effluent of WWTPs, application of biosolids to soil, or leachates from landfills. It has also been pointed out that NP fate in technical systems such as WWTPs determines whether bare, coated, chemically or physically transformed particles are released, and via which pathway (as effluent or biosolid) [18-21].

So far emission and environmental concentration levels have been estimated using material flow models following the NP life cycle [22]. Calculation models assume that produced NP will be released either to waste streams or directly to environmental compartments, and more realistic approaches account for the delayed release during use due to in-use NP stocks. NP emissions are also controlled by (i) aging or weathering [23,24,19,25,26], (ii) the fate of the NP during use [20,27,28] and (iii) the waste management system [29,30]. Production volumes, however, may give a good indication of the emission of specific NPs. Available data on production volumes differs greatly depending on the way of data collection. $TiO_2$ NP and $SiO_2$ NP are certainly the most relevant materials in terms of worldwide productions volumes (> 10,000 t/a in 2010), followed by $CeO_2$ NP, $FeO_x$ NP, $AlO_x$ NP, and ZnO NP, and carbon nanotubes (CNT) (100 to 1,000 t/a in 2010). The production volume of Ag NP was estimated with approximately 55 t/a worldwide in 2010 [31].

First attempts to estimate NP emissions during the life-cycle indicated that most NPs are emitted during use phase and after disposal e.g. on landfills [30], while during production not more than 2% of the production volume is released [32]. Depending on the type and application of NPs they are either directly released into the environment, or indirectly via technical compartments and waste streams or enter in-use stock

causing a delayed release [22],[30,33-35]. The release pattern and masses depend on the NP type and its application. For instance Sun et al. [22] studied emission patterns in the EU in 2014 of $TiO_2$ NP, ZnO NP, Ag NP and CNTs considering landfills, sediments, and soil as sink for NP. They found that $TiO_2$ NPs accumulate in sludge treated soils followed by sediments and landfills (approx. 8,400 and 7,600 and 7,000 tons). The dominating emission pathway of $TiO_2$ NP occurs via wastewater (85% of total $TiO_2$ NP emissions) [47, [30]]. For example, $TiO_2$ NPs are accumulated in sewage sludge during wastewater treatment, which is in many countries ultimately deployed onto soils. It was estimated that approximately 36% of $TiO_2$ NP emissions occur via this pathway. A lower portion of the sewage sludge is deposited onto landfills directly or after incineration which equals approximately 30% of total emitted $TiO_2$ NP. $TiO_2$ NP emissions via wastewater effluent account for approximately 33% [22]. ZnO NP, which are mostly used in cosmetics, electronics and medicine accumulate in sediments (1,300 tons), in natural and urban soil (300 tons) as well as in landfills (200 tons). The dominating emission pathway occurs, just as for $TiO_2$ NP, via wastewater since both are used in cosmetics [47]. CNTs and Ag NPs show different emission pattern. CNTs are predominantly emitted via production and use directly to landfills. Hence, approximately 90% of the CNT production is accumulated in landfills, approximately 10% in soils and < 1% in sediments and air [22]. Due to their usage, Ag NPs are emitted from production and use to both landfills and wastewater.

Global estimation of NP emissions indicate that landfills (approximately 63–91 %) and soils (approximately 8-28%) receive the largest share followed by emissions into the aquatic environment and air (7% and 1.5%, respectively of the production volumes) [30]. Such estimations allow to identify applications with potentially high environmental implication. A potential increase in outdoor applications of NP may elevate their mass flows directly into the environment [36]. For example, NP emission from façade paints, such as photocatalytic active compounds, e.g. $TiO_2$ NP, has been demonstrated previously [37,19,38].

Besides emission of engineered NPs there are particulate emissions of anthropogenic NPs which are not intentionally produced as NP. For instance, particulate emissions from traffic, such as palladium, were identified to be in nanoscale [39,40]. NP release might also be intended due to their direct application in environmental compartments, for instance, for groundwater remediation such as iron-based NP [41-43] or when applying nano-pesticides directly to agricultural fields [44,45]. Although some

information on NP emission is available, it is of high importance to quantify their amounts and concentrations in the environment. Quantification of NP emissions into the aquatic environment has by now, however, been hampered by the lack of appropriate analytical techniques [5].

**Predicting and Measuring Nanoparticles in Natural Ecosystems**

Computational modelling was suggested as a way forward estimating environmental concentrations because straight forward analytical methods were not available for detection of NPs in the environment [46,47]. Material flow models rely on life cycle information and production volumes, which were not necessarily available in sufficient detail, limiting their accuracy [48]. Very recently, more advanced models use probabilistic approaches [49] that consider dynamic input rates, in-use stocks as well as the continuous rise in production volumes [22]. These models allow predicting the time dependent material flow of specific NP (e.g. $TiO_2$ NP) in technical systems and environmental compartments. These models estimate NP concentrations in surface waters to be in the lower ng/L or µg/L range depending on the type of NP. For instance, mean NP concentrations in surface water were estimated for $TiO_2$ with approximately 2.2 µg/L ($Q_{0.15}$ 0.19 µg/L to $Q_{0.85}$ 4.4 µg/L) and for Ag NP with 1.5 ng/L ($Q_{0.15}$ 0.4 µg/L to $Q_{0.85}$ 2.8 ng/L) for the EU in 2014 [22]. Although these models hardly consider NP specific fate mechanisms [e.g., sedimentation 50], first studies assessing the actual presence of NP in the aquatic environment [36,51,35,52] are in consensus with modelling results [16]. For instance, analytical studies revealed $TiO_2$ NP surface water concentrations between 3 ng/L and 1.6 µg/L, confirming the high variation of modelling results in a comparable concentration range. However, analytical limitations, namely the lack of specific and sensitive analytical methods in complex matrixes, did not yet allow to formally assess for the assumption that the increasing production and market volume of NP will ultimately lead to an increase in environmental concentrations. Complementary analytical techniques have been used to determine and characterize metal-based NPs in different environmental compartment [53,51]. Concentration and size of metal based NPs such Au, Ag, Cu, $TiO_2$, in surface water and soils have been, for example, determined by single particle inductively coupled plasma mass spectrometry (sp-ICP-MS) [53,54] or fractionation techniques in combination with light scattering and elemental detection [55]. Structural information and information on particle size have been derived from electron microscopy as a complementary

technique [51]. Among others the NP surface chemistry including surface charge or functionalization controls NP fate. Therefore, surface characterization methods are important to understand NP fate processes [56].

For complex types of NPs such as core shell structures a multi-element technique e.g. sp-ICP-Time of Flight (ToF)-MS was developed [57] and has recently been successfully applied to determine engineered $CeO_2$ NP in soil [58]. This technique is of high importance to differentiate between engineered NPs and natural NPs by detecting impurities in natural NPs which are not present in engineered NPs. Such analyses will help to validate model outputs on environmental NPs concentrations.

In comparison to the analysis of inorganic NPs in environmental compartments, organic NP analysis it is still in its infancy. In fact, analytical techniques for organic NPs have been developed for example for fullerenes and CNTs [59,52] but they are hampered by insufficient selectivity with regards to the high environmental background concentrations of carbon. To improve the analysis of organic NP in complex media such surface water or soil, more efficient extraction methods are needed [60].

Recently, considerable progress has been made overcoming some of the analytical problems (natural particle counterparts, low concentrations, matrix interferences) [61,62,58], opening new possibilities that foster our understanding on both sources and fate of NPs in the environment. However, future work should focus on the differentiation between engineered and natural NP, the detection of organic NP and the characterization of the NP surfaces.

## Fate of Nanoparticles in the Environment

NP in the environment undergo aging processes such as chemical transformation, aggregation, disaggregation. The interplay between these processes and the NP transport determine the fate and ultimately the ecotoxicological potential of NP [63-65]. Since particle properties and environmental conditions control these aging and transport processes [65,45,66], a direct transfer of data to even slightly deviating conditions is difficult and can even be misleading. Here we analyse the current state of the art regarding NP fate and conclude if this knowledge is sufficient to allow for extrapolations from well-defined and controlled laboratory conditions to complex, real world scenarios.

Alterations in chemical speciation, dissolution, degradation as well as alteration of the surface properties by precipitation and ad- or desorption are important chemical transformation processes of NP, which have frequently been investigated both in aquatic and soil ecosystems (Fig. 1). A general remark in this context: functionalization of NP surfaces, which makes the particles' properties more beneficial for industrial purposes [67,68], will strongly control transformation processes in the environment [66,69,70]. A thorough characterization of NP surface chemistry [i.e. the formation or loss of coating 71] over time seems therefore mandatory to understand NP fate [72,73], but is still highly challenging. The present paper, however, specifically focuses on dissolution, passivation, aggregation, adsorption, sedimentation, and deposition as a selection of the most relevant processes under field conditions (see Fig. 2).

*Chemical Transformation*

Dissolution of NP (Fig. 2a) is driven directly by the particle chemistry. Dissolution of Ag NP, for instance, requires aerobic conditions. In such environments, an oxide layer ($Ag_2O$) can be formed around the particle, which releases $Ag^+$ [74]. In a range of studies, it was uncovered that Ag NP dissolution rates are triggered by particle-inherent factors including surface coating, size, shape and state of aggregation, as well as environmental parameters such as pH, dissolved organic carbon, and temperature [see for a more detailed assessment of the mechanisms 11,75-80]. Koser et al. [81] used equilibrium speciation calculations, based on a broad basis of literature data, to successfully predict Ag dissolution in several artificial media. This suggests that the scientific community was indeed capable of advancing the knowledge to a state that allows for reasonably accurate predictions and modelling.

A passivation process frequently occurring under various environmental conditions is the sulfidation of NP (Fig. 2b) that include Ag NP, ZnO NP and CuO NP [e.g. 82,79,83]. Sulfidation of Ag NP, for instance, can lead to the formation of core-shell $Ag^0$-$Ag_2S$ structures or hollow $Ag_2S$ NP [84]. The mechanisms of sulfidation are given elsewhere [66,84-86]. Sulfidation leads to nearly inert NP surfaces with consequence for their reactivity [Fig. 2, 84,87,] and thus toxicity [66], while sulfidised NP can still be toxic to microorganisms [88].

### *Colloidal Stability*

Colloidal stability of NP is one of the key factors controlling their fate and effects [89,12]. When released into the environment, NP interact with the variety of dissolved or particulate, inorganic or organic compounds influencing NP aggregation dynamics and thus colloidal stability [90]. Ultimately, exposure conditions are controlled by NP aggregation. By focusing on factors controlling homo-aggregation (interaction between the same NP) and hetero-aggregation (interaction between different NP or between NP and natural colloids [such as montmorillonite, maghemite, kaolinite but also microorganisms, algae, and proteins 91,92], as well as disaggregation, we also discuss the processes determining NP fate.

Homo-aggregation of NP (Fig. 2c) is positively correlated with their concentration in the media. Since predicted environmental concentrations are rather low (in the pg/L to the low µg/L range for surface waters [16]), homo-aggregation is less likely due to the low probability for collisions. Nonetheless, this factor is relevant – but largely ignored – for laboratory based ecotoxicological investigations that often use high NP concentrations compared to predicted environmental concentrations [76]. Under field conditions, the ionic strength of the surrounding medium seems more relevant as aggregation rates increase with ionic strength [e.g. 93,94]. The aggregation dynamics are in most cases characterized by classical Derjaguin-Landau-Verwey-Overbeek (DLVO) theory [95,96]. Furthermore, multivalent cations are more efficient than monovalent cations [97], whereas the efficiency within both groups of cations depends on their respective identity as judged by critical coagulation concentrations (CCCs): the aggregation of citrate-coated Ag NP was, for instance, more efficient for $Ca^{2+}$ than $Mg^{2+}$ [76], which may be explained by the higher ability of $Ca^{2+}$ to form citrate complexes [98]. At the same time, the impact of cations and anions can be concentration dependent. Whereas high concentrations of $Cl^-$ ions enhance the aggregation of Ag NP due to the bridging by AgCl [99], low concentrations may stabilise NP via the formation of negatively charged surface precipitates [76]. Similarly, soils and soil extracts modulate NP aggregation [100].

In addition to ionic strength, homo-aggregation is also influenced by a range of environmental variables. The surface charge of NP changes with pH, which is reflected by the isoelectric point (IEP; i.e. the pH at which NP do not carry a net charge). The IEP varies substantially among commercially available NP [101,102], suggesting that even at the same pH the fate and thus the interaction of NP with organisms might vary

substantially [103]. Furthermore, natural organic matter (NOM) can increase or reduce colloidal stability of NP as a function of its quality and quantity as well as the ionic strength of the medium [e.g., 104]: At low ionic strength, NOM stabilizes negatively charged NP through electrostatic and/or steric forces [76,100]. Due to the formation of cation-NOM bridges among NP, NOM can enhance aggregation at high ionic strength [e.g., 97]. Positively charged NP may also increase aggregation in presence of NOM as shown for the combination of negatively charged NOM and $TiO_2$ NP due to charge screening [105]. Until now the effects of several individual factors like surface coating of NP, ionic strength, and valence and type of cations on the fate of NP are characterized to reasonable degree. However, less is known on how the interplay between these individual factors affects the fate of NP under realistic environmental conditions.

In contrast to homo-aggregation, hetero-aggregation (Fig. 2d) is considered to be of higher environmental relevance given the several orders of magnitude higher concentration of natural colloids [106] relative to NP [16]. Quik et al. [107], for example, indicated that hetero-aggregation is the main mechanism removing $CeO_2$ NP from the water phase through sedimentation. The aggregation kinetics of NP and natural colloids or other NP are particularly fast if they are differently charged [108,92]. The presence of NOM, in contrast, reduces hetero-aggregation due to electrostatic and steric stabilization [109]. Besides electrostatic forces, bridging by polymers, hydrogen as well as chemical bonding were reported as mechanisms inducing hetero-aggregation. This process is, thus, highly complex and amongst others triggered by NP surface properties, their aging status, interacting particulate phases, chemical composition of the surrounding environment and the properties of natural inorganic, organic and biological colloids.

However, only a few publications assessed aggregation in complex field-relevant media [e.g. 110,100,93], complicating any conclusion about the general relevance of the processes detailed above. Even less is known about the reversibility of NP aggregation in natural systems [93]. As disaggregation is mainly triggered by changing environmental conditions, experiments in simplified artificial systems are falling too short to properly address the dynamics of aggregation and disaggregation in real aquatic systems. This calls for experimental designs capable of simulating such fluctuating conditions. Furthermore, low and environmentally relevant NP concentrations should be used in future studies to avoid potentially confounding

implications of NP homo-aggregation, which is, as outlined above, less likely under currently predicted environmental concentrations of NP compared to hetero-aggregation.

## *Transport in Porous Media*

Most of the published data on NP mobility in porous media was generated using water saturated artificial columns frequently made of quartz sand [e.g. 111] while only a few involved natural soil [e.g. 92]. Similar to aquatic ecosystems, ionic strength triggers NPs' fate: NP retention and deposition in porous media (Fig. 2) is positively related to the ionic strength of the pore water [112], likely driven by quick NP aggregation [e.g. 111]. At high levels of ionic strength retention rates can further increase due to the "ripening effect" [i.e., increasing attraction forces between NP in the liquid phase and NP already deposited onto soil 113]. Hetero-aggregation of Ag NP with soil colloids, in contrast, can even enhance NP mobility by the size-exclusion effect [92, 112]. Furthermore, electrostatic and steric repulsion forces induced by NOM often lead to higher mobility [e.g. 114, 112], while a decreasing pH has the opposite effect [e.g. 111]. In contrast to water saturated systems, unsaturated porous media are less frequently but increasingly assessed [see for instance, 115]. Relative to water saturated porous media, unsaturated systems have often a higher retention potential [e.g. 116], while Fang et al. [117] found only marginal differences regarding the retention of $TiO_2$ NP between saturated and unsaturated porous media. This pattern may be explained by the non-equilibrium sorption to solid-water interface and equilibrium sorption to air water interface [118]. Moreover, the water film straining during drying could increase NP retention [116] and is thus of potentially high relevance in unsaturated porous media. The impact of ionic strength, type of cations, NOM but also pH on NP fate is comparable among aquatic systems and porous media irrespective of whether the latter is saturated or unsaturated. Therefore, we refer to the subchapters above for a more detailed description.

Driven by the few number of studies [e.g., 100] and the partly contradictory outcomes particularly for unsaturated porous media, a reliable prediction of NP fate in soil ecosystems seems difficult. Thus, a more systematic approach is urgently needed uncovering the role of soil properties on NP fate. One important step would be to assess NP fate in natural soils instead of porous media made of artificial substrate such as quartz sand. Although there are certainly challenges from the analytical side,

i.e. inorganic NP might occur at high levels in natural soils and form a substantial background contamination, which can be overcome with the help of modelling, those data are likely of higher field-relevance. In natural soils, for instance, microorganisms, inorganic and organic particles might form complex bio-geochemical interfaces that interact with NP and as a consequence will influence their fate [119] and toxicity. Those insights can, however, barely be inferred from experiments using highly artificial substrates. On the way to indeed using natural soils, it may however, be feasible to employ more complex artificial soils containing amongst others also natural organic matter.

In summary, predominantly qualitative information on particle fate in aquatic and porous media is available and key factors which control fate processes have been identified. Particle surface properties and NP concentration are most relevant and need to be characterised carefully – also throughout the experiments. Environmental key factors controlling NP fate processes are ionic strength, type and charge of ions, pH, type and concentration of NOM in all environmental compartments, while the degree of water saturation is an additional factor for porous media. Quantitative systematic data are rare [45,64,12,50] but fundamental for process understanding and ultimately for the development of reliable and predictive fate models. Future studies should, thus, qualitatively and quantitatively assess NP fate under environmentally relevant conditions, reflecting amongst others realistic NP concentrations, environmental conditions but also reaction and residence times. These data will certainly support the recent developments in NP fate modelling, namely simulations of individual fate processes and fate predictions in rivers and porous media [64,120-123]. As their validation is largely lacking, this aspect should be addressed in future work.


**Effects of Nanoparticles and their Mechanisms of Toxicity**

Roughly a decade ago and thus with the initiation of the research field "nano-ecotoxicology", Moore [124] as well as Hund-Rinke and Simon [125] suggested that NP have the potential to cause harmful effects in biota by the formation of reactive oxygen species (ROS) that could affect biological structures (Fig. 3a). Moore [124] also pointed to the potential of NP to function as carriers for other pollutants (Fig. 2d) – an assumption that will be addressed in more detail in the next chapter. While it is evident from the literature that oxidative stress can indeed be a driver for many NP-induced effects [126], the last decade of research showed that NP have the ability to act via

multiple pathways of which the induction of oxidative stress is one. In the following we briefly highlight the current state of the art with regard to central aspects supposedly driving the ecotoxicity of NP.

No mechanism of toxicity can be considered as generic for all NP [126]. Oxidative stress is, however, a frequently reported phenomenon [127,128]. Just to name a few other relevant mechanisms, physiological implications that can go as far as reproductive failure by modifying hormones or hatching enzymes were reported [129,130]. Those effects indicate implications in population development and suggest the potential for transgenerational effects [131,132]. In addition, algae [133] and aquatic plants [134] were altered in their photosynthetic pigment composition and showed effects in photosystem II, while we refer to Thwala et al. [135] for a more detailed review. Similarly, several recent reviews have covered NP accumulation in terrestrial plants which can cause biochemical and physiological changes [136-138]: Cao and co-workers, for instance, documented impacts on carbon fixation as well as water use efficiency during photosynthesis in response to $CeO_2$NP exposure [139]. The latter may have indirect effects on soil organisms via implications in soil moisture. Besides this massive diversity regarding the mechanisms of toxicity among NP, species and ecosystems, some more general questions attracted attention among researchers, namely the relevance of ions released (dissolved) from NP for NP-induced effects.

## Effects of Nanoparticles on Individuals and Populations

### Effects of ion-releasing NPs

Certain NP are prone to dissolution, i.e. the release of ions from the NP surface, during their entire (aquatic) life cycle [Fig. 2 & 3, 140]. In such cases researchers were interested in uncovering the relevance but also the mechanism of toxicity induced by those ions released from NP. Against this background, Ag NP have frequently been assessed, suggesting that Ag ions released from these NP explained a large proportion of the observed toxicity for various test organisms [e.g., 141,142,143] and soil microbial communities [144]. Additionally, the mechanisms of toxicity, for example for snails [143] and periphyton [141], were largely comparable between Ag ions and Ag NP. These observations contradict other findings, highlighting more severe implications by Ag NP than what could be explained exclusively by the Ag ions measured [145]. Differences in gene expression and transcriptomic profile point

towards distinct mechanisms of toxicity in aquatic [146,147] and terrestrial organisms [148]. Nonetheless and in line with the extensive literature review by Völker et al. [149] it may be suggested that Ag NP and Ag ions share common mechanisms of action. This conclusion also implies that the Ag NP induced toxicity, which largely depends on the particle surface properties, diameter and exposure time [150], can mainly be explained by the quantity of released ions [sensu 151,152]. Ag NP are, moreover, sulfidized (see above, Fig. 2b) in wastewater treatment plants and trapped in sewage sludge. As a consequence of the usage of sewage sludge as fertilizer for crop production in various countries, soil organisms are directly exposed to $Ag_2S$ NP, Ag NP and $Ag^+$ ions. The form of Ag directly influences the location and speciation (metallic, ionic, thiol, NP) in which Ag is stored in wheat roots [153]. In cucumber and wheat, $Ag_2S$ NP remained in their NP-form and were translocated from the roots to leaf tissue, reducing plant growth and activating plant defence mechanisms [154]. Internalisation (Fig 3c) or physical adherence, such as biological surface coating (inhibiting e.g. photosynthesis, nutrient uptake or movement) are also considered as possible mechanisms of toxicity for "inert" NP, i.e. those not releasing toxic ions [Fig. 3, 155,156].

CuO NP exposure resulted in a different pattern relative to Cu ions. This was shown for protein regulation and gene expression in marine mussels [157] and zebrafish gills [146]. Similarly, Mortimer et al. [158] indicated CuO particle-related effects in the membranes' fatty acid composition of protozoa pointing towards distinct mechanisms of toxicity induced by Cu ions relative to CuO NPs. Also in wheat grown on sand, CuO NP reduced root length and simultaneously increased root hair length with no effect on shoot growth, while Cu ions reduced both root and shoot growth [159]. A recent study by Pradhan et al. [160], however, suggests that aquatic fungi from metal contaminated ecosystems have a higher tolerance towards CuO NP driven by elevated enzymatic activity. This observation may indicate a specific adaptation of fungi towards Cu ions, supporting fungi to withstand CuO NP stress, which might indicate a common mechanism of toxicity. On the other hand, a more generic defence mechanism might have been strengthened by the long-term adaptation towards metal stress in general, which resulted in an evolution of co-tolerance towards CuO NP.

Similar to CuO NP, the mechanism of toxicity induced by ZnO NP seems to deviate from its ionic counterpart. Fernandez-Cruz et al. [161], for instance, suggested that cytotoxic effects in fish cells are mainly particle-related, which is supported by studies

uncovering difference in gene expression [162,163] and thus different mechanisms of toxicity [164]. Recent evidence with soil nematodes (*Caenorhabditis elegans*) indicates a higher ecotoxicological potential of ZnO NP relative to $Zn^{2+}$ ions [165].

It is hence not possible to draw a generic conclusion regarding the relevance of toxic metal ions released from NP relative to the effects induced by the NP themselves. This relationship is rather driven by the NP identity and coating, the biological system and the environmental conditions (e.g. complexation with NOM) under which the studies are performed. For instance, gene expression profiling in enchytraeids (*Enchytraeus crypticus*) suggested deviating mechanisms of toxicity for different Ag NP products [166]. Also the uptake and toxicity of Ag NP in earthworms are triggered by the particle coating. Makama et al. [167] reported size-dependent effects only for PVP-coated Ag NP. The uptake of Ti through the roots into basil was highest when exposed to $TiO_2$ NP with hydrophobic relative to hydrophilic coatings, causing alterations in the content of several essential elements and sugar [168]. A long-term study with two agricultural soils and different plant species looked at the effects of ZnO NP [169]. In this study, acidic soils stimulated Zn accumulation, ROS production and photosynthetic pigments of beans relative to calcareous systems, while the opposite pattern was observed in tomatoes [169].

### *Effects of NPs not releasing toxic ions*

For NP that are only marginally or not releasing toxic metal ions during the aquatic life cycle, "biological surface coating" (i.e., the attachment or adsorption of NP to the organisms' outer surface, Fig. 3d) is suggested as potential toxicity trigger [170]. The acute toxicity of $TiO_2$ NP and $Fe_3O_4$ NP in daphnids, for instance, was attributed to a physical inhibition of moulting, ultimately inducing death [155,156]. At the same time, biological surface coating could alter daphnids' swimming behaviour with potential chronic effects [171]. These effects are usually more pronounced at smaller initial particle sizes, while evidence suggest that the surface area is the driving force for toxicity [7,172,173].

## Nanoparticle induced effects over multiple generations

### *Impact of natural organic material on NP-induced effects*

As highlighted earlier, aquatic invertebrates have shown an increase in sensitivity in filial generations as a consequence of the exposure of the parental [131] or subsequent generations [132] towards $TiO_2$ NP. Similarly, at Au NP concentrations inducing only negligible mortality in the parental generation of the soil organism *C. elegans*, the reproduction of subsequent generations (F1-F4) was substantially impaired [174]. In a full lifespan test, CuO NP caused more severe effects compared to standard test duration [175]. Also, plants exposed to $CeO_2$ NP in their parental generation showed response in the filial generation with implications in the grains' nutrient composition, growth and physiology [176]. Despite the current lack of mechanistic understanding regarding the underlying processes, these insights support the idea of long-term effects in natural populations of aquatic and terrestrial organisms. Importantly, such effects are not covered by most standardized test systems. More systematic research is needed addressing the mechanistic basis of these phenomena as well the evolutionary potential of populations and communities to adapt to these emerging stressors.

## Interactions of Nanoparticles in a complex environment

In the environment, NP will interact with their abiotic surrounding, which influences their fate and ecotoxicological potential [177,81]. The relevance of natural organic molecules attaching to NP (Fig. 2e) has recently been reviewed elsewhere [178], which is why we give only a few examples here. Dissolved organic matter (DOM) coats NP and thereby stabilizes particle size [179] due to steric or electrostatic repulsion [180]. These processes are more effective with increasing hydrophobicity or aromaticity of the DOM, ultimately reducing their ecotoxicological potential - likely by reducing the availability of reactive surfaces [181]. In situations where artificial (e.g. polyvinylpyrrolidone, gum arabic or citrate) or natural OM coats Ag NP, the release of potentially toxic ions into the surrounding environment [66,182] or the NP bioavailability [183] is reduced. On the contrary, humic acid elevated the release of ions from Pb NP [184]. Bicho et al. [185] reported that soil and soil-water extracts could elevate effects of NP (here Europium polyoxometalates encapsulated in $SiO_2$ NP) relative to their absence.

Thus, it becomes apparent that soil properties influence the toxicity of NP to soil organisms. Especially the organic matter content, soil texture, ionic composition and pH affect the fate and bioavailability of NP [186,187,112], which leads to differences in toxicity. With a decrease in organic carbon in standard Lufa soils the toxic effects of PVP coated AgNP to *Enchytraeus crypticus* increased [188]. Less toxicity of AgNP was also observed for an entire test battery of dicotyledonous and monocotyledonous plants, Collembola and earthworms in soil with higher silt than sand content [189]. With a rise in soil pH ZnONP effects on *F. candida* reproduction decreased [190].

When considering time as a factor, aging of NP in presence of DOM for 48 h reduced or did not influence the toxicity of Ag and ZnO NP, respectively [191]. In contrast, the aging of $TiO_2$ NP in presence of DOM for 1 and 3 days slightly increased toxicity for daphnids, while aging for longer time periods (e.g., 6 days) reduced NP induced effects substantially as NP agglomerates exceeded the size range retained by daphnids' filter apparatus [192]. Similarly, Collembola (*Folsomia candida*) showed more severe effects in their reproductive output with increasing aging duration of Ag NP in spiked sewage sludge [193]. It is suspected that this is due to the continuous release of silver ions from AgNP.

Algal cells fed by invertebrates may enhance the uptake and toxicity of NP [194]. The adsorption of NP to algal cell surfaces (Fig. 2f) could accelerate their sedimentation (Fig. 2g), which forces pelagic consumers to invest more energy in collecting their food near the sediment [195]. Bundschuh et al. [196], in contrast, uncovered an increase in *Daphnia* growth and partly reproduction after allowing an interaction between algae and $TiO_2$ NP for 1 to 3 days. Moreover, NP ingested together with the food could negatively influence digestion by clogging the gut with negative consequences on life history strategies of primary consumers in autotrophic food webs [195]. Similar patterns have been observed for detritus-based food webs [197]. Altogether, these observations suggest highly complex interactions between organic material (irrespective whether of particulate or dissolved nature), NP and biota, but are also pointing to a lack of mechanistic understanding.

### NP-triggered alterations in the ecotoxicity of co-occurring contaminants

Aquatic and terrestrial ecosystems are also commonly exposed to mixtures of chemical stressors, which raised concerns about the potential of NP to act as carriers for organic and inorganic chemical stressors of anthropogenic origin [198]. Schwab et al. [199] reported, for instance, an elevated herbicide (diuron) induced toxicity applied at environmentally relevant concentrations in the presence of carbon-based NP. Similarly, the acute toxicity of the insecticide bifenthrin was increased in presence of fullerene NP, while its chronic effects were not affected [200]. In line with these observations, a recent review suggested that carbon-based NP could also act as Trojan horse for metal ions. The potential of carbon-based NP to act as "Trojan horse" for other contaminants strongly depends on the characteristics of the surrounding environment [see for a more detailed discussion 201]. This conclusion is challenged by Sanchis et al. [202], reporting for most combinations of carbon-based NP and organic co-contaminants antagonistic effects for daphnids and bacteria.

Also, the combined exposure of metallic NP with other chemical stressors delivered contradictory results. The presence of $TiO_2$ NP reduced the uptake of phenols [203] and polycyclic aromatic hydrocarbons [204], which, however, did not necessarily reduce the combined toxic effects of those organic chemicals with $TiO_2$ NP, suggesting a significant contribution of the NP to the biological responses. On the contrary, the accumulation of perfluorooctanesulfonate in fish was facilitated in presence of $TiO_2$ NP. This pattern was particularly pronounced at the bottom of the experimental systems as a consequence of the adsorption of perfluorooctanesulfonate onto $TiO_2$ NP surfaces and the subsequent aggregation and deposition of perfluorooctanesulfonate-loaded NP [205]. Similarly, $TiO_2$ NP increase the uptake of metal ions [206] from the water phase and at high concentrations of OM also from sediments [207], in biota ultimately elevating biological responses.

Other publications indicate the opposite pattern, namely a reduction in metal ion induced effects in presence of $nTiO_2$ or $Al_2O_3$ NP in algae [208,209] or mussels [210], with an even more pronounced reduction in presence of DOM [211]. Follow-up studies suggested that the direction and magnitude of effects caused by a combined exposure of $TiO_2$ NP and metal ions is triggered by the charge of the most toxic metal ion [212]. Although the underlying mechanisms are not well understood yet [213] and the NP concentrations used in those experiments often exceed environmentally relevant concentrations by at least one order of magnitude, interactions of NP with co-

contaminants will occur most likely under field conditions. The relevance of such interactions in both direction and magnitude for effects caused by co-contaminants in wildlife remains to be resolved.

**NP-effects in communities and consequences for trophic interaction**

McKee and Filser [214] reviewed interactions of metal-based NP in soils and pointed out the relevance of species interactions for fate and bioavailability of these NP, next to abiotic parameters. They stated that particularly biotic interactions might explain the negative consequences of NP on ecosystem processes such as carbon dioxide emission, nitrogen or phosphorous fluxes [215] that could not be detected from short-term, single species tests [214]. Button et al. [216], for instance, did not detect any negative effects on microbial community structure and function in wetland systems when exposed for 28 days to ionic Ag, citrate- and PVP-coated Ag NP (at 100 µg/L). These microbial communities, however, developed an Ag resistance, indicating an existing potential to adapt to such emerging stressors by elevating the production of extracellular polymers [217], while the costs of this adaptation remain unclear. Evidence is increasing that nitrifiers are among the most sensitive microorganisms towards Ag NP [218-220], even when the NP are sulfidized [88]. Nitrite production rate was also reduced by about 30% in presence of 200 mg magnetite ($Fe_3O_4$) NP/L [219], a concentration considered as rather low in soils remediated from organic contamination [221]. This relatively low effect threshold (given that iron oxides are mostly being considered harmless to beneficial) is supported by a range of further studies reporting sometimes surprisingly strong negative effects on microorganisms exposed to iron oxide NP [214,222,223].

When actively spraying Ag NP as growth promoter on several plant species, root and shoot mass of cowpea and *Brassica* increased, while only for the latter in a dose dependent manner [218]. For wheat, in turn, shoot mass remained stable and root mass decreased with increasing Ag NP exposure [218]. These authors also reported increased bacterial counts and higher abundances of P-solubilizing bacteria in pure soil (without plants) following Ag NP exposure while at higher Ag NP concentration the abundance of N-fixing bacteria decreased. In the rhizosphere of plants treated with Ag NP, however, the microbial responses varied with plant species and thus deferred from the pure soil [218]. An experiment with $Fe_3O_4$ NP and *Zea mays* documented a reduction in the diversity of arbuscular mycorrhizal fungi accompanied by a decreased

catalase activity, plant biomass, phosphorous content, carbon transfer to the fungi and impaired root colonization and phosphatase activity [222]. These examples emphasize that the interactions between soil microorganisms, plants and NP are highly complex, warranting further research. Addressing the underlying processes will ultimately support a well-informed decision making about potential environmental risks of NP when applied to agricultural fields.

Recent studies highlight the potential for indirect effects of NP on invertebrate species via microorganisms. Antisari et al. [224] reported for Co NP a reduction in soil microbial biomass and changes in its community composition, which may partly explain alterations in earthworms' fatty acid composition. The uptake of $TiO_2$ NP via contaminated food seems to be of high relevance for terrestrial [225,226] and aquatic invertebrates [227]. This direct uptake pathway increases NP exposure and might influence the food quality through impacts on food-associated microorganisms.

In aquatic systems, structural [228,229] and functional [230,141] changes, such as photosynthetic efficiency and leaf decomposition were reported, although often at rather high concentrations. These examples suggest that NP can indeed affect species but also species interactions [231] at various trophic levels. At the same time, neither the mechanisms driving these changes nor the consequences for the wider food web or whole ecosystems have yet even been addressed.


**CONCLUSION**

Over the past decade our understanding of sources, fate and effects of NP in the environment has made significant progress. Besides the call to consider environmental relevant concentrations of NPs as well as to monitor the fate of NP during biological testing, there are multiple open questions that need further consideration. A more systematic approach is urgently needed uncovering the role of soil properties (including saturated and unsaturated systems) for NP fate and thus the risk of groundwater contamination by NP. We have, for instance, learned that ions released from NP can in some situations fully explain the effects observed in organisms. It is currently, however, not possible to properly describe under which conditions this simplified assumption should be rejected and other mechanisms need to be considered. The impact of coating – either as intended functionalization or based on natural processes – on the fate and effects of NP is currently underrepresented in literature [but see, 232]. As those coatings are likely of high field relevance, we strongly

recommend their inclusion in future projects. Although most studies highlight effects at relatively high NP concentrations, more recent approaches document sublethal implications at field relevant levels particularly over multiple generations [as reviewed in 177]. Thus, the impact of NP under current and future exposure scenarios (including co-exposure to other stressors) on communities, ecosystems, ecosystem functions as well as interactions across ecosystem boundaries deserves special attention. Particularly for sparingly soluble or insoluble NP that may accumulate in certain environmental compartments (e.g. sediments) over time, investigations covering multiple years of (repeated) exposure and assessment are suggested to properly assess their potential long-term implications in aquatic and terrestrial ecosystems. This aspect directly links to the acknowledgement of NP-induced alterations in horizontal and vertical trophic interactions with food webs.

## ETHICS APPROVAL AND CONSENT TO PARTICIPATE

Not applicable.

## CONSENT FOR PUBLICATION

Not applicable.

## AVAILABILITY OF DATA MATERIAL

Not applicable.

## COMPETING INTERESTS

We declare no conflict of interest.

## AUTHORS' CONTRIBUTIIONS

MB initiated the paper; all authors contributed to the content in various ways. Therefore, only the main responsibilities for each of the chapters are highlighted. Introduction: MB, RS; Pathways of Nanoparticles into Natural Ecosystems: SW, MB; Predicting and Measuring Nanoparticles in Natural Ecosystems: SW; Fate of Nanoparticles in the Environment: GM, SW, GS; Effects of Nanoparticles and their Mechanisms of Toxicity: MB, RS; Effects of Nanoparticles on Individuals and Populations: JF, MM, MB, RS; Nanoparticle induced effects over multiple generations: JF, MM, SL; Interactions of Nanoparticles in a complex environment: JF, MM, MB, SL; Effects in communities and trophic interaction: JF, MM. Figures: SW, SL. All authors edited the final version of this manuscript.
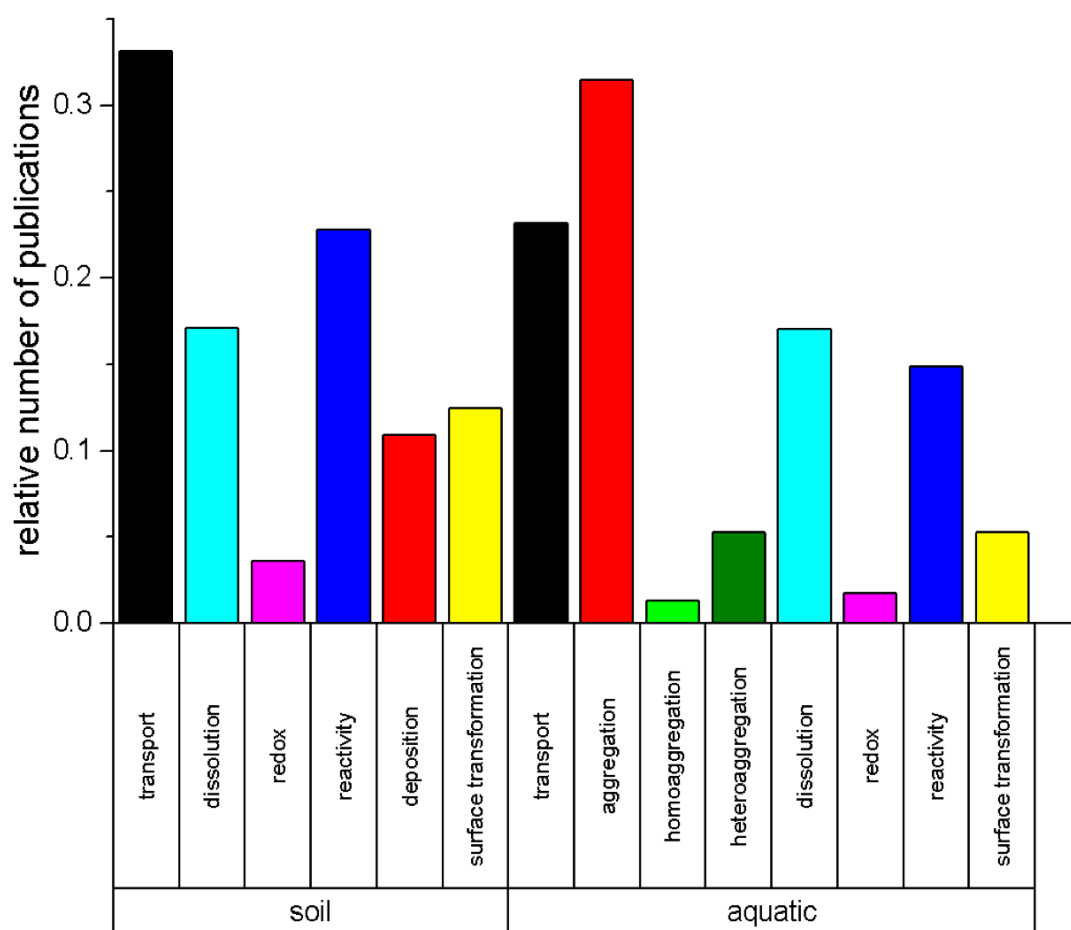
**Figure 1.** Relative number of publications compared to total number of publications found between 2007 and 2017 in soil and aquatic environments (search criteria: nano* & environ* & *system*, NOT effect* & NOT *tox*; process search criteria: transp*, agg*, homoagg*, heteroagg*, dissol*, redox*, surface* transfo*, reacti*, deposition*; system search criteria: soil*, aqua*; only web-of-science category *environmental science* considered).
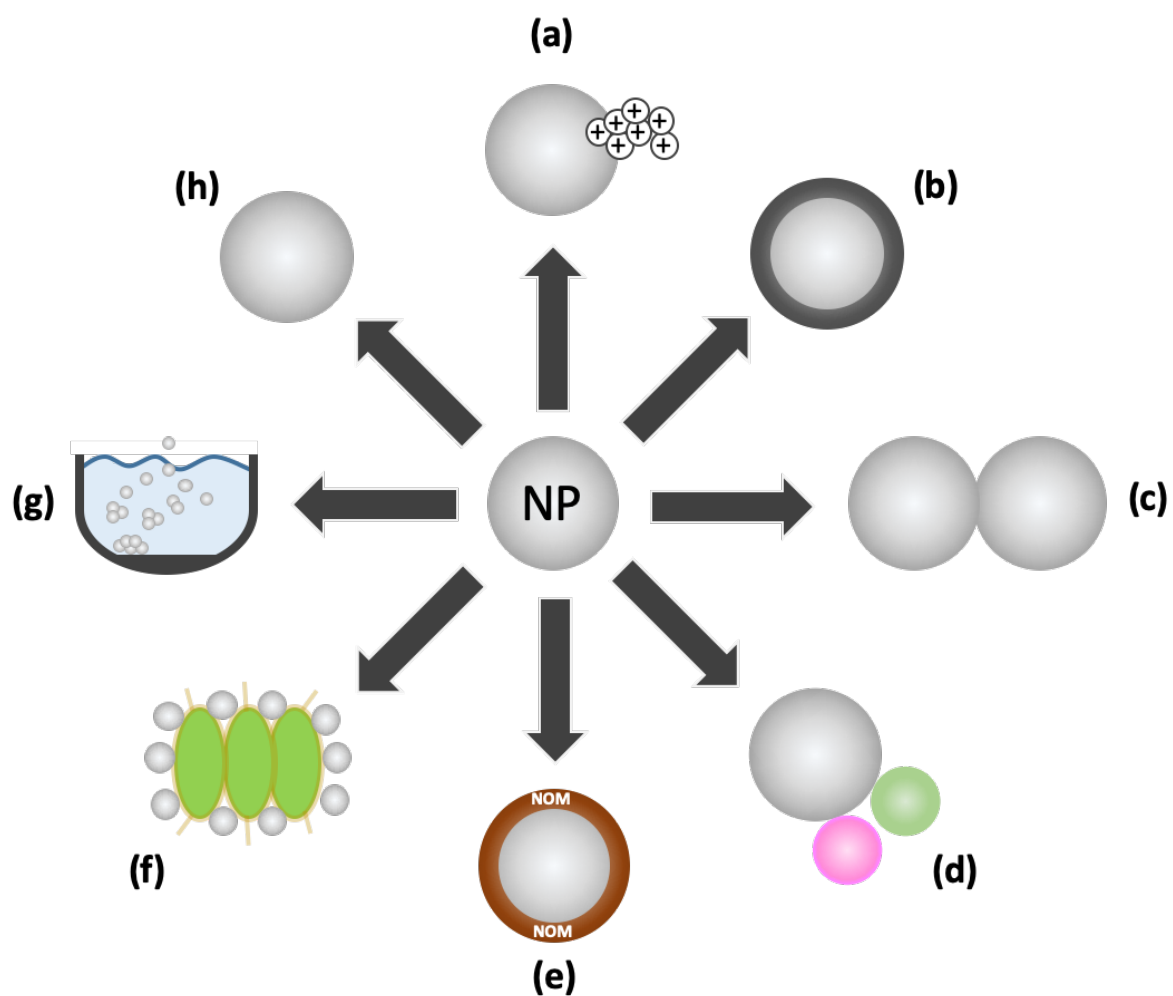
**Figure 2.** Interactions and fate of NP in the environment considering (a) dissolution, (b) sulfidation, (c) homo-aggregation, (d) hetero-aggregation, (e) coating with NOM, (f) NP adsorption on biological surfaces, (g) sedimentation/deposition, and (h) persistence.
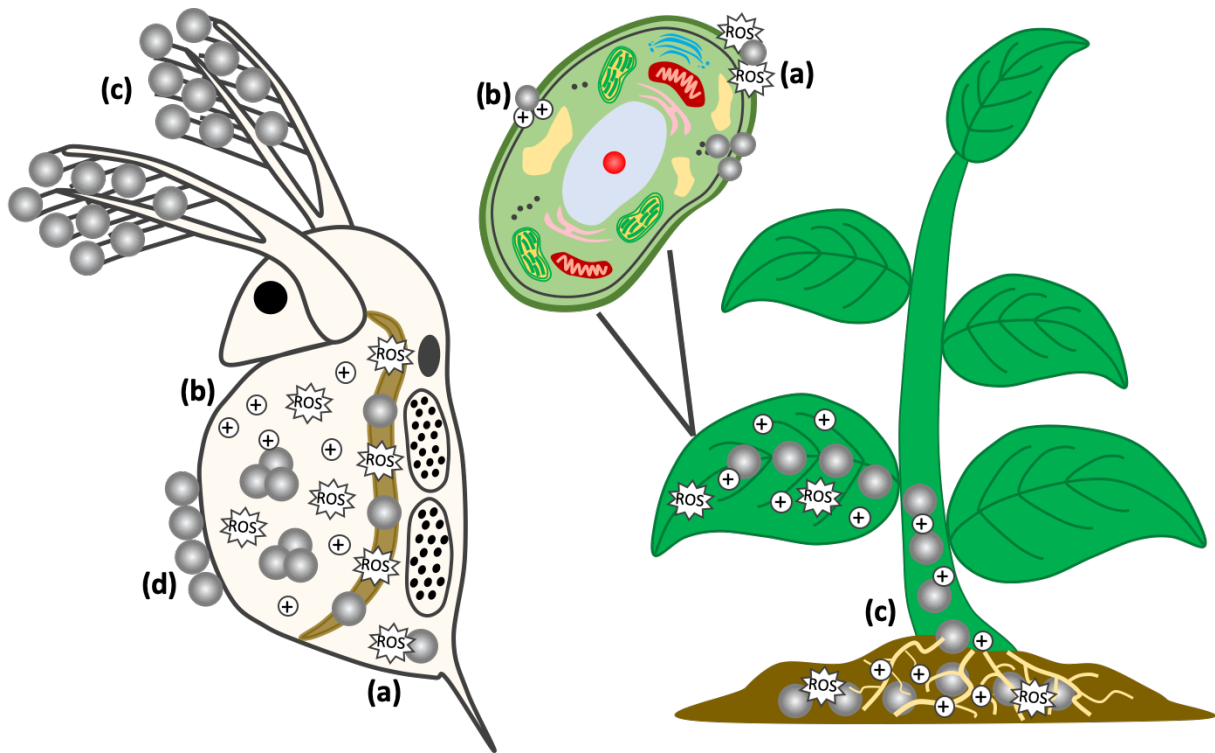
**Figure 3.** Potential ecotoxicity of NP in aquatic and terrestrial regimes, illustrating the potential (a) uptake, (b) distribution, (c) biological surface coating, locally acting mechanisms as (d) ion release, and (e) formation of ROS.

**REFERENCES**

1. PEN (2013) The Project on Emerging Nanotechnologies. Available online (1462013) http://www.nanotechproject.org/

2. Ito A, Shinkai M, Honda H, Kobayashi T (2005) Medical application of functionalized magnetic nanoparticles. J Biosci Bioeng 100:1-11

3. Semenzin E, Lanzellotto E, Hristozov D, Critto A, Zabeo A, Giubilato E, Marcomini A (2015) Species sensitivity weighted distribution for ecological risk assessment of engineered nanomaterials: The n-TiO2 case study. Environ Toxicol Chem 34:2644-2659

4. Nowack B, Bucheli TD (2007) Occurrence, behavior and effects of nanoparticles in the environment. Environ Pollut 150 (1):5-22

5. von der Kammer F, Ferguson PL, Holden PA, Masion A, Rogers KR, Klaine SJ, Koelmans AA, Horne N, Unrine JM (2012) Analysis of engineered nanomaterials in complex matrices (environment and biota): general considerations and conceptual case studies. Environ Toxicol Chem 31 (1):32-49.

6. Klaine SJ, Alvarez PJ, Batley GE, Fernandes TF, Handy RD, Lyon DY, Mahendra S, McLaughlin MJ, Lead JR (2008) Nanomaterials in the Environment: Behavior, Fate, Bioavailability, and Effects. Environ Toxicol Chem 27 (9):1825-1851

7. Seitz F, Rosenfeldt RR, Schneider S, Schulz R, Bundschuh M (2014) Size-, surface- and crystalline structure composition-related effects of titanium dioxide nanoparticles during their aquatic life cycle. Sci Total Environ 493:891-897

8. Petersen EJ, Diamond SA, Kennedy AJ, Goss GG, Ho K, Lead J, Hanna SK, Hartmann NB, Hund-Rinke K, Mader B, Manier N, Pandard P, Salinas ER, Sayre P (2015) Adapting OECD Aquatic Toxicity Tests for Use with Manufactured Nanomaterials: Key Issues and Consensus Recommendations. Environ Sci Technol 49 (16):9532-9547.

9. Freixa A, Acuña V, Sanchís J, Farré M, Barceló D, Sabater S (2018) Ecotoxicological effects of carbon based nanomaterials in aquatic organisms. Sci Total Environ 619–620:328–337

10. Petersen EJ, Zhang LW, Mattison NT, O'Carroll DM, Whelton AJ, Uddin N, Nguyen T, Huang QG, Henry TB, Holbrook RD, Chen KL (2011) Potential release pathways, environmental fate, and ecological risks of carbon nanotubes. Environ Sci Technol 45 (23):9837-9856

11. Furtado LM, Bundschuh M, Metcalfe CD (2016) Monitoring the environmental fate and transformation of silver nanoparticles in natural waters. UB/TIB Hann 97:449–455

12. Schaumann GE, Phillippe A, Bundschuh M, Metrevelli G, Klitzke S, Rakcheev D, Grün A, Kumahor S, Kühn M, Baumann T, Lang F, Manz W, Schulz R, Vogel H-J (2015) Understanding the fate and biological effects of Ag- and TiO2-nanoparticles in the environment: the quest for advanced analytics and interdisciplinary concepts. Sci Total Environ 535:3-19

13. Leopold K, Philippe A, Wörle K, Schaumann GE (2016) Analytical strategies to the determination of metal-containing nanoparticles in environmental samples. Trends Anal Chem 84:107-120

14. Hansen SF, Heggelund LR, Besora PR, Mackevica A, Boldrin A, Baun A (2016) Nanoproducts - what is actually available to European consumers? Environ-Sci Nano 3 (1):169-180

15. Gottschalk F, Sonderer T, Scholz RW, Nowack B (2009) Modeled environmental concentrations of engineered nanomaterials (TiO2, ZnO, Ag, CNT, Fullerenes) for different regions. Environ Sci Technol 43 (24):9216-9222.

16. Gottschalk F, Sun TY, Nowack B (2013) Environmental concentrations of engineered nanomaterials: Review of modeling and analytical studies. Environ Pollut 181:287-300

17. Tolaymat T, El Badawy A, Genaidy A, Abdelraheem W, Sequeira R (2017) Analysis of metallic and metal oxide nanomaterial environmental emissions. Journal of Cleaner Production 143:401-412

18. Al-Kattan A, Wichser A, Vonbank R, Brunner S, Ulrich A, Zuin S, Arroyo Y, Golanski L, Nowack B (2015) Characterization of materials released into water from paint containing nano-SiO2. Chemosphere 119:1314-1321

19. Kaegi R, Sinnet B, Zuleeg S, Hagendorfer H, Mueller E, Vonbank R, Boller M, Burkhardt M (2010) Release of silver nanoparticles from outdoor facades. Environ Pollut 158 (9):2900-2905

20. Kaegi R, Voegelin A, Sinnet B, Zuleeg S, Hagendorfer H, Burkhardt M, Siegrist H (2011) Behavior of metallic silver nanoparticles in a pilot wastewater treatment plant. Environ Sci Technol 45 (9):3902-3908

21. Zuin S, Gaiani M, Ferrari A, Golanski L (2013) Leaching of nanoparticles from experimental water-borne paints under laboratory test conditions. Journal of Nanoparticle Research 16 (1)

22. Sun TY, Bornhoft NA, Hungerbuhler K, Nowack B (2016) Dynamic probabilistic modeling of environmental emissions of engineered nanomaterials. Environ Sci Technol 50 (9):4701-4711

23. Bressot C, Manier N, Pagnoux C, Aguerre-Chariol O, Morgeneyer M (2017) Environmental release of engineered nanomaterials from commercial tiles under standardized abrasion conditions. J Hazard Mater 322:276-283

24. Duncan TV, Pillai K (2015) Release of engineered nanomaterials from polymer nanocomposites: diffusion, dissolution and desorption. ACS Applied Materials & Interfaces 7 (1):2-19

25. Olabarrieta J, Zorita S, Peña I, Rioja N, Monzón O, Benguria P, Scifo L (2012) Aging of photocatalytic coatings under a water flow: Long run performance and TiO2 nanoparticles release. Applied Catalysis B: Environmental 123:182-192

26. Wohlleben W, Meyer J, Muller J, Muller P, Vilsmeier K, Stahlmecke B, Kuhlbusch TAJ (2016) Release from nanomaterials during their use phase: combined mechanical and chemical stresses applied to simple and multi-filler nanocomposites mimicking wear of nano-reinforced tires. Environ-Sci Nano 3 (5):1036-1051

27. Kinsinger N, Honda R, Keene V, Walker SL (2015) Titanium dioxide nanoparticle removal in primary prefiltration stages of water treatment: role of coating, natural organic matter, source water, and solution chemistry. Environ Eng Sci 32 (4):292-300

28. Mitrano DM, Rimmele E, Wichser A, Erni R, Height M, Nowack B (2014) Presence of nanoparticles in wash water from conventional silver and nano-silver textiles. ACS nano 8 (7):7208-7219

29. Gottschalk F, Ort C, Scholz RW, Nowack B (2011) Engineered nanomaterials in rivers - exposure scenarios for Switzerland at high spatial and temporal resolution. Environ Pollut 159 (12):3439-3445.

30. Keller AA, McFerran S, Lazareva A, Suh S (2013) Global life cycle releases of engineered nanomaterials. Journal of Nanoparticle Research 15 (6):1692

31. Piccinno F, Gottschalk F, Seeger S, Nowack B (2012) Industrial production quantities and uses of ten engineered nanomaterials in Europe and the world. Journal of Nanoparticle Research 14 (9):1109

32. Gottschalk F, Nowack B (2011) The release of engineered nanomaterials to the environment. Journal of Environmental Monitoring 13:1145–1155

33. Kim B, Murayama M, Colman BP, Hochella MF (2012) Characterization and environmental implications of nano- and larger TiO2 particles in sewage sludge, and soils amended with sewage sludge. Journal of Environmental Monitoring 14 (4):1129-1137

34. Ma R, Levard C, Judy JD, Unrine JM, Durenkamp M, Martin B, Jefferson B, Lowry GV (2014) Fate of zinc oxide and silver nanoparticles in a pilot wastewater treatment plant and in processed biosolids. Environ Sci Technol 48 (1):104-112

35. Mitrano DM, Mehrabi K, Dasilva YAR, Nowack B (2017) Mobility of metallic (nano)particles in leachates from landfills containing waste incineration residues. Environ-Sci Nano 4 (2):480-492

36. Baalousha M, Yang Y, Vance ME, Colman BP, McNeal S, Xu J, Blaszczak J, Steele M, Bernhardt E, Hochella MF (2016) Outdoor urban nanomaterials: The emergence of a new, integrated, and critical field of study. Sci Total Environ 557:740-753

37. Bossa N, Chaurand P, Levard C, Borschneck D, Miche H, Vicente J, Geantet C, Aguerre-Chariol O, Michel FM, Rose J (2017) Environmental exposure to TiO2 nanomaterials incorporated in building material. Environ Pollut 220:1160-1170

38. Kaegi R, Ulrich A, Sinnet B, Vonbank R, Wichser A, Zuleeg S, Simmler H, Brunner S, Vonmont H, Burkhardt M, Boller M (2008) Synthetic TiO2 nanoparticle emission from exterior facades into the aquatic environment. Environ Pollut 156 (2):233-239.

39. Ermolin MS, Fedotov PS, Ivaneev AI, Karandashev VK, Fedyunina NN, Eskina VV (2017) Isolation and quantitative analysis of road dust nanoparticles. Journal of Analytical Chemistry 72 (5):520-532

40. Prichard HM, Fisher PC (2012) Identification of platinum and palladium particles emitted from vehicles and dispersed into the surface environment. Environ Sci Technol 46 (6):3149-3154

41. Filser J, Arndt D, Baumann J, Geppert M, Hackmann S, Luther EM, Pade C, Prenzel K, Wigger H, Arning J, Hohnholt MC, Koser J, Kuck A, Lesnikov E, Neumann J, Schutrumpf S, Warrelmann J, Baumer M, Dringen R, von Gleich A, Swiderek P, Thoming J (2013) Intrinsically green iron oxide nanoparticles? From synthesis via (eco-)toxicology to scenario modelling. Nanoscale 5 (3):1034-1046.

42. Weil M, Meissner T, Busch W, Springer A, Kuhnel D, Schulz R, Duis K (2015) The oxidized state of the nanocomposite Carbo-Iron (R) causes no adverse effects on growth, survival and differential gene expression in zebrafish. Sci Total Environ 530:198-208.

43. Weil M, Meissner T, Springer A, Bundschuh M, Hübler L, Schulz R, Duis K (2016) Oxidized Carbo-Iron causes reduced reproduction and lower tolerance of juveniles in the amphipod *Hyalella azteca*. Aquatic Toxicology 181:94–103

44. Kah M (2015) Nanopesticides and nanofertilizers: emerging contaminants or opportunities for risk mitigation? Frontiers in chemistry 3:64.

45. Wagner S, Gondikas A, Neubauer E, Hofmann T, von der Kammer F (2014) Spot the difference: engineered and natural nanoparticles in the environment-release, behavior, and fate. Angewandte Chemie-International Edition 53 (46):12398-12419

46. Boxall AB, Tiede K, Chaudhry Q (2007) Engineered nanomaterials in soils and water: how do they behave and could they pose a risk to human health? Nanomedicine 2 (6):919-927

47. Mueller NC, Nowack B (2008) Exposure modeling of engineered nanoparticles in the environment. Environ Sci Technol 42 (12):4447-4453

48. Caballero-Guzman A, Nowack B (2016) A critical review of engineered nanomaterial release data: Are current data useful for material flow modeling? Environ Pollut 213:502-517

49. Sun TY, Gottschalk F, Hungerbuhler K, Nowack B (2014) Comprehensive probabilistic modelling of environmental emissions of engineered nanomaterials. Environ Pollut 185:69-76.

50. Baalousha M, Cornelis G, Kuhlbusch TAJ, Lynch I, Nickel C, Peijnenburg W, van den Brink NW (2016) Modeling nanomaterial fate and uptake in the environment: current knowledge and future trends. Environ-Sci Nano 3 (2):323-345.

51. Gondikas AP, von der Kammer F, Reed RB, Wagner S, Ranville JF, Hofmann T (2014) Release of TiO2 nanoparticles from sunscreens into surface waters: a one-year survey at the old Danube recreational lake. Environ Sci Technol 48:5415–5422

52. Bauerlein PS, Emke E, Tromp P, Hofman JAMH, Carboni A, Schooneman F, de Voogt P, van Wezel AP (2017) Is there evidence for man-made nanoparticles in the Dutch environment? Sci Total Environ 576:273-283

53. Gondikas A, von der Kammer F, Kaegi R, Borovinskaya O, Neubauer E, Navratilova J, Praetorius A, Cornelis G, Hofmann T (2018) Where is the nano? Analytical approaches for the detection and quantification of TiO2 engineered nanoparticles in surface waters. Environmental Sciecne: Nano in press:10.1039/c1037en00952f

54. Laborda F, Bolea E, Cepria G, Gomez MT, Jimenez MS, Perez-Arantegui J, Castillo JR (2016) Detection, characterization and quantification of inorganic engineered nanomaterials: A review of techniques and methodological approaches for the analysis of complex samples. Anal Chim Acta 904:10-32.

55. Philippe A, Schaumann GE (2014) Evaluation of hydrodynamic chromatography coupled with uv-visible, fluorescence and inductively coupled plasma mass spectrometry detectors for sizing and quantifying colloids in environmental media. PLoS ONE 9 (2):0090559

56. Grainger DW, Castner DG (2008) Nanobiomaterials and nanoanalysis: opportunities for improving the science to benefit biomedical technologies. Advanced Materials 20:867–877

57. Borovinskaya O, Gschwind S, Hattendorf B, Tanner M, Gunther D (2014) Simultaneous mass quantification of nanoparticles of different composition in a mixture by microdroplet generator-ICPTOFMS. Anal Chem 86 (16):8142-8148.

58. Praetorius A, Gundlach-Graham A, Goldberg E, Fabienke W, Navratilova J, Gondikas A, Kaegi R, Gunther D, Hofmann T, von der Kammer F (2017) Single-particle multi-element fingerprinting (spMEF) using inductively-coupled plasma time-of-flight mass spectrometry (ICP-TOFMS) to identify engineered nanoparticles against the elevated natural background in soils. Environ-Sci Nano 4 (2):307-314

59. Gogos A, Kaegi R, Zenobi R, Bucheli TD (2014) Capabilities of asymmetric flow field-flow fractionation coupled to multi-angle light scattering to detect carbon nanotubes in soot and soil. Environ-Sci Nano 1 (6):584-594.

60. Petersen EJ, Flores-Cervantes DX, Bucheli TD, Elliott LCC, Fagan JA, Gogos A, Hanna S, Kagi R, Mansfield E, Bustos ARM, Plata DL, Reipa V, Westerhoff P, Winchester MR (2016) Quantification of Carbon Nanotubes in Environmental Matrices: Current Capabilities, Case Studies, and Future Prospects. Environ Sci Technol 50 (9):4587-4605.

61. Navratilova J, Praetorius A, Gondikas A, Fabienke W, von der Kammer F, Hofmann T (2015) Detection of engineered copper nanoparticles in soil using single particle ICP-MS. Int J Env Res Pub He 12 (12):15756-15768

62. Nowack B, Baalousha M, Bornhoft N, Chaudhry Q, Cornelis G, Cotterill J, Gondikas A, Hassellov M, Lead J, Mitrano DM, von der Kammer F, Wontner-Smith T (2015) Progress towards the validation of modeled environmental concentrations of engineered nanomaterials by analytical measurements. Environ-Sci Nano 2 (5):421-428

63. Navarro E, Piccapietra F, Wagner B, Marconi F, Kaegi R, Odzak N, Sigg L, Behra R (2008) Toxicity of silver nanoparticles to *Chlamydomonas reinhardtii*. Environ Sci Technol 42 (23):8959-8964

64. Dale AL, Casman EA, Lowry GV, Lead JR, Viparelli E, Baalousha M (2015) Modeling nanomaterial environmental fate in aquatic systems. Environ Sci Technol 49 (5):2587-2593.

65. Peijnenburg WJGM, Baalousha M, Chen JW, Chaudry Q, Von der kammer F, Kuhlbusch TAJ, Lead J, Nickel C, Quik JTK, Renker M, Wang Z, Koelmans AA (2015) A Review of the properties and processes determining the fate of engineered nanomaterials in the aquatic environment. Crit Rev Environ Sci Technol 45 (19):2084-2134.

66. Levard C, Hotze EM, Lowry GV, Brown GE (2012) Environmental transformations of silver nanoparticles: impact on stability and toxicity. Environ Sci Technol 46 (13):6900-6914.

67. Sekine R, Khaksar M, Brunetti G, Donner E, Scheckel KG, Lombi E, Vasilev K (2013) Surface immobilization of engineered nanomaterials for in situ study of their environmental transformations and fate. Environ Sci Technol 47 (16):9308-9316.

68. Sivry Y, Gelabert A, Cordier L, Ferrari R, Lazar H, Juillot F, Menguy N, Benedetti MF (2014) Behavior and fate of industrial zinc oxide nanoparticles in a carbonate-rich river water. Chemosphere 95:519-526.

69. Stankus DP, Lohse SE, Hutchison JE, Nason JA (2011) Interactions between natural organic matter and gold nanoparticles stabilized with different organic capping agents. Environ Sci Technol 45 (8):3238-3244.

70. Li Y, Zhang W, Niu JF, Chen YS (2013) Surface-coating-dependent dissolution, aggregation, and reactive oxygen species (ROS) generation of silver nanoparticles under different irradiation conditions. Environ Sci Technol 47 (18):10293-10301.

71. Auffan M, Pedeutour M, Rose J, Masion A, Ziarelli F, Borschneck D, Chaneac C, Botta C, Chaurand P, Labille J, Bottero JY (2010) Structural degradation at the surface of a TiO2-based nanomaterial used in cosmetics. Environ Sci Technol 44 (7):2689-2694.

72. Baer DR, Engelhard MH, Johnson GE, Laskin J, Lai JF, Mueller K, Munusamy P, Thevuthasan S, Wang HF, Washton N, Elder A, Baisch BL, Karakoti A, Kuchibhatla SVNT, Moon D (2013) Surface characterization of nanomaterials and nanoparticles:

Important needs and challenging opportunities. J Vac Sci Technol A 31 (5). doi:Artn 050820

73. Barton LE, Auffan M, Bertrand M, Barakat M, Santaella C, Masion A, Borschneck D, Olivi L, Roche N, Wiesner MR, Bottero JY (2014) Transformation of pristine and citrate-functionalized CeO2 nanoparticles in a laboratory-scale activated sludge reactor. Environ Sci Technol 48 (13):7289-7296.

74. Elzey S, Grassian VH (2010) Agglomeration, isolation and dissolution of commercially manufactured silver nanoparticles in aqueous environments. Journal of Nanoparticle Research 12 (5):1945-1958.

75. Mitrano DM, Ranville JF, Bednar A, Kazor K, Hering AS, Higgins CP (2014) Tracking dissolution of silver nanoparticles at environmentally relevant concentrations in laboratory, natural, and processed waters using single particle ICP-MS (spICP-MS). Environ-Sci Nano 1 (3):248-259.

76. Metreveli G, Frombold B, Seitz F, Grün A, Phillippe A, Rosenfeldt RR, Bundschuh M, Schulz R, Manz W, Schaumann GE (2016) Impact of chemical composition of ecotoxicological test media on the stability and aggregation status of silver nanoparticles. Environmental Science: Nano 3:418-433

77. Khaksar M, Jolley DF, Sekine R, Vasilev K, Johannessen B, Donner E, Lombi E (2015) In situ chemical transformations of silver nanoparticles along the water-sediment continuum. Environ Sci Technol 49 (1):318-325.

78. Dale AL, Lowry GV, Casman EA (2013) Modeling nanosilver transformations in freshwater sediments. Environ Sci Technol 47 (22):12920-12928.

79. Brunetti G, Donner E, Laera G, Sekine R, Scheckel KG, Khaksar M, Vasilev K, De Mastro G, Lombi E (2015) Fate of zinc and silver engineered nanoparticles in sewerage networks. Water Res 77:72-84.

80. Liu JY, Hurt RH (2010) Ion release kinetics and particle persistence in aqueous nano-silver colloids. Environ Sci Technol 44 (6):2169-2175.

81. Koser J, Engelke M, Hoppe M, Nogowski A, Filser J, Thoming J (2017) Predictability of silver nanoparticle speciation and toxicity in ecotoxicological media. Environ-Sci Nano 4 (7):1470-1483.

82. Lowry GV, Espinasse BP, Badireddy AR, Richardson CJ, Reinsch BC, Bryant LD, Bone AJ, Deonarine A, Chae S, Therezien M, Colman BP, Hsu-Kim H, Bernhardt ES, Matson CW, Wiesner MR (2012) Long-term transformation and fate of manufactured Ag nanoparticles in a simulated large scale freshwater emergent wetland. Environ Sci Technol 46 (13):7027-7036.

83. Gogos A, Thalmann B, Voegelin A, Kaegi R (2017) Sulfidation kinetics of copper oxide nanoparticles. Environmental Science:-Nano in press

84. Thalmann B, Voegelin A, Morgenroth E, Kaegi R (2016) Effect of humic acid on the kinetics of silver nanoparticle sulfidation. Environ-Sci Nano 3 (1):203-212

85. Kaegi R, Voegelin A, Ort C, Sinnet B, Thalmann B, Krismer J, Hagendorfer H, Elumelu M, Mueller E (2013) Fate and transformation of silver nanoparticles in urban wastewater systems. Water Res 47 (12):3866-3877.

86. Baalousha M, Arkill KP, Romer I, Palmer RE, Lead JR (2015) Transformations of citrate and Tween coated silver nanoparticles reacted with Na2S. Sci Total Environ 502:344-353.

87. Liu JY, Pennell KG, Hurt RH (2011) Kinetics and mechanisms of nanosilver oxysulfidation. Environ Sci Technol 45 (17):7345-7353.

88. Kraas M, Schlich K, Knopf B, Wege F, Kagi R, Terytze K, Hund-Rinke K (2017) Long-term effects of sulfidized silver nanoparticles in sewage sludge on soil microflora. Environmental Toxocilogy and Chemistry.

89. Lowry GV, Gregory KB, Apte SC, Lead JR (2012) Transformations of nanomaterials in the environment. Environ Sci Technol 46 (13):6893-6899.

90. Sani-Kast N, Labille J, Ollivier P, Slomberg D, Hungerbuhler K, Scheringer M (2017) A network perspective reveals decreasing material diversity in studies on nanoparticle interactions with dissolved organic matter. Proc Natl Acad Sci U S A 114 (10):E1756-E1765.

91. Wang H, Adeleye AS, Huang Y, Li F, Keller AA (2015) Heteroaggregation of nanoparticles with biocolloids and geocolloids. Advances in Colloid and Interface Science 226:24-36.

92. Cornelis G, Pang L, Doolette C, Kirby JK, McLaughlin MJ (2013) Transport of silver nanoparticles in saturated columns of natural soils. Sci Total Environ 463-464:120-130.

93. Metreveli G, Philippe A, Schaumann GE (2015) Disaggregation of silver nanoparticle homoaggregates in a river water matrix. Sci Total Environ 535:35-44.

94. Adam V, Loyaux-Lawniczak S, Labille J, Galindo C, del Nero M, Gangloff S, Weber T, Quaranta G (2016) Aggregation behaviour of TiO2 nanoparticles in natural river water. Journal of Nanoparticle Research 18:13

95. Derjaguin BV, Landau L (1941) Theory of the stability of strongly charged lyophobic sols and of the adhesion of strongly charged particles in solutions of electrolytes. Progress in Surface Science 14:633-662

96. Verwey EJW, Overbeek JTG (1948) Theory of the stability of lyophobic colloids. Elsevier, Amsterdam

97. Baalousha M, Nur Y, Romer I, Tejamaya M, Lead JR (2013) Effect of monovalent and divalent cations, anions and fulvic acid on aggregation of citrate-coated silver nanoparticles. Sci Total Environ 354:119-131

98. Field TB, Coburn J, McCourt JL, McBryde WAE (1975) Composition and stability of some metal citrate and diglycolate complexes in aqueous solution. Anal Chim Acta 74:101-106

99. Li X, Lenhart JJ, Walker HW (2012) Aggregation kinetics and dissolution of coated silver nanoparticles. Langmuir 28:1095-1104

100. Klitzke S, Metreveli G, Peters A, Schaumann GE, Lang F (2015) The fate of silver nanoparticles in soil solution - Sorption of solutes and aggregation. Sci Total Environ 535:54-60

101. Petosa AR, Jaisi DP, Quevedo IR, Elimelech M, Tufenkji N (2010) Aggregation and deposition of engineered nanomaterials in aquatic environments: role of physicochemical interactions. Environ Sci Technol 44 (17):6532-6549.

102. Omar FM, Aziz HA, Stoll S (2014) Aggregation and disaggregation of ZnO nanoparticles: Influence of pH and adsorption of Suwannee River humic acid. Sci Total Environ 468:195-201

103. El Badawy AM, Silva RG, Morris B, Scheckel KG, Suidan MT, Tolaymat TM (2011) Surface charge-dependent toxicity of silver nanoparticles. Environ Sci Technol 45 (11):283-287

104. Philippe A, Schaumann GE (2014) Interactions of dissolved organic matter with natural and engineered inorganic colloids: a review. Environ Sci Technol 48 (16):8946-8962.

105. Zhou DX, Ji ZX, Jiang XM, Dunphy DR, Brinker J, Keller AA (2013) Influence of material properties on TiO2 nanoparticle agglomeration. PLoS One 8 (11):e81239

106. Atteia O, Perret D, Adatte T, Kozel R, Rossi P (1998) Characterization of natural colloids from a river and spring in a karstic basin. Environ Geol 34 (4):257-269

107. Quik JTK, Stuart MC, Wouterse M, Peijnenburg W, Hendriks AJ, van de Meent D (2012) Natural colloids are the dominant factors in the sedimentation of nanoparticles. Environ Toxicol Chem 31 (5):1019-1022

108. Huynh KA, McCaffery JM, Chen KL (2012) Heteroaggregation of multiwalled carbon nanotubes and hematite nanoparticles: rates and mechanisms. Environ Sci Technol 46 (11):5912-5920.

109. Quik JT, Velzeboer I, Wouterse M, Koelmans AA, van de Meent D (2014) Heteroaggregation and sedimentation rates for nanomaterials in natural waters. Water Researcg 48:269-279.

110. Tso CP, Zhung CM, Shih YH, Tseng YM, Wu SC, Doong RA (2010) Stability of metal oxide nanoparticles in aqueous solutions. Water Sci Technol 61 (1):127-133.

111. Solovitch N, Labille J, Rose J, Chaurand P, Borschneck D, Wiesner MR, Bottero JY (2010) Concurrent aggregation and deposition of TiO2 nanoparticles in a sandy porous media. Environ Sci Technol 44 (13):4897-4902.

112. Cornelis G, Hund-Rinke K, Kuhlbusch T, van den Brink N, Nickel C (2014) Fate and bioavailability of engineered nanoparticles in soils: A review. Crit Rev Environ Sci Technol 44:2720-2764

113. Jiang X, Tong M, Kim H (2012) Influence of natural organic matter on the transport and deposition of zinc oxide nanoparticles in saturated porous media. Journal of Colloid and Interface Science 386 (1):34-43.

114. Sagee O, Dror I, Berkowitz B (2012) Transport of silver nanoparticles (AgNPs) in soil. Chemosphere 88 (5):670-675.

115. Kumahor SK, Hron P, Metreveli G, Schaumann GE, Klitzke S, Lang F, Vogel HJ (2016) Transport of soil-aged silver nanoparticles in unsaturated sand. J Contam Hydrol 195:31-39.

116. Liu L, Gao B, Wu L, Morales VL, Yang LY, Zhou ZH, Wang H (2013) Deposition and transport of graphene oxide in saturated and unsaturated porous media. Chem Eng J 229:444-449.

117. Fang J, Xu MJ, Wang DJ, Wen B, Han JY (2013) Modeling the transport of TiO2 nanoparticle aggregates in saturated and unsaturated granular media: Effects of ionic strength and pH. Water Res 47 (3):1399-1408.

118. Kumahor SK, Hron P, Metreveli G, Schaumann GE, Vogel HJ (2015) Transport of citrate-coated silver nanoparticles in unsaturated sand. Sci Total Environ 535:113-121.

119. Hoppe M, Mikutta R, Utermann J, Duijnisveld W, Guggenberger G (2014) Retention of sterically and electrosterically stabilized silver nanoparticles in soils. Environ Sci Technol 48 (21):12628-12635

120. Markus AA, Parsons JR, Roex EWM, de Voogt P, Laane RWPM (2015) Modeling aggregation and sedimentation of nanoparticles in the aquatic environment. Sci Total Environ 506:323-329.

121. de Klein JJM, Quik JTK, Bauerlein PS, Koelmans AA (2016) Towards validation of the NanoDUFLOW nanoparticle fate model for the river Dommel, The Netherlands. Environ-Sci Nano 3 (2):434-441.

122. Meesters JAJ, Quik JTK, Koelmans AA, Hendriks AJ, van de Meent D (2016) Multimedia environmental fate and speciation of engineered nanoparticles: a probabilistic modeling approach. Environ-Sci Nano 3 (4):715-727.

123. Praetorius A, Scheringer M, Hungerbuhler K (2012) Development of environmental fate models for engineered nanoparticles - a case study of TiO2 nanoparticles in the Rhine River. Environ Sci Technol 46:6705-6713.

124. Moore MN (2006) Do nanoparticles present ecotoxicological risks for the health of the aquatic environment? Environ Int 32:967-976

125. Hund-Rinke K, Simon M (2006) Ecotoxic effect of photocatalytic active nanoparticles TiO2 on algae and daphnids. Environmental Science and Pollution Research 13 (4):225-232.

126. von Moos N, Slaveykova VI (2014) Oxidative stress induced by inorganic nanoparticles in bacteria and aquatic microalgae - state of the art and knowledge gaps. Nanotoxicology 8 (6):605-630.

127. Mwaanga P, Carraway ER, van den Hurk P (2014) The induction of biochemical changes in D*aphnia magna* by CuO and ZnO nanoparticles. Aquatic Toxicology 150:201-209.

128. Wu Y, Zhou QF (2012) Dose- and time-related changes in aerobic metabolism, chorionic disruption, and oxidative stress in embryonic medaka (*Oryzias latipes*): underlying mechanisms for silver nanoparticle developmental toxicity. Aquatic Toxicology 124:238-246

129. Muller EB, Lin SJ, Nisbet RM (2015) Quantitative adverse outcome pathway analysis of hatching in zebrafish with CuO nanoparticles. Environ Sci Technol 49 (19):11817-11824.

130. Nair PMG, Park SY, Lee SW, Choi J (2011) Differential expression of ribosomal protein gene, gonadotrophin releasing hormone gene and Balbiani ring protein gene in silver nanoparticles exposed *Chironomus riparius*. Aquatic Toxicology 101 (1):31-37.

131. Bundschuh M, Seitz F, Rosenfeldt RR, Schulz R (2012) Titanium dioxide nanoparticles increase sensitivity in the next generation of the water flea *Daphnia magna*. PLoS One 7 (11):e48956.

132. Jacobasch C, Völker C, Giebner S, Völker J, Alsenz H, Potouridis T, Heidenreich H, Kayser G, Oehlmann J, Oetken M (2014) Long-term effects of nanoscaled titanium dioxide on the cladoceran *Daphnia magna* over six generations. Environ Pollut 186:180-186.

133. Zou XY, Li PH, Huang Q, Zhang HW (2016) The different response mechanisms of W*olffia globosa*: Light-induced silver nanoparticle toxicity. Aquatic Toxicology 176:97-105.

134. Jiang HS, Yin LY, Ren NN, Zhao ST, Li Z, Zhi YW, Shao H, Li W, Gontero B (2017) Silver nanoparticles induced reactive oxygen species via photosynthetic energy transport imbalance in an aquatic plant. Nanotoxicology 11 (2):157-167.

135. Thwala M, Klaine SJ, Musee N (2016) Interactions of metal-based engineered nanoparticles with aquatic higher plants: A review of the state of current knowledge. Environ Toxicol Chem 35 (7):1677-1694.

136. Du WC, Tan WJ, Peralta-Videa JR, Gardea-Torresdey JL, Ji R, Yin Y, Guo HY (2017) Interaction of metal oxide nanoparticles with higher terrestrial plants: Physiological and biochemical aspects. Plant Physiol Bioch 110:210-225.

137. Marslin G, Sheeba CJ, Franklin G (2017) Nanoparticles alter secondary metabolism in plants via ROS burst. Front Plant Sci 8. doi:ARTN 832

138. Tripathi DK, Shweta, Singh S, Singh S, Pandey R, Singh VP, Sharma NC, Prasad SM, Dubey NK, Chauhan DK (2017) An overview on manufactured nanoparticles in plants: Uptake, translocation, accumulation and phytotoxicity. Plant Physiol Bioch 110:2-12.

139. Cao ZM, Stowers C, Rossi L, Zhang WL, Lombardini L, Ma XM (2017) Physiological effects of cerium oxide nanoparticles on the photosynthesis and water use efficiency of soybean (*Glycine max* (L.) Merr.). Environ-Sci Nano 4 (5):1086-1094.

140. Batley GE, Kirby JK, McLaughlin MJ (2013) Fate and risks of nanomaterials in aquatic and terrestrial environments. Accounts of chemical research 46 (3):854-862.

141. Gil-Allué C, Schirmer K, Tlili A, Gessner MO, Behra R (2015) Silver nanoparticle effects on stream periphyton during short-term exposures. Environ Sci Technol 49 (2):1165-1172.

142. Jo HJ, Choi JW, Lee SH, Hong SW (2012) Acute toxicity of Ag and CuO nanoparticle suspensions against *Daphnia magna*: the importance of their dissolved fraction varying with preparation methods. J Hazard Mater 227-228:301-308.

143. Volker C, Kampken I, Boedicker C, Oehlmann J, Oetken M (2015) Toxicity of silver nanoparticles and ionic silver: Comparison of adverse effects and potential toxicity mechanisms in the freshwater clam *Sphaerium corneum*. Nanotoxicology 9 (6):677-685.

144. Doolette CL, Gupta VVSR, Lu Y, Payne JL, Batstone DJ, Kirby JK, Navarro DA, McLaughlin MJ (2016) Quantifying the sensitivity of soil microbial communities to silver sulfide nanoparticles using metagenome sequencing. Plos One 11 (8): e0161979

145. Nair PM, Park SY, Choi J (2013) Evaluation of the effect of silver nanoparticles and silver ions using stress responsive gene expression in *Chironomus riparius*. Chemosphere 92 (5):592-599.

146. Griffitt RJ, Hyndman K, Denslow ND, Barber DS (2009) Comparison of molecular and histological changes in zebrafish gills exposed to metallic nanoparticles. Toxicol Sci 107 (2):404-415.

147. Poynton HC, Lazorchak JM, Impellitteri CA, Blalock BJ, Rogers K, Allen HJ, Loguinov A, Heckrnan JL, Govindasmawy S (2012) Toxicogenomic responses of nanotoxicity in *Daphnia magna* exposed to silver nitrate and coated silver nanoparticles. Environ Sci Technol 46 (11):6288-6296.

148. Patricia CS, Nerea GV, Erik U, Elena SM, Eider B, Dario DW, Manu S (2017) Responses to silver nanoparticles and silver nitrate in a battery of biomarkers measured in coelomocytes and in target tissues of *Eisenia fetida* earthworms. Ecotoxicol Environ Saf 141:57-63.

149. Völker C, Oetken M, Oehlmann J (2013) The biological effects and possible modes of action of nanosilver. Reviews in Environmental Contamination and Toxicology 233:81-106

150. Yang YF, Cheng YH, Liao CM (2017) Nematode-based biomarkers as critical risk indicators on assessing the impact of silver nanoparticles on soil ecosystems. Ecological Indicators 75:340-351.

151. Hoheisel SM, Diamond S, Mount D (2012) Comparison of nanosilver and ionic silver toxicity in *Daphnia magna* and *Pimephales promelas*. Environ Toxicol Chem 31 (11):2557-2563.

152. Seitz F, Rosenfeldt RR, Strom K, Metrevelli G, Schaumann GE, Schulz R, Bundschuh M (2015) Effects of silver nanoparticle properties, media pH and dissolved organic matter on toxicity to *Daphnia magna*. Ecotoxicol Environ Saf 111:263-270

153. Pradas del Real AE, Vidal V, Carriere M, Castillo-Michel HA, Levard C, Chaurand P, Sarret G (2017) Ag nanoparticles and wheat roots: a complex interplay. Environ Sci Technol in press:doi:10.1021/acs.est.1027b00422

154. Wang P, Lombi E, Sun SK, Scheckel KG, Malysheva A, McKenna BA, Menzies NW, Zhao FJ, Kopittke PM (2017) Characterizing the uptake, accumulation and toxicity of silver sulfide nanoparticles in plants. Environ-Sci Nano 4 (2):448-460.

155. Dabrunz A, Duester L, Prasse C, Seitz F, Rosenfeldt RR, Schilde R, Schaumann GE, Schulz R (2011) Biological surface coating and molting inhibition as mechanisms of TiO2 nanoparticle toxicity in *Daphnia magna* PLoS One 6 (5):e20112

156. Baumann J, Koser J, Arndt D, Filser J (2014) The coating makes the difference: Acute effects of iron oxide nanoparticles on *Daphnia magna*. Sci Total Environ 484:176-184.

157. Gomes T, Chora S, Pereira CG, Cardoso C, Bebianno MJ (2014) Proteomic response of mussels *Mytilus galloprovincialis* exposed to CuO NPs and Cu2+: An exploratory biomarker discovery. Aquatic Toxicology 155:327-336.

158. Mortimer M, Kasemets K, Vodovnik M, Marinsek-Logar R, Kahru A (2011) Exposure to CuO nanoparticles changes the fatty acid composition of protozoa *Tetrahymena thermophila*. Environ Sci Technol 45 (15):6617-6624.

159. Adams J, Wright M, Wagner H, Valiente J, Britt D, Anderson A (2017) Cu from dissolution of CuO nanoparticles signals changes in root morphology. Plant Physiol Bioch 110:108-117.

160. Pradhan A, Seena S, Schlosser D, Gerth K, Helm S, Dobritzsch M, Krauss GJ, Dobritzsch D, Pascoal C, Cassio F (2015) Fungi from metal-polluted streams may have high ability to cope with the oxidative stress induced by copper oxide nanoparticles. Environ Toxicol Chem 34 (4):923-930.

161. Fernandez-Cruz ML, Lammel T, Connolly M, Conde E, Barrado AI, Derick S, Perez Y, Fernandez M, Furger C, Navas JM (2013) Comparative cytotoxicity induced

by bulk and nanoparticulated ZnO in the fish and human hepatoma cell lines PLHC-1 and Hep G2. Nanotoxicology 7 (5):935-952.

162. Nair PMG, Chung IM (2015) Alteration in the expression of antioxidant and detoxification genes in *Chironomus riparius* exposed to zinc oxide nanoparticles. Comp Biochem Phys B 190:1-7.

163. Su GY, Zhang XW, Giesy JP, Musarrat J, Saquib Q, Alkhedhairy AA, Yu HX (2015) Comparison on the molecular response profiles between nano zinc oxide (ZnO) particles and free zinc ion using a genome-wide toxicogenomics approach. Environmental Science and Pollution Research 22 (22):17434-17442.

164. Marisa I, Matozzo V, Munari M, Binelli A, Parolini M, Martucci A, Franceschinis E, Brianese N, Marin MG (2016) In vivo exposure of the marine clam Ruditapes philippinarum to zinc oxide nanoparticles: responses in gills, digestive gland and haemolymph. Environmental Science and Pollution Research 23 (15):15275-15293.

165. Huang CW, Li SW, Liao VHC (2017) Chronic ZnO-NPs exposure at environmentally relevant concentrations results in metabolic and locomotive toxicities in *Caenorhabditis elegans*. Environ Pollut 220:1456-1464.

166. Gomes SIL, Roca CP, Scott-Fordsmand JJ, Amorim MJB (2017) High-throughput transcriptomics reveals uniquely affected pathways: AgNPs, PVP-coated AgNPs and Ag NM300K case studies. Environ-Sci Nano 4 (4):929-937.

167. Makama S, Piella J, Undas A, Dimmers WJ, Peters R, Puntes VF, van den Brink NW (2016) Properties of silver nanoparticles influencing their uptake in and toxicity to the earthworm *Lumbricus rubellus* following exposure in soil. Environ Pollut 218:870-878.

168. Tan WJ, Du WC, Barrios AC, Armendariz R, Zuverza-Mena N, Ji ZX, Chang CH, Zink JI, Hernandez-Viezcas JA, Peralta-Videa JR, Gardea-Torresdey JL (2017) Surface coating changes the physiological and biochemical impacts of nano-TiO2 in basil (*Ocimum basilicum*) plants. Environ Pollut 222:64-72.

169. Garcia-Gomez C, Obrador A, Gonzalez D, Babin M, Fernandez MD (2017) Comparative effect of ZnO NPs, ZnO bulk and ZnSO4 in the antioxidant defences of

two plant species growing in two agricultural soils under greenhouse conditions. Sci Total Environ 589:11-24.

170. Oberdörster E, Zhu S, Blickley TM, McClellan-Green P, Haasch ML (2006) Ecotoxicology of carbon-based engineered nanoparticles: effects of fullerene (C60) on aquatic organisms. Carbon 44:1112-1120

171. Noss C, Dabrunz A, Rosenfeldt RR, Lorke A, Schulz R (2013) Three-dimensional analysis of the swimming behavior of *Daphnia magna* exposed to nanosized titanium dioxide. PLoS One 8 (11):e80960

172. Van Hoecke K, De Schamphelaere KAC, Van der Meeren P, Lucas S, Janssen CR (2008) Ecotoxicity of silica nanoparticles to the green alga *Pseudokirchneriella subcapitata*: importance of surface area. Environ Toxicol Chem 27 (9):1948-1957

173. Van Hoecke K, Quik JTK, Mankiewicz-Boczek J, De Schamphelaere KAC, Elsaesser A, Van der Meeren P, Barnes C, McKerr G, Howard CV, Van De Meent D, Rydzynski K, Dawson KA, Salvati A, Lesniak A, Lynch I, Silversmit G, De Samber B, Vincze L, Janssen CR (2009) Fate and Effects of CeO2 Nanoparticles in Aquatic Ecotoxicity Tests. Environ Sci Technol 43 (12):4537-4546.

174. Moon J, Kwak JI, Kim SW, An YJ (2017) Multigenerational effects of gold nanoparticles in *Caenorhabditis elegans*: continuous versus intermittent exposures. Environ Pollut 220:46-52.

175. Goncalves MFM, Gomes SIL, Scott-Fordsmand JJ, Amorim MJB (2017) Shorter lifetime of a soil invertebrate species when exposed to copper oxide nanoparticles in a full lifespan exposure test. Sci Rep-Uk 7. doi:ARTN 1355

176. Rico CM, Johnson MG, Marcus MA, Andersen CP (2017) Intergenerational responses of wheat (*Triticum aestivum* L.) to cerium oxide nanoparticles exposure. Environ-Sci Nano 4 (3):700-711.

177. Bundschuh M, Seitz F, Rosenfeldt RR, Schulz R (2016) Effects of nanoparticles in fresh waters – risks, mechanisms and interactions. Freshw Biol 61:2185–2196.

178. Docter D, Westmeier D, Markiewicz M, Stolte S, Knauer SK, Stauber RH (2015) The nanoparticle biomolecule corona: lessons learned - challenge accepted? Chem Soc Rev 44 (17):6094-6121.

179. Hall S, Bradley T, Moore JT, Kuykindall T, Minella L (2009) Acute and chronic toxicity of nano-scale TiO2, particles to freshwater fish, cladocerans, and green algae, and effects of organic and inorganic substrate on TiO2 toxicity. Nanotoxicology 3 (2):91-97

180. Hyung H, Fortner JD, Hughes JB, Kim JH (2007) Natural organic matter stabilizes carbon nanotubes in the aqueous phase. Environ Sci Technol 41 (1):179-184.

181. Seitz F, Rosenfeldt RR, Müller M, Lüderwald S, Schulz R, Bundschuh M (2016) Quantity and quality of natural organic matter influence the ecotoxicity of titanium dioxide nanoparticles. Nanotoxicology 10 (10):1415-1421

182. Park S, Woodhall J, Ma G, Veinot JGC, Boxall AB (2015) Does particle size and surface functionality affect uptake and depuration of gold nanoparticles by aquatic invertebrates? Environ Toxicol Chem 34 (4):850-859

183. Li CC, Wang YJ, Dang F, Zhou DM (2016) Mechanistic understanding of reduced AgNP phytotoxicity induced by extracellular polymeric substances. J Hazard Mater 308:21-28.

184. Chiang CW, Ng DQ, Lin YP, Chen PJ (2016) Dissolved organic matter or salts change the bioavailability processes and toxicity of the nanoscale tetravalent lead corrosion product PbO2 to medaka fish. Environ Sci Technol 50 (20):11292-11301.

185. Bicho RC, Soares AMVM, Nogueira HIS, Amorim MJB (2016) Effects of europium polyoxometalate encapsulated in silica nanoparticles (nanocarriers) in soil invertebrates. Journal of Nanoparticle Research 18 (12).

186. Tourinho PS, van Gestel CAM, Lofts S, Svendsen C, Soares AMVM, Loureiro S (2012) Metal-based nanoparticles in soil: Fate, behavior, and effects on soil invertebrates. Environ Toxicol Chem 31 (8):1679-1692.

187. Handy RD, Cornelis G, Fernandes T, Tsyusko O, Decho A, Sabo-Attwood T, Metcalfe C, Steevens JA, Klaine SJ, Koelmans AA, Horne N (2012) Ecotoxicity test methods for engineered nanomaterials: practical experiences and recommendations from the bench. Environ Toxicol Chem 31 (1):15-31.

188. Topuz E, van Gestel CAM (2017) The effect of soil properties on the toxicity and bioaccumulation of Ag nanoparticles and Ag ions in *Enchytraeus crypticus*. Ecotoxicol Environ Saf 144:330-337.

189. Velicogna JR, Ritchie EE, Scroggins RP, Princz JI (2016) A comparison of the effects of silver nanoparticles and silver nitrate on a suite of soil dwelling organisms in two field soils. Nanotoxicology 10 (8):1144-1151.

190. Waalewijn-Kool PL, Ortiz MD, Lofts S, van Gestel CAM (2013) The effect of pH on the toxicity of zinc oxide nanoparticles to *Folsomia candida* in amended field soil. Environ Toxicol Chem 32 (10):2349-2355.

191. Cupi D, Hartmann NB, Baun A (2015) The influence of natural organic matter and aging on suspension stability in guideline toxicity testing of silver, zinc oxide, and titanium dioxide nanoparticles with *Daphnia magna*. Environ Toxicol Chem 34 (3):497-506.

192. Seitz F, Rosenfeldt RR, Lüderwald S, Schulz R, Bundschuh M (2015) Aging of TiO2 nanoparticles transiently increases their toxicity to the pelagic microcrustacean *Daphnia magna*. PLoS One 10 (5):e0126021

193. McKee MS, Engelke M, Zhang X, Lesnikov E, Köser J, Eickhorst T, Filser  J (2017) Collembola reproduction decreases with aging of silver nanoparticles in a sewage sludge-treated soil. Frontiers in Environmental Sciences 5:19

194. Jackson BP, Bugge D, Ranville JF, Chen CY (2012) Bioavailability, toxicity, and bioaccumulation of quantum dot nanoparticles to the amphipod *Leptocheirus plumulosus*. Environ Sci Technol 46 (10):5550-5556.

195. Campos B, Rivetti C, Rosenkranz P, Navas JM, Barata C (2013) Effects of nanoparticles of TiO(2) on food depletion and life-history responses of *Daphnia magna*. Aquatic Toxicology 130-131C:174-183.

196. Bundschuh M, Vogt R, Seitz F, Rosenfeldt RR, Schulz R (2016) Do titanium dioxide nanoparticles induce food depletion for filter feeding organisms? A case study with *Daphnia magna*. Environ Pollut 214:840-846

197. Rosenfeldt RR, Seitz F, Zubrod JP, Feckler A, Merkel T, Lüderwald S, Bundschuh R, Schulz R, Bundschuh M (2015) Does the presence of titanium dioxide nanoparticles

reduce copper toxicity? A factorial approach with the benthic amphipod Gammarus fossarum. Aquatic Toxicology 165:154-159

198. Zhang XZ, Sun HW, Zhang ZY, Niu Q, Chen YS, Crittenden JC (2007) Enhanced bioaccumulation of cadmium in carp in the presence of titanium dioxide nanoparticles. Chemosphere 67 (1):160-166.

199. Schwab F, Bucheli TD, Camenzuli L, Magrez A, Knauer K, Sigg L, Nowack B (2013) Diuron sorbed to carbon nanotubes exhibits enhanced toxicity to *Chlorella vulgaris*. Environ Sci Technol 47 (13):7012-7019.

200. Brausch KA, Anderson TA, Smith PN, Maul JD (2010) Effects of functionalized fullerenes on bifenthrin and tribufos toxicity to *Daphnia magna*: Survival, reproduction, and growth rate. Environ Toxicol Chem 29 (11):2600-2606.

201. Boncel S, Kyziol-Komosinska J, Krzewska I, Czupiol J (2015) Interactions of carbon nanotubes with aqueous/aquatic media containing organic/inorganic contaminants and selected organisms of aquatic ecosystems - A review. Chemosphere 136:211-221.

202. Sanchis J, Olmos M, Vincent P, Farre M, Barcelo D (2016) New insights on the influence of organic co-contaminants on the aquatic toxicology of carbon nanomaterials. Environ Sci Technol 50 (2):961-969.

203. Fang Q, Shi XJ, Zhang LP, Wang QW, Wang XF, Guo YY, Zhou BS (2015) Effect of titanium dioxide nanoparticles on the bioavailability, metabolism, and toxicity of pentachlorophenol in zebrafish larvae. J Hazard Mater 283:897-904.

204. Farkas J, Bergum S, Nilsen EW, Olsen AJ, Salaberria I, Ciesielski TM, Baczek T, Konieczna L, Salvenmoser W, Jenssen BM (2015) The impact of TiO2 nanoparticles on uptake and toxicity of benzo(a)pyrene in the blue mussel (*Mytilus edulis*). Sci Total Environ 511:469-476.

205. Qiang LW, Pan XY, Zhu LY, Fang SH, Tian SY (2016) Effects of nano-TiO2 on perfluorooctanesulfonate bioaccumulation in fishes living in different water layers: Implications for enhanced risk of perfluorooctanesulfonate. Nanotoxicology 10 (4):471-479.

206. Fan WH, Cui MM, Liu H, Wang CA, Shi ZW, Tan C, Yang XP (2011) Nano-TiO2 enhances the toxicity of copper in natural water to *Daphnia magna*. Environ Pollut 159 (3):729-734.

207. Ma TW, Wang M, Gong SJ, Tian B (2017) Impacts of sediment organic matter content and pH on ecotoxicity of coexposure of TiO2 nanoparticles and cadmium to freshwater snails *Bellamya aeruginosa*. Arch Environ Contam Toxicol 72 (1):153-165.

208. Chen JY, Qian Y, Li HR, Cheng YH, Zhao MR (2015) The reduced bioavailability of copper by nano-TiO2 attenuates the toxicity to *Microcystis aeruginosa*. Environmental Science and Pollution Research 22 (16):12422-12429.

209. Li XM, Zhou SY, Fan WH (2016) Effect of nano-Al2O3 on the toxicity and oxidative stress of copper towards *Scenedesmus obliquus*. Int J Env Res Pub He 13:6. doi:ARTN 575

210. Della Torre C, Balbi T, Grassi G, Frenzilli G, Bernardeschi M, Smerilli A, Guidi P, Canesi L, Nigro M, Monaci F, Scarcelli V, Rocco L, Focardi S, Monopoli M, Corsi I (2015) Titanium dioxide nanoparticles modulate the toxicological response to cadmium in the gills of *Mytilus galloprovincialis*. J Hazard Mater 297:92-100.

211. Fan WH, Peng RS, Li XM, Ren JQ, Liu T, Wang XR (2016) Effect of titanium dioxide nanoparticles on copper toxicity to *Daphnia magna* in water: Role of organic matter. Water Res 105:129-137.

212. Rosenfeldt RR, Seitz F, Schulz R, Bundschuh M (2014) Heavy metal uptake and toxicity in the presence of titanium dioxide nanoparticles: A factorial approach using *Daphnia magna*. Environ Sci Technol 48:6965-6972

213. Canesi L, Ciacci C, Balbi T (2015) Interactive effects of nanoparticles with other contaminants in aquatic organisms: Friend or foe? Mar Environ Res 111:128-134.

214. McKee MS, Filser J (2016) Impacts of metal-based engineered nanomaterials on soil communities. Environ-Sci Nano 3 (3):506-533.

215. Wang XH, Li J, Liu R, Hai RT, Zou DX, Zhu XB, Luo N (2017) Responses of bacterial communities to CuO nanoparticles in activated sludge system. Environ Sci Technol 51 (10):5368-5376.

216. Button M, Auvinen H, Van Koetsem F, Hosseinkhani B, Rousseau D, Weber KP, Du Laing G (2016) Susceptibility of constructed wetland microbial communities to silver nanoparticles: A microcosm study. Ecological Engineering 97:476-485.

217. Ergon-Can T, Koseoglu-Imer DY, Algur OF, Koyuncu I (2016) Effect of different nanomaterials on the metabolic activity and bacterial flora of activated sludge medium. Clean-Soil Air Water 44 (11):1508-1515.

218. Pallavi Mehta CM, Srivastava R, Arora S, Sharma AK (2016) Impact assessment of silver nanoparticles on plant growth and soil bacterial diversity. 3 Biotech 6. doi:ARTN 254

219. Michels C, Perazzoli S, Soares HM (2017) Inhibition of an enriched culture of ammonia oxidizing bacteria by two different nanoparticles: Silver and magnetite. Sci Total Environ 586:995-1002.

220. Wang JA, Shu KH, Zhang L, Si YB (2017) Effects of silver nanoparticles on soil microbial communities and bacterial nitrification in suburban vegetable soils. Pedosphere 27 (3):482-490.

221. Filser J, Arndt D, Baumann J, Geppert M, Hackmann S, Luther EM, Pade C, Prenzel K, Wigger H, Arning J, Hohnholt MC, Koser J, Kuck A, Lesnikov E, Neumann J, Schutrumpf S, Warrelmann J, Baumer M, Dringen R, von Gleich A, Swiderek P, Thoming J (2013) Intrinsically green iron oxide nanoparticles? From synthesis via (eco-)toxicology to scenario modelling. Nanoscale 5 (3):1034-1046.

222. Cao JL, Feng YZ, Lin XG, Wang JH, Xie XQ (2017) Iron oxide magnetic nanoparticles deteriorate the mutual interaction between arbuscular mycorrhizal fungi and plant. J Soils Sediments 17 (3):841-851.

223. Rashid MI, Shahzad T, Shahid M, Imran M, Dhavamani J, Ismail IMI, Basahi JM, Almeelbi T (2017) Toxicity of iron oxide nanoparticles to grass litter decomposition in a sandy soil. Sci Rep-Uk 7. doi:ARTN 4196510.1038/srep41965

224. Antisari LV, Carbone S, Gatti A, Ferrando S, Nacucchi M, De Pascalis F, Gambardella C, Badalucco L, Laudicina VA (2016) Effect of cobalt and silver nanoparticles and ions on *Lumbricus rubellus* health and on microbial community of earthworm faeces and soil. Appl Soil Ecol 108:62-71.

225. Jemec A, Kos M, Drobne D, Koponen IK, Vuki J, Ferreira NGC, Loureiro S, McShane HVA (2016) In field conditions, commercial pigment grade TiO2 was not harmful to terrestrial isopods but reduced leaf litter fragmentation. Sci Total Environ 571:1128–1135

226. Garcia-Velasco N, Gandariasbeitia M, Irizar A, Soto M (2016) Uptake route and resulting toxicity of silver nanoparticles in *Eisenia fetida* earthworm exposed through Standard OECD Tests. Ecotoxicology 25 (8):1543-1555.

227. Lüderwald S, Schell T, Seitz F, Rosenfeldt RR, Newton K, Dackermann V, Schulz R, Bundschuh M (in preparation) Exposure pathway depended impacts of silver and titanium dioxide nanoparticles on *Gammarus fossarum*.

228. Das P, Williams CJ, Fulthorpe RR, Hoque ME, Metcalfe CD, Xenopoulos MA (2012) Changes in bacterial community structure after exposure to silver nanoparticles in natural waters. Environ Sci Technol 46 (16):9120-9128.

229. Bour A, Mouchet F, Cadarsi S, Silvestre J, Verneuil L, Baque D, Chauvet E, Bonzom J-M, Pagnout C, Clivot H, Fourquaux I, Tella M, Auffan M, Gauthier L, Pinelli E (2016) Toxicity of CeO2 nanoparticles on a freshwater experimental trophic chain: A study in environmentally relevant conditions through the use of mesocosms. Nanotoxicology 10:245-255.

230. Pradhan A, Seena S, Pascoal C, Cassio F (2011) Can metal nanoparticles be a threat to microbial decomposers of plant litter in streams? Microb Ecol 62:58-68.

231. Kalčíková G, Englert D, Rosenfeldt RR, Seitz F, Schulz R, Bundschuh M (2014) Combined effect of UV-irradiation and TiO2-nanoparticles on the predator-prey interaction of gammarids and mayfly nymphs. Environ Pollut 186:136-140

232. Pang C, Neubauer N, Boyles M, Brown D, Kanase N, Hristozov D, Fernandes T, Stone V, Wohlleben W, Marcomini A (2017) Releases from transparent blue automobile coatings containing nanoscale copper phthalocyanine and their effects on J774 A1 macrophages. Nanoimpact 7:75-83.

**Appendix A. 2**

# A blessing in disguise? Natural organic matter reduces the UV light-induced toxicity of nanoparticulate titanium dioxide

Lüderwald, S., Dackermann, V., Seitz, F., Adams, E., Feckler, A., Schilde, C., Schulz, R., Bundschuh, M.

**HIGHLIGHTS**

- Environmental parameters meaningfully modify nanoparticle toxicity
- UV light enhances the toxicity of titanium dioxide nanoparticles
- Natural organic matter increases ROS formed by titanium dioxide
- Oxidative stress and acute toxicity are reduced by natural organic matter
- Adverse nanoparticle effects potentially at predicted environmental concentrations

# ABSTRACT

Besides their economic value, engineered inorganic nanoparticles (EINPs) may pose a risk for the integrity of ecosystems. Among EINPs, titanium dioxide ($nTiO_2$) is frequently used and released into surface waters in the µg range. There, $nTiO_2$ interacts with environmental factors, influencing its potential to cause adverse effects on aquatic life. Although factors like ultra violet (UV) light and natural organic matter (NOM) are considered as ubiquitous, their joint impact on $nTiO_2$-induced toxicity is poorly understood. This study addressed the acute toxicity of $nTiO_2$ (P25; 0.00-64.00 mg/L; ~60 nm) at ambient UV light (0.00-5.20 W $UVA/m^2$) and NOM levels (seaweed extract; 0.00-4.00 mg TOC/L), using the immobility of *Daphnia magna* as response variable. Confirming previous studies, effects caused by $nTiO_2$ were elevated with increasing UV radiation (up to ~280 fold) and mitigated by higher NOM levels (up to ~12 fold), possibly due to reduced reactive oxygen species (ROS; measured as $^\bullet OH$ radicals) formation at lower UV intensities. However, contradicting to former studies, $nTiO_2$-mediated ROS formation was not proportional to increasing NOM levels: lower concentrations (0.04-0.40 mg TOC/L) slightly diminished, whereas a higher concentration (4.00 mg TOC/L) promoted the ROS quantity, irrespective of UV intensity. Measured ROS levels do not fully explain the observed $nTiO_2$-induced toxicity, whereas increasing acetylcholinesterase and glutathione-S-transferase activities in daphnids (in presence of 8.00 mg/L $nTiO_2$ and elevated UV intensity) point towards neurotoxic and oxidative stress as a driver for the observed effects. Hence, despite higher $^\bullet OH$ levels in the treatments where 4.00 mg TOC/L were present, NOM was still capable of reducing $nTiO_2$-induced stress and ultimately adverse effects in aquatic life.

## KEYWORDS

## INTRODUCTION

Engineered inorganic nanoparticles (EINPs) have experienced an increasing demand for commercial and industrial purposes (Farré et al. 2009, Scheringer 2008). Driven by their unique physicochemical properties (e.g. size, surface area, surface reactivity, charge, and shape), EINPs possess a broad range of possible applications, which include amongst others cosmetics, pharmacy, and medicine (Ito et al. 2005, Semenzin et al. 2015, Xiong et al. 2011). One of the most frequently manufactured and used EINP is titanium dioxide ($nTiO_2$; Keller and Lazareva 2014, Aitken et al. 2006, Piccinno et al. 2012), and as a consequence of its frequent use, it is inevitably released into surface waters through various pathways including facade paint runoff and wastewater treatment plant effluents (Kaegi et al. 2008, Kiser et al. 2009, Westerhoff et al. 2011). To determine the potential environmental risk associated with the use of $nTiO_2$, numerous studies assessed the ecotoxicological impact of $nTiO_2$ on aquatic organisms (e.g. Amiano et al. 2012, Rosenfeldt et al. 2015, Zhu et al. 2010).

In this context, one important factor modulating the fate and effect of EINPs in surface waters is omnipresent natural organic matter (NOM). Titanium dioxide nanoparticles coated with NOM can be stabilized in the surrounding medium (Chappell et al. 2009), and exhibit a diminished toxicity towards aquatic organisms (Schaumann et al. 2015). This altered toxicity positively correlates with the NOM's aromaticity and hydrophobicity (Seitz et al. 2016) by reducing bioavailability and reactivity of EINPs. Another factor of environmental relevance is the presence of UV light, which triggers the photocatalytic properties of $nTiO_2$ due to the formation of reactive oxygen species (ROS; Bhatkhande et al. 2002). This photocatalytic activity considerably enhances the ecotoxicological potential of $nTiO_2$ already at ambient UV intensities (Bar-Ilan et al. 2013, Marcone et al. 2012). ROS formed by $nTiO_2$ impair biological systems through, for instance, damaging fatty acids within cell membranes and consequently causing oxidative stress (Cabiscol et al. 2000).

There are studies available assessing the effect of both parameters UV and NOM on EINP toxicity (e.g. Li et al. 2016, Zhang et al. 2018, Wormington et al. 2017), however, mechanistic and systematic approaches facilitating an understanding of their joint effects on aquatic life are still limited. Therefore, the present study aims at a systematic assessment of the individual and combined effects of varying ambient NOM levels and UV intensities on the ecotoxicological potential of $nTiO_2$, using the immobility of the water flea *Daphnia magna* as response variable. The experimental design largely

followed the OECD guideline 202 (OECD 2004), with an elongated exposure duration of 96 h (Dabrunz et al. 2011). Additionally, the illumination conditions were changed from laboratory light to field relevant UV intensities (0.00-5.20 W UVA m²; wavelength: 315-380 nm; exposure period: 8 h/day; (Amiano et al. 2012, Häder et al. 2007) and NOM levels (seaweed extract; 0.00-4.00 mg TOC/L; Marinure®, Glenside, Scotland; (Ryan et al. 2009). With the aim to relate the photocatalytic activity of nTiO$_2$ under the different exposure scenarios to the ecotoxicological impact, the formation of ROS was quantified during the course of the experiments, using ˙OH radicals as a proxy. Additionally, glutathione-S-transferase (GST) activity, glutathione (GSH) content, as well as acetylcholinesterase (AChE) activity were determined in *Daphnia*. These biomarkers are involved in the defense system towards oxidative and neurotoxic stress and can inform about the mechanisms of EINP toxicity (Barata et al. 2005, Kim et al. 2010, Ulm et al. 2015). It was hypothesized that the presence of NOM mitigates the toxicity of UV irradiated nTiO$_2$ towards *D. magna*, a pattern that should be explained by (i) suppression of ROS formation (as proposed by Wormington et al. 2017) through EINP surface coating, and (ii) reduced biomarker responses within the different treatments.

## MATERIAL AND METHODS

### Test Substance

The applied nTiO$_2$ product P25 (consisting of Anatase and Rutile; ratio: ~75:25) was purchased as powder (AEROXIDE® TiO$_2$ P25, Evonik, Germany). The advertised primary particle size of the powder was 21 nm with a surface area of 50 ±15 m$^2$/g. Using deionized water as dispersant, an additive free suspension (80 g nTiO$_2$/L) was prepared by stirred media milling (PML 2, Bühler AG, Switzerland). This suspension was diluted with deionized water (stock suspension; 2.00 g nTiO$_2$/L; nominal concentration) and pH stabilized (~3.25) by applying 120 µL of 2M HCl/L. The intensity-weighted monodispersed average particle size of the stock suspension was 59.60 ±3.78 nm (mean ±SD; Tab. 1) according to dynamic light scattering (*n*=3; 60 measurements each; temperature: 20°C; pinhole: 100 µm; DelsaNano C, Beckman Coulter, Germany). Prior to its application (i.e. before spiking of nTiO$_2$ to the test medium), the stock suspension (2.00 g nTiO$_2$/L) was sonicated for 10 minutes (SONOREX DIGITEC DT 514 H, Bandelin, Germany; nominal power: 215 W; sonication frequency: 35 Hz) to ensure a homogeneous particle distribution and thus

an accurate transfer of particles to the test medium. Since inductively coupled plasma mass spectrometry – described in Rosenfeldt et al. (2014) – revealed no substantial differences between measured and nominal concentrations at the test initiation, this study is exclusively based on the nominal $nTiO_2$ concentration (see also in Seitz et al. 2015a).

**Table 1.** Particle size distribution, cumulated diameter expressed as average diameter (nm ±SD; $n$=3), polydispersity index (PI), 10th, 50th and 90th percentile of the particle distribution in the $nTiO_2$ stock suspension.

| Individual Measurement | Cumulated Diameter (nm) | PI | D (10%) | D (50%) | D (90%) |
|---|---|---|---|---|---|
| 1 | 60.9 | 0.06 | 35.9 | 60.6 | 104.1 |
| 2 | 55.3 | 0.21 | 28.3 | 59.1 | 120.8 |
| 3 | 62.5 | 0.15 | 28.7 | 66.1 | 157.0 |
| Average Diameter: | 59.6 ±3.8 | 0.14 | 30.9 | 61.9 | 127.3 |

To investigate $nTiO_2$ size changes during each of the acute toxicity tests, the particle size distribution was analyzed approximately five minutes after the application to the test medium (ASTM ±NOM; ASTM 2007) as well as after 48, and 96 h at a nominal concentration of 2.00 mg $nTiO_2$/L (ASTM ±NOM, ±UV; Tab. S1).

**Test Organism**

*D. magna* (Eurofins-GAB, Germany) were kept in a permanent culture within a climate-controlled chamber (Weiss Environmental Technology Inc., Germany) at 20 ±1°C with a 16:8 h (light:dark) photoperiod (luminescent tubes; visible light intensity: 3.14 W/m$^2$; UVA: 0.01 W/m$^2$; UVB: 0.01 W/m$^2$; as detailed in Dabrunz et al. 2011). Groups of 25 adult organisms were kept in 1.5 L of reconstituted hard freshwater, according to the ASTM International Standard Guide E729 (ASTM 2007), additionally enriched with selenium, vitamins (thiamine hydrochloride, cyanocobalamin, and biotin; ASTM), and with seaweed extract (SW; 8.00 mg TOC/L; Marinure®, Glenside, Scotland). A renewal of the medium was performed three times a week and the animals were fed on a daily basis with the green algae *Desmodesmus* sp. (200 µg C/organism).

## Toxicity Studies

All experiments followed the OECD guideline 202 (OECD 2004), whereas the test duration was prolonged to 96 h, as recommended for nanoparticle testing (Dabrunz et al. 2011, Karimi et al. 2018). Moreover, instead of luminescent tubes, UV fluorescent lamps (Magic Sun 23/160 R 160 W, Heraeus, Germany; UVA output: 44 W, UVB output: 1.1%) were used as light source with a 8:16 h (light:dark) photoperiod at comparably low but still environmentally relevant intensities (Häder et al. 2007).

In particular, 20 acute tests structured in test series (TS) I-V were conducted. The nominal $nTiO_2$ concentrations applied for all test series were 0.00, 0.10, 0.20, 1.00, 2.00, 4.00, 8.00, 16.00, 32.00, and 64.00 mg/L. Each test series consisted of four acute tests with varying nominal NOM concentrations (applying SW as conventional representative (Seitz et al. 2016, OECD 2008); at 0.00, 0.04, 0.40, and 4.00 mg TOC/L), while using ASTM as test medium. Prior to its application, a SW sample (8.00 mg TOC/L, diluted in 50 mL test medium, and $nTiO_2$-free) was analysed at the DOC-LABOR (Karlsruhe, Germany), allowing for a detailed characterization of the substance (*inter alia* TOC content; Tab. S2, contains the data as per Seitz et al. 2016). SW was chosen as NOM source, given its recommendation in the OECD guideline 211 as additive for long-term culturing of *D. magna* and chronic *Daphnia* experiments (OECD 2008).

TS I was conducted in total darkness, whereas TS II-V were characterized by the presence of increasing UVA intensities: 0.40-0.60 (II), 1.00-1.40 (III), 2.20-2.60 (IV) and 4.80-5.20 (V) W/m$^2$ (Magic Sun 23/160 R 160W, Heraeus, Germany; UVA output: 44W, UVB output: 1.1%; measured with a RM12 radiometer, Dr. Göbel UV-Electronic GmbH, Germany). The different UVA intensities were achieved by attaching differently UV-porous curtains below the UV lamps. For all acute toxicity tests five juvenile daphnids (age <24 h) were exposed to the respective combination of $nTiO_2$, NOM and UV levels per replicate, while each treatment was replicated four times. Every 24 h, daphnids were visually checked for their mobility (i.e. after 24, 48, 72 and 96 h of exposure). Finally, immobility data was used in order to calculate $nTiO_2$ 96-h $EC_{50}$ concentrations for the respective treatments. $EC_{50}$ values of this study are based on 96 h exposure duration, as calculations for shorter exposure times were partly not possible since dose-response relationship could not always be observed. Animals were considered as immobile when the test beaker was gently agitated and no movement was recognizable within 10 sec.

## ROS Analysis

The amount of $^{\bullet}OH$ radicals was used as a proxy for ROS, as they are predominantly formed by $nTiO_2$ (Kim et al. 2013) when illuminated by UV light ($\lambda$ <365 nm (Ahmed et al. 2010) besides other oxygen radicals (*inter alia* $^{\bullet}O_2^{-}$, $^{\bullet}OOH$, and $H_2O_2$; Brezová et al. 2005, Hirakawa et al. 2004). ROS were monitored for each TS and NOM level at three $nTiO_2$ concentrations (0.00, 4.00, and 8.00 mg/L; $n$=3), generally following the method by Tang et al. (2005). Thereby, the amount of $^{\bullet}OH$ was measured in relative fluorescence units, emitted by the reaction product of disodium terephthalate and $^{\bullet}OH$, using a microplate reader (MPR; Tecan Infinite® M200, Tecan Group Ltd., Switzerland) at excitation and emission wavelengths of 310 and 430 nm, respectively. For each acute toxicity study a second set of replicates was prepared and used for the $^{\bullet}OH$ quantification. After 0, 48 and 96 h of UV illumination, 20 mL of an aqueous solution containing 1.30 g disodium terephthalate/L (Alfa Aesar GmbH & Co. KG, Germany) were added and the disodium terephthalate was allowed to react with $^{\bullet}OH$ for 5 minutes (Feckler et al. 2015). Subsequently, 200 µL of each replicate were transferred into a microplate (96F Nunclon Delta Black Microwell SI, Nunc GmbH & Co. KG, Germany) and analysed in the MPR. Thereby, the measured amount of relative fluorescence units was interpreted as a quantitative estimation for ROS.

## Biomarker Assays

Enzymatic assays were conducted as part of additional experiments according the procedure of Mingo et al. (2017), modified for the application to *D. magna* (Barata et al. 2005), and measured colorimetrically using the MPR. As these methods require relatively high biomasses, approximately 600 neonates (age <24 h) were raised for 5 days in a 15-L aquarium. Subsequently, these daphnids (instead of juveniles of an age below 24 h) were exposed under static conditions for 48 h to one of 12 treatments characterised by all possible combinations of $nTiO_2$ (0.00 or 8.00 mg/L), NOM (0.00 or 4.00 mg TOC/L), and UVA radiation (0.00, 0.40-0.60, or 2.20-2.60 W/m$^2$). Each treatment was replicated 10 times, containing 5 daphnids per replicate in 50 mL of test medium. After 48 h, the daphnids from each replicate (henceforth referred to as sample) were immediately shock frozen in liquid nitrogen and stored at -80 °C.

For the measurements, frozen samples were thawed on ice and subsequently homogenized in a mixer mill (Retsch MM 301, Retsch GmbH, Germany) for 60 sec,

after adding 35 mg silica beads and 200 µL lysis buffer (containing 25 mM Tris-HCl and 0.1% Triton X-100). Following, each replicate was centrifuged at 4 °C for 3 min at 4,200 rpm. Both steps were repeated. The supernatant was stored at -80 °C until further use. Total protein contents were determined with the MPR at 25 °C following the method of Bradford applying Bovine Serum Albumin (BSA) as standard (Bradford 1976).

AChE activity was measured following the procedure of Ellman et al. (1961). The reaction medium contained 180 µL potassium phosphate (85 mM, pH 7.4, including 0.425 mM 5.50´dithio-bis(2-nitrobenzoicacid); DTNB), 10 µL acetylthiocholine (1 mM), and 10 µL of the sample. Reaction media were analysed at 25 °C in the MPR, measuring the absorbance at 405 nm every 60 sec for 10 min, and enzymatic activity was expressed as mmol/mg$^{-1}$ protein/min, using a molar extinction coefficient of 1.36 × 10$^4$ M$^{-1}$ cm$^{-1}$.

GST activity was determined using the method of Habig et al. (1974). The reaction medium comprised of 150 µL potassium phosphate buffer (100 mM, pH 6.5, containing 0.1% Triton-X 100), 10 µL 1-chloro-2,4- dinitrobenzene (40 mM; CDNB), 20 µL Glutathione (200 mM), as well as 20 µL sample. Reaction media were analysed at 25 °C in the MPR, measuring the absorbance at 340 nm every 60 sec for 10 min, and enzymatic activity was expressed as mmol/mg$^{-1}$ protein/min, using a molar extinction coefficient of 0.00503 µM$^{-1}$.

Glutathione (GSH) was quantified using the method of Griffith and Owen (Griffith 1980). The reaction medium contained 80 µL of 0.3 mM NADPH and 6 mM DTNB in a 7:1 ratio (NADPH and DTNB was prior dissolved in 125 mM Na-phosphate buffer containing 6.3 mM Na-EDTA, at pH 7.5), 10 µL glutathione reductase/mL glutathione reaction buffer, and 20 µL sample. A GSH standard and the increment of absorbance at 405 after 60 sec at 25 °C (using the MPR) was used to calculate the GSH concentrations.

**Statistical Analysis**

The data obtained after 96 h of exposure served as basis for the calculation of EC$_{50}$ values, defined as the concentration of the test substance (here: nTiO$_2$) causing immobility in 50% of the test organisms. Therefore, the immobilization data of each experiment was corrected for control mortality (never exceeding 10%) using Abbott's formula. Following, the dataset was used for fitting dose-response models (Ritz and

Streibig 2005). The selection of the most appropriate models was based on Akaike's information criterion and visual judgment. The 96-h $EC_{50}$ values were tested for statistically significant differences among factor combinations by applying Bonferroni adjusted confidence interval (CI) testing (Wheeler et al. 2006).

Biomarkers assays were assessed for the applicability of parametric testing by applying the Shapiro-Wilk Normality Test and the Bartlett Test of Homogeneity of Variances. If the requirements for parametric testing were met, a one-way ANOVA was implemented. If the requirements were not met a Kruskal-Wallis Test was applied on the data. Ultimately, either Dunnett's (parametric) or Wilcoxon rank sum tests (nonparametric) were applied as *post-hoc* evaluation for statistically significant differences ($p < 0.05$) and in case of multiple comparisons *p*-values were Bonferroni adjusted. All statistical analyses and figures were implemented with the statistical software environment R for Mac (version 3.4.4) and additional packages (Lemon 2006, Core Team R 2013).

## RESULTS

### Acute Toxicity Tests

#### Test Series I: 0.00 W UVA/m$^2$

In darkness it was not possible to calculate 96-h $EC_{50}$ values, since none of the applied test concentrations (0.00-64.00 mg/L) caused at least 50% immobility in the respective treatments, except in absence of NOM (96-h $EC_{50}$: 28.83 mg $nTiO_2$/L, 95% CI: 13.30-44.37 mg/L).

#### *Test Series II: 0.40-0.60 W UVA/m$^2$*

At the lowest applied UV radiation of 0.40-0.60 W UVA/m$^2$ the toxicity of $nTiO_2$ to *D. magna* was significantly (up to ~8-fold) reduced by NOM concentrations ≥0.40 mg TOC/L, relative to the absence of NOM (Fig. 1; Fig. S1 B). The 96-h $EC_{50}$ increased from 1.08 mg $nTiO_2$/L (95% CI: 0.74-1.42 mg/L) at 0.00 mg TOC/L, to 12.12 mg $nTiO_2$/L (95% CI: 5.70-18.54 mg/L) at 0.40 mg TOC/L, and 8.94 mg $nTiO_2$/L (95% CI: 5.25-12.62 mg/L) at 4.00 mg TOC/L.

### Test Series III: 1.00-1.40 W UVA/m²

At an intensity of 1.00-1.40 W UVA/m² the presence of 0.04 mg TOC/L (96-h $EC_{50}$: 0.25 mg nTiO$_2$/L, 95% CI: 0.06-0.40 mg/L) caused an approx. 3.5-fold higher toxicity of nTiO$_2$, compared to the absence of TOC (96-h $EC_{50}$: 0.84 mg nTiO$_2$/L, 95% CI:0.60-1.09 mg/L), whereas for higher NOM concentrations the toxic potential of nTiO$_2$ was reduced by ~1.5-fold (at 0.40 mg TOC/L; 96-h $EC_{50}$: 1.16 mg nTiO$_2$/L, 95% CI: 0.98-1.34 mg/L) and a factor of ~5 (at 4.00 mg TOC/L; 96-h $EC_{50}$: 4.26 mg nTiO$_2$/L, 95% CI: 3.84-4.67 mg/L; Fig. 1; Fig. S1 B), respectively.
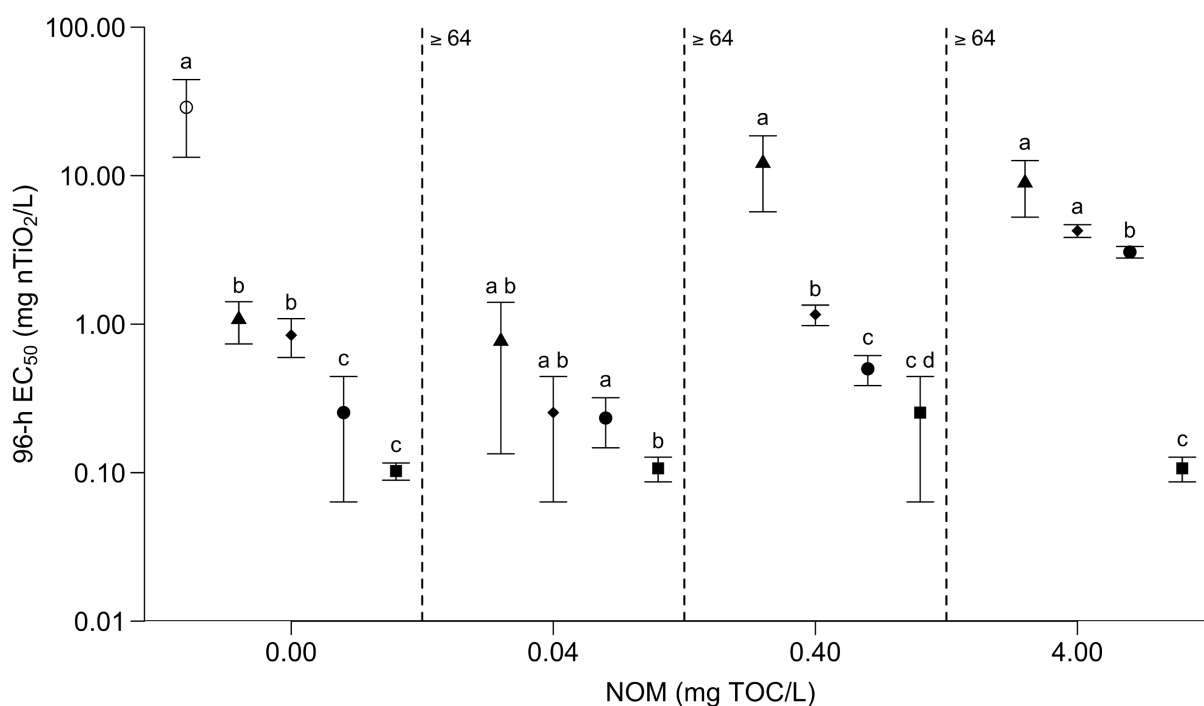


**Figure 1.** 96-h $EC_{50}$ (±95% CI) of *D. magna*, exposed to nTiO$_2$ (0.00-64.00 mg/L) in ASTM +NOM (0.00-4.00 mg TOC/L), in the presence of UV light (0.00-5.20 W UVA/m²). ○=TS I (0.00 W UVA/m²), ▲=TS II (0.40-0.60 W UVA/m²), ◆=TS III (1.00-1.40 W UVA/m²), ●=TS IV (2.20-2.60 W UVA/m²), and ■=TS V (4.80-5.20 W UVA/m²). Different letters denote statistically significant difference between individual TS but within one NOM level. ≥64 represents the treatments where a 96-h $EC_{50}$ calculation was not possible due to less than 50% observed immobility of the test organism at the highest applied nTiO$_2$ concentration (64.00 mg/L).

114

### Test Series IV: 2.20-2.60 W UVA/m$^2$

TS IV revealed a similar pattern as observed for TS II and III, i.e. in presence of 2.20-2.60 W UVA/m$^2$, NOM concentrations ≥0.40 mg TOC/L reduced the toxicity of nTiO$_2$ by a factor from ~2 (0.40 mg TOC/L; 96-h EC$_{50}$: 0.50 mg nTiO2/L, 95% CI: 0.39-0.61 mg/L) to ~12 (4.00 mg TOC/L; 96-h EC$_{50}$: 3.06 mg nTiO2/L, 95% CI: 2.79-3.33 mg/L; Fig. 1; Fig. S1 D), relative to a TOC absence (96-h EC$_{50}$: 0.25 mg nTiO$_2$/L, 95% CI: 0.06-0.44 mg/L).

### Test Series V: 4.80-5.20 W UVA/m$^2$

At the highest applied UV radiation nTiO$_2$ caused for all investigated NOM concentrations 96-h EC$_{50}$ values between 0.10-0.25 mg/L and therefore the strongest impact on *Daphnias*' survival among all TS (Fig. 1; Fig. S1 E).

### Comparison of Test Series I-V

Generally, the nTiO$_2$-induced toxicity in *D. magna* increased with increasing UV radiation: in the absence of NOM, for instance, the 96-h EC$_{50}$ decreased by a factor of ~2.5 (TS II), ~8.0 (TS III), ~10.0 (TS IV), and ~280.0 (TS V; Fig. 1; Fig. S1; Tab. S3) relative to TS I (no UV). Moreover, with exception of TS V, NOM levels beyond 0.04 mg/L caused within a particular UV intensity a reduction in nTiO$_2$ toxicity (with a factor of max. ~5.5 (TS I), ~8.0 (TS II), ~5.0 (TS III), and ~12.0 (TS IV; Fig. 1; Fig. S1; Tab. S3). Furthermore, it was noticeable that the effect of NOM on the nTiO$_2$ toxicity was repealed at the highest UV intensity (TS V; 4.80-5.20 W UVA/m$^2$), which showed almost identical EC$_{50}$ values among all investigated NOM levels ( 0.10≤ 96-h EC$_{50}$ ≤0.25 mg nTiO$_2$/L).

### ROS Quantification

In the absence of UV light, the potential of nTiO$_2$ to form ROS was the lowest – irrespective of the NOM (0.00-4.00 mg TOC/L) or particle concentration (0.00-8.00 mg/L) – with an amount of ~70 fluorescence units (data not shown). With increasing UV intensity and TOC concentration the quantity of ROS produced increased from 105 ±1 (mean ±SD, *n*=3, 0.00 mg TOC/L, 0.00 mg nTiO$_2$/L) up to 42,000 ±640 (mean ±SD; *n*=3; 4.00 mg TOC/L; 8.00 mg nTiO$_2$/L; c.f. Figs. 2 A-D) fluorescence units. Moreover, increasing nTiO$_2$ concentrations additionally favoured the formation of ROS, for all

applied UV light intensities (Figs. 2 A-D). On the contrary, the $nTiO_2$ induced ROS formation was not inversely related to increasing NOM levels: whereas lower concentrations (0.04-0.40 mg TOC/L) partly mitigated the ROS production marginally, a higher concentration (4.00 mg TOC/L) elevated this variable. The latter effect increased with increasing UV intensity (c.f. Figs. 2 A-D).
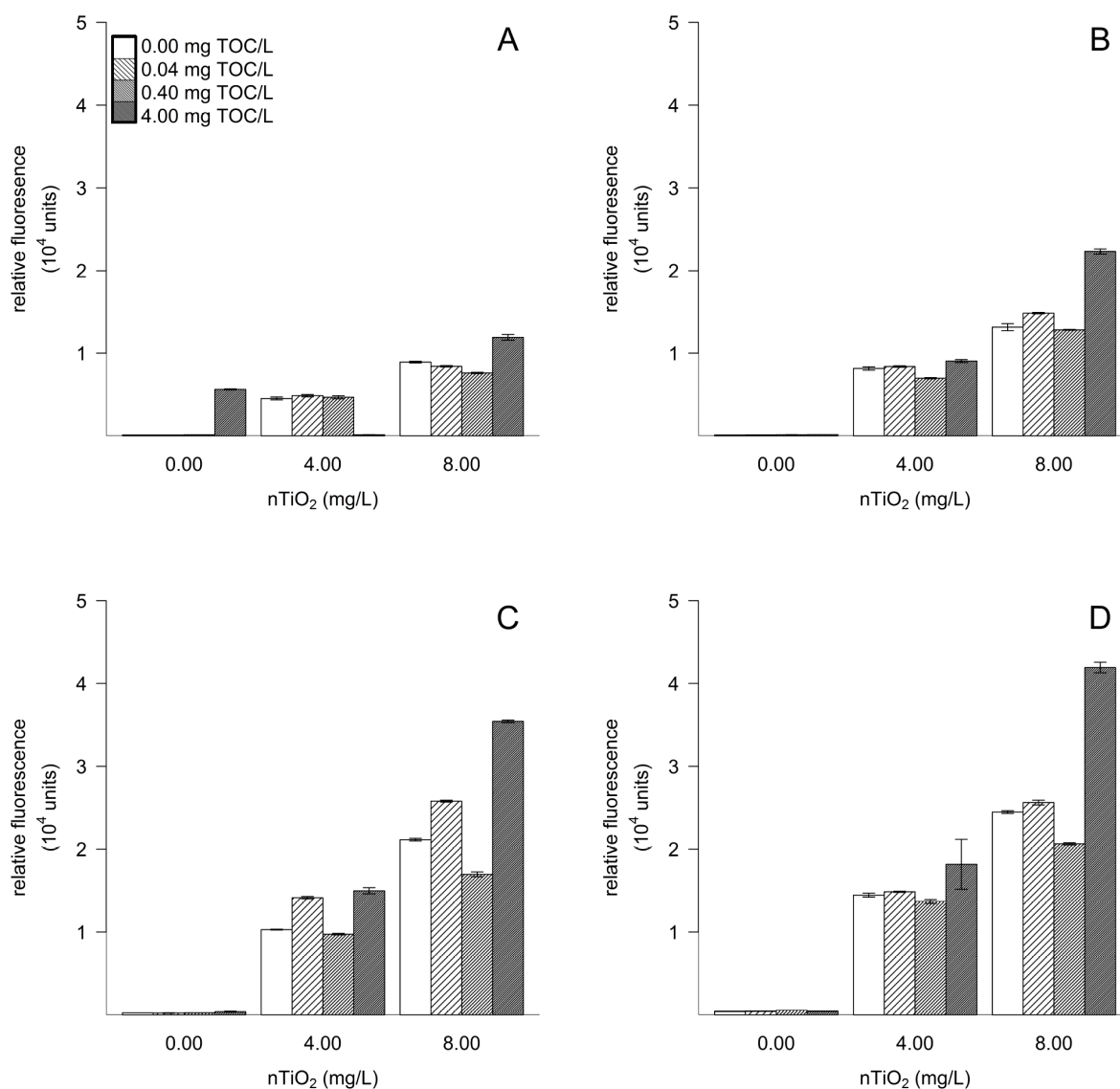


**Figure 2:** Mean relative fluorescence ($10^4$ units ±SD, $n$=3), representative for ROS formation of $nTiO_2$ (0.00, 4.00 and 8.00 mg/L), measured in ASTM +NOM (0.00, 0.04, 0.40 and 4.00 mg TOC/L) after 96 h in the presence of different UV light intensities (A: 0.40-0.60 W UVA/m²; B: 1.00-1.40 W UVA/m²; C: 2.20-2.40 W UVA/m²; D: 4.80-5.20 W UVA/m²). Mean relative fluorescence of approx. 70 fluorescence units in the absence of UV is not shown.

**Biomarker Assays**

Within the control treatment (absence of $nTiO_2$) we observed a significant 1.7-fold increase of AChE activity with increasing UV intensity (comparing 0.00 vs. 2.20-2.60 W UVA/$m^2$; Fig. 3 A). In the presence of NOM, AChE activity was not affected independent of the applied UV intensity. When $nTiO_2$ (8.00 mg/L) was applied the effect of UV radiation on the AChE activity was even more pronounced and was significantly (up to 2.6-fold) elevated compared to the control (at 2.20-2.60 W UVA/$m^2$; Fig.3 A). The combination of $nTiO_2$ and NOM resulted in a reduced effect but the same pattern relative to the $nTiO_2$ only treatment (Fig. 3 A).

For the control, as well as the NOM treatment the presence of UV radiation revealed no significant impact on the GST activity. In presence of $nTiO_2$ and UV ($nTiO_2$, and $nTiO_2$ +NOM), however, GST levels were significantly increased up to 6.5-fold, relative to the control (comparing 0.40-0.60 W UVA/$m^2$, control vs. $nTiO_2$; Fig. 3 B). When $nTiO_2$ and NOM were jointly present, we observed a reduced GST activity compared to the $nTiO_2$ only treatment – however solely at medium UV intensities (0.40-0.60 W UVA/$m^2$).

Glutathione (GSH) content was neither significantly affected by UV, NOM, nor $nTiO_2$, relative to the control (Fig. 3 C). However, except for the $nTiO_2$ treatment we observed the tendency to an increased GSH content at 0.40-0.60 W UVA/$m^2$ (for the control, NOM, and $nTiO_2$ +NOM treatment), followed by a decrease at 2.20-2.60 W UVA/$m^2$, comparable to GSH contents in darkness (Fig. 3 C).
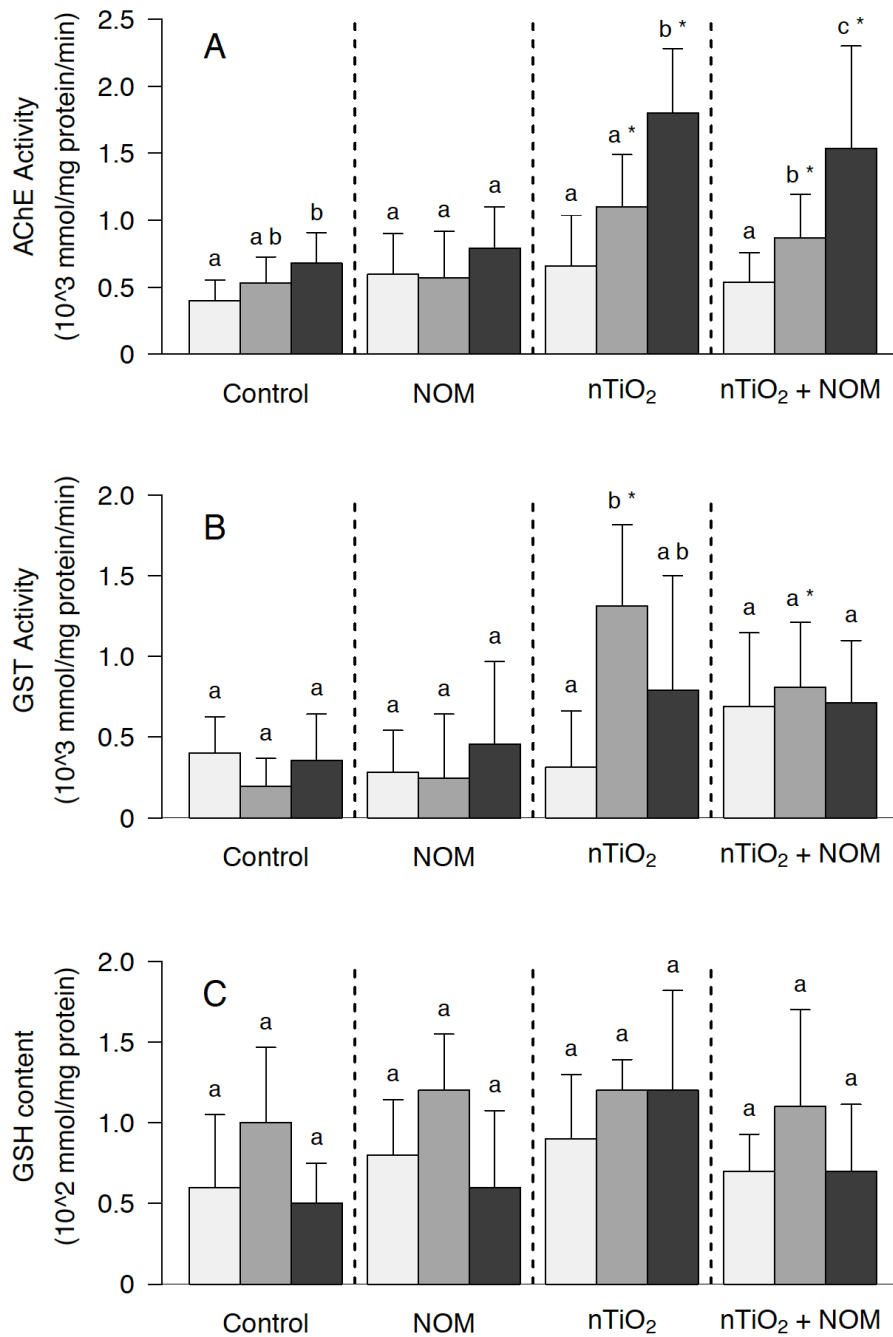
**Figure 3.** Median (A) AChE activity (±SD; mmol/mg protein/min), (B) GST activity (±SD; mmol/mg protein/min), and (C) GSH content (±SD; mmol/mg protein) in *D. magna* after being exposed for 48 h to the control, NOM (SW, 4.00 mg TOC/L), $nTiO_2$ (P25, 8.00 mg/L), as well as the combination of $nTiO_2$ +NOM (P25, 8.00 mg/L; SW, 4.00 mg TOC/L). The shading of the bars indicates the applied UVA intensities (light grey: 0.00 $W/m^2$, medium grey: 0.40-0.60 $W/m^2$, and dark grey: 2.20-2.60 $W/m^2$). Different letters denote statistically significant difference between increasing UVA intensities within one treatment. Asterisks denote statistically significant difference to the control treatment at the respective applied UVA intensity.

**DISCUSSION**

In our study the toxic potential of $nTiO_2$ for *D. magna* generally decreased with an increasing NOM concentration (≥0.40 mg TOC/L) by a factor of up to ~8.5 (e.g. TS II; 0.40-0.60 W UVA/m²; 96-h $EC_{50}$: 1.07 mg $nTiO_2$/L (0.00 mg TOC/L) to 8.93 mg $nTiO_2$/L (4.00 mg TOC/L); Fig. 1). This pattern may be explained by the coating of both, the EINPs and test species with NOM (Schaumann et al. 2015, Klaine et al. 2008). This assumption is indirectly supported by zeta potential measurements whose values became more negative with increasing NOM concentrations (as detailed in Seitz et al. 2016; Tab. S4) indicating an increased NOM surface adsorption. This process modifies the bioavailability of the nanoparticles and ultimately reduces their toxicity – at least in terms of survival (cf. Seitz et al. 2015a, Hall et al. 2009, Brame et al. 2014, Kolts et al. 2008).

Thereby, the NOM coverage of the particles as well as the organism prevented an attachment of $nTiO_2$ to the daphnias' surface (Lin et al. 2012), proposed as being one mode of toxic action of $nTiO_2$ (=biological surface coating (Dabrunz et al. 2011). Hall et al. (2009), for instance, observed a decreased acute $nTiO_2$ toxicity for *Ceriodaphnia dubia* depicted by an increased 48-h $LC_{50}$ value (lethal concentration required to kill 50% of the test organisms) from 7.60 mg $TiO_2$/L in the absence of TOC to >100 mg $nTiO_2$/L in the presence of 1.50 mg TOC/L. Similarly, in our study a reduction of $nTiO_2$-induced toxicity was observable at NOM concentrations ≥0.40 mg TOC/L (Fig. 1). Moreover, NOM is suggested to act as an additional source of energy for *D. magna*, which can already increase energy reserves in the organisms after 96 h, resulting in a generally higher stress tolerance (Seitz et al. 2015a, Bergman Filho et al. 2011, Bouchnak and Steinberg 2010).

Contrary to NOM, UV light enhanced the toxic potential of $nTiO_2$ towards *D. magna* by a factor of up to ~280 (Fig. 1). This distinct increase in $nTiO_2$-induced toxicity was already detected at low but environmentally relevant intensities as low as 5.20 W UVA/m². As intensities can range from 2.6 W UVA/m² (northern Spain during summer, afternoon in the shade; Amiano et al. 2012) to more than 50 W UVA/m² (western South America during summer, at clear sky; Häder et al. 2007)), the impact of UV light on the toxic potential of $nTiO_2$ will likely vary drastically across the globe but also depends on the time of day and season.

Our findings are supported by a range of earlier publications describing elevated $nTiO_2$ toxicity with increasing UV intensity (e.g. Marcone et al. 2012, Kalčíková et al. 2014,

Ma et al. 2012a, Mansfield et al. 2015). This increase in toxicity is due to $nTiO_2$'s photocatalytic properties, forming ROS when illuminated with UV light (Johnston et al. 2009, Ma et al. 2012b). These ROS are primarily composed of hydroxyl ($^{\bullet}OH$) and super oxide ($O_2^-$) radicals (Kim et al. 2013, Nowotny 2008). As a consequence, aquatic organisms like *D. magna*, may suffer from oxidative stress, for instance through lipid peroxidation within cell membranes, oxidative damage of proteins or mutation of DNA (Cabiscol et al. 2000, Buonocore et al. 2010). Thus, the elevated $nTiO_2$ toxicity with increasing UV intensities seems to be most likely driven by an amplified formation of ROS. This assumption is underpinned by the supplementing ROS measurements, revealing with 24,500-42,000 relative fluorescence units (0.00-4.00 mg TOC/L; 8.00 mg $nTiO_2$/L) the highest quantity of ROS at the highest UV intensity (4.80-5.20 W UVA/$m^2$; cf. Fig. 2 A-D). Besides the UV intensity, the concentration of $nTiO_2$ also positively influenced the formation of ROS (Fig. 2), which can be explained by an increased availability of reactive surface area (Seitz et al. 2012).

Accordingly, the biomarker assays revealed a significantly elevated AChE activity in *D. magna* with increasing UV radiation in presence of $nTiO_2$ (8.00 mg/L), indicating a neurotoxic effect of $nTiO_2$. This might be explained by a possible interaction of $nTiO_2$ or ROS with the animals' acetylcholine receptors affecting their binding efficiency and potentially causing an increased AChE synthesis. A similar mechanism was proposed by Bainy et al. (2006) for Cd in the digestive gland of the brown mussel *Perna perna*. Likewise, Ulm et al. (2015) observed an increased AChE activity in *D. magna* as a result of an acute (48-h) exposure to nanoparticulate silver, which was assumed to be triggered by a *de novo* synthesis of the enzyme as response to an initial AChE inhibition. Moreover, an exposure to $nTiO_2$ could also lead to an enhancement of the enzyme-substrate comlex, ultimately accelerating the AChE activity, a response that was already observed within fish when being exposed to sublethal Cu concentrations (Romani et al. 2003). Likewise, the activity of GST was partly significantly increased by $nTiO_2$ exposure at UV intensities $\geq$0.40-0.60 W UVA/$m^2$, relative to the absence of $nTiO_2$ (for both the $nTiO_2$, and $nTiO_2$ +NOM treatment; Fig. 3 B). This can possibly be attributed to the GST involvement during the detoxification of xenobiotics (i.e. $nTiO_2$) but also the production of cytotoxic aldehydes during lipid peroxidation (Booth and O'Halloran 2001, Halliwell and Gutteridge 1995).

The interaction of the factors NOM and $nTiO_2$ revealed an increasing formation of ROS with increasing UV intensities. However, the relationship between NOM content and ROS quantity did not follow a general progression, as increasing NOM quantities up to 0.40 mg TOC/L seemed to marginally suppress the formation of ROS. On the other hand, 4.00 mg TOC/L caused a comparably distinctive ROS enhancement irrespective of the applied UV intensity (Fig. 2 A-D). In this context, transformations related to the photoreactivity of metals, EINPs, and organic matter might play a crucial role (Aiken et al. 2011). For instance, interactions of NOM and sunlight have the potential to trigger a range of reactions governing the speciation of metals and their related surface chemistry (Aiken et al. 2011). During such reactions NOM can serve as a light-adsorbing entity (primary chromophore) having the ability to affect photochemical transformations (Garg et al. 2011). This can occur either directly due to bonding activities (e.g. serving as ligand or as sorbent on nanoparticle surfaces), or indirectly by forming highly reactive intermediates (e.g. organic radicals) and ROS (e.g. singlet oxygen ($^1O_2$), hydrogen peroxide ($H_2O_2$), super oxide ($O_2^-$), or hydroxyl radicals ($^{\bullet}OH$); Aiken et al. 2011). Therefore, it seems likely that in our study NOM at concentrations >0.40 mg TOC/L additionally promoted ROS formations in the form of $^{\bullet}OH$ radicals. Furthermore, it also seems plausible that NOM concentrations up to 0.40 mg TOC/L resulted in an increased amount of less stabilized and therefore bigger particles. This might have reduced $TiO_2$ surface availability for interaction with the UV light and thus ROS formation, relative to NOM at concentrations >0.40 mg TOC/L. This assumption is supported by the particle size monitoring, revealing a trend of smaller particle sizes at NOM concentrations $\geq$0.4 mg TOC/L, even though this trend is not completely applicable for all the TS conducted (Tab. S1). Still, at lower NOM concentrations ($\leq$0.40 mg/L) a higher sedimentation of $TiO_2$ particles was visually observed (potentially relocating the $TiO_2$ particles from the water body towards the bottom of the test vessel), relative to the highest NOM concentration (4.00 mg TOC/L) and regardless of the applied UV intensity.

This outcome, however, partly contradicts the bioassay results with *D. magna* where at constant UV-intensities, $nTiO_2$ toxicity decreased with increasing NOM content. At the same time, higher NOM concentrations elevated the formation of ROS – which are known to cause oxidative stress and drive $nTiO_2$ toxicity (Cabiscol et al. 2000). This observation, however, is in sharp contrast to an earlier publication, suggesting that the presence of NOM reduces $nTiO_2$ toxicity as result of an ROS quenching mechanism at

a given UVA intensity (Wormington et al. 2017). Despite the higher ROS levels in the present study, our biomarker assays support the observation on *Daphnia* immobility with GST activities being to some extent reduced when comparing the responses in presence relative to the absence of NOM at the same UV intensity and $nTiO_2$ concentration (Fig. 3 B).

This phenomenon, namely a lower toxicity despite an elevated formation of ROS, may also be explained by the substantially reduced interaction of ROS with *D. magna* in the presence of NOM, relative to its absence (Brame et al. 2014). Firstly, NOM can act as protection film by coating the daphnids surface (Lin et al. 2012), consequently shielding or reducing the impact of mostly locally acting ROS on the test organism (Feckler et al. 2015). Secondly, in our test system NOM might have functioned as an antioxidant (Fabrega et al. 2009), with the ability to interact with ROS partly releasing *Daphnia* from harmful radical reactions (Brame et al. 2014). This process may be relevant to our study, since NOM hinders oxidation processes more when interacting with $^{\cdot}OH$ than with other radicals (Brame et al. 2014). Therefore, it seems plausible that NOM concentrations beyond 0.40 mg TOC/L, on one hand, amplify the formation of ROS (Fig. 2), but, on the other hand, protect against their potential negative implications which was also supported by our biomarker analyses (Fig. 1 & 3).

**CONCLUSION**

Since NOM is a ubiquitous substance within surface waters with concentrations in the mg/L range (Ryan et al. 2009), the risk associated with the acute exposure of aquatic organisms to $nTiO_2$ may be moderate in the presence of comparably low UV intensities. Our study, however, investigated UV intensities at the lower end of those measured in the field (Häder et al. 2007). Therefore, the interaction of NOM and UV light in presence of $nTiO_2$ might deviate from the observations of the present study when assessing worst-case scenarios (i.e. high levels of UV intensities).

We clearly displayed that moving the test conditions of EINPs towards a more field-relevant approach meaningfully modifies the risk of $nTiO_2$ for aquatic organisms, namely a 96-h $EC_{50}$ variation by a factor of up to ~280. Furthermore, when considering risk assessment factors that are typically applied for studies like ours (Amiard-Triquet et al. 2015, Syberg and Hansen 2016), adverse effects on aquatic systems can already be assumed at currently predicted environmental $nTiO_2$-concentrations (Gondikas et al. 2014). As the demand for EINPs like $nTiO_2$ is predicted to continuously increase in

the near future (Farré et al. 2009, Scheringer 2008), their release into waterbodies will most likely be facilitated. Moreover, the number of factors influencing the direction and intensity of EINP toxicity in nature is not only limited to NOM and UV radiation (Bergman Filho et al. 2011, Lüderwald et al. 2016, Seitz et al. 2015 b), which calls for a systematic assessment of the impact of such factors individually and in combination for a more reliable EINP risk assessment.

## ACKNOWDLEDGEMENTS

## REFERENCES

Ahmed, S.; Rasul, M. G.; Martens, W. N.; Brown, R.; Hashib, M. A., Heterogeneous photocatalytic degradation of phenols in wastewater: a review on current status and developments. *Desalination* **2010**, *261*, (1-2), 3-18. http://dx.doi.org/10.1016/j.desal.2010.04.062.

Aiken, G. R.; Hsu-Kim, H.; Ryan, J. N., Influence of dissolved organic matter on the environmental fate of metals, nanoparticles, and colloids. *Environ. Sci. Technol.* **2011**, *45*, (8), 3196-3201. 10.1021/es103992s.

Aitken, R. J.; Chaudhry, M. Q.; Boxall, A. B. A.; Hull, M., Manufacture and use of nanomaterials: current status in the UK and global trends. *Occup. Med-C.* **2006**, *56*, (5), 300-306. 10.1093/occmed/kql051.

Amiano, I.; Olabarrieta, J.; Vitorica, J.; Zorita, S., Acute toxicity of nanosized $TiO_2$ to *Daphnia magna* under UVA irradiation. *Environ. Toxicol. Chem.* **2012**, *31*, (11), 2564-2566. http://dx.doi.org/10.1002/etc.1981.

Amiard-Triquet, C.; Amiard, J.-C.; Mouneyrac, C., Aquatic ecotoxicology: advancing tools for dealing with emerging risks. *Academic Press, Waltham, USA* **2015**. http://dx.doi.org/10.1016/B978-0-12-800949-9.00001-2.

ASTM E729-96, Standard guide for conducting acute toxicity tests on test materials with fishes, macroinvertebrates, and amphibians. *ASTM International, West Conshohocken* **2007**, *NA*, (NA), 1-22. 10.1520/C0033-03R06.

Bainy, A.; Medeiros, M.; Di Mascio, P.; Almeida, E., In vivo effects of metals on the acetylcholinesterase activity of the *Perna perna* mussel's digestive gland. *Biotemas* **2006**, *19,* (1), 35-39. https://doi.org/10.5007/%25x.

Barata, C.; Varo, I.; Navarro, J. C.; Arun, S.; Porte, C., Antioxidant enzyme activities and lipid peroxidation in the freshwater cladoceran *Daphnia magna* exposed to redox cycling compounds. *Comp. Biochem. Phys. C.* **2005**, *140*, (2), 175-186. https://doi.org/10.1016/j.cca.2005.01.013.

Bar-Ilan, O.; Chuang, C. C.; Schwahn, D. J.; Yang, S.; Joshi, S.; Pedersen, J. A.; Hamers, R. J.; Peterson, R. E.; Heideman, W., $TiO_2$ Nanoparticle exposure and illumination during zebrafish development: mortality at parts per billion concentrations. *Environ. Sci. Technol.* **2013**, *47*, (9), 4726-4733. 10.1021/es304514r.

Bhatkhande, D. S.; Pangarkar, V. G.; Beenackers, A., Photocatalytic degradation for environmental applications - a review. *J. Chem. Technol. Biotechnol.* **2002**, *77*, (1), 102-116. https://doi.org/10.1002/jctb.532.

Bergman Filho, T.; Soares, A.; Loureiro, S., Energy budget in *Daphnia magna* exposed to natural stressors. *Environ. Sci. Pollut. Res.* **2011**, *18*, (4), 655-662. 10.1007/s11356-010-0413-0.

Booth, L. H.; O'Halloran K., A comparison of biomarker responses in the earthworm *Aporrectodea caliginosa* to the organophosphorus insecticides diazinon and chlorpyrifos. *Environ. Toxicol. Chem.* **2001**, *20*, (11), 2494-2502. 10.1002/etc.5620201115.

Bouchnak, R.; Steinberg, C. E. W., Modulation of longevity in *Daphnia magna* by food quality and simultaneous exposure to dissolved humic substances. *Limnologica* **2010**, *40*, (2), 86-91. http://dx.doi.org/10.1016/j.limno.2009.11.010.

Buonocore, G.; Perrone, S.; Tataranno, M. L., Oxygen toxicity: chemistry and biology of reactive oxygen species. *Semin. Fetal Neonatal Med.* **2010**, *15*, (4), 186-190. http://dx.doi.org/10.1016/j.siny.2010.04.003.

Bradford, M. M., A rapid and sensitive method for the quantitation of microgram quantities of protein utilizing the principle of protein-dye binding. *Anal. Biochem.* **1976**, *72*, (1), 248-254. https://doi.org/10.1016/0003-2697(76)90527-3.

Brame, J.; Long, M.; Li, Q.; Alvarez, P., Trading oxidation power for efficiency: Differential inhibition of photo-generated hydroxyl radicals versus singlet oxygen. *Water Res.* **2014**, *60*, (NA), 259-266. http://dx.doi.org/10.1016/j.watres.2014.05.005.

Brezová, V.; Gabčová, S.; Dvoranová, D.; Staško, A., Reactive oxygen species produced upon photoexcitation of sunscreens containing titanium dioxide (an EPR study). *J. Photoch. Photobio. B.* **2005**, *79*, (2), 121-134. http://dx.doi.org/10.1016/j.jphotobiol.2004.12.006.

Cabiscol, E.; Tamarit, J.; Ros, J., Oxidative stress in bacteria and protein damage by reactive oxygen species. *Int. Microbiol.* **2000**, *3*, (1), 3-8. http://hdl.handle.net/10459.1/56751.

Chappell, M. A.; George, A. J.; Dontsova, K. M.; Porter, B. E.; Price, C. L.; Zhou, P.; Morikawa, E.; Kennedy, A. J.; Steevens, J. A., Surfactive stabilization of multi-walled carbon nanotube dispersions with dissolved humic substances. *Environ. Pollut.* **2009**, *157*, (4), 1081-1087. http://dx.doi.org/10.1016/j.envpol.2008.09.039.

Core Team R, R: a language and environment for statistical computing. *R Foundation for Statistical Computing: Vienna, Austria* **2013**. https://www.R-project.org/.

Dabrunz, A.; Duester, L.; Prasse, C.; Seitz, F.; Rosenfeldt, R.; Schilde, C.; Schaumann, G. E.; Schulz, R., Biological surface coating and molting inhibition as mechanisms of $TiO_2$ nanoparticle toxicity in *Daphnia magna*. *PLoS ONE* **2011**, *6*, (5), e20112. 10.1371/journal.pone.0020112.

Ellman, G. L.; Courtney, K. D.; Andres, V.; Featherstone, R. M., A new and rapid colorimetric determination of acetylcholinesterase activity. *Biochem. Pharmacol.* **1961**, *7*, (2), 88-95. https://doi.org/10.1016/0006-2952(61)90145-9.

Fabrega, J.; Fawcett, S. R.; Renshaw, J. C.; Lead, J. R., Silver nanoparticle impact on bacterial growth: effect of pH, concentration, and organic matter. *Environ. Sci. Technol.* **2009**, *43*, (19), 7285-7290. 10.1021/es803259g.

Farre, M.; Gajda-Schrantz, K.; Kantiani, L.; Barcelo, D., Ecotoxicity and analysis of nanomaterials in the aquatic environment. *Anal. Bioanal. Chem.* **2009**, *393*, (1), 81-95. 10.1007/s00216-008-2458-1.

Feckler, A.; Rosenfeldt, R. R.; Seitz, F.; Schulz, R.; Bundschuh, M., Photocatalytic properties of titanium dioxide nanoparticles affect habitat selection of and food quality for a key species in the leaf litter decomposition process. *Environ. Pollut.* **2015**, *196*, (NA), 276-283. http://dx.doi.org/10.1016/j.envpol.2014.09.022.

Garg, S.; Rose, A. L.; Waite, T. D., Photochemical production of superoxide and hydrogen peroxide from natural organic matter. *Geochim. Cosmochimica Acta* **2011**, *75*, (15), 4310-4320. http://dx.doi.org/10.1016/j.gca.2011.05.014.

Gondikas, A. P.; Kammer, F. v. d.; Reed, R. B.; Wagner, S.; Ranville, J. F.; Hofmann, T., Release of $TiO_2$ nanoparticles from sunscreens into surface waters: a one-year survey at the old Danube recreational lake. *Environ. Sci. Technol.* **2014**, *48*, (10), 5415-5422. 10.1021/es405596y.

Griffith, O. W., Determination of glutathione and glutathione disulfide using glutathione reductase and 2-vinylpyridine. *Anal. Biochem.* **1980**, *106*, (1), 207-212. https://doi.org/10.1016/0003-2697(80)90139-6.

Habig, W. H.; Pabst, M. J.; Jakoby, W. B., Glutathione s-transferases: the first enzymatic step in mercapturic acid formation. *J. Biol. Chem.* **1974**, *249*, (22), 7130-7139. http://www.jbc.org/content/249/22/7130.abstract.

Häder, D. P.; Lebert, M.; Schuster, M.; del Campo, L.; Helbling, E. W.; McKenzie, R., ELDONET - a decade of monitoring solar radiation on five continents. *Photochem. Photobiol.* **2007**, *83*, (6), 1348-1357. 10.1111/j.1751-1097.2007.00168.x.

Hall, S.; Bradley, T.; Moore, J. T.; Kuykindall, T.; Minella, L., Acute and chronic toxicity of nano-scale $TiO_2$ particles to freshwater fish, cladocerans, and green algae, and effects of organic and inorganic substrate on $TiO_2$ toxicity. *Nanotoxicology* **2009**, *3*, (2), 91-97. 10.1080/17435390902788078.

Halliwell, B.; Gutteridge, J. M. C., The definition and measurement of antioxidants in biological systems. *Free Radical Bio. Med.* **1995**, *18*, (1), 125-126. https://doi.org/10.1016/0891-5849(95)91457-3.

Hirakawa, K.; Mori, M.; Yoshida, M.; Oikawa, S.; Kawanishi, S., Photo-irradiated titanium dioxide catalyzes site specific DNA damage via generation of hydrogen peroxide. *Free Radic. Res.* **2004**, *38*, (5), 439-447. 10.1080/1071576042000206487.

Ito, A.; Shinkai, M.; Honda, H.; Kobayashi, T., Medical application of functionalized magnetic nanoparticles. *J. Biosci. Bioeng.* **2005**, *100*, (1), 1-11. http://dx.doi.org/10.1263/jbb.100.1.

Johnston, H. J.; Hutchison, G. R.; Christensen, F. M.; Peters, S.; Hankin, S.; Stone, V., Identification of the mechanisms that drive the toxicity of $TiO_2$ particulates: the contribution of physicochemical characteristics. *Part. Fibre Toxicol.* **2009**, *6*, (NA), 33. 10.1186/1743-8977-6-33.

Kalčíková, G.; Englert, D.; Rosenfeldt, R. R.; Seitz, F.; Schulz, R.; Bundschuh, M., Combined effect of UV-irradiation and $TiO_2$-nanoparticles on the predator-prey interaction of gammarids and mayfly nymphs. *Environ. Pollut.* **2014**, *186*, (0), 136-140. http://dx.doi.org/10.1016/j.envpol.2013.11.028.

Kaegi, R.; Ulrich, A.; Sinnet, B.; Vonbank, R.; Wichser, A.; Zuleeg, S.; Simmler, H.; Brunner, S.; Vonmont, H.; Burkhardt, M.; Boller, M., Synthetic $TiO_2$ nanoparticle emission from exterior facades into the aquatic environment. *Environ. Pollut.* **2008**, *156*, (2), 233-239. 10.1016/j.envpol.2008.08.004.

Karimi, S.; Troeung, M.; Wang, R.; Draper, R.; Pantano, P., Acute and chronic toxicity of metal oxide nanoparticles in chemical mechanical planarization slurries with *Daphnia magna. Environ. Sci.:Nano.* **2018**, *5*, (NA), 1670-1684. 10.1039/C7EN01079F.

Keller, A. A.; Lazareva, A., Predicted releases of engineered nanomaterials: from global to regional to local. *Environ. Sci. Tech. Let.* **2014**, *1*, (1), 65-70. 10.1021/ez400106t.

Kiser, M. A.; Westerhoff, P.; Benn, T.; Wang, Y.; Perez-Rivera, J.; Hristovski, K., Titanium nanomaterial removal and release from wastewater treatment plants. *Environ. Sci. Technol.* **2009**, *43*, (17), 6757-6763. 10.1021/es901102n.

Kim, C.; Park, H.-j.; Cha, S.; Yoon, J., Facile detection of photogenerated reactive oxygen species in $TiO_2$ nanoparticles suspension using colorimetric probe-assisted spectrometric method. *Chemosphere* **2013**, *93*, (9), 2011-2015. http://dx.doi.org/10.1016/j.chemosphere.2013.07.023.

Kim, K. T.; Klaine, S. J.; Cho, J.; Kim, S. H.; Kim, S. D., Oxidative stress responses of *Daphnia magna* exposed to $TiO_2$ nanoparticles according to size fraction. *Sci. Total Environ.* **2010**, *408*, (10), 2268-2272. 10.1016/j.scitotenv.2010.01.041.

Klaine, S. J.; Alvarez, P. J. J.; Batley, G. E.; Fernandes, T. F.; Handy, R. D.; Lyon, D. Y.; Mahendra, S.; McLaughlin, M. J.; Lead, J. R., Nanomaterials in the environment: behavior, fate, bioavailability, and effects. *Environ. Toxicol. Chem.* **2008**, *27*, (9), 1825-1851. https://doi.org/10.1897/08-090.1.

Kolts, J. M.; Brooks, M. L.; Cantrell, B. D.; Boese, C. J.; Bell, R. A.; Meyer, J. S., Dissolved fraction of standard laboratory cladoceran food alters toxicity of waterborne silver to *Ceriodaphnia dubia*. *Environ. Toxicol. Chem.* **2008**, *27*, (6), 1426-1434. 10.1897/07-326.1.

Lemon, J., Plotrix: a package in the red light district of R. *R-News* **2006**, *6*, (4), 8-12. https://CRAN.R-project.org/package=plotrix.

Li, S.; Ma, H.; Wallis, L. K.; Etterson, M. A.; Riley, B.; Hoff, D. J.; Diamond, S. A., Impact of natural organic matter on particle behavior and phototoxicity of titanium dioxide nanoparticles. *Sci. Total Environ.* **2016**, *542*, (Pt A), 324-333. https://doi.org/10.1016/j.scitotenv.2015.09.141.

Lin, D.; Ji, J.; Long, Z.; Yang, K.; Wu, F., The influence of dissolved and surface-bound humic acid on the toxicity of $TiO_2$ nanoparticles to *Chlorella* sp. *Water Res.* **2012**, *46*, (14), 4477-4487. http://dx.doi.org/10.1016/j.watres.2012.05.035.

Lüderwald, S.; Seitz, F.; Seisenbaeva, G. A.; Kessler, V. G.; Schulz, R.; Bundschuh, M., Palladium nanoparticles: Is there a risk for aquatic ecosystems? *Bull. Environ. Contam. Toxicol.* **2016**, *97*, (2), 153-158. 10.1007/s00128-016-1803-x.

Ma, H.; Brennan, A.; Diamond, S. A., Photocatalytic reactive oxygen species production and phototoxicity of titanium dioxide nanoparticles are dependent on the solar ultraviolet radiation spectrum. *Environ. Toxicol. Chem.* **2012b**, *31*, (9), 2099-2107. 10.1002/etc.1916.

Ma, H.; Brennan, A.; Diamond, S. A., Phototoxicity of $TiO_2$ nanoparticles under solar radiation to two aquatic species: *Daphnia magna* and Japanese medaka. *Environ. Toxicol. Chem.* **2012a**, *31*, (7), 1621-1629. 10.1002/etc.1858.

Mansfield, C. M.; Alloy, M. M.; Hamilton, J.; Verbeck, G. F.; Newton, K.; Klaine, S. J.; Roberts, A. P., Photo-induced toxicity of titanium dioxide nanoparticles to *Daphnia magna* under natural sunlight. *Chemosphere* **2015**, *120*, (NA), 206-210. http://dx.doi.org/10.1016/j.chemosphere.2014.06.075.

Marcone, G. P. S.; Oliveira, A. C.; Almeida, G.; Umbuzeiro, G. A.; Jardim, W. F., Ecotoxicity of $TiO_2$ to *Daphnia similis* under irradiation. *J. Hazard. Mater.* **2012**, *211-212*, (NA), 436-442. 10.1016/j.jhazmat.2011.12.075.

Mingo, V.; Lötters, S.; Wagner, N., The use of buccal swabs as a minimal-invasive method for detecting effects of pesticide exposure on enzymatic activity in common wall lizards. *Environ. Pollut.* **2017**, *220*, 53-62. https://doi.org/10.1016/j.envpol.2016.09.022.

Nowotny, J., Titanium dioxide-based semiconductors for solar-driven environmentally friendly applications: impact of point defects on performance. *Energy Environ. Sci.* **2008**, *1*, (5), 565-572. 10.1039/B809111K.

OECD, Test no. 202: *Daphnia* sp. acute immobilisation test. OECD guideline for testing of chemicals. *OECD Publishing*, *Paris*. **2004**, *Section 2*, (NA), 1-12. https://doi.org/10.1787/9789264069947-en.

OECD, Test no. 211: *Daphnia magna* reproduction test. OECD guideline for testing of chemicals. *OECD Publishing, Paris*. **2008**, *Section 2*, (NA), 1-23. https://doi.org/10.1787/9789264185203-en.

Piccinno, F.; Gottschalk, F.; Seeger, S.; Nowack, B., Industrial production quantities and uses of ten engineered nanomaterials in Europe and the world. *J. Nanopart. Res.* **2012**, *14*, (9), 1-11. 10.1007/s11051-012-1109-9.

Ritz, C.; Streibig, J. C., Bioassay analysis using R. *J. Statist. Softw.* **2005**, *12*, (5), 1-22. 10.18637/jss.v012.i05.

Romani, R.; Antognelli, C.; Baldracchini, F.; De Santis, A.; Isani, G.; Giovannini, E.; Rosi, G., Increased acetylcholinesterase activities in specimens of *Sparus auratus* exposed to sublethal copper concentrations. *Chem-Biol. Interact.* **2003**, *145*, (3), 321-329. https://doi.org/10.1016/S0009-2797(03)00058-9.

Rosenfeldt, R. R.; Seitz, F.; Schulz, R.; Bundschuh, M., Heavy metal uptake and toxicity in the presence of titanium dioxide nanoparticles: a factorial approach using *Daphnia magna*. *Environ. Sci. Technol.* **2014**, *48*, (12), 6965-6972. 10.1021/es405396a.

Rosenfeldt, R. R.; Seitz, F.; Senn, L.; Schilde, C.; Schulz, R.; Bundschuh, M., Nanosized titanium dioxide reduces copper toxicity — the role of organic material and the crystalline phase. *Environ. Sci. Technol.* **2015**, *49*, (3), 1815-1822. 10.1021/es506243d.

Ryan, A. C.; Tomasso, J. R.; Klaine, S. J., Influence of pH, hardness, dissolved organic carbon concentration, and dissolved organic matter source on the acute toxicity of copper to *Daphnia magna* in soft waters: implications for the biotic ligand model. *Environ. Toxicol. Chem.* **2009**, *28*, (8), 1663-1670. 10.1897/08-361.1.

Schaumann, G. E.; Philippe, A.; Bundschuh, M.; Metreveli, G.; Klitzke, S.; Rakcheev, D.; Grün, A.; Kumahor, S. K.; Kühn, M.; Baumann, T.; Lang, F.; Manz, W.; Schulz, R.; Vogel, H.-J., Understanding the fate and biological effects of Ag- and $TiO_2$-nanoparticles in the environment: the quest for advanced analytics and interdisciplinary concepts. *Sci. Total Environ.* **2015**, *535*, (NA), 3-19. http://dx.doi.org/10.1016/ j.scitotenv.2014.10.035.

Scheringer, M., Nanoecotoxicology: Environmental risks of nanomaterials. *Nat. Nanotechnol.* **2008**, *3*, (6), 322-323. 10.1038/nnano.2008.145.

Seitz, F.; Bundschuh, M.; Dabrunz, A.; Bandow, N.; Schaumann, G. E.; Schulz, R., Titanium dioxide nanoparticles detoxify pirimicarb under UV irradiation at ambient intensities. *Environ. Toxicol. Chem.* **2012**, *31*, (3), 518-523. 10.1002/etc.1715.

Seitz, F.; Lüderwald, S.; Rosenfeldt, R. R.; Schulz, R.; Bundschuh, M., Aging of $TiO_2$ nanoparticles transiently increases their toxicity to the pelagic microcrustacean *Daphnia magna*. *PLoS ONE* **2015a**, *10*, (5), e0126021. 10.1371/journal.pone.0126021.

Seitz, F.; Rosenfeldt, R. R.; Müller, M.; Lüderwald, S.; Schulz, R.; Bundschuh, M., Quantity and quality of natural organic matter influence the ecotoxicity of titanium dioxide nanoparticles. *Nanotoxicology* **2016**, *10*, (10), 1-7. 10.1080/17435390.2016.1222458.

Seitz, F.; Rosenfeldt, R. R.; Storm, K.; Metreveli, G.; Schaumann, G. E.; Schulz, R.; Bundschuh, M., Effects of silver nanoparticle properties, media pH and dissolved organic matter on toxicity to *Daphnia magna*. *Environ. Saf.* **2015b,** *111*, (NA), 263-270. http://dx.doi.org/10.1016/j.ecoenv.2014.09.031.

Semenzin, E.; Lanzellotto, E.; Hristozov, D.; Critto, A.; Zabeo, A.; Giubilato, E.; Marcomini, A., Species sensitivity weighted distribution for ecological risk assessment of engineered nanomaterials: The n-TiO$_2$ case study. *Environ. Toxicol. Chem.* **2015**, *34*, (11), 2644-2659. 10.1002/etc.3103.

Syberg, K.; Hansen, S. F., Environmental risk assessment of chemicals and nanomaterials — the best foundation for regulatory decision-making? *Sci. Total Environ.* **2016**, *541*, 784-794. 10.1016/j.ecoenv.2007.05.010.

Tang, B.; Zhang, L.; Geng, Y., Determination of the antioxidant capacity of different food natural products with a new developed flow injection spectrofluorimetry detecting hydroxyl radicals. *Talanta* **2005**, *65*, (3), 769-775. http://dx.doi.org/10.1016/j.talanta.2004.08.004.

Ulm, L.; Krivohlavek, A.; Jurašin, D.; Ljubojević, M.; Šinko, G.; Crnković, T.; Žuntar, I.; Šikić, S.; Vinković Vrček, I., Response of biochemical biomarkers in the aquatic crustacean *Daphnia magna* exposed to silver nanoparticles. *Environ. Sci. Pollut. Res.* **2015**, *22*, (24), 19990-19999. 10.1007/s11356-015-5201-4.

Westerhoff, P.; Song, G.; Hristovski, K.; Kiser, M. A., Occurrence and removal of titanium at full scale wastewater treatment plants: implications for TiO$_2$ nanomaterials. *J. Environ. Monitor.* **2011**, *13*, (5), 1195-203. 10.1039/c1em10017c.

Wheeler, M. W.; Park, R. M.; Bailer, A. J., Comparing median lethal concentration values using confidence interval overlap or ratio tests. *Environ. Toxicol. Chem.* **2006**, *25*, (5), 1441-1444. 10.1897/05-320r.1.

Wormington, A. M.; Coral, J.; Alloy, M. M.; Delmaré C. L.; Mansfield, C. M.; Klaine, S. J.; Bisesi, J. H.; Roberts, A. P., Effect of natural organic matter on the photo-induced toxicity of titanium dioxide nanoparticles. *Environ. Toxicol. Chem*. **2017**, *36*, (6), 1661-1666. doi:10.1002/etc.3702.

Xiong, D.; Fang, T.; Yu, L.; Sima, X.; Zhu, W., Effects of nano-scale $TiO_2$, ZnO and their bulk counterparts on zebrafish: acute toxicity, oxidative stress and oxidative damage. *Sci. Total Environ.* **2011**, *409*, (8), 1444-1452. http://dx.doi.org/10.1016/j.scitotenv.2011.01.015.

Zhang, Y.; Blewett, T. A.; Val, A. L.; Goss, G. G., UV-induced toxicity of cerium oxide nanoparticles ($CeO_2$ NPs) and the protective properties of natural organic matter (NOM) from the Rio Negro Amazon River. *Environ. Sci-Nano*. **2018**, *5*, (2), 476-486. 10.1039/C7EN00842B.

Zhu, X. S.; Chang, Y.; Chen, Y. S., Toxicity and bioaccumulation of $TiO_2$ nanoparticle aggregates in *Daphnia magna*. *Chemosphere* **2010**, *78*, (3), 209-215. 10.1016/j.chemosphere.2009.11.013.

# A blessing in disguise? Natural organic matter reduces the UV light-induced toxicity of nanoparticulate titanium dioxide

Lüderwald, S., Dackermann, V., Seitz, F., Adams, E., Feckler, A., Schilde, C., Schulz, R., Bundschuh, M.

**Table S1.** Average particle size (nm ±SD; $n$=3) and respective polydispersity index (PI) of $nTiO_2$ (2.00 mg/L) in the test medium (ASTM) at different NOM levels (0.00-4.00 mg TOC/L) and UV light (0.00-5.20 W UVA/m²) intensities after 0, 48 and 96 h. NA=not applicable due to an insufficient scattered light intensity.

| Level | Intensity (W UVA /m²) | NOM (mg TOC/L) | 0 h | PI | 48 h | PI | 96 h | PI |
|---|---|---|---|---|---|---|---|---|
| I | 0.00 | 0.00 | 407.6 ±3.59 | 0.26-0.31 | 2171.4 ±202.61 | 0.67-0.77 | 200.3 ±1.15 | 0.26-0.29 |
| I | 0.00 | 0.04 | 496.9 ±48.45 | 0.22-0.29 | 4897.4 ±1308.83 | 1.13-1.44 | 2136.3 ±552.30 | 0.82-1.11 |
| I | 0.00 | 0.40 | 200.3 ±1.15 | 0.26-0.29 | 231.4 ±3.89 | 0.24-0.27 | 273 ±3.94 | 0.2-0.24 |
| I | 0.00 | 4.00 | 364.8 ±36.31 | 0.20-0.25 | 329.5 ± 20.48 | 0.21-0.30 | 283.1 ±4.42 | 0.27-0.29 |
| II | 0.40-0.60 | 0.00 | 253.4 ±15.75 | 0.25-0.29 | 3033.8 ±353.75 | 0.69-0.87 | NA | NA |
| II | 0.40-0.60 | 0.04 | 4272.5 ±297.61 | 1.17-1.38 | 3853.8 ±919.43 | 0.89-1.26 | 4890.2 ±887.35 | 1.11-1.39 |
| II | 0.40-0.60 | 0.40 | 284.1 ±24.25 | 0.17-0.3 | 3192.9 ±322.18 | 0.88-1.05 | 4112.8 ±339.22 | 1.02-1.17 |
| II | 0.40-0.60 | 4.00 | 211.2 ±45.10 | 0.14-0.33 | 1984.2 ±138.7 | 0.61-0.71 | 4427.5 ±862.47 | 1.16-1.43 |
| III | 1.00-1.40 | 0.00 | 445.7 ±37.44 | 0.25-0.28 | 2744 ±121.65 | 0.86-0.91 | NA | NA |
| III | 1.00-1.40 | 0.04 | 3872.6 ±327.56 | 1.09-1.34 | NA | NA | NA | NA |
| III | 1.00-1.40 | 0.40 | 351.8 ±57.47 | 0.19-0.27 | 2518 ±275.98 | 0.75-0.87 | NA | NA |
| III | 1.00-1.40 | 4.00 | 287.7 ±11.55 | 0.29-0.30 | 287.7 ±11.55 | 0.29-0.30 | NA | NA |
| IV | 2.20-2.60 | 0.00 | 587.9 ±67.51 | 0.25-0.30 | 4637 ±566.3 | 1.17-1.25 | 2813.8 ±468.79 | 0.72-0.79 |
| IV | 2.20-2.60 | 0.04 | 943.7 ±110.41 | 0.34-0.42 | 4436.4 ±439.27 | 0.96-1.26 | 2178.3 ±228.43 | 0.55-0.67 |
| IV | 2.20-2.60 | 0.40 | 217.2 ±1.91 | 0.23-0.26 | 2368.2 ±242.12 | 0.77-0.90 | 3367 ±160.21 | 1.01-1.05 |
| IV | 2.20-2.60 | 4.00 | 382.6 ±82.54 | 0.19-0.28 | 2241.6 ±270.37 | 0.69-0.83 | NA | NA |
| V | 4.80-5.20 | 0.00 | 1076.1 ±51.06 | 0.38-0.43 | NA | NA | NA | NA |
| V | 4.80-5.20 | 0.04 | 818.4 ±66.76 | 0.31-0.38 | NA | NA | NA | NA |
| V | 4.80-5.20 | 0.40 | 2535.1 ±316.26 | 0.76-0.93 | NA | NA | NA | NA |
| V | 4.80-5.20 | 4.00 | 1250.8 ±201.61 | 0.42-0.55 | 3720.9 ±753.97 | 0.91-1.24 | 4738.1 ± 366.99 | 1.16-1.24 |

**Table S2.** Characterization of dissolved organic carbon properties as well as N and S information for the applied NOM (i.e., Seaweed Extract (SW), determined via LC-OCD-NOD or gained by either CHNS-analyses; modified following Seitz et al. (2016).

| Type | | HOC[b] | | DOC | | | | | | | | SUVA[a] (L/mg*m) | N (%(w/w)) | S (%(w/w)) |
|---|---|---|---|---|---|---|---|---|---|---|---|---|---|---|
| | | | | | CDOC[c] | | | | | | | | | |
| | Total (µg C/L) | Total (µg C/L) | Total (µg C/L) | BIO-polymers | Humic substance | | | Building blocks (µg C/L) | LMW[d] neutrals (µg C/L) | LMW[d] acids (µg C/L) | | | | |
| | | | | Total (µg C/L) | Total (µg C/L) | Aromaticity (L/mg*m) | Mol. weight (g/mol) | | | | | | | |
| SW | 1277 | 366 | 911 | 71 | 196 | 4.96 | 954 | 285 | 312 | 48 | | 2.13 | 0.46 | 0.77 |

[a] specific UV absorbance

[b] Hydrophobic organic carbon

[c] Chromatographic dissolved organic carbon

[d] Low molecular neutrals/organic acids

**Table S3.** 96-h $EC_{50}$ values (half maximal effective concentration) of $nTiO_2$ for the differently assessed UV intensities (0.00-5.20 W $UVA/m^2$) and NOM concentrations (0.00-4.00 mg TOC/L), as well as their respective standard errors (SE), lower (LCI) and upper (UCI) 95% confidence intervals. NA=not applicable, since the modeled $EC_{50}$ values exceeded the highest applied $nTiO_2$ concentration (64.00 mg/L).

| Test series | UV Intensity (W $UVA/m^2$) | NOM content (mg TOC/L) | 96-h $EC_{50}$ (mg $nTiO_2$/L) | SE | LCI | UCI |
|---|---|---|---|---|---|---|
| I | 0.00 | 0.00 | 28.83 | 7.54 | 13.30 | 44.37 |
| I | 0.00 | 0.04 | NA | NA | NA | NA |
| I | 0.00 | 0.40 | NA | NA | NA | NA |
| I | 0.00 | 4.00 | NA | NA | NA | NA |
| II | 0.40-0.60 | 0.00 | 1.08 | 0.17 | 0.74 | 1.42 |
| II | 0.40-0.60 | 0.04 | 0.77 | 0.31 | 0.13 | 1.40 |
| II | 0.40-0.60 | 0.40 | 12.12 | 3.17 | 5.70 | 18.54 |
| II | 0.40-0.60 | 4.00 | 8.94 | 1.82 | 5.25 | 12.62 |
| III | 1.00-1.40 | 0.00 | 0.84 | 0.12 | 0.60 | 1.09 |
| III | 1.00-1.40 | 0.04 | 0.25 | 0.09 | 0.06 | 0.44 |
| III | 1.00-1.40 | 0.40 | 1.16 | 0.09 | 0.98 | 1.34 |
| III | 1.00-1.40 | 4.00 | 4.26 | 0.21 | 3.84 | 4.67 |
| IV | 2.20-2.60 | 0.00 | 0.25 | 0.09 | 0.06 | 0.44 |
| IV | 2.20-2.60 | 0.04 | 0.23 | 0.04 | 0.15 | 0.32 |
| IV | 2.20-2.60 | 0.40 | 0.50 | 0.06 | 0.39 | 0.61 |
| IV | 2.20-2.60 | 4.00 | 3.06 | 0.13 | 2.79 | 3.33 |
| V | 4.80-5.20 | 0.00 | 0.10 | 0.09 | 0.09 | 0.12 |
| V | 4.80-5.20 | 0.04 | 0.11 | 0.01 | 0.09 | 0.13 |
| V | 4.80-5.20 | 0.40 | 0.25 | 0.09 | 0.06 | 0.44 |
| V | 4.80-5.20 | 4.00 | 0.11 | 0.01 | 0.09 | 0.13 |

**Table S4.** Mean zeta potential (mV ±SD; $n$=3) of the applied P25 nanoparticles (assessed at 4.00 mg $nTiO_2$/L) in ASTM, in presence of increasing NOM concentrations (SW, 0.00-4.00 mg TOC/L), assessed directly after the application of the P25 nanoparticles (~1 min) into the respective medium (as detailed in Seitz et al. 2016).

| TOC (mg/L) | Zeta Potential (mV) |
|---|---|
| 0.00 | -10.79 (±0.46) |
| 0.04 | -9.77 (±0.24) |
| 0.40 | -21.48 (±0.80) |
| 4.00 | -21.22 (±0.26) |
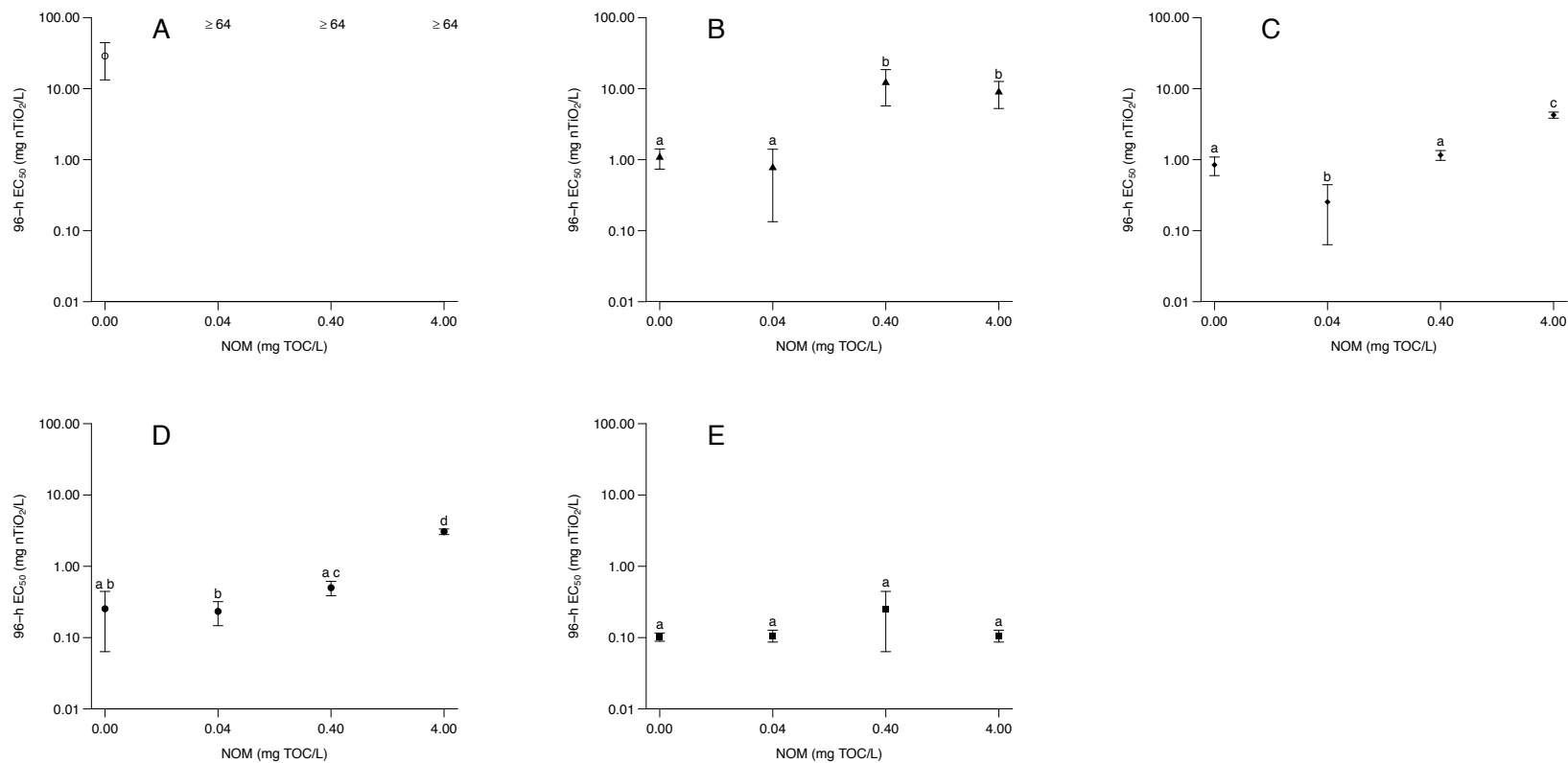
**Figure S1.** 96-h EC$_{50}$ (±95% CI) of *D. magna*, exposed to nTiO$_2$ (0.00-64.00 mg/L) in ASTM ±NOM (0.00-4.00 mg TOC/L), in the presence of (A): 0.00 W UVA/m$^2$ (TS I), (B): 0.40-0.60 W UVA/m$^2$ (TS II), (C): 1.00-1.40 W UVA/m$^2$ (TS III), (D): 2.20-2.60 W UVA/m$^2$ (TS IV), and (E): 4.80-5.20 W UVA/m$^2$ (TS V); Different letters denote statistically significant difference between individual TS but within one NOM level.

141
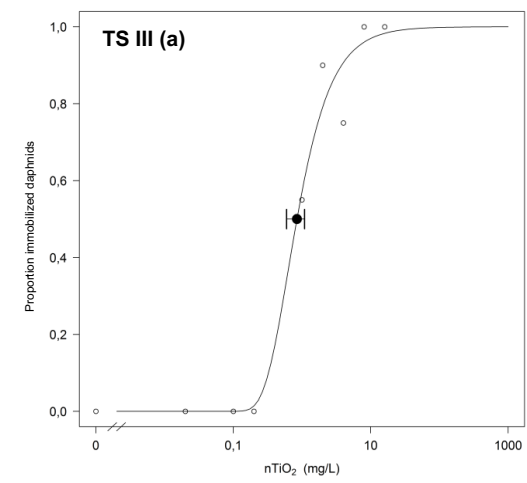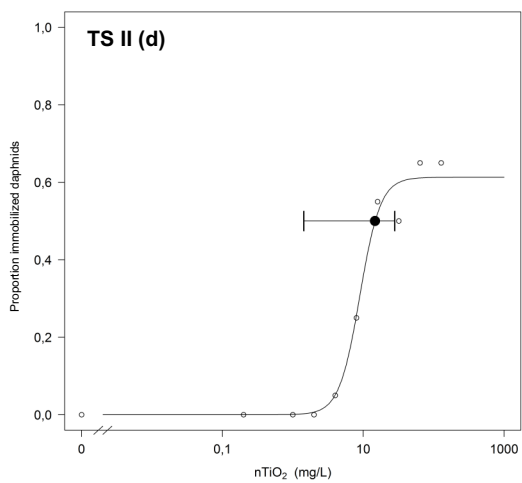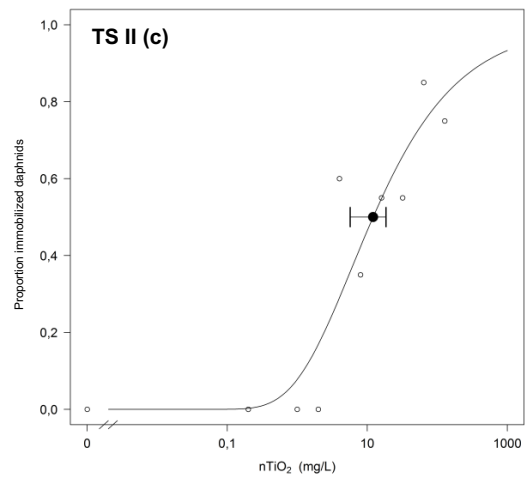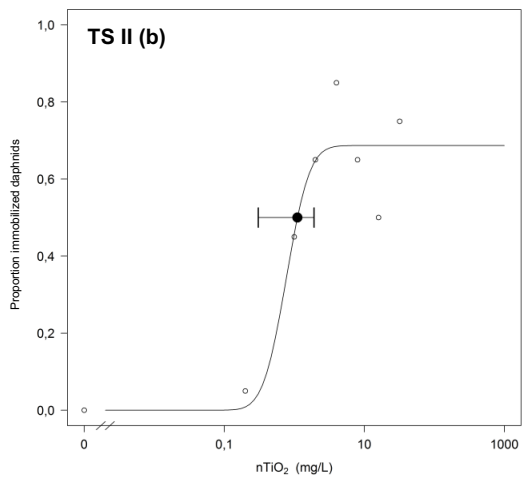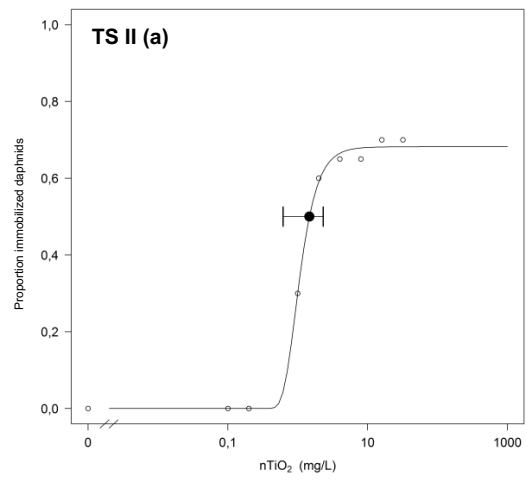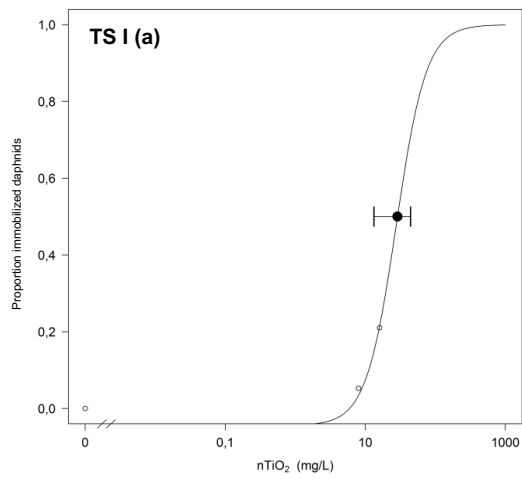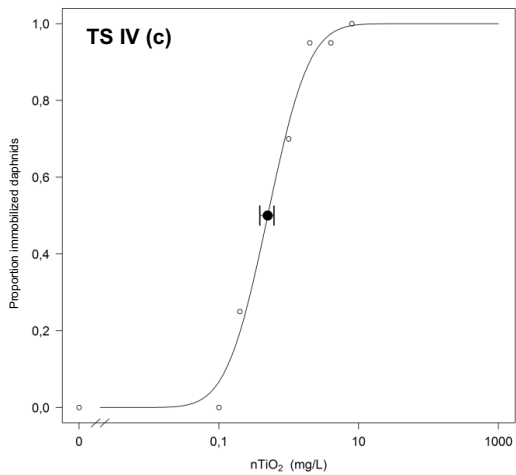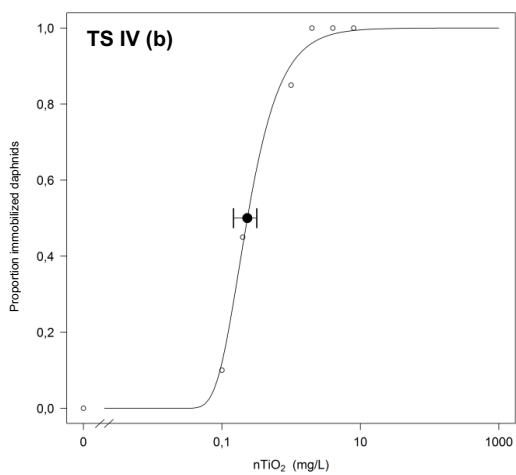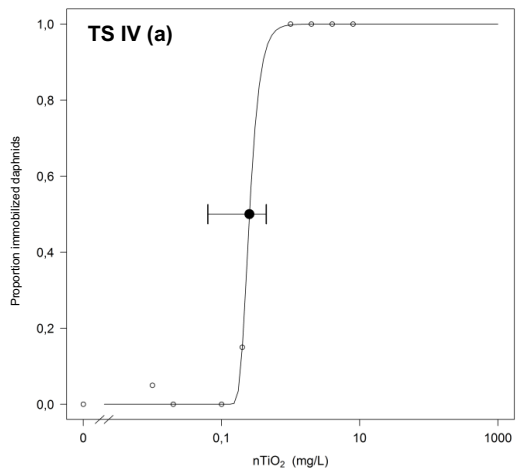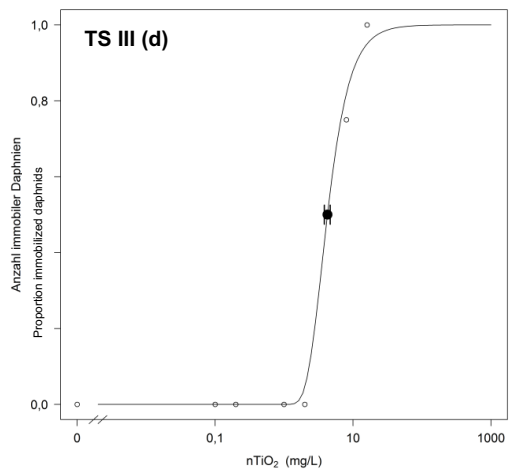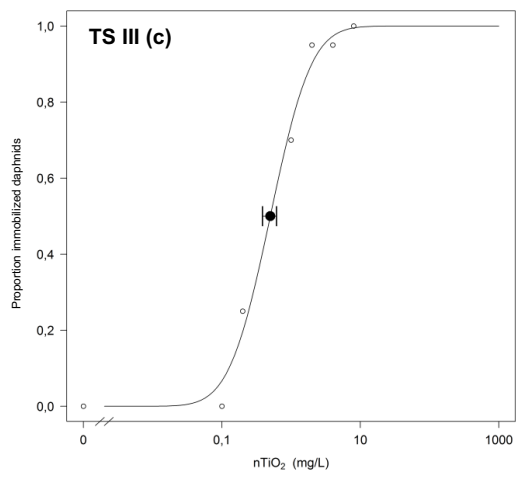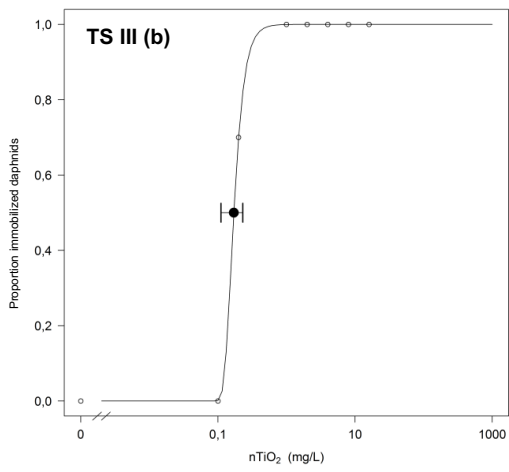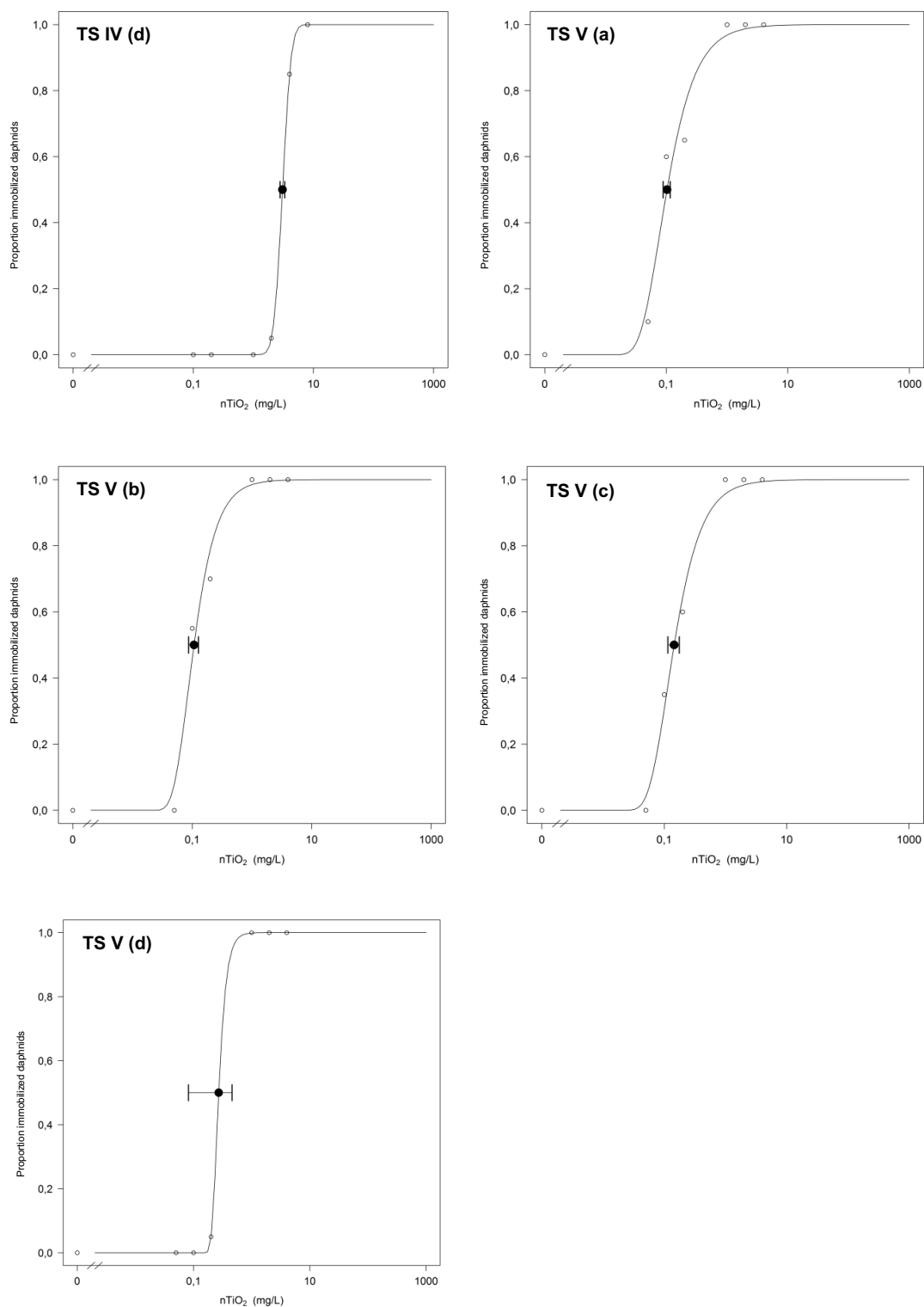
**Fig. S3.** Dose-response models of the calculated 96-h EC50 values for the conducted TS: (TS I): 0.00 W UVA/m², (TS II): 0.40-0.60 W UVA/m², (TS III): 1.00-1.40 W UVA/m², (TS IV): 2.20-2.60 W UVA/m², and (TS V): 4.80-5.20 W UVA/m²; (a)=0.00 mg TOC /L, (b)=0.04 mg TOC/L, (c)=0.40 mg TOC/L, and (d)=4.00 mg TOC/L.

# Reduction of pesticide toxicity under field relevant conditions? The interaction of titanium dioxide nanoparticles, UV, and NOM

Lüderwald, S., Meyer, F., Gerstle, V., Friedrichs, L., Rolfing, K., Bakanov, N., Schulz, R., Bundschuh, M.

**ABSTRACT**

Illumination of photoactive Engineered nanomaterials (ENMs) with UV triggers the formation of reactive intermediates, consequently altering the ecotoxicological potential of co-occurring organic micropollutants including pesticides due to catalytic degradation. Simultaneously, natural organic matter (NOM) adsorbs onto ENMs' surfaces, altering their surface properties, but also absorbs light reducing the photo(cata)lytic transformation of pesticides. Interactions between these environmental factors (i) impacts the ecotoxicity of photoactive ENMs, and (ii) indirectly the degradation of pesticides. We assessed the impact of field-relevant UV radiation (up to 2.6 W UVA m²), NOM (4 mg TOC/L), and photoactive ENM ($nTiO_2$, 50 μg/L) presence on the acute toxicity of six pesticides in *Daphnia magna*.

We selected azoxystrobin, dimethoate, malathion, parathion, permethrin, and pirimicarb, based on varying photolytic, and hydrolytic and hydrophobic properties. Increasing UVA alone partially reduced pesticide toxicity due to enhanced degradation. Even at 50 μg/L, $nTiO_2$ reduced but also increased pesticide toxicity, which is attributable to (i) more efficient degradation, and probably (ii) photocatalytic-induced formation of toxic byproducts. NOM (i) partially reduced pesticide toxicity, not evidently accompanied by enhanced pesticide degradation, but also (ii) inhibition in pesticide degradation, effectively increasing the pesticide toxicity. Predicting the ecotoxicological potential of pesticides based on their hydro- and photolysis or interaction with NOM was hardly possible, which was additionally promoted by the presence of $nTiO_2$.

**KEYWORDS**

Photolysis, Photocatalysis, Titanium dioxide, Pesticide, UV radiation, Natural organic matter

## INTRODUCTION

In recent years, the application of engineered nanomaterials (ENMs) has increased rapidly (Keller 2014). Consequently, ENMs are likely to enter the aquatic environment, mainly through run-off from agricultural fields treated with sewage sludge as fertilizer or the release of wastewater (Gottschalk 2011; Westerhoff 2011). Once in a surface water, the fate of ENMs is influenced by a multitude of environmental factors. The irradiation with ultra violet (UV)-light is a factor, which is of particular concern for phtocatalytically active metal oxides such as nano-sized titanium dioxide ($nTiO_2$) or zinc oxide (nZnO) (Valenzuela 2002; Ouyang 2019). Under these conditions, the formation of reactive oxygen species (ROS) is triggered (Ma 2012b). This formation of ROS is also supporting water treatment (Thiruvenkatachari 2008) by reducing the ecotoxicological potential of co-occurring organic micropollutants including pesticides (Hariharan 2006; Bundschuh 2011; Seitz 2012). In addition to UV, natural organic matter (NOM) is known for its potential to alter the surface properties of ENMs by adsorption (Aiken 2011). Moreover, NOM adsorbs light affecting the photo(cata)lytic transformation of organic micropollutants (Garg 2011). The interaction with these environmental factors has significant influences on the ecotoxicological potential of photoactive ENMs (Bar-Ilan 2013; Lüderwald 2019) and indirectly the degradation of organic micropollutants (Thiruvenkatachari 2008; Seitz 2012). It remains, however unclear whether similar effects can be observed at field relevant levels of ENM, UV and NOM.

Consequently, our study aims at addressing the presence of comparably low UV radiation (up to 2.6 W UVA m²) recorded during summers' afternoon in the shade (Häder 2007; Amiano 2012)), a field-relevant NOM (4 mg TOC/L, seaweed extract; (Ryan 2009)), and photoactive ENM concentration ($nTiO_2$, P25, 50 µg/L) on the acute toxicity of six pesticides towards the model organism *Daphnia magna*. We selected $nTiO_2$ as it is one of the most frequently applied ENMs, which is used in personal care products, coatings, paints, and pigments (Piccinno 2012; Keller 2014). Moreover, its predicted environmental concentration is in the µg/L range (Gottschalk 2013; Peters 2018) and thus at the same order of magnitude as the concentration tested here (Gondikas 2014). As pesticides we selected azoxystrobin (AZO), dimethoate (DIM), malathion (MAL), parathion (PAR), permethrin (PER), and pirimicarb (PIR), as model pesticides because of their varying photolytic (p-), and hydrolytic (h-) 50% degradation time ($DT_{50}$), and organic carbon/water partitioning coefficient ($K_{OC}$; Tab. 1). The

pesticide concentrations were quantified for each exposure scenario right after the application (0 h), as well as after experiment termination (96 h), allowing to unveil degradation efficacy, resulting ecotoxicological potential and the influence of UV radiation, $nTiO_2$, and NOM on this process.

We hypothesized that increasing UV radiation leads to an enhanced degradation of the pesticides and therefore reduced acute toxicity. Moreover, we expected this effect to be even more pronounced in the presence of $nTiO_2$ and/or NOM as a result of an amplified pesticide degradation. Finally, we anticipated this impact to be of varying magnitude for the different pesticides, depending on their physiochemical properties. More specifically, the pesticides with a comparably low p-$DT_{50}$s might undergo UV-induced detoxification, whereas for the pesticides with low susceptibility towards photolytic degradation the presence of $nTiO_2$ and NOM will induce their detoxification due to photocatalytic degradation.

**Table 1.** Pesticides, product and supplier information, along with the applied concentration ranges, photolytic and hydrolytic 50% degradation time (p- and h-DT$_{50}$), and organic carbon/water partition coefficient (K$_{OC}$) of the used in the present study. DT$_{50}$ and K$_{OC}$ values are based on the active ingredient of the respective pesticide and were obtained from the "Pesticides Properties DataBase" (PPDB; Lewis 2016), and "PubChem" (National Center for Biotechnology Information).

| Pesticide | Applied Product | Supplier | Nominal concentrations (µg/L) | p-DT$_{50}$ (days) at 20° C | h-DT$_{50}$ (days) at 20° C | K$_{OC}$ |
|---|---|---|---|---|---|---|
| Azoxystrobin (AZO) | Ortiva® | Syngenta Agro GmbH | 28.4, 56.8, 113.6, 227.2, 454.5, 909.1 | 8.7 | stable | 589 |
| Dimethoate (DIM) | Perfekthion® | BASF SE | 50, 100, 20, 400, 800, 1600, 3200 | 175 | 68 | 5-50 |
| Malathion (MAL) | PESTANAL®, analytical standard | Sigma-Aldrich | 0.1, 0.2, 0.4, 0.8, 1.25, 2.5, 5 | 98 | 6.2 | 1800 |
| Parathion (PAR) | PESTANAL®, analytical standard | Sigma-Aldrich | 0.3, 0.6, 1.25, 2.5, 5, 10 | 30 | 260 | 7660 |
| Permethrin (PER) | PESTANAL®, analytical standard | Sigma-Aldrich | 0.09, 0.18, 0.4, 0.7, 1.4, 2.8, 5.6 | 1 | 31 | 100000 |
| Pirimicarb (PIR) | Pirimor® | Syngenta Agro GmbH | 5, 10, 20, 40, 60, 80 | 0.5-6 | stable | 56-800 |

## MATERIAL AND METHODS

### Nanoparticle characterization

The utilized $nTiO_2$ was acquired as powder (AEROXIDE® $TiO_2$ P25; Anatase-Rutile ratio: ~75:25; Evonik) with an advertised primary particle size of 21 nm, and a surface area of 50 ±15 $m^2$/g (Brunauer-Emmett-Teller). At the Institute for Particle Technology (TU Braunschweig, Germany) an additive free dispersion (80 g $nTiO_2$/L) was prepared by stirred media milling (PML 2, Bühler AG) using deionized water as dispersant. Following, this dispersion was diluted with deionized water (stock dispersion, 2 g $nTiO_2$/L, nominal concentration) and pH stabilized (~3.25) by applying 120 µL of 2 M HCl/L. The intensity-weighted average hydrodynamic diameter of the stock dispersion was ~80 nm, measured via dynamic light scattering (DelsaNano C, Beckman Coulter) applying the following conditions: $n$=3, 60 measurements each; temperature=20°C (Tab. 2). Before the application, the stock dispersion was sonicated for 10 minutes with a nominal power of 215 W and a sonication frequency of 35 Hz (SONOREX DIGITEC DT 514 H, Bandelin) to provide a homogeneous particle distribution. Transmission electron microscopy images of the ENM can be found in Fig. S1.

**Table 2.** Particle size distribution of the applied $nTiO_2$ stock dispersion ($n$=3), i.e. intensity weighted average diameter, polydispersity index (PI), as well as the 10th, 50th, and 90th percentile.

| Rep. No | Avg. diameter (nm) | PI | $D_{10\%}$ (nm) | $D_{50\%}$ (nm) | $D_{90\%}$ (nm) |
|---------|---------------------|------|------------------|------------------|------------------|
| 1 | 80.1 | 0.19 | 45.2 | 86.1 | 166.4 |
| 2 | 84.8 | 0.20 | 48.9 | 87.9 | 159.8 |
| 3 | 86.0 | 0.16 | 51.2 | 88.6 | 155.1 |
| Mean | 83.5 | 0.18 | 48.4 | 87.6 | 160.4 |

### Pesticides

The pesticides applied in this study were either purchased as commercially available products (for AZO, DIM and PIR), or as an analytical standard (for MAL, PAR, and PER), and diluted in the respective test medium in order to achieve the desired nominal concentrations of the active ingredient (Tab. 1). Their selection is motivated by varying degrees of p- and h-$DT_{50}$, ranging from 0.5–175 p-$DT_{50}$ (days), and 6.2–260 or stable h-$DT_{50}$ (days; Tab. 1). Thereby, varying degrees in p- and h-$DT_{50}$ will determine the rate of photolytic, photocatalytic, and hydrolytic degradation and therefore the potential

of degradation and detoxification towards *D. magna*. Moreover, the pesticides were characterized by a high variation in their $K_{OC}$, ranging from 5–100000, respectively (Tab. 1). This broad range of adsorption capacity could influence the pesticides' interaction with NOM, which is likely to have an impact on their ecotoxicological potential.

**Test organism**

*Daphnia magna* (obtained from Eurofins-GAB GmbH, Germany) were kept in mass culture inside a climate-controlled chamber (Weiss Environmental Technology Inc., Germany) at 20 ±1°C applying a 16:8 h (light:dark) photoperiod (fluorescent tubes; Osram L 58W/840 lumilux cool white; visible light intensity: 3.14 W/m$^2$; UVA: 0.01 W/m$^2$; UVB: 0.01 W/m$^2$). Thereby, groups of 25 adult females were kept in 1.5 L of reconstituted hard freshwater, according to the ASTM International Standard Guide E729 (ASTM 2007), that was additionally enriched with selenium, vitamins (thiamine hydrochloride, cyanocobalamin, and biotin), and seaweed extract (SW; 8 mg TOC/L; Marinure®). A renewal of the medium was carried out three times a week and the organisms were daily fed on the green algae *Desmodesmus* sp. (corresponding to 200 µg C/organism/d).

**Bioassay setup**

For each pesticide four individual exposure scenario were realized, which in the following sections are referred to as test series (TS): (1) pesticide exposure only (PEST), (2) pesticide exposure in the presence of 50 µg/L nTiO$_2$ (PEST+nTiO$_2$), (3) pesticide exposure in the presence of 4 mg TOC/L (PEST+NOM), and (4) combination of pesticide exposure in the presence of 50 µg/L nTiO$_2$ and 4 mg TOC/L (PEST+nTiO$_2$ + NOM). Each TS covered 4 levels with increasing UVA radiation, applying comparatively low but environmentally relevant levels (0–2.6 W UVA/m$^2$, UVA I–UVA IV; (Häder 2007); Tab. 3). The different UVA levels of radiation were achieved by attaching UV-porous curtains of varying efficiency to the UV tubes (as per Lüderwald 2019).

The tests were based on the OECD TG No. 202 (OECD 2004), with the following two adaptions: (i) the test duration was prolonged to 96 h, as recommended for testing with nanomaterials (Dabrunz 2011; Karimi 2018), and (ii) instead of fluorescent tubes, UV fluorescent tubes (Magic Sun 23/160 R 160 W, Heraeus, Germany; UVA output: 44 W,

UVB output: 1.1%, measured with a RM12 radiometer, Dr. Göbel UV-Electronic GmbH) were used as light source applying a 8:16 h (light:dark) rhythm. As test medium the vitamin and selenium enriched culture medium without SW was used (see section 2.3).

For each acute toxicity test one replicate consisted of five juvenile *Daphnia* (age <24 h), exposed to the respective pesticide concentration, TS and UVA radiation (=treatment), while each treatment was replicated four times. Each day daphnids were visually checked for their immobility (i.e. after 24, 48, 72 and 96 h of exposure). Immobility data was used to calculate the pesticides' 96-h EC50 values for the respective exposure scenarios.

SW was chosen as NOM representative, given its recommendation in standard test guidelines as additive for long-term culturing of *D. magna* and chronic *Daphnia* experiments (OECD 2008). Prior application, a SW subsample (8 mg TOC/L, diluted in 50 mL test medium, pesticide- and $nTiO_2$-free) was analyzed as part of an earlier study at the DOC-LABOR (Karlsruhe, Germany), providing a more detailed characterization (contains data as per Seitz 2016; Tab. S1).

**Table 3.** Applied exposure scenarios for the acute toxicity bioassays. Each scenario was applied to each of the six pesticides (AZO, DIM, MAL, PAR, PER, and PIR). *Before the start of the experiments, UVA radiation was measured at the water-surface of the test vessels, and were randomly placed in the areas that were in the UV-range respectively listed (section 2.4).

| Test series (TS) | UVA-level | UV radiation* (W UVA/ $m^2$) | $nTiO_2$ (µg/L) | NOM (mg TOC/L) |
|---|---|---|---|---|
| PEST | UVA-I | 0 | 0 | 0 |
| | UVA-II | 0.4–0.6 | 0 | 0 |
| | UVA-III | 1–1.4 | 0 | 0 |
| | UVA-IV | 2.2–2.6 | 0 | 0 |
| PEST +$nTiO_2$ | UVA-I | 0 | 50 | 0 |
| | UVA-II | 0.4–0.6 | 50 | 0 |
| | UVA-III | 1–1.4 | 50 | 0 |
| | UVA-IV | 2.2–2.6 | 50 | 0 |
| PEST +NOM | UVA-I | 0 | 0 | 4 |
| | UVA-II | 0.4–0.6 | 0 | 4 |
| | UVA-III | 1–1.4 | 0 | 4 |
| | UVA-IV | 2.2–2.6 | 0 | 4 |
| PEST+$nTiO_2$+NOM | UVA-I | 0 | 50 | 4 |
| | UVA-II | 0.4–0.6 | 50 | 4 |
| | UVA-III | 1–1.4 | 50 | 4 |
| | UVA-IV | 2.2–2.6 | 50 | 4 |

## Chemical analysis

We were aiming to unveil the influence of $nTiO_2$, UVA radiation, and NOM on the degradation and therefore possibly altering acute toxicity of pesticides over the course of the experiments. Therefore, water samples were taken at the highest applied pesticide concentration for each exposure scenario right after the pesticide application (0 h), as well as after the termination of the experiments (96 h).

Samples (10 mL) were stored in liquid scintillation vials (glass, 20 mL), at -20°C until realizing analysis via ultra-high-performance liquid chromatography (Thermo Fischer Sientific). The concentrations were determined using an external standard calibration applying matrix-aligned standards. For the first AZO experiment samples were taken at 1818.2 µg/L, although the following experiments were conducted with 909.1 µg/L as highest concentration. To keep the chemical analysis comparable, all further AZO samplings were performed at 1818.2 µg/L. Due to a malfunctioning freezer PAR and PER samples could not be analyzed (Tab. 4).

## Statistical Analysis

After 96-h of exposure immobility data in each of the treatment combinations was used to calculate EC50 values (Tab. S2), which is the concentration of the respective pesticide, that caused immobility in 50% of the test organisms. This was done by fitting adequate dose-response models (Ritz 2005). The most appropriate model was selected based on Akaike's information criterion and visual judgement (Fig. S2; Tab. S2). Statistical significance between EC50 values among the different exposure scenarios was tested by applying Bonferroni adjusted confidence interval (CI) testing (Wheeler 2006). 96-h EC50s referred in the following sections are based on nominal applied concentrations if not explicitly declared else. Measured based 96-h EC50s were calculated and are available in Tab. S2, as well as depicted in Fig. S3.

# RESULTS
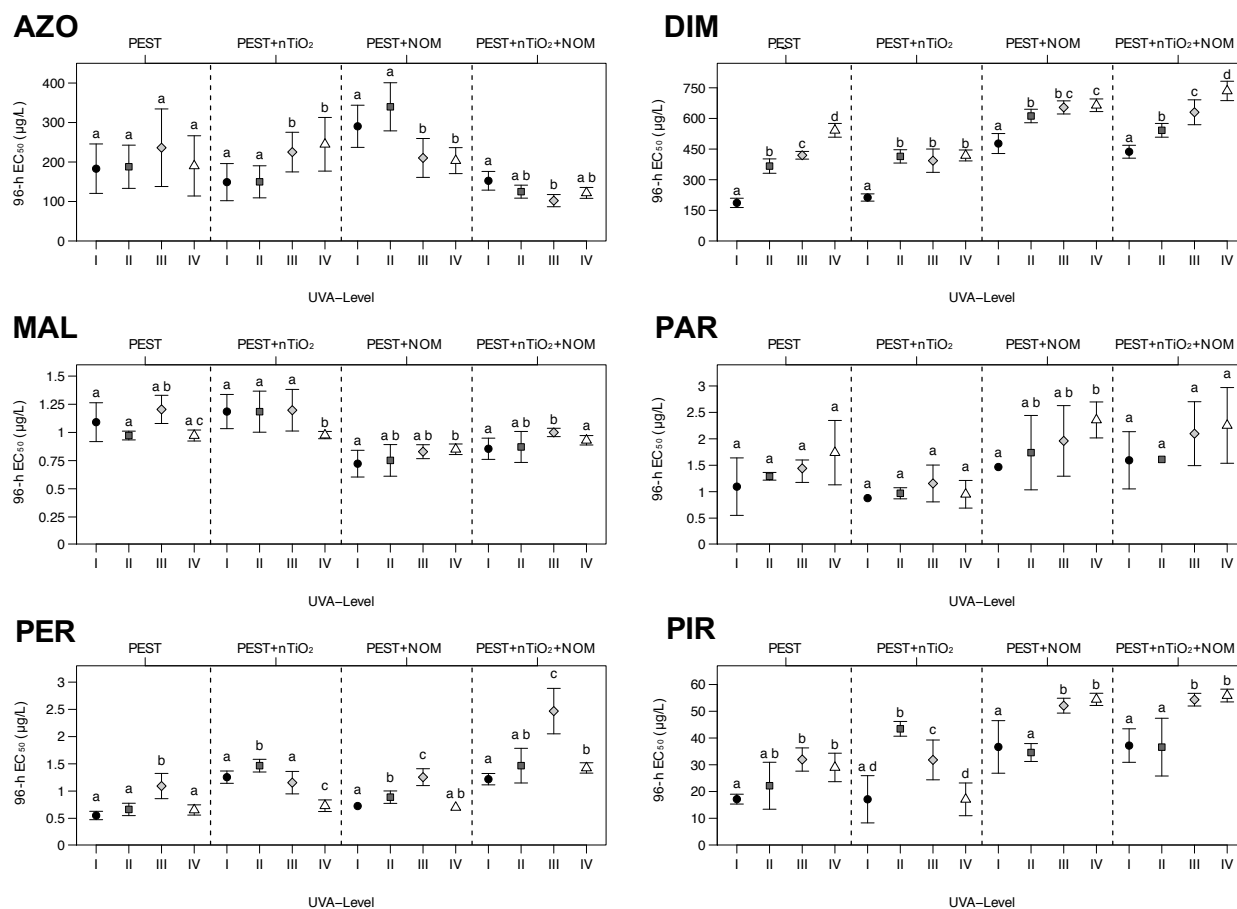


**Figure 1.** 96-h EC50s (µg/L ±95% CI) of *D. magna* for the six pesticides azoxystrobin (AZO), dimethoate (DIM), malathion (MAL), parathion (PAR), permethrin (PER), and pirimicarb (PIR) based on nominal concentrations, under varying UVA radiation (I: 0.00 W UVA/m$^2$, II: 0.40–0.60W UVA/m$^2$, III: 1.00–1.40W UVA/m$^2$, and IV: 2.20–2.60W UVA/m$^2$), and TS (PEST, PEST+nTiO$_2$, PEST+NOM, and PEST+nTiO$_2$+NOM; Tab. 3). For more information on the applied pesticides and concentrations see Tab. 1. Different letters denote statistically significant difference between individual UVA levels but within one TS.

## Azoxystrobin (AZO)

In absence of NOM and nTiO$_2$ (PEST), increasing UVA radiation did not have a significant impact on AZO toxicity with 96-h EC50 values ranging between 180 and 240 µg/L (UVA-I and UVA-III, respectively; Fig. 1). There was also no meaningful photo-induced degradation of AZO over 96 h (Tab. 4), except for UVA-III (~20% relative to the other TS). In PEST+nTiO$_2$, a UVA radiation ≥UVA-III caused an up to 1.6-fold decrease in AZO toxicity. This is in accordance with the measured AZO concentrations, showing a ~30% reduction at UVA-IV after 96 h compared to UVA-I

(Tab. 4). At low UVA radiation, PEST+NOM revealed generally an up to 2-fold reduced AZO toxicity relative to the other TS (Fig. 1). However, PEST+NOM caused a significantly (up to ~1.4-fold) enhanced toxicity starting with the UVA-III treatment (UVA-III: 210 µg/L and UVA-IV: 205 µg/L), relative to the absence of UV (290 µg/L; Fig. 1). This contradicts the measured AZO concentrations showing a 25 and 30% higher degradation than at UV-I and UVA-II, respectively (Tab. 4). When combining PEST+nTiO$_2$+NOM, increasing UVA radiation lead to the highest observed AZO toxicity amongst the four TS. At UVA-III and UVA-IV, the 96-h EC50 values were significantly reduced by 1.25- and 1.5-fold (UVA-III: 100 µg/L and UVA-IV: 120 µg/L, respectively) relative to UVA-I (150 µg/L; Fig. 1) and despite a more than 10% AZO degradation after 96h.

**Dimethoate (DIM)**

The absence of NOM and nTiO$_2$ (PEST) revealed a continuous decrease of DIM toxicity with increasing UVA radiation with the 96-h EC50 value increasing up to 3-fold from approx. 185 to 540 µg/L (Fig. 1). In presence of nTiO$_2$, the toxicity of DIM decreased around 2-fold by increasing UVA radiation from UVA-I to UVA-II (96-h EC50: ~210 µg/L, and 415 µg/L, respectively; Fig. 1), but reached a plateau and did not further decrease at higher UVA levels. Similarly, during PEST+NOM with a generally lower DIM toxicity (factor of ~1.7 relative to PEST+nTiO$_2$), leading to 96-h EC50s of up to 660 µg/L (Fig. 1). Also, in the PEST+nTiO$_2$+NOM TS toxicity was reduced with increasing UVA (Fig. 1). The lowest DIM degradation was observed in TS PEST with a maximum of ~10%, despite the up to 3-fold observed toxicity reduction (0h vs. 96h at UVA-IV). For PEST+nTiO$_2$, PEST+NOM and PEST+nTiO$_2$+NOM, the concentration of DIM was reduced by up to 30% (Tab. 4).

**Malathion (MAL)**

Increasing UVA radiation alone did not change MAL 96-h EC50 values meaningfully, they fluctuated by a factor of 1.2 (Fig. 1). The TS PEST+nTiO$_2$ influenced MAL toxicity to a similar extend (1.2-fold) but this impact was statistically significant at the highest UVA level (Fig. 1). In presence of NOM, MAL toxicity was enhanced compared to PEST and PEST+nTiO$_2$ with increasing 96-h EC50 at higher UVA radiation, which was partly significant (Fig. 1). Similarly, PEST+nTiO$_2$+NOM revealed a by tendency reduced MAL toxicity relative PEST+NOM (up to ~1.2-fold; Fig. 1). MAL concentration decreased

over the study duration, a pattern enhanced by increasing UVA radiation with the lowest decrease in presence of $nTiO_2$ alone (30%) and the highest in the other TS (70%).

### Parathion (PAR)

Increasing UVA radiation alone induced a non-significant trend of a reduced PAR toxicity by up to 70% (Fig. 1). Compared to PEST, PAR toxicity was generally higher in presence of $nTiO_2$ by a factor between 1.2–1.8-fold (comparing the respective UVA levels of both TS). Nonetheless, in PEST+$nTiO_2$ the 96-h- EC50 increased from ~0.85 µg/L at UVA-I to ~1.15 µg/L at UVA-III, followed by a decrease to 0.95 µg/L at UVA-IV (Fig 1). Even if not statistically significant, the presence of NOM in both PEST+NOM and PEST+$nTiO_2$+NOM favored the lowest observed PAL toxicity further decreasing with enhancing UVA radiation (Fig. 1).

### Permethrin (PER)

In absence of $nTiO_2$ or NOM, UVA levels lead to a significant decrease of PER toxicity by a factor of 2 at UVA-III, followed by a recurring decrease at UVA-IV to nearly the same level as observed at UVA-I (Fig. 1). A similar pattern was observed in presence of $nTiO_2$ (PEST+$nTiO_2$; Fig 1). The addition of NOM (PEST+NOM) promoted the mitigation of PER toxicity at UVA-I and UVA-II by a factor of ~1.3, relative to the absence of NOM. Compared to PEST+$nTiO_2$, however, the 96-h EC50s of PEST+NOM at UVA-I and UVA-II were ~1.7-fold lower, a pattern which was not confirmed for UVA-III and UVA-IV (Fig. 1). Combining PEST+$nTiO_2$+NOM induced a 2.2-fold reduced PER toxicity, relative to PEST.

### Pirimicarb (PIR)

With increased UVA radiation but in absence of $nTiO_2$ and NOM (PEST), PIR toxicity decreased by up to ~1.9-fold, which was partly significant (Fig. 1). In presence of $nTiO_2$ PIR toxicity was decreased at lower UVA radiation, while this impact vanished at the highest UVA radiation tested (Fig 1). The presence of NOM irrespective of the $nTiO_2$ presence and UVA radiation revealed the highest reduction in PIR toxicity. These pattern in toxicity are confirmed by chemical analysis with decreasing PIR concentrations at increasing UVA radiation. This decrease was up to 90% (UVA-IV; Tab. 4).

**Table 4.** Measured concentrations of AZO, DIM, MAL, and PIR in TS 1–4, at varying UVA radiations (UVA-I-IV), approx. 10 min (0 h) after pesticide application to the respective test medium and exposure scenario, as well as after the termination of the experiments (96 h). Due to a malfunctioning freezer PAR and PER samples were not suitable for chemical analysis and are therefore not listed. Δ illustrates the relative degradation in % after 96 h referring to the 0-h concentrations of the respective test series, whereas negative values indicate pesticide degradation. NA=not assessable.

| TS | UVA | Time (h) | AZO (µg/L) | Δ (%) | DIM (µg/L) | Δ (%) | MAL (µg/L) | Δ (%) | PIR (µg/L) | Δ (%) |
|---|---|---|---|---|---|---|---|---|---|---|
| PEST | - | 0 | 1396 | - | 2900 | - | 6.3 | - | 69.6 | - |
| | I | 96 | 1817 | 30 | 2862 | -1 | 2.0 | -68 | 80.7 | 16 |
| | II | 96 | 1867 | 34 | 2633 | -9 | 2.7 | -58 | 67.6 | -3 |
| | III | 96 | 1476 | 6 | 2688 | -7 | 2.1 | -66 | 30.0 | -57 |
| | IV | 96 | 1713 | 23 | 2532 | -13 | 2.0 | -68 | 14.6 | -79 |
| PEST | - | 0 | 1443 | - | 2856 | - | 2.6 | - | 64.7 | - |
| + | I | 96 | 1693 | 17 | 2827 | -1 | 1.3 | -48 | 91.9 | 42 |
| nTiO$_2$ | II | 96 | 1648 | 14 | 2804 | -2 | 2.2 | -14 | 7.0 | -89 |
| | III | 96 | 1441 | 0 | 2946 | 3 | 1.1 | -58 | <LOD | NA |
| | IV | 96 | 1186 | -18 | 1983 | -31 | 0.9 | -65 | <LOD | NA |
| PEST | - | 0 | 1533 | - | 2989 | - | 4.4 | - | 35.6 | - |
| + | I | 96 | 1575 | 3 | 2798 | -6 | 3.2 | -29 | 43.0 | 21 |
| NOM | II | 96 | 1431 | -7 | 2887 | -3 | 3.1 | -29 | 22.7 | -36 |
| | III | 96 | 1200 | -22 | 2652 | -11 | 2.9 | -35 | 17.5 | -51 |
| | IV | 96 | 1066 | -30 | 2150 | -28 | 3.2 | -29 | 9.2 | -74 |
| PEST | - | 0 | 1496 | - | 2981 | - | 2.9 | - | 37.0 | - |
| + | I | 96 | 1520 | 2 | 2837 | -5 | 2.1 | -30 | 38.8 | 5 |
| nTiO$_2$ | II | 96 | 1275 | -15 | 2841 | -5 | 2.0 | -31 | 29.4 | -20 |
| + | III | 96 | 1356 | -9 | 2700 | -9 | 2.2 | -25 | 13.8 | -63 |
| NOM | IV | 96 | 1228 | -18 | 2028 | -32 | 0.9 | -71 | 4.4 | -88 |

## DISCUSSION

### Influence of UVA illumination (test series: PEST)

In our study UVA illumination of the pesticides resulted in two effect patterns: (i) decreasing pesticide toxicity with increasing UVA illumination, and (ii) constant pesticide toxicity independent of the applied UVA radiation. Decreasing pesticide toxicity with increasing UVA illumination was hypothesized for substances with a high photolytic potential as represented by a low p-$DT_{50}$; a pattern which was observed for DIM, PAR, and PIR. In principle the reduction of DIM and PIR toxicity were confirmed by chemical analysis: DIM and PIR concentrations were substantially reduced by up to approx. 15% and 80%, respectively (Tab.4). These observations are in line with earlier studies with DIM (Evgenidou 2006) and PIR (e.g. (Schwack 1993; Romero 1994; Pirisi 1996; Seitz 2012), highlighting a more efficient photodegradation for PIR. Although not confirmed by chemical analyses in our study, Zoh et al. (2006) highlighted an 80% reduction in PAR under natural solar radiation (average intensity: 6.4–19 $W/m^2$) within 150 min confirming its photolytic properties (see also Tab. 1). Hence, the reduction in PAR toxicity reported in our study is likely driven by its photolysis, though less efficient relative to PIR and DIM.

Steady pesticide toxicity regardless of the applied UVA radiation was observed for AZO, MAL, and PER suggesting no detoxification. Indeed, the degradation of AZO was negligible with increasing UVA illumination (Tab. 4). Although the UV-visible (UV/VIS) absorption spectrum of AZO slightly overlaps with the solar light spectrum suggesting UV-induced photodegradation could theoretically occur, our observation is in line with Boudina et al. (2007). Contrasting to AZO, MAL was even in darkness (UVA-I) degraded by up to approx. 70% (Tab. 4) suggesting hydrolysis as a dominating detoxification pathway with little additional impact through photolysis (Tab. 1). For PER we would have assumed a fast degradation in presence of UVA followed by a significant detoxification, given the low p-$DT_{50}$ of 1 d. The mostly steady 96-h EC50 with increasing UV radiation could be driven by the "knock down" through fast interference with sodium channels leading to rapid paralysis finally resulting in death, a mode of action typical for pyrethroids such as PER (United States 2006; Ensley 2007). Consequently, the responses of the test organisms to PER exposure may have occurred faster than any potential degradation.

**Influence of UVA illumination + nTiO$_2$ (test series PEST+nTiO$_2$)**

Combining UVA radiation with nTiO$_2$ resulted in three patterns: (i) enhanced pesticide degradation compared to nTiO$_2$-absence, along with toxicity reduction (ii) low UVA radiation-induced a reduction while high UVA radiation enhanced toxicity, and (iii) steady 96-h EC50s despite increasing UVA radiation, while the toxicity was generally higher compared to nTiO$_2$-absence (PEST).

In our study, more efficient pesticide degradation relative to the absence of nTiO$_2$ was observed for AZO (PEST: -23% vs. PEST + nTiO$_2$: 18%; UVA-IV), DIM (PEST: 13% vs. PEST + nTiO$_2$: 31%; UVA-IV), and PIR (PEST: 79% vs. PEST + nTiO$_2$: <LOQ; UVA-IV), being partly accompanied by an additional detoxification. An amplified degradation is known to be triggered by solar illumination of a co-occurring photocatalyst like nTiO$_2$, inducing various redox reactions (Konstantinou 2003). This results in the formation of ROS (Turchi 1989; Low 1991; Pelizzetti 1999), finally leading to mineralization and detoxification of organic compounds such as pesticides (Hoffmann 1995; Robert 2002).

Solar illumination of a co-occurring photocatalyst has been documented as efficient treatment technology for organic micropollutants in general and for pesticides, including AZO, DIM, and PIR, in particular. However, those studies mainly focused on environmentally irrelevant concentrations of photocatalysts (mg-g/L range) and UV radiation that may be considered as relatively high (up to 30 W/m2, see Malato 2001; Kim 2006; Chen 2007; Navarro 2009). Our observations are largely in line with those studies, and furthermore demonstrate that photocatalytic degradation and detoxification of pesticides, is even taking place under conditions very close to concentrations considered field relevant (i.e., 50 µg nTiO$_2$/L; Fig. 1). Moreover, the lower p-DT$_{50}$ seemed to foster the degradation efficiency of PIR (0.5–6 d; up to <LOQ), relative to AZO (8.7 d; up to 18%), and DIM (175 d; up to 30%).

On the downside, the presence of nTiO$_2$ at higher UVA radiation also resulted in increased toxicity in *D. magna* as demonstrated for MAL, PER, and PIR (Fig. 1) despite elevated pesticide degradation (measured for MAL and PIR samples; Tab. 4). MAL, PER, and PIR are acting as acetylcholinesterase inhibitor, which is known as fast-acting mode of action (Cambon 1979; Xuereb 2009). This, in combination with the highest applied UVA radiation along with the presence of nTiO$_2$, might have facilitated the pesticide degradation, but potentially resulted in a synergistic stress (through ROS) causing an increased toxicity while outweighing degradation-triggered detoxification.

In support of this assumption, Johnson et al. (2015) observed sublethal toxicity of $nTiO_2$ when illuminated with UVA radiation in the eastern oyster *Crassostrea virginica* at a concentration as low as 50 µg/L (sensu Amiano 2012).

The 96-h EC50s of DIM that indicate higher toxicity at TS PEST + $nTiO_2$ than at TS PEST despite more efficient degradation (Tab. 4), could, additionally, be induced by the formation of metabolites that are more toxic than the parent substance (Evgenidou 2006; Farner Budarz 2017). It was shown that during photocatalytic degradation with $nTiO_2$, DIM is degraded into nine by-products (Evgenidou 2006), whereas the major by-product, omethoate (Van Scoy 2016) is 90-fold more toxic relative to the mother compound (PPDB). Likewise, the photocatalysis (UV=5.8 $W/m^2$; $TiO_2$=120 mg/L) of MAL sharply increases its toxicity towards *Vibrio fischeri*, whereas no increase in toxicity was observed when treating MAL with UV alone (Li 2019). Hence, also for MAL, a formation of toxic by-products at the highest applied UVA radiation seems likely.

With a medium p-$DT_{50}$ of 30 d, PAR might have been subjected to photolytic degradation in the presence of UVA, which was shown to be significantly amplified in the presence of the photocatalyst $nTiO_2$ (Evgenidou 2007). However, photocatalytic transformation of PAR can lead to the formation of paraoxon (Evgenidou 2007). Paraoxons's acute toxicity towards *D. magna* is approx. 10-times higher relative to the parent compound (Guilhermino 1996), being the potential trigger for the increased PAR toxicity in TS PEST + $nTiO_2$, compared to TS PEST.

In essence, we demonstrated a distinctive impact of field-relevant UVA radiation (up to 2.6 W UVA/ $m^2$) on $nTiO_2$ induced toxicity applied at very low and thus indeed environmentally relevant concentrations. UVA- and $nTiO_2$-induced effects were observed at radiation intensities and concentrations 2.5-300-fold and 4-2000-fold, respectively, lower than applied in existing studies (e.g. Romero 1994; Zoh 2006; Evgenidou 2007; Seitz 2012). Our observations seem to be triggered by a combination $nTiO_2$ exerting direct negative effects on aquatic biota (i.e. formation of ROS; (Amiano 2012)) and an alteration of the toxic potential of co-occurring pesticides. The latter might either be a reduced toxicity as a consequence of elevated photolytic degradation or an increased toxicity induced by the formation of toxic by-products. Furthermore, this impact seems partly explained by the pesticides' physico-chemical properties (i.e. p- and h-$DT_{50}$).

## Influence of UVA illumination in presence of NOM (test series: PEST+(nTiO₂)+ NOM)

The application of NOM resulted in two contrasting patterns: (i) a reduced pesticide toxicity in the presence of NOM, not accompanied by an enhanced pesticide degradation, and (ii) NOM-induced inhibition in pesticide degradation increasing pesticide toxicity on a relative scale. This is not in line with our expectations as we hypothesized NOM to amplify the degradation and therefore detoxification of pesticides. Furthermore, there was no clear relationship between $K_{OC}$ and degradation efficiency, or detoxification observable. More precisely, higher adsorption tendencies towards NOM, triggered by comparably high $K_{OC}$s did not reveal specific impact on the pesticides' degradation or toxicity (Tab. 4; Tab. S2).

The generally detoxifying effect of NOM was observed for DIM, PAR, and PIR (relative to PEST, and PEST+nTiO₂; Fig. 1), which could not be linked to a higher pesticide degradation for DIM and PIR (Tab. 4). The lower pesticide toxicity seems, hence, driven by the potential of NOM to serve as energy source with a positive effect on the fitness of *D. magna*, as NOM increases the lifespan and offspring along with a higher tolerance towards other stressors (Bouchnak 2010; Bergman Filho 2011). In addition to an increased fitness and stress tolerance of *D. magna*, NOM could directly interact with the pesticide by adsorption reducing dissolved pesticide concentration and consequently bioavailability (Yang 2006). Moreover, NOM is prone to transformations induced by light (Sulzberger 2009) potentially triggered by photoreactive intermediates originating from illuminated ENMs such as nTiO₂ (Aiken 2011). This will most likely have an influence on nTiO₂-mediated photocatalytic reactions, i.e. the formation of ROS (Ma 2012b; Kim 2013), and consequently the detoxification of micropollutants (Bundschuh 2011), demonstrated by the degradation efficiency and resulting detoxification of DIM being most effective in the presence of nTiO₂ and NOM.

Contrastingly, absorption of UVA radiation by NOM could lead to a UVA-attenuating shading effect (Albrektienė 2012), decreasing photolysis/photocatalysis potential of certain pesticides indirectly (Garbin 2007). The apparently increased toxicity of MAL in presence of NOM may, thus, be based on a shading-triggered decreased UVA-availability for photolysis, consequently leading to the reduced potential for pesticide degradation or the formation of less-toxic metabolites. This is a mechanism that has also been suggested for the insecticide fipronil (Bejarano 2005). While acting as light-absorbing entity, NOM is also suggested to induce the formation of reactive

intermediates, (e.g. ROS; Garbin 2007; Aiken 2011), that are known to be toxic for aquatic life (Cabiscol 2000; Buonocore 2010).

## CONCLUSION

Our study shows that exposing pesticides to degradation promoting factors like UV radiation, $nTiO_2$ and NOM at field relevant conditions does not necessarily lead to their detoxification. While existing studies are mainly focusing on detoxifying pretreatments of contaminated waters (e.g. Zoh 2006; Seitz 2012), our study is among the first pointing out the direct impact of a more complex field-relevant setup on potential degradation and detoxification of pesticides through photo(cata)lysis (c.f. Farner Budarz 2017). We conclude that the impact on the resulting ecotoxicological potential of the pesticide seems mainly driven by the specific treatment process, i.e. photolysis vs. photocatalysis (Li 2019), rather than by physico-chemical properties of the pesticide. In nature, the detoxification of those micropollutants seems strongly affected by the presence of NOM (Garbin 2007; Aiken 2011). More specifically, the presence of NOM potentially amplifies the detoxification of pesticides on the one hand by facilitating photocatalytic degradation. On the other hand, photocatalytic degradation can also enhance the ecotoxicological potential due to the formation of byproducts that are more toxic than the parent pesticide. The impact of UVA, photoactive ENMs, and NOM on the degradation and detoxification of pesticides under artificial and ideal conditions seem therefore not suitable for reliable ecotoxicological projections.

## ACKNOWLEDGEMENTS

**REFERENCES**

Aiken GR, Hsu-Kim H, Ryan JN. 2011. Influence of dissolved organic matter on the environmental fate of metals, nanoparticles, and colloids. *Environ Sci Technol* 45:3196-3201. DOI: 10.1021/es103992s.

Albrektienė R, Rimeika M, Zalieckienė E, Šaulys V, Zagorskis A. 2012. Determination of organic matter by UV absorption in the ground water. *J Environ Eng Landsc* 20:163-167. DOI: 10.3846/16486897.2012.674039.

Amiano I, Olabarrieta J, Vitorica J, Zorita S. 2012. Acute toxicity of nanosized $TiO_2$ to *Daphnia magna* under UVA irradiation. *Environ Toxicol Chem* 31:2564-2566. DOI: 10.1002/etc.1981.

ASTM E729-96. 2007. Standard guide for conducting acute toxicity tests on test materials with fishes, macroinvertebrates, and amphibians. *ASTM International, West Conshohocken* 1–22. DOI: https://doi.org/10.1520/C0033-03R06.

Bar-Ilan O, Chuang CC, Schwahn DJ, Yang S, Joshi S, Pedersen JA, Hamers RJ, Peterson RE, Heideman W. 2013. $TiO_2$ nanoparticle exposure and illumination during zebrafish development: mortality at parts per billion concentrations. *Environ Sci Technol* 47:4726-4733. DOI: 10.1021/es304514r.

Bejarano AC, Chandler GT, Decho AW. 2005. Influence of natural dissolved organic matter (DOM) on acute and chronic toxicity of the pesticides chlorothalonil, chlorpyrifos and fipronil on the meiobenthic estuarine copepod *Amphiascus tenuiremis*. *J Exp Mar Biol Ecol* 321:43-57. DOI: https://doi.org/10.1016/j.jembe.2005.01.003.

Bergman Filho T, Soares A, Loureiro S. 2011. Energy budget in *Daphnia magna* exposed to natural stressors. *Environ Sci Pollut Res* 18:655-662. DOI: 10.1007/s11356-010-0413-0.

Bouchnak R, Steinberg CEW. 2010. Modulation of longevity in *Daphnia magna* by food quality and simultaneous exposure to dissolved humic substances. *Limnologica* 40:86-91. DOI: http://dx.doi.org/10.1016/j.limno.2009.11.010.

Boudina A, Emmelin C, Baaliouamer A, Païssé O, Chovelon JM. 2007. Photochemical transformation of azoxystrobin in aqueous solutions. *Chemosphere* 68:1280-1288. DOI: https://doi.org/10.1016/j.chemosphere.2007.01.051.

Bundschuh M, Zubrod JP, Seitz F, Stang C, Schulz R. 2011. Ecotoxicological evaluation of three tertiary wastewater treatment techniques via meta-analysis and feeding bioassays using *Gammarus fossarum*. *J Hazard Mater* 192:772-8. DOI: 10.1016/j.jhazmat.2011.05.079.

Buonocore G, Perrone S, Tataranno ML. 2010. Oxygen toxicity: chemistry and biology of reactive oxygen species. *Semin Fetal Neonatal M* 15:186-190. DOI: http://dx.doi.org/ 10.1016/j.siny.2010.04.003.

Cabiscol E, Tamarit J, Ros J. 2000. Oxidative stress in bacteria and protein damage by reactive oxygen species. *Int Microbiol* 3:3-8. DOI: 10.2436/im.v3i1.9235.

Cambon C, Declume C, Derache R. 1979. Effect of the insecticidal carbamate derivatives (carbofuran, pirimicarb, aldicarb) on the activity of acetylcholinesterase in tissues from pregnant rats and fetuses. *Toxicol Appl Pharmacol* 49:203-208. DOI: 10.1016/0041-008x(79)90242-4

Chen JQ, Wang D, Zhu MX, Gao CJ. 2007. Photocatalytic degradation of dimethoate using nanosized $TiO_2$ powder. *Desalination* 207:87-94. DOI: 10.1016/j.desal. 2006.06.012.

Dabrunz A, Duester L, Prasse C, Seitz F, Rosenfeldt R, Schilde C, Schaumann GE, Schulz R. 2011. Biological surface coating and molting inhibition as mechanisms of $TiO_2$ nanoparticle toxicity in *Daphnia magna*. *PLoS ONE* 6:e20112. DOI: doi:10.1371/journal.pone.0020112.

Ensley S. 2007. Chapter 41 - Pyrethrins and pyrethroids. In Gupta RC, ed, *Veterinary Toxicology.* Academic Press, pp. 494-498. DOI: https://doi.org/10.1016/B978-012370467-2/50138-3.

Evgenidou E, Konstantinou I, Fytianos K, Albanis T. 2006. Study of the removal of dichlorvos and dimethoate in a titanium dioxide mediated photocatalytic process through the examination of intermediates and the reaction mechanism. *J Hazard Mater* 137:1056-1064. DOI: 10.1016/j.jhazmat.2006.03.042.

Evgenidou E, Konstantinou I, Fytianos K, Poulios I, Albanis T. 2007. Photocatalytic oxidation of methyl parathion over $TiO_2$ and ZnO suspensions. *Catal Today* 124:156-162. DOI: https://doi.org/10.1016/j.cattod.2007.03.033.

Farner Budarz J, Cooper EM, Gardner C, Hodzic E, Ferguson PL, Gunsch CK, Wiesner MR. 2017. Chlorpyrifos degradation via photoreactive $TiO_{(2)}$ nanoparticles: assessing the impact of a multi-component degradation scenario. *J Hazard Mater* 372:61-68. DOI: 10.1016/j.jhazmat.2017.12.028.

Garbin JR, Milori DMBP, Simões ML, da Silva WTL, Neto LM. 2007. Influence of humic substances on the photolysis of aqueous pesticide residues. *Chemosphere* 66:1692-1698. DOI: https://doi.org/10.1016/j.chemosphere.2006.07.017.

Garg S, Rose AL, Waite TD. 2011. Photochemical production of superoxide and hydrogen peroxide from natural organic matter. *Geochimica et Cosmochimica Acta* 75:4310-4320. DOI: http://dx.doi.org/10.1016/j.gca.2011.05.014.

Gondikas AP, Kammer Fvd, Reed RB, Wagner S, Ranville JF, Hofmann T. 2014. Release of $TiO_2$ nanoparticles from sunscreens into surface waters: a one-year survey at the old Danube recreational lake. *Environ Sci Technol* 48:5415-5422. DOI: 10.1021/es405596y.

Gottschalk F, Nowack B. 2011. The release of engineered nanomaterials to the environment. *Journal of Environmental Monitoring* 13:1145-1155. DOI: 10.1039/C0EM00547A.

Gottschalk F, Sun T, Nowack B. 2013. Environmental concentrations of engineered nanomaterials: review of modeling and analytical studies. *Environ Pollut* 181:287-300. DOI: http://dx.doi.org/10.1016/j.envpol.2013.06.003.

Guilhermino L, Lopes MC, Carvalho AP, Soared AMVM. 1996. Inhibition of acetylcholinesterase activity as effect criterion in acute tests with juvenile *Daphnia magna*. *Chemosphere* 32:727-738. DOI: https://doi.org/10.1016/0045-6535(95)00360-6.

Häder DP, Lebert M, Schuster M, del Campo L, Helbling EW, McKenzie R. 2007. ELDONET - a decade of monitoring solar radiation on five continents. *Photochem Photobiol* 83:1348-1357. DOI: 10.1111/j.1751-1097.2007.00168.x.

Hariharan C. 2006. Photocatalytic degradation of organic contaminants in water by ZnO nanoparticles: Revisited. *Applied Catalysis A: General* 304:55-61. DOI: https://doi.org/10.1016/j.apcata.2006.02.020.

Hoffmann MR, Martin ST, Choi W, Bahnemann DW. 1995. Environmental applications of semiconductor photocatalysis. *Chemical Reviews* 95:69-96. DOI: 10.1021/cr00033a004.

Johnson BD, Gilbert SL, Khan B, Carroll DL, Ringwood AH. 2015. Cellular responses of eastern oysters, *Crassostrea virginica*, to titanium dioxide nanoparticles. *Mar Environ Res* 111:135-143. DOI: https://doi.org/10.1016/j.marenvres.2015.06.019.

Karimi S, Troeung M, Wang R, Draper R, Pantano P. 2018. Acute and chronic toxicity of metal oxide nanoparticles in chemical mechanical planarization slurries with *Daphnia magna*. *Environ Sci-Nano* 5:1670-1684. DOI: 10.1039/C7EN01079F.

Keller AA, Lazareva A. 2014. Predicted releases of engineered nanomaterials: from global to regional to local. *Environ Sci Tech Let* 1:65-70. DOI: 10.1021/ez400106t.

Kim C, Park H-j, Cha S, Yoon J. 2013. Facile detection of photogenerated reactive oxygen species in $TiO_2$ nanoparticles suspension using colorimetric probe-assisted spectrometric method. *Chemosphere* 93:2011-2015. DOI: http://dx.doi.org/10.1016/j.chemosphere.2013.07.023.

Kim TS, Kim JK, Choi K, Stenstrom MK, Zoh KD. 2006. Degradation mechanism and the toxicity assessment in $TiO_2$ photocatalysis and photolysis of parathion. *Chemosphere* 62:926-933. DOI: 10.1016/j.chemosphere.2005.05.038.

Konstantinou IK, Albanis TA. 2003. Photocatalytic transformation of pesticides in aqueous titanium dioxide suspensions using artificial and solar light: intermediates and degradation pathways. *Appl Catal B-Environmental* 42:319-335. DOI: https://doi.org/10.1016/S0926-3373(02)00266-7.

Lewis KA, Tzilivakis J, Warner DJ, Green A. 2016. An international database for pesticide risk assessments and management. *Human and Ecological Risk Assessment: An International Journal* 22:1050-1064. DOI: 10.1080/10807039.2015.1133242.

Li W, Zhao Y, Yan X, Duan J, Saint CP, Beecham S. 2019. Transformation pathway and toxicity assessment of malathion in aqueous solution during UV photolysis and photocatalysis. *Chemosphere* 234:204-214. DOI: https://doi.org/10.1016/j.chemosphere.2019.06.058.

Low GKC, McEvoy SR, Matthews RW. 1991. Formation of nitrate and ammonium ions in titanium dioxide mediated photocatalytic degradation of organic compounds containing nitrogen atoms. *Environ Sci Technol* 25:460-467. DOI: 10.1021/es00015a013.

Lüderwald S, Dackermann V, Seitz F, Adams E, Feckler A, Schilde C, Schulz R, Bundschuh M. 2019. A blessing in disguise? Natural organic matter reduces the UV light-induced toxicity of nanoparticulate titanium dioxide. *Sci Total Environ* 663:518-526. DOI: https://doi.org/10.1016/j.scitotenv.2019.01.282.

Ma H, Brennan A, Diamond SA. 2012b. Photocatalytic reactive oxygen species production and phototoxicity of titanium dioxide nanoparticles are dependent on the solar ultraviolet radiation spectrum. *Environ Toxicol Chem* 31:2099-2107. DOI: 10.1002/etc.1916.

Malato S, Caceres J, Aguera A, Mezcua M, Hernando D, Vial J, Fernandez-Alba AR. 2001. Degradation of imidacloprid in water by photo-fenton and $TiO_2$ photocatalysis at a solar pilot plant: a comparative study. *Environ Sci Technol* 35:4359-4366. DOI: 10.1021/es000289k.

National Center for Biotechnology Information. PubChem Database. Dimethoate, CID=3082, https://pubchem.ncbi.nlm.nih.gov/compound/Dimethoate (accessed on June 9, 2019).

National Center for Biotechnology Information. PubChem Database. Pirimicarb, CID=31645, https://pubchem.ncbi.nlm.nih.gov/compound/Pirimicarb (accessed on June 9, 2019).

Navarro S, Fenoll J, Vela N, Ruiz E, Navarro G. 2009. Photocatalytic degradation of eight pesticides in leaching water by use of ZnO under natural sunlight. *J Hazard Mater* 172:1303-1310. DOI: https://doi.org/10.1016/j.jhazmat.2009.07.137.

OECD. 2004. Test no. 202: *Daphnia* sp. acute immobilisation test. OECD guideline for testing of chemicals, section 2. *OECD Publishing, Paris* pp. 1–12 https://doi.org/10.1787/ 9789264069947-en.

OECD. 2008. Test no. 211: *Daphnia magna* reproduction test. OECD guideline for testing of chemicals, section 2. *OECD Publishing, Paris* pp. 1–23. DOI: https://doi.org/ 10.1787/9789264185203-en.

Ouyang W, Santiago ARP, Cerdán-Gómez K, Luque R. 2019. Chapter 5 - Nanoparticles within functional frameworks and their applications in photo(electro)catalysis. In Prieto JP, Béjar MG, eds, *Photoactive Inorganic Nanoparticles*. Elsevier, pp 109-138. DOI: https://doi.org/10.1016/ B978-0-12-814531-9.00005-1

Pelizzetti E, Minero C. 1999. Role of oxidative and reductive pathways in the photocatalytic degradation of organic compounds. *Colloids and Surfaces A: Physicochemical and Engineering Aspects* 151:321-327. DOI: https://doi.org/10.1016/S0927-7757(98)00580-9.

Peters RJB, van Bemmel G, Milani NBL, den Hertog GCT, Undas AK, van der Lee M, Bouwmeester H. 2018. Detection of nanoparticles in Dutch surface waters. *Sci Total Environ* 621:210-218. DOI: https://doi.org/10.1016/j.scitotenv.2017.11.238.

Piccinno F, Gottschalk F, Seeger S, Nowack B. 2012. Industrial production quantities and uses of ten engineered nanomaterials in Europe and the world. *Journal of Nanoparticle Research* 14:1-11. DOI: 10.1007/s11051-012-1109-9.

Pirisi FM, Cabras P, Garau VL, Melis M, Secchi E. 1996. Photodegradation of pesticides. Photolysis rates and half-life of pirimicarb and its metabolites in reactions in water and in solid phase. *J Agric Food Chem* 44:2417-2422. DOI: https://doi.org/10.1021/jf9501711.

Ritz, C., Streibig, J.C., 2005. Bioassay analysis using R. *J. Stat. Softw* 12:1–22. DOI: https://doi.org/10.18637/jss.v012.i05.

Robert D, Malato S. 2002. Solar photocatalysis: a clean process for water detoxification. *Sci Total Environ* 291:85-97. DOI: https://doi.org/10.1016/S0048-9697(01)01094-4.

Romero E, Schmitt P, Mansour M. 1994. Photolysis of pirimicarb in water under natural and simulated sunlight conditions. *Pestic Sci* 41:21-26. DOI: https://doi.org/10.1002/ps.2780410105.

Rosenfeldt RR., Seitz F, Haigis A, Höger J, Zubrod J.P, Schulz R, Bundschuh M. 2016. Nanosized titanium dioxide influences copper-induced toxicity during aging as a function of environmental conditions. *Environ. Toxicol. Chem*. 35:1766–1774. DOI: https://doi.org/10.1002/etc.3325.

Ryan AC, Tomasso JR, Klaine SJ. 2009. Influence of pH, hardness, dissolved organic carbon concentration, and dissolved organic matter source on the acute toxicity of copper to *Daphnia magna* in soft waters: implications for the biotic ligand model. *Environ Toxicol Chem* 28:1663-1670. DOI: 10.1897/08-361.1.

Schwack W, Kopf G. 1993. Photodegradation of the carbamate insecticide pirimicarb. *Z Lebensm Unters Forch* 197:264-268. DOI: https://doi.org/10.1007/BF01185283.

Seitz F, Bundschuh M, Dabrunz A, Bandow N, Schaumann GE, Schulz R. 2012. Titanium dioxide nanoparticles detoxify pirimicarb under UV irradiation at ambient intensities. *Environ Toxicol Chem* 31:518-523. DOI: 10.1002/etc.1715.

Seitz F, Rosenfeldt RR, Müller M, Lüderwald S, Schulz R, Bundschuh M. 2016. Quantity and quality of natural organic matter influence the ecotoxicity of titanium dioxide nanoparticles. *Nanotoxicology* 10:1415-1421. DOI: 10.1080/17435390.2016.1222458.

Sulzberger B, Durisch-Kaiser E. 2009. Chemical characterization of dissolved organic matter (DOM): a prerequisite for understanding UV-induced changes of DOM absorption properties and bioavailability. *Aquatic Sciences* 71:104-126. DOI: 10.1007/s00027-008-8082-5.

Thiruvenkatachari R, Vigneswaran S, Moon IS. 2008. A review on UV/TiO2 photocatalytic oxidation process (Journal Review). *Korean Journal of Chemical Engineering* 25:64-72. DOI: 10.1007/s11814-008-0011-8.

Turchi CS, Ollis DF. 1989. Mixed reactant photocatalysis: intermediates and mutual rate inhibition. *J Catal* 119:483-496. DOI: https://doi.org/10.1016/0021-9517(89)90176-0.

United States. Environmental Protection Agency. Prevention, Pesticides, and Toxic Substances. 2006. Reregistration Eligibility Decision (RED) for Permethrin. *U.S. Environmental Protection Agency, Prevention, Pesticides and Toxic Substances*. EP 5.2:P 42/18.

Valenzuela MA, Bosch P, Jiménez-Becerrill J, Quiroz O, Páez AI. 2002. Preparation, characterization and photocatalytic activity of ZnO, Fe2O3 and ZnFe2O4. *J Phottoch Photobio A* 148:177-182. DOI: http://dx.doi.org/10.1016/S1010-6030(02)00040-0.

Van Scoy A, Pennell A, Zhang X. 2016. Environmental fate and toxicology of dimethoate. *Rev Environ Contam Toxicol* 237:53-70. DOI: 10.1007/978-3-319-23573-8_3.

Westerhoff P, Song G, Hristovski K, Kiser MA. 2011. Occurrence and removal of titanium at full scale wastewater treatment plants: implications for $TiO_2$ nanomaterials. *Journal of Environmental Monitoring* 13:1195-1203. DOI: 1 0.1039/c1em10017c.

Wheeler MW, Park RM, Bailer AJ. 2006. Comparing median lethal concentration values using confidence interval overlap or ratio tests. *Environ Toxicol Chem* 25:1441-1444. DOI: 10.1897/05-320r.1.

Xuereb B, Lefevre E, Garric J, Geffard O. 2009. Acetylcholinesterase activity in *Gammarus fossarum* (Crustacea Amphipoda): linking AChE inhibition and behavioural alteration. *Aquat Toxicol* 94:114-122. DOI: 10.1016/j.aquatox.2009.06.010.

Yang W, Gan J, Hunter W, Spurlock F. 2006. Effect of suspended solids on bioavailability of pyrethroid insecticides. *Environ Toxicol Chem* 25:1585-1591. DOI: 10.1897/05-448R.1.

Zoh KD, Kim TS, Kim JG, Choi K, Yi SM. 2006. Parathion degradation and toxicity reduction in solar photocatalysis and photolysis. *Water Sci Technol* 53:1-8. DOI: https://doi.org/10.2166 /wst.2006.069.

**Supporting Information of Appendix A. 3**

**Reduction of pesticide toxicity under field relevant conditions? The interaction of titanium dioxide nanoparticles, UV, and NOM**

Lüderwald, S., Meyer, F., Gerstle, V., Friedrichs, L., Rolfing, K., Bakanov, N., Schulz, R., Bundschuh, M.

**Table S1.** Characterization of dissolved organic carbon properties as well as N and S information for the applied NOM (i.e., Seaweed Extract (SW)), determined via LC-OCD-NOD or gained by CHNS-analyses. The table is modified from Seitz et al. (2016).

| | | HOC[b] | DOC | | CDOC[c] | | | | | | | SUVA[a] (L/mg*m) | N (%(w/w)) | S (%(w/w)) |
|---|---|---|---|---|---|---|---|---|---|---|---|---|---|---|
| Type | Total (µg C/L) | Total (µg C/L) | Total (µg C/L) | BIO-polymers Total (µg C/L) | Humic substance Total (µg C/L) | Aromaticity (L/mg*m) | Mol.weight (g/mol) | Building blocks (µg C/L) | LMW[d] neutrals (µg C/L) | LMW[d] acids (µg C/L) | | | | |
| SW | 1277 | 366 | 911 | 71 | 196 | 4.96 | 954 | 285 | 312 | 48 | | 2.13 | 0.46 | 0.77 |

[a] Specific UV absorbance
[b] Hydrophobic organic carbon
[c] Chromatographic dissolved organic carbon
[d] Low molecular neutrals/organic acids

**Table S2**. Derived 96-h EC$_{50}$s (based on nominal and measured pesticide concentrations, where available) for the applied pesticides, along with the corresponding standard error, 95% CI, as well as the dose-response models fitted to the respective immobilization data.

| Pesticide | TS | UV level | 96-h EC50 (µg/L) | Standard error | Lower 95% CI | Upper 95% CI | Model |
|---|---|---|---|---|---|---|---|
| **Based on nominal concentrations** | | | | | | | |
| **AZO** | 1 | I | 183.13 | 30.46 | 120.52 | 245.74 | W1.2 |
| | | II | 187.97 | 26.63 | 133.23 | 242.72 | W2.2 |
| | | III | 236.16 | 47.79 | 137.93 | 334.39 | W2.2 |
| | | IV | 190.18 | 37.10 | 113.92 | 266.44 | W1.2 |
| | 2 | I | 149.02 | 22.88 | 102.00 | 196.04 | W1.2 |
| | | II | 149.83 | 19.75 | 109.23 | 190.43 | LN.2 |
| | | III | 225.13 | 24.42 | 174.93 | 275.32 | LN.2 |
| | | IV | 244.90 | 32.99 | 176.96 | 312.83 | W2.2 |
| | 3 | I | 290.44 | 25.98 | 237.05 | 343.84 | LN.2 |
| | | II | 339.80 | 29.58 | 278.87 | 400.73 | W2.2 |
| | | III | 210.29 | 23.95 | 161.05 | 259.52 | W1.2 |
| | | IV | 203.52 | 16.00 | 170.63 | 236.40 | LL.2 |
| | 4 | I | 152.46 | 11.52 | 128.78 | 176.15 | W2.2 |
| | | II | 124.93 | 7.99 | 108.50 | 141.36 | W1.2 |
| | | III | 102.17 | 7.50 | 86.75 | 117.59 | LL.2 |
| | | IV | 121.80 | 6.70 | 108.03 | 135.57 | LL.2 |
| **DIM** | 1 | I | 186.56 | 11.15 | 163.79 | 209.33 | LN.2 |
| | | II | 366.73 | 17.22 | 331.55 | 401.90 | W1.2 |
| | | III | 419.65 | 9.20 | 400.86 | 438.45 | W1.2 |
| | | IV | 541.86 | 16.49 | 508.19 | 575.53 | LN.2 |
| | 2 | I | 212.90 | 8.68 | 195.16 | 230.63 | W1.2 |
| | | II | 414.20 | 15.98 | 381.56 | 446.84 | W2.2 |
| | | III | 393.18 | 27.94 | 336.11 | 450.24 | LN.2 |
| | | IV | 418.79 | 13.12 | 392.00 | 445.57 | W2.2 |

| | | | | | | |
|---|---|---|---|---|---|---|
| | 3 | I | 477.15 | 23.96 | 428.21 | 526.08 | W2.2 |
| | | II | 611.97 | 16.20 | 578.89 | 645.04 | LN.2 |
| | | III | 653.97 | 15.72 | 621.86 | 686.07 | LN.2 |
| | | IV | 664.52 | 15.14 | 633.61 | 695.43 | W2.2 |
| | 4 | I | 437.00 | 15.45 | 405.44 | 468.55 | W1.2 |
| | | II | 541.86 | 16.49 | 508.19 | 575.53 | LN.2 |
| | | III | 630.22 | 29.85 | 569.26 | 691.19 | LN.2 |
| | | IV | 734.66 | 23.24 | 687.21 | 782.12 | LL.2 |
| MAL | 1 | I | 1.09 | 0.08 | 0.92 | 1.26 | LN.2 |
| | | II | 0.97 | 0.02 | 0.93 | 1.01 | LN.2 |
| | | III | 1.20 | 0.06 | 1.08 | 1.33 | LN.2 |
| | | IV | 0.97 | 0.02 | 0.92 | 1.02 | LN.2 |
| | 2 | I | 1.19 | 0.07 | 1.03 | 1.34 | LN.2 |
| | | II | 1.18 | 0.09 | 1.00 | 1.37 | LN.2 |
| | | III | 1.20 | 0.09 | 1.01 | 1.38 | LL.2 |
| | | IV | 0.98 | 0.02 | 0.94 | 1.01 | LN.2 |
| | 3 | I | 0.72 | 0.06 | 0.60 | 0.84 | W2.2 |
| | | II | 0.75 | 0.07 | 0.61 | 0.89 | W2.2 |
| | | III | 0.83 | 0.03 | 0.77 | 0.89 | LN.2 |
| | | IV | 0.85 | 0.02 | 0.80 | 0.90 | W1.2 |
| | 4 | I | 0.86 | 0.05 | 0.76 | 0.95 | LN.2 |
| | | II | 0.87 | 0.07 | 0.73 | 1.01 | LN.2 |
| | | III | 1.00 | 0.02 | 0.96 | 1.04 | LN.2 |
| | | IV | 0.93 | 0.02 | 0.89 | 0.97 | LN.2 |
| PAR | 1 | I | 1.10 | 0.26 | 0.55 | 1.64 | LN.2 |
| | | II | 1.29 | 0.04 | 1.22 | 1.36 | LL.2 |
| | | III | 1.44 | 0.08 | 1.18 | 1.60 | W2.2 |
| | | IV | 1.74 | 0.30 | 1.13 | 2.35 | W2.2 |
| | 2 | I | 0.88 | 0.00 | 0.87 | 0.89 | LL.3u |

| | | | | | | | |
|---|---|---|---|---|---|---|---|
| | | II | 0.97 | 0.05 | 0.86 | 1.08 | W2.2 |
| | | III | 1.16 | 0.17 | 0.81 | 1.50 | W2.2 |
| | | IV | 0.95 | 0.13 | 0.69 | 1.21 | W2.4 |
| | 3 | I | 1.47 | 0.00 | 1.46 | 1.48 | W1.2 |
| | | II | 1.74 | 0.34 | 1.04 | 2.44 | W1.2 |
| | | III | 1.96 | 0.32 | 1.29 | 2.63 | LN.2 |
| | | IV | 2.36 | 0.17 | 2.02 | 2.70 | W2.2 |
| | 4 | I | 1.59 | 0.26 | 1.05 | 2.14 | LN.2 |
| | | II | 1.61 | 0.01 | 1.58 | 1.64 | LL.5 |
| | | III | 2.10 | 0.29 | 1.49 | 2.70 | LN.2 |
| | | IV | 2.25 | 0.35 | 1.54 | 2.97 | W2.2 |
| PER | 1 | I | 0.55 | 0.04 | 0.47 | 0.63 | W1.2 |
| | | II | 0.66 | 0.06 | 0.55 | 0.78 | W1.2 |
| | | III | 1.09 | 0.11 | 0.86 | 1.32 | W2.2 |
| | | IV | 0.65 | 0.05 | 0.56 | 0.75 | LL.3u |
| | 2 | I | 1.26 | 0.06 | 1.14 | 1.37 | W2.2 |
| | | II | 1.47 | 0.06 | 1.35 | 1.58 | W2.2 |
| | | III | 1.15 | 0.10 | 0.95 | 1.36 | LN.2 |
| | | IV | 0.73 | 0.05 | 0.62 | 0.84 | W1.2 |
| | 3 | I | 0.73 | 0.01 | 0.70 | 0.75 | W1.2 |
| | | II | 0.89 | 0.06 | 0.77 | 1.00 | W1.2 |
| | | III | 1.26 | 0.08 | 1.10 | 1.41 | W2.2 |
| | | IV | 0.70 | 0.00 | 0.69 | 0.71 | W1.2 |
| | 4 | I | 1.22 | 0.05 | 1.11 | 1.32 | W1.2 |
| | | II | 1.47 | 0.15 | 1.15 | 1.79 | W1.2 |
| | | III | 2.47 | 0.20 | 2.05 | 2.89 | W2.2 |
| | | IV | 1.42 | 0.05 | 1.33 | 1.52 | W2.2 |
| PIR | 1 | I | 17.16 | 0.90 | 15.32 | 19.00 | W2.2 |
| | | II | 22.16 | 4.27 | 13.38 | 30.94 | W1.2 |

| | | | | | | |
|---|---|---|---|---|---|---|
| | | III | 31.96 | 2.11 | 27.62 | 36.30 | W2.2 |
| | | IV | 29.00 | 2.59 | 23.68 | 34.33 | W2.2 |
| | 2 | I | 17.10 | 4.29 | 8.27 | 25.93 | LN.2 |
| | | II | 43.44 | 1.34 | 40.68 | 46.19 | W2.2 |
| | | III | 31.82 | 3.62 | 24.37 | 39.26 | W2.2 |
| | | IV | 17.08 | 2.98 | 10.96 | 23.20 | LN.2 |
| | 3 | I | 36.67 | 4.78 | 26.84 | 46.49 | W2.2 |
| | | II | 34.58 | 1.63 | 31.24 | 37.92 | W2.2 |
| | | III | 52.10 | 1.35 | 49.32 | 54.88 | W2.2 |
| | | IV | 54.45 | 1.11 | 52.17 | 56.73 | W2.2 |
| | 4 | I | 37.18 | 3.05 | 30.92 | 43.44 | W1.2 |
| | | II | 36.59 | 5.25 | 25.80 | 47.39 | W2.2 |
| | | III | 54.34 | 1.15 | 51.97 | 56.70 | W2.2 |
| | | IV | 55.88 | 1.16 | 53.50 | 58.26 | W2.2 |

**Based on measured concentrations**

| | | | | | | |
|---|---|---|---|---|---|---|
| AZO | 1 | I | 140.57 | 23.38 | 92.51 | 188.63 | W1.2 |
| | | II | 144.29 | 20.44 | 102.27 | 186.31 | W2.2 |
| | | III | 181.28 | 36.68 | 105.87 | 256.68 | W2.2 |
| | | IV | 175.27 | 35.15 | 103.02 | 247.52 | W2.2 |
| | 2 | I | 118.27 | 18.15 | 80.95 | 155.58 | W1.2 |
| | | II | 118.91 | 15.68 | 86.69 | 151.13 | LN.2 |
| | | III | 178.66 | 19.38 | 138.83 | 218.50 | LN.2 |
| | | IV | 194.36 | 26.18 | 140.44 | 248.27 | W2.2 |
| | 3 | I | 244.83 | 21.90 | 199.82 | 289.84 | LN.2 |
| | | II | 286.43 | 24.94 | 235.07 | 337.79 | W2.2 |
| | | III | 177.26 | 20.19 | 135.76 | 218.76 | W1.2 |
| | | IV | 171.56 | 13.49 | 143.84 | 199.28 | LL.2 |
| | 4 | I | 125.48 | 9.48 | 105.99 | 144.97 | W2.2 |
| | | II | 102.82 | 6.58 | 89.30 | 116.34 | W1.2 |

|  |  |  |  |  |  |  |  |
|---|---|---|---|---|---|---|---|
|  |  | III | 84.09 | 6.17 | 71.40 | 96.78 | LL.2 |
|  |  | IV | 100.24 | 5.51 | 88.91 | 111.57 | LL.2 |
| DIM | 1 | I | 169.06 | 10.10 | 148.43 | 189.70 | LN.2 |
|  |  | II | 316.54 | 13.60 | 288.76 | 344.32 | W1.2 |
|  |  | III | 380.30 | 8.34 | 363.27 | 397.33 | W1.2 |
|  |  | IV | 491.05 | 14.94 | 460.53 | 521.56 | LN.2 |
|  | 2 | I | 190.00 | 7.75 | 174.17 | 205.83 | W1.2 |
|  |  | II | 369.65 | 14.26 | 340.52 | 398.78 | W2.2 |
|  |  | III | 350.89 | 24.94 | 299.96 | 401.82 | LN.2 |
|  |  | IV | 373.75 | 11.71 | 349.84 | 397.66 | W2.2 |
|  | 3 | I | 445.67 | 22.38 | 399.96 | 491.38 | W2.2 |
|  |  | II | 571.59 | 15.13 | 540.69 | 602.49 | LN.2 |
|  |  | III | 610.82 | 14.68 | 580.83 | 640.81 | LN.2 |
|  |  | IV | 620.67 | 14.14 | 591.81 | 649.54 | W2.2 |
|  | 4 | I | 407.04 | 14.39 | 377.65 | 436.43 | W1.2 |
|  |  | II | 504.71 | 15.36 | 473.35 | 536.07 | LN.2 |
|  |  | III | 587.02 | 27.80 | 530.23 | 643.80 | LN.2 |
|  |  | IV | 684.29 | 21.64 | 640.10 | 728.49 | LL.2 |
| MAL | 1 | I | 1.38 | 0.11 | 1.16 | 1.60 | LN.2 |
|  |  | II | 1.23 | 0.02 | 1.18 | 1.28 | LN.2 |
|  |  | III | 1.52 | 0.08 | 1.36 | 1.68 | LN.2 |
|  |  | IV | 1.23 | 0.03 | 1.17 | 1.29 | LN.2 |
|  | 2 | I | 0.61 | 0.04 | 0.53 | 0.68 | LN.2 |
|  |  | II | 0.61 | 0.05 | 0.51 | 0.70 | LN.2 |
|  |  | III | 0.61 | 0.05 | 0.52 | 0.71 | LL.2 |
|  |  | IV | 0.50 | 0.01 | 0.48 | 0.52 | LN.2 |
|  | 3 | I | 0.64 | 0.05 | 0.54 | 0.74 | W2.2 |
|  |  | II | 0.67 | 0.06 | 0.54 | 0.79 | W2.2 |
|  |  | III | 0.73 | 0.03 | 0.68 | 0.79 | LN.2 |

|     |   |     |       |      |       |       |      |
|-----|---|-----|-------|------|-------|-------|------|
|     |   | IV  | 0.75  | 0.02 | 0.71  | 0.79  | W1.2 |
|     | 4 | I   | 0.50  | 0.03 | 0.45  | 0.56  | LN.2 |
|     |   | II  | 0.51  | 0.04 | 0.43  | 0.59  | LN.2 |
|     |   | III | 0.59  | 0.01 | 0.57  | 0.61  | LN.2 |
|     |   | IV  | 0.55  | 0.01 | 0.52  | 0.57  | LN.2 |
| **PIR** | 1 | I   | 14.92 | 0.78 | 13.32 | 16.52 | W2.2 |
|     |   | II  | 19.28 | 3.71 | 11.64 | 26.91 | W1.2 |
|     |   | III | 27.80 | 1.84 | 24.02 | 31.58 | W2.2 |
|     |   | IV  | 25.22 | 2.25 | 20.59 | 29.86 | W2.2 |
|     | 2 | I   | 13.82 | 3.47 | 6.69  | 20.96 | LN.2 |
|     |   | II  | 35.12 | 1.08 | 32.89 | 37.35 | W2.2 |
|     |   | III | 25.72 | 2.93 | 19.70 | 31.74 | W2.2 |
|     |   | IV  | 13.80 | 2.41 | 8.86  | 18.75 | LN.2 |
|     | 3 | I   | 16.32 | 2.13 | 11.95 | 20.70 | W2.2 |
|     |   | II  | 15.39 | 0.72 | 13.90 | 16.88 | W2.2 |
|     |   | III | 23.19 | 0.60 | 21.95 | 24.43 | W2.2 |
|     |   | IV  | 24.88 | 0.44 | 23.97 | 25.79 | W2.2 |
|     | 4 | I   | 17.19 | 1.41 | 14.30 | 20.09 | W1.2 |
|     |   | II  | 16.92 | 2.43 | 11.93 | 21.91 | W2.2 |
|     |   | III | 25.12 | 0.53 | 24.03 | 26.22 | W2.2 |
|     |   | IV  | 25.84 | 0.54 | 24.74 | 26.94 | W2.2 |
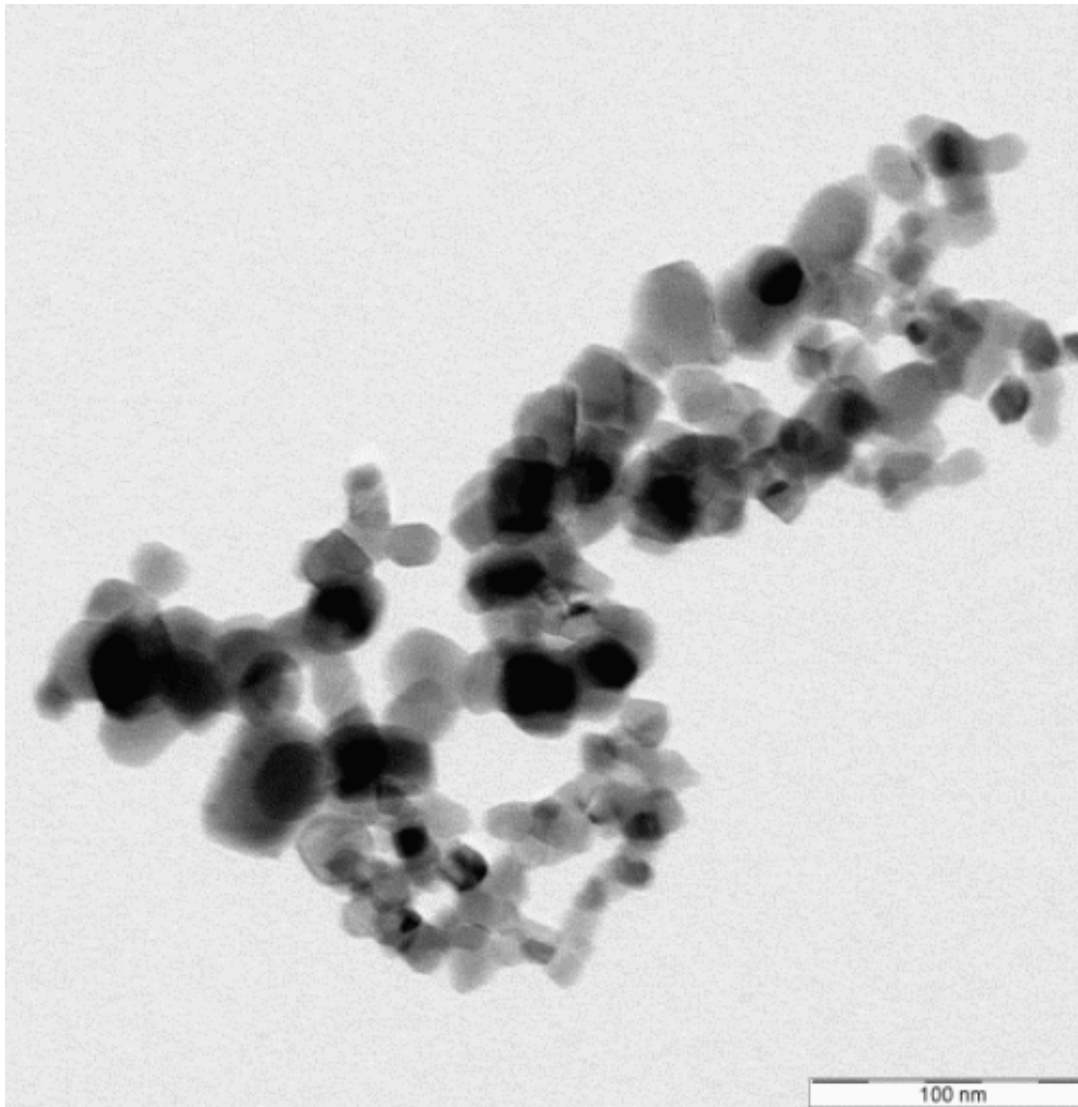
**Figure S1:** Transmission electron microscopy image of the applied nTiO$_2$ product stock dispersions (200 keV Zeiss 922 Omega; scale bar: 100 nm); taken from Rosenfeldt et al. (2016).
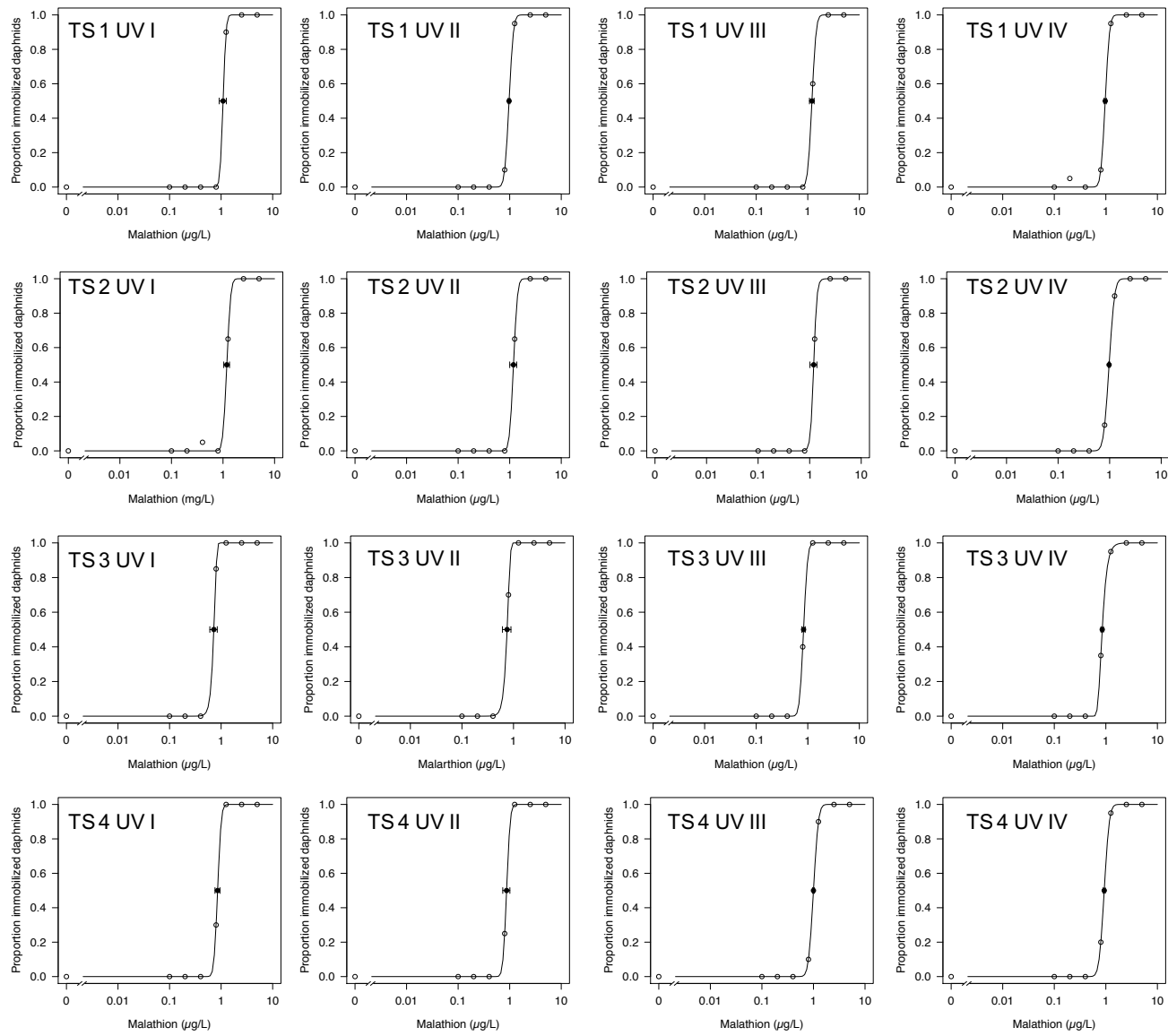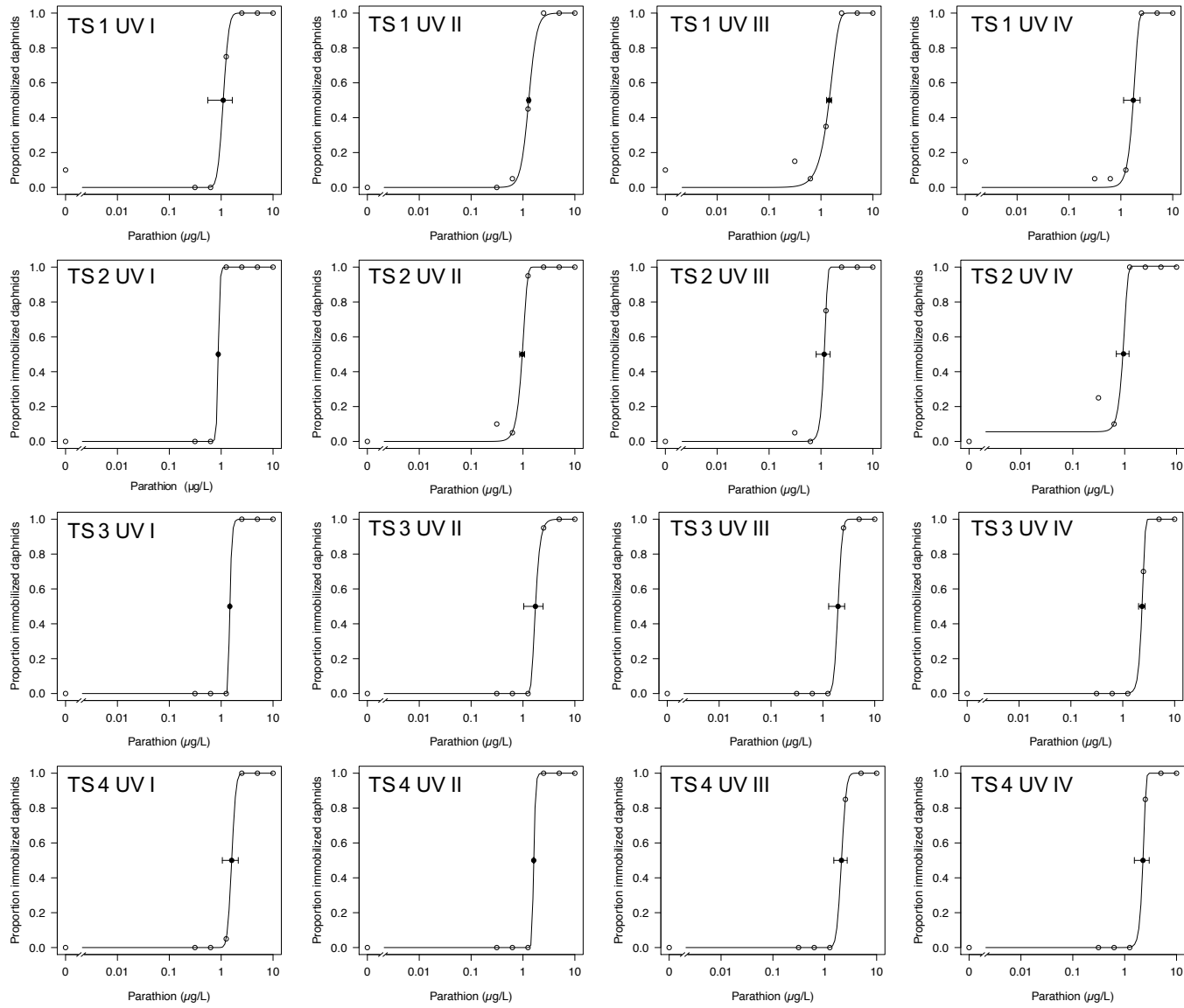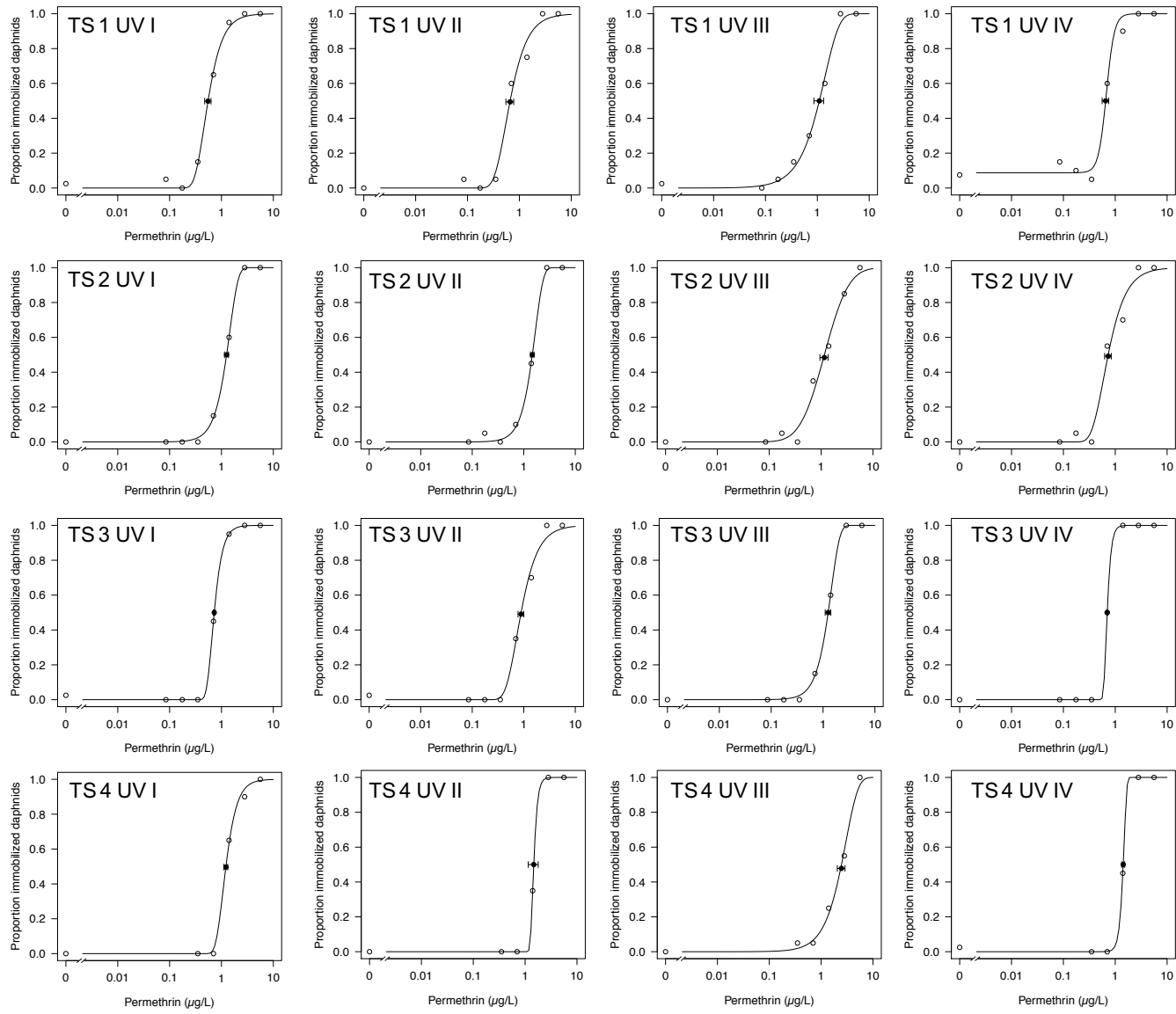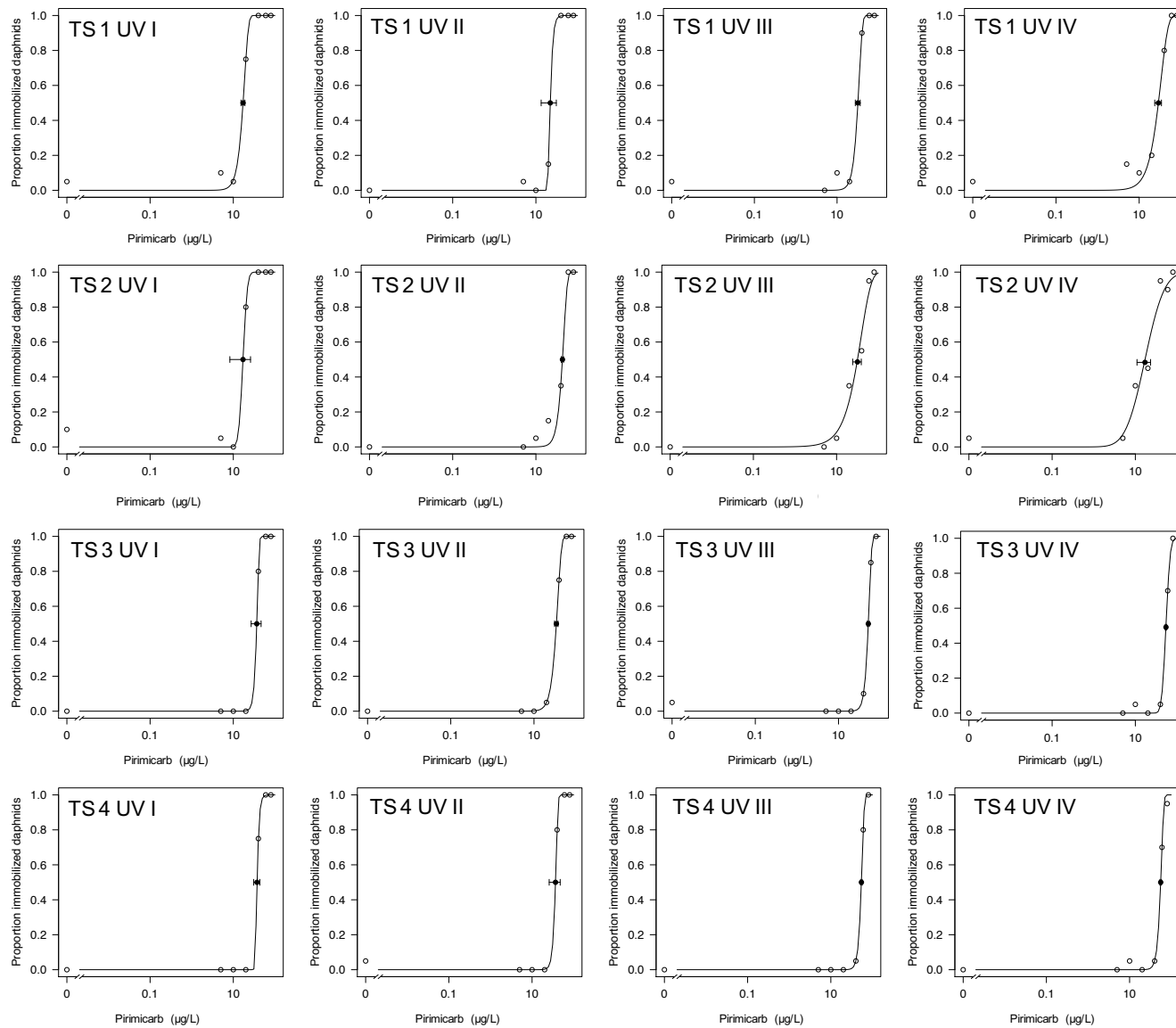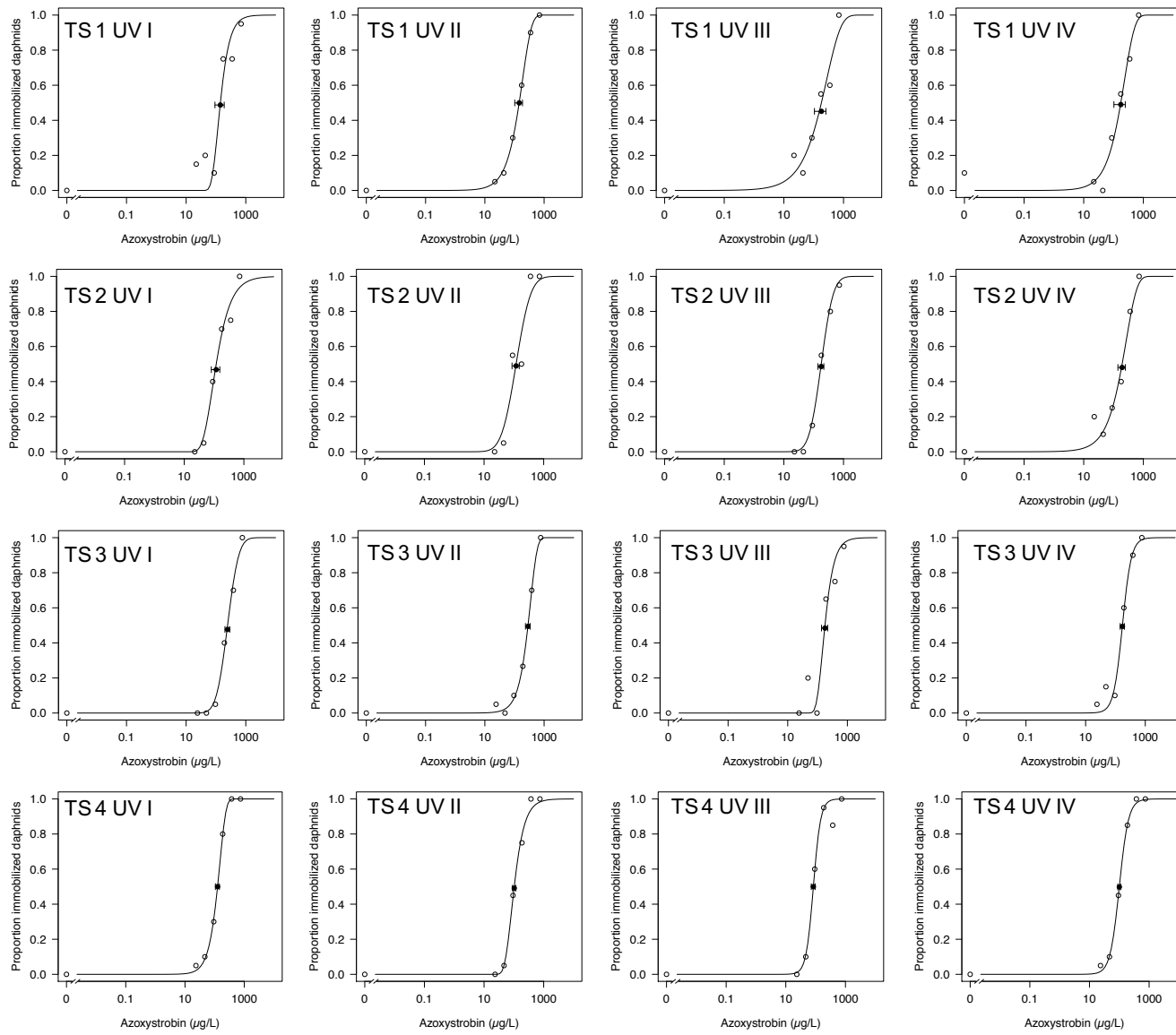
A

A
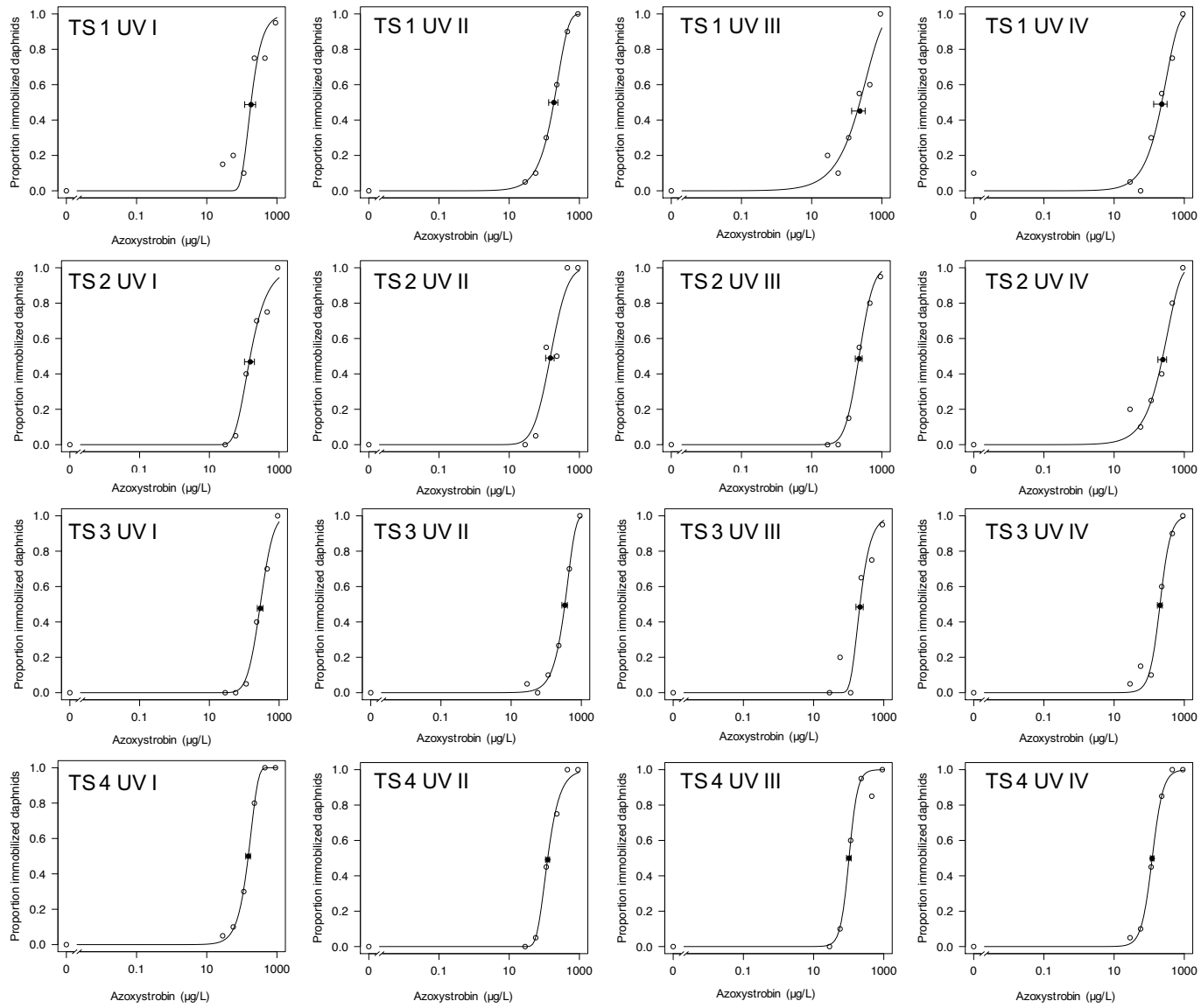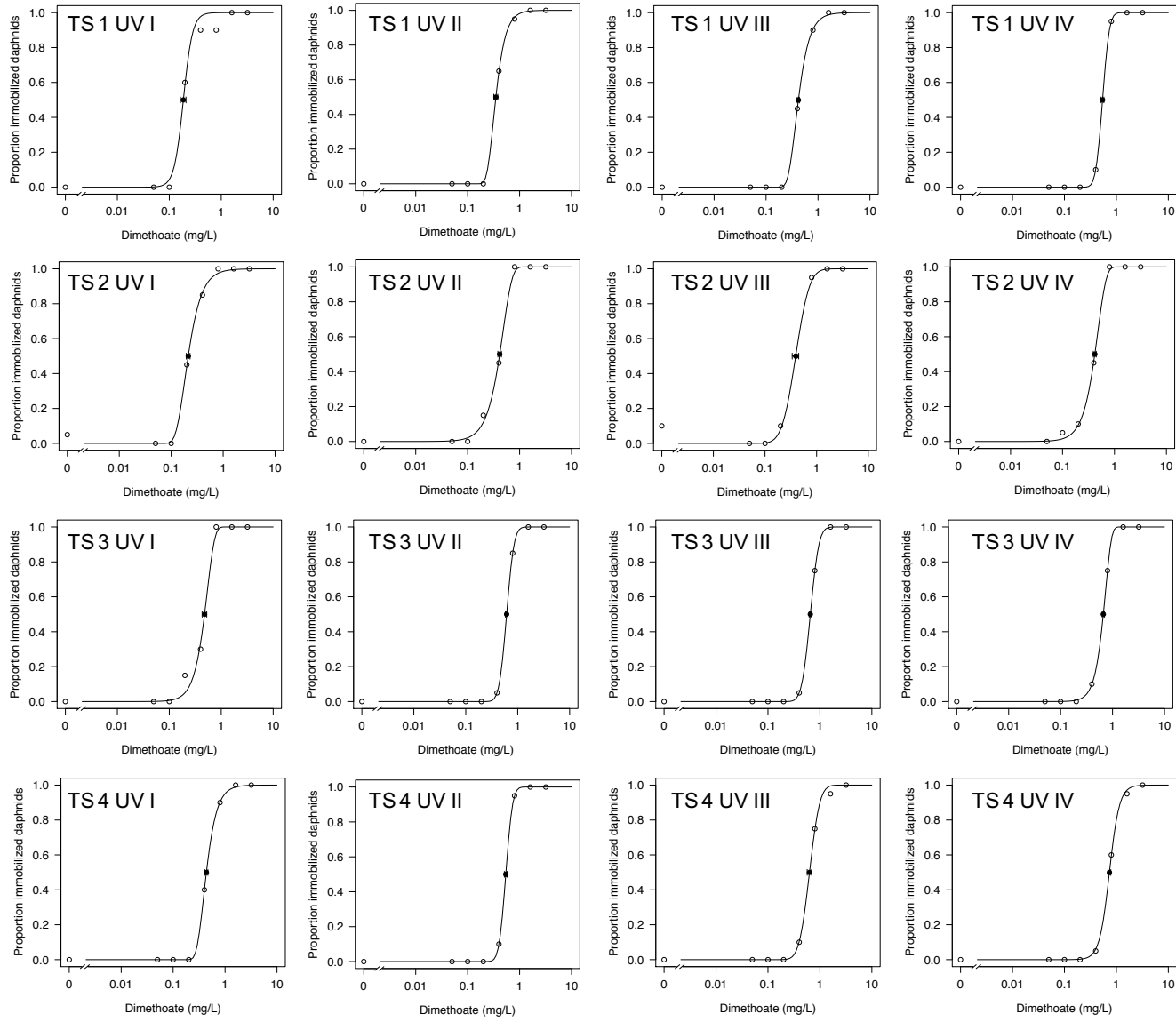
**B**

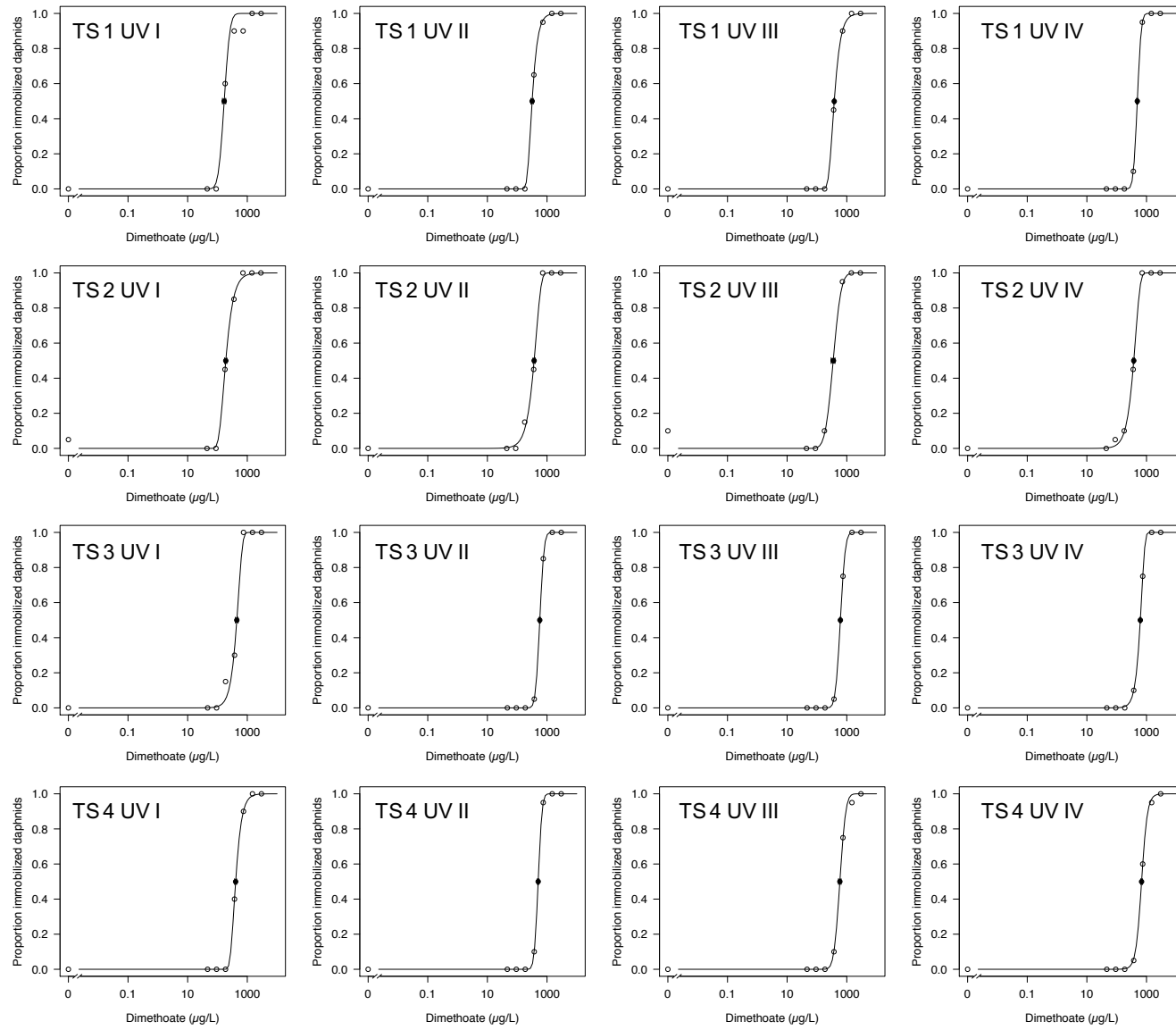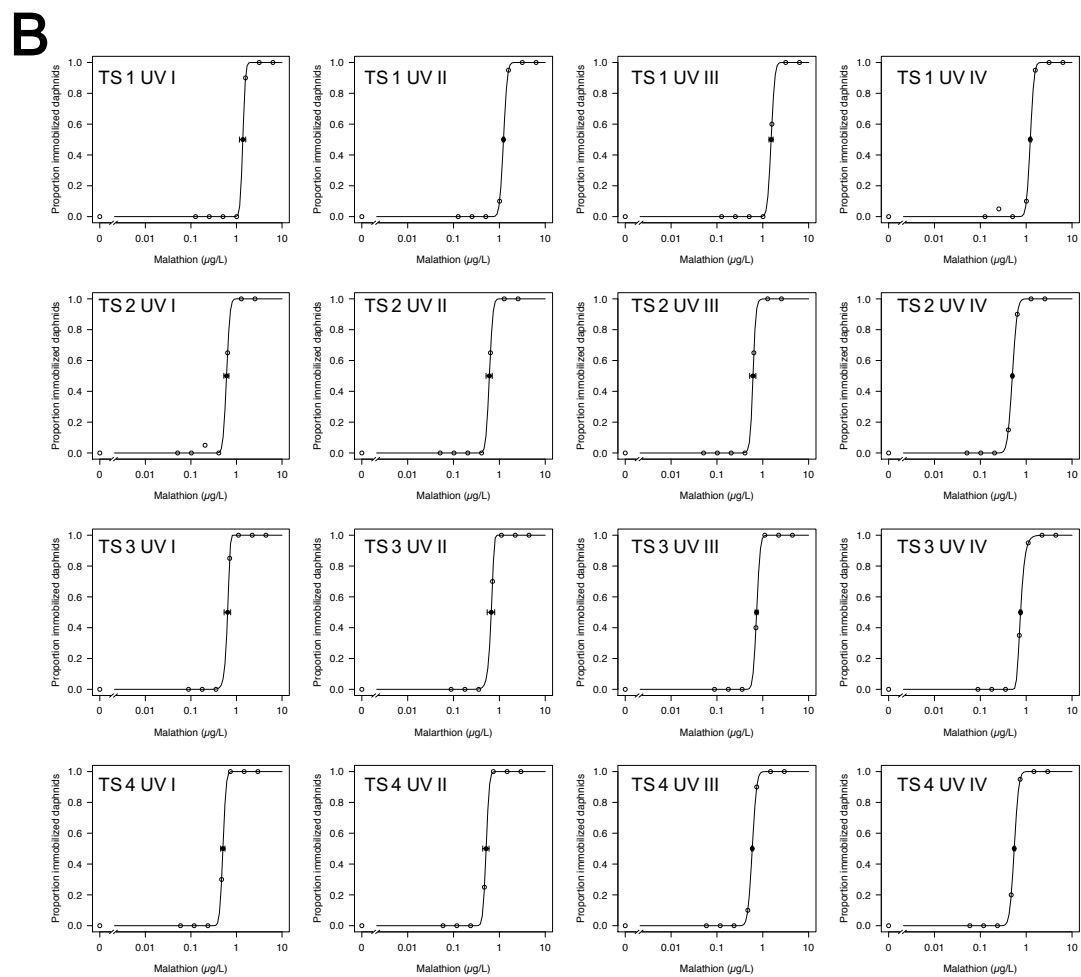**Figure S2:** Dose-response models of the calculated 96-h EC$_{50}$s for the different test series (TS) based on (A) nominal and where applicable (B) measured concentrations for AZO, DIM, MAL, (PAR, PER), and PIR. TS 1 = PEST, TS 2 = PEST+nTiO$_2$, TS 3 = PEST+NOM, TS 4 = PEST+nTiO$_2$+NOM.
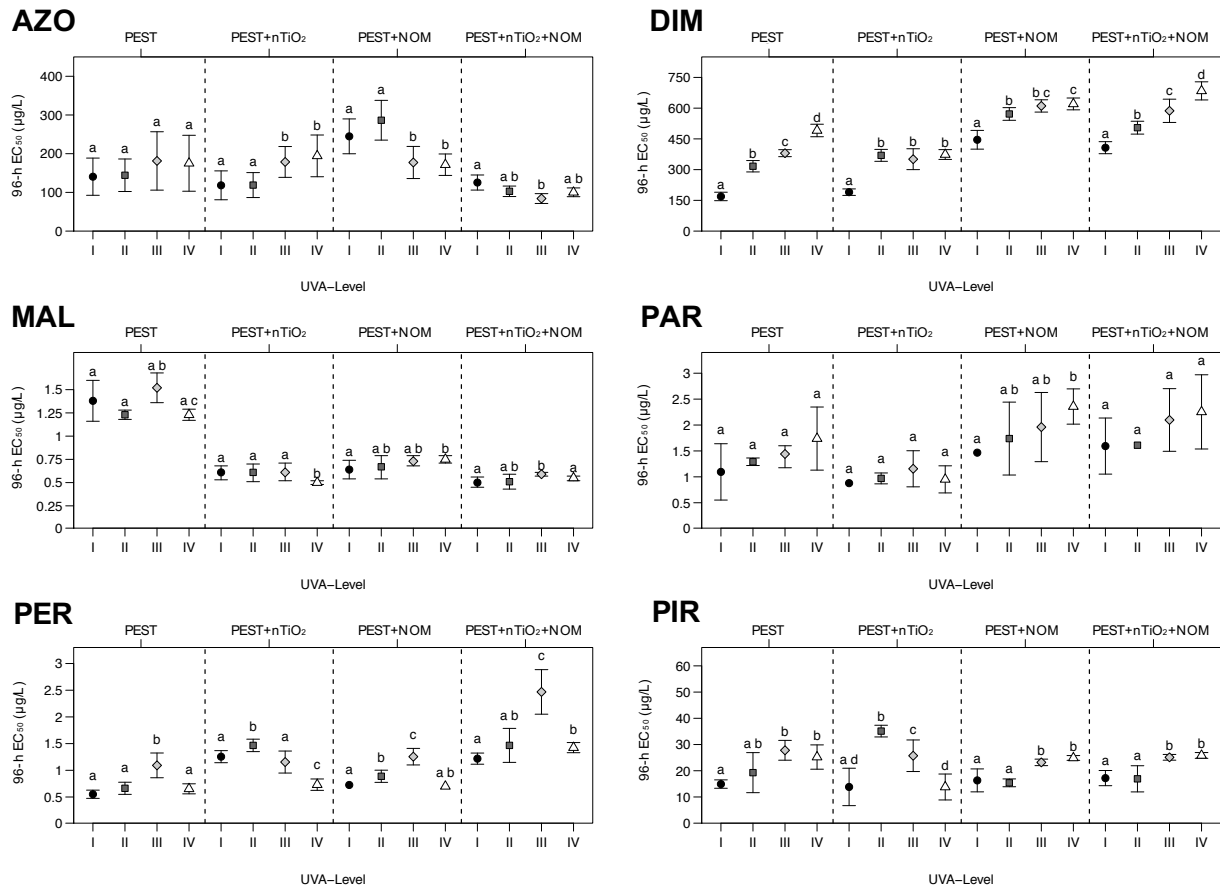
**Figure S3.** 96-h EC$_{50}$ (µg/L ±95% CI) of *D. magna* for the six pesticides azoxystrobin (AZO), dimethoate (DIM), malathion (MAL), parathion (PAR), permethrin (PER), and pirimicarb (PIR) based on measured concentrations, under varying UVA radiation (I: 0.00 W UVA/m$^2$, II: 0.40–0.60W UVA/m$^2$, III: 1.00–1.40W UVA/m$^2$, and IV: 2.20–2.60W UVA/m$^2$), and TS (PEST, PEST+nTiO$_2$, PEST+NOM, and PEST+nTiO$_2$+NOM; Tab. 3). For more information on the applied pesticides and concentrations see Tab. 1. Different letters denote statistically significant difference between individual UVA levels but within one TS.

**Exposure pathway dependent effects of titanium dioxide and silver nanoparticles on the benthic amphipod *Gammarus fossarum***

Lüderwald, S., Schell, T., Newton, K., Salau, R., Seitz, F., Rosenfeldt, R., Dackermann, V., Metreveli, G., Schulz, R., Bundschuh, M.

**HIGHLIGHTS**

- Exposure pathway dependent effects are triggered by nanoparticle intrinsic properties
- Energy assimilation is a promising variable to assess chronic nanoparticle effects
- *G. fossarum* seems not threatened by nanoparticle exposure at predicted environmental concentrations

## ABSTRACT

The increasing production of engineered inorganic nanoparticles (EINPs) elevates their release into aquatic ecosystems raising concerns about associated environmental risks. Numerous investigations indicate sediments as the final sink, facilitating the exposure of benthic species to EINPs. Although reports of sub-lethal EINP effects on benthic species are increasing, the importance of exposure pathways (either waterborne or dietary) is poorly understood. This study investigates the influence of two EINPs, namely titanium dioxide ($nTiO_2$) and silver (nAg), on the benthic model organism *Gammarus fossarum* specifically addressing the relative relevance of these pathways. For each type of EINP an individual 30-day long bioassay was conducted, applying a two-factorial test design. The factors include the presence or absence of the EINPs ($nTiO_2$: ~80 nm, 4 mg/L or nAg: ~30 nm, 0.125 mg/L; $n$=30) in the water phase (waterborne), combined with a preceding 6-day long aging of their diet (black alder leaves) also in presence or absence of the EINPs (dietary). Response variables were mortality, food consumption, feces production and energy assimilation. Additionally, the physiological fitness was examined using lipid content and dry weight of the organisms as measures. Results revealed a significantly reduced energy assimilation (up to ~30%) in *G. fossarum* induced by waterborne exposure towards $nTiO_2$. In contrast, the dietary exposure towards nAg significantly increased the organisms' energy assimilation (up to ~50%). Hence, exposure pathway dependent effects of EINPs cannot be generalized and remain particle specific resting upon their intrinsic properties affecting their potential to interact with the surrounding environment. As a result of the different properties of the EINPs used in this study, we clearly demonstrated variations in type and direction of observed effects in *G. fossarum*. The results of the present study are thus supporting current approaches for nano-specific grouping that might enable an enhanced accuracy in predicting EINP effects facilitating their environmental risk assessment.

## KEYWORDS

## INTRODUCTION

Nanotechnology has become one of the major technologies of the 21st century (Forster et al., 2011; Rao et al., 2015). Engineered inorganic nanoparticles (EINPs) are intensively used in commercial products and for industrial purposes (Keller and Lazareva, 2014; Stark et al., 2015). Among EINPs, nano-sized titanium dioxide ($nTiO_2$) and silver (nAg) are frequently manufactured and used, for instance, in sunscreens or as anti-microbial agents (Aitken et al., 2006; Piccinno et al., 2012). As a consequence, $nTiO_2$ and nAg will inevitably be released into surface waters through point (wastewater treatment plant effluents) and non-point (e.g. runoff) sources (Kaegi et al., 2008; Kiser et al., 2009; Westerhoff et al., 2011).

In surface waters EINPs are subjected to hetero- and homo-agglomeration (Adam et al., 2016; Markus et al., 2011; Petosa et al., 2010), ultimately altering their fate, along with the risk of exposure for different types of aquatic organisms (Klaine et al., 2008). Particularly in an initial stage, EINPs might possess an ecotoxicological impact on pelagic species (Dabrunz et al., 2011; Lovern and Klaper, 2006; Rosenkranz et al., 2009; Seitz et al., 2013), whereas the formation of EINP agglomerates leads to their elevated sedimentation, suggesting sediments as a final sink (Baun et al., 2008; Velzeboer et al., 2014), and increases the exposure of benthic species (von der Kammer et al., 2010). Although effect assessments using benthic organisms are gaining more and more attention (e.g. Mehennaoui et al., 2016; Rajala et al., 2018; Rosenfeldt et al., 2015), the majority of studies addressing EINP toxicity have been performed on pelagic organisms (i.e. *Daphnia magna*; Baun et al., 2008; Lovern and Klaper, 2006). Nonetheless, there are studies reporting different degrees of nAg accumulation in *D. magna* between a waterborne and dietary exposure (Ribeiro et al., 2017). Others are pointing out stronger effects of waterborne exposure (e.g. for *Asellus aquaticus*, and *Gammarus fossarum*) compared to diet related effects, though related to pesticide exposure (Feckler et al., 2016; Zubrod et al., 2015). Croteau et al. (2011, 2014), for instance, were investigating the bioaccumulation of nanosized Ag and CuO in *Lymnaea stagnalis* comparing waterborne and dietary exposure over 24 hours. However, to the best of our knowledge, studies allowing an assessment for the relative importance of both exposure pathways utilizing a series of response variables and different types of EINPs inducing potential long-term effects in benthic organism are limited.

To uncover the effects provoked by the different exposure pathways, two individual 30-day long bioassays using *Gammarus fossarum* as benthic model species were carried out, differentiating between waterborne and diet-related exposure pathways (Fig. 1). This organism was chosen as it can be affected by either a direct waterborne exposure of sedimented EINP agglomerates, as well as indirectly through EINPs adsorbed to the consumed food (leaf litter). The experiments were performed with two types of EINPs, namely $nTiO_2$ and nAg as representatives for chemically stable (non-dissolving) and ion-releasing (dissolving) EINP, respectively (Bundschuh et al., 2018). The EINP concentrations used in this study were selected to increase the probability of distinctive sub-lethal effects allowing an assignment of the different exposure pathways to the observed effects. Mortality (as evidence for possible acute effects), food consumption, feces production, and energy assimilation (as sensitive and robust sub-lethal response variables; see Maltby et al., 2002) were used as response variables. Furthermore, after the termination of the experiments, the physiological fitness of the animals was determined using their lipid content and dry weight as measures. As we expected a higher EINP exposure via the waterborne pathway relative to a dietary exposure, we hypothesized the effects on gammarids to be less pronounced for the latter. The combination of both exposure pathways is assumed to reveal additive effects on the test organism.

## MATERIAL AND METHODS

### Test substances

The applied $nTiO_2$ (consisting of Anatase and Rutile; ratio: ~75:25) was purchased as powder (AEROXIDE® $TiO_2$ P25; Evonik, Germany). The advertised size of the primary particles was 21 nm with a surface area of 50 ±15 $m^2$/g (Brunauer-Emmett-Teller). Using deionized water as dispersant, an additive free dispersion (80 g $nTiO_2$/L) was prepared at the Institute for Particle Technology (TU Braunschweig, Germany) by stirred media milling (PML 2, Bühler AG, Switzerland). This dispersion was diluted with deionized water (stock dispersion, 2 g $nTiO_2$/L, nominal concentration) and pH stabilized (~3.25) by applying 120 µL of 2 M HCl/L.

The nAg (citrate coated) was synthesized following a citrate reduction method (Turkevich et al., 1951) modified by Metreveli et al. (2016). Briefly, trisodium citrate ($Na_3C_6H_5O_7$, 5 mmol, Sigma-Aldrich) and silver nitrate ($AgNO_3$, 1 mmol, ≥99.9% p.a., Carl Roth) were dissolved separately in deionized water. Following, pH value was

adjusted to 11 by adding sodium hydroxide (NaOH, 1 N standard solution, Carl Roth, Germany). Subsequently, the trisodium citrate solution was brought to the boil in a glass beaker under permanent stirring on a heatable magnetic stirrer. Once the trisodium nitrate solution started boiling, the silver nitrate solution was added drop by drop within a period of 5 min. The boiling procedure was continued for another approx. 20 min, followed by a cool down to room temperature. The nAg was stored in darkness at 4°C until further use.

The intensity-weighted average hydrodynamic diameters of the EINPs in the stock dispersions were ~80 nm ($nTiO_2$) and ~30 nm (nAg) according to measurements with a dynamic light scattering device (DelsaNano C, Beckman Coulter, Germany) under following conditions: $n=3$, 60 measurements each; temperature: 20°C; pinhole: 100 µm (Tab. 1). Prior to their application, the dispersions were sonicated for 10 minutes with a nominal power of 215 W and a sonication frequency of 35 Hz (SONOREX DIGITEC DT 514 H, Bandelin, Germany) to ensure a homogeneous particle distribution. Transmission electron microscopy images of the applied $nTiO_2$ and nAg stock dispersions can be found in Fig. S1.

**Table 1.** Particle size distribution, i.e. intensity weighted average diameter and polydispersity index (PI) of $nTiO_2$ and nAg, measured in the stock dispersions and the bioassay after 0, 24 and 48 hours in the presence of two leaf discs and a gammarid (mean ±SD, $n=3$; 60 measurements each).

| Substance | Time (hours) | Average diameter (nm) | PI |
|---|---|---|---|
| $nTiO_2$ | Stock | 83.9 ±2.5 | 0.16 |
| | 0 | 534.4 ±18.8 | 0.24 |
| | 24 | 2823.0 ± 214.1 | 0.88 |
| | 48 | 2237.3 ±172.9 | 0.82 |
| nAg | Stock | 35.8 ±1.1 | 0.36 |
| | 0 | 544.8 ±29.3 | 0.24 |
| | 24 | 3234.3 ±959.3 | 1.17 |
| | 48 | 4931.7 ±589.9 | 1.58 |

## Test Organism

Seven days before the start of the experiments, *G. fossarum* were kick-sampled in the Hainbach stream, Germany (49°14'N, 8°03'E), upstream of any agricultural activity, settlement or wastewater inlet. There, the local population is exclusively composed of the cryptic lineage B (Feckler et al., 2014). During their acclimatization to laboratory conditions, organisms were kept in a climate-controlled chamber (Weiss Environmental Technology Inc., Germany) at 16 ±1°C in darkness and fed *ad libitum* with conditioned black alder leaves (see 2.3). The adaption to the test medium SAM-5S (Borgmann, 1996), was done by increasing the ratio of stream water and test medium from 70:30 (day 1), to 50:50 (day 2), to 30:70 (day 3), ending up with 100% test medium from day 4 onwards. Only male (identified by their position during precopula pairing) and visually non-parasitized gammarids (excluding animals with a visible bright red spot within their tissue) with a cephalothorax diameter ranging from 1.6 to 2.0 mm were used for the experiment.

## Leaf Disc Preparation

Black alder leaves (*Alnus glutinosa*) were collected in October 2014 and 2015 close to Landau, Germany (49°11'N, 8°05'E) and stored in a freezer at -20° until they were used for the experiments (unconditioned leaves; Fig. 1 A). The leaf discs were prepared according to the procedure described by Zubrod et al. (2010). Summarized, unconditioned leaves were introduced in fine-mesh gauze bags, and subsequently inserted into the Rodenbach stream near Grünstadt in Germany (49°33′ N, 8°02′ E) for 14 days, upstream from agricultural activity or wastewater inlets in order to build up a microbial community on the leaves (conditioned leaves; Fig. 1 A). At our facilities, discs of 2 cm diameter were cut out from unconditioned leaves and added to the conditioned leaves and kept in darkness for 10 days in a permanently aerated aquarium containing nutrient medium (Dang et al., 2005; Fig. 1 C). Afterwards, the leaf discs were dried for approximately 24 hours at 60° C to achieve a constant weight and subsequently weighed to the nearest 0.01 mg.
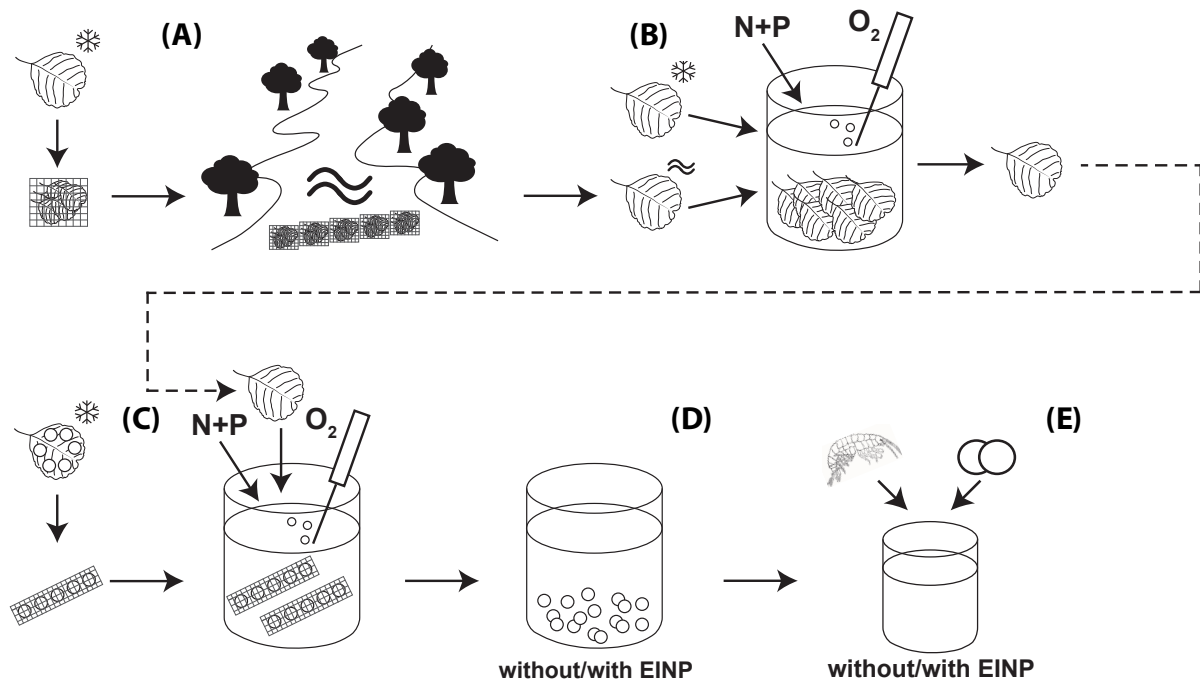
**Figure 1.** Schematic visualization of the conducted experiments: (A) conditioning of fresh leaf material; (B) conditioned leaf material and fresh leaf material kept in nutrient medium (N+P) to generate the microbial inoculum for the experiments; (C) nylon gauze strips containing leaf discs, kept together with the microbial inoculum; (D) watering/aging of the leaf discs in the presence and absence of the EINPs; (E) a single gammarid and the respectively treated leaf discs in the presence or absence of the EINPs in the water body; modified after Feckler et al. (2016).

**Experimental Setup**

Two individual 30-day long bioassays with *G. fossarum* were carried out (one for each EINP) following a 2 × 2 factorial test design. The first factor was denoted by the presence or absence of the EINPs in the water body (either $nTiO_2$: ~80 nm, 4 mg/L or nAg: ~30 nm, 0.125 mg/L; Fig. 1 E). The second factor was characterized by EINP exposure via the diet. This was implemented by a 6-day long aging of black alder leaf discs in the test medium in presence or absence of the EINPs (either $nTiO_2$: ~80 nm, 4 mg/L or nAg: ~30 nm, 0.125 mg/L; Fig. 1 D) preceding the introduction into the test system.

The individual factors and their possible combinations resulted in four treatments: the EINP-free control, EINP exposure via the water phase (EINP-W), EINP exposure through the diet (EINP-F) and the combination of waterborne and dietary exposure (EINP-WxF). A single replicate consisted of a 225 mL polystyrene beaker filled with 150 mL test medium, a single male gammarid, and two pre-weighed leaf discs (Fig. 1

197

E), whereas each treatment was replicated 30 times. During the experiments, all beakers were placed in a climate-controlled chamber (Weiss Environmental Technology Inc., Germany) at 16 ±1°C in total darkness and gently aerated.

A constant EINP exposure was guaranteed by changing the test medium of each treatment every third day. After a careful transfer of the animals and the leaf discs into the new medium, the old medium of each replicate was individually filtered over pre-weighed glass fiber filters with a pore size of 1-3 μm (GF 6, Whatman GmbH, Germany) to quantify the feces produced by the organisms. Prior to their use, the filters were incinerated at 400 °C for 5 hours to remove any organic residues that could influence the filtration process or their weight. After the incineration the filters were stored in an oven at 60 °C to keep a constant weight and were then pre-weighed to the nearest 0.01 mg.

In order to quantify the leaf consumption and feces production of each individual gammarid (see 2.5), every other medium exchange (after 6 days) the individual leaf discs and filters were replaced by new ones. The old leaf discs and filters were dried for approximately 24 hours at 60 °C to achieve a constant weight weighed again to the nearest 0.01 mg. To quantify the impact of EINP residuals on the filters, that could influence their weight and leading to misinterpretations of the leaf consumption or feces production in the treatments containing EINPs, five additional beakers with two pre-weighed leaf discs each (treated as described above), and no gammarids, were set up.

Additionally, during each medium exchange the mortality of the test organisms was recorded. After the termination of the experiments the remaining gammarids were blotted dry, frozen in liquid nitrogen and stored at -80° C for the analysis of total lipid content, and dry weight, representing the physiological fitness of the organisms.

**Endpoint calculations**

*Food consumption*

The leaf consumption (C) was expressed as mg leaf dry mass, consumed per gammarid and day and based on the following equation (Naylor et al., 1989):

$$C = \frac{L_a \times (1 - \frac{L_s - L_e}{L_s}) - L_r}{t} \tag{1}$$

$L_a$ is the initial dry weight of the leaf discs provided for a single gammarid. $L_s$ represents the initial mean dry weight of five replicates containing leaf discs in absence of gammarids, $L_e$ the mean dry weight of the same five replicates in absence of gammarids after six days, serving as a correction factor for leaf mass loss induced by microbial decomposition or leaching. $L_r$ represents the residues of $L_a$ after providing the leaf discs to a gammarid for 6 days (t).

## *Feces production*

The feces production (F) was calculated as mg feces (dry mass) per gammarid and day (Naylor et al., 1989), modified by Zubrod et al. (2010), using the following equation:

$$F = \frac{F_f - F_i - F_c}{t} \tag{2}$$

$F_f$ is the final weight of the filter (including feces) and $F_i$ the initial weight of the filter (excluding feces). $F_c$ represents the average change in weight of 5 additional filters (handled like $F_f$, but without feces), serving as correction factor to consider filter weight changes evoked by the filtration method, e.g. adsorption of EINP agglomerates or general mass loss evoked by mechanical abrasion during the filtration. The observation time was 6 days (t).

## *Energy Assimilation*

The energy assimilation (A) was expressed as mg assimilated leaf material per gammarid and day and was calculated as difference between C (leaf consumption) and F (feces production).

## *Total lipid content and dry weight*

Test organisms used for the quantification of their physiological fitness (*n*=15; per treatment) were freeze-dried for 24 hours and individually weighed to the nearest 0.01 mg. Moreover, the dry weight of these individuals was used to quantify their growth during the 30-day exposure period. The determination of the total lipid content was based on the method described by van Handel (1985) and modified as per Zubrod et al. (2011), utilizing a sulfo-phospho-vanillin-reaction (Knight et al., 1972).

## Data analysis

All statistical analyses and figures were performed with the statistical software R for Mac (Core Team, 2013; version 3.4.4). By using the Shapiro-Wilk Normality Test and the Bartlett Test of Homogeneity of Variances, the data sets were assessed for the applicability of parametric testing. If the requirements were not met, the data set was rank-transformed and evaluated for statistically significant differences by applying the Kruskal-Wallis Test followed by the Wilcoxon signed-rank Test for multiple comparisons (Bonferroni adjustment). The sub-lethal endpoints (feces production, leaf consumption and energy assimilation), as well as the physiological fitness parameters (dry weight and lipid content) were assessed with two-factorial ANOVAs allowing the assessment of individual effects of the factors and their combination (Tab. S1). The impact on mortality was assessed using testing for equality of proportions with continuity correction.

## RESULTS

### Mortality

Exposure to $nTiO_2$ did not significantly affect the mortality of *Gammarus*, regardless of the exposure pathway (Tab. 2). The highest mortality rate was observed within the control (10%), followed by EINP-W and $nTiO_2$ EINP-WxF (6.7%), as well as EINP-F (3.3%). Results for the nAg bioassay revealed a significant impact ($p$=0.008) on *Gammarus* survival in the combined exposure scenario (W×F), indicated by a mortality rate of 27%, relative the control (0%).

**Table 2.** Recorded mortality after the 30-day exposure towards $nTiO_2$ and nAg, within the different treatments as absolute value and percentage.

|  | Control | | EINP-W | | EINP-F | | EINP-WxF | |
| --- | --- | --- | --- | --- | --- | --- | --- | --- |
|  | $nTiO_2$ | nAg | $nTiO_2$ | nAg | $nTiO_2$ | nAg | $nTiO_2$ | nAg |
| **Mortality (absolute)** | 3 | 0 | 2 | 2 | 1 | 0 | 2 | 8 |
| **Mortality (%)** | 10 | 0 | 6.7 | 6.7 | 3.3 | 0 | 6.7 | 27 |

### Food Consumption, Feces Production, and Energy Assimilation

EINP exposure did not – irrespective of the exposure pathway – significantly affect the overall leaf consumption of *G. fossarum* over the study duration of 30 days, relative to the control (Fig. 2 A-B). Likewise, the feces production of the organism was not affected by the exposure to $nTiO_2$ and nAg when compared to the EINP-free control (Fig. 2 A-B). In the treatments where $nTiO_2$ was applied to the water phase (EINP-W; EINP-WxF) *Gammarus* showed a significantly reduced energy assimilation relative to the control (Fig. 2 A). This reduction ranged from about 20% (EINP-WxF) to almost 30% (EINP-W). Contrastingly, the treatments that received nAg through the provided food (EINP-F; EINP-WxF) revealed a significantly increased energy assimilation when compared to the control. This increase was almost 40% for the combined (EINP-WxF; Fig. B) and about 50% when exposed via the diet only (EINP-F; Fig. 2 B).
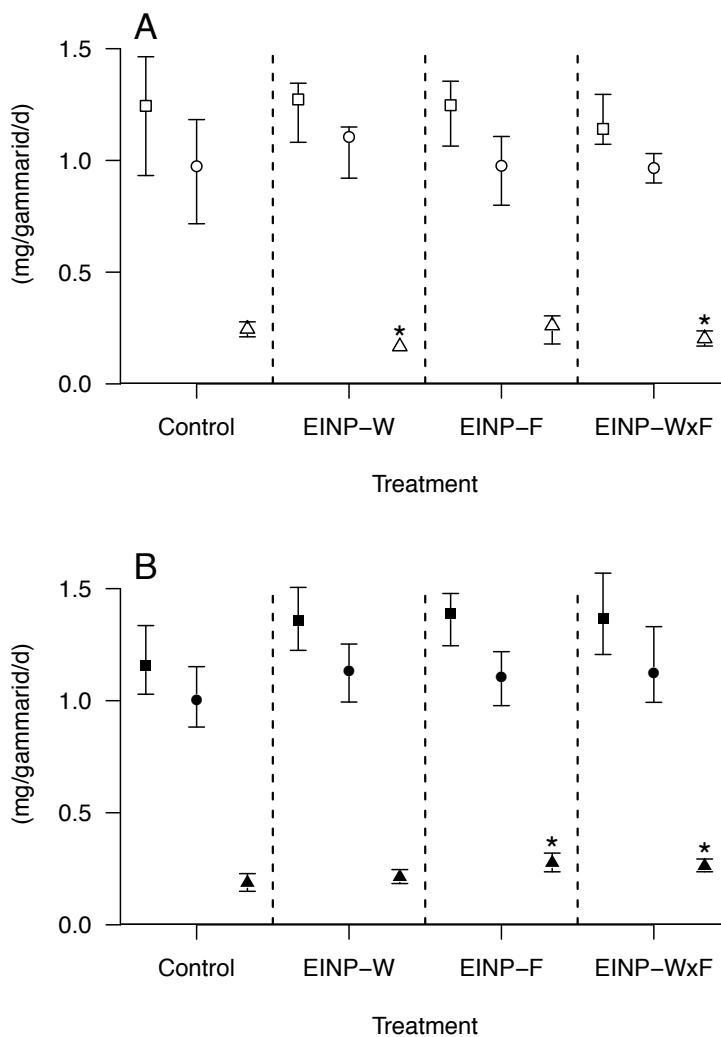
**Figure 2.** Median leaf consumption (squares), feces production (circles), and energy assimilation (triangles; ±95% CI) of *G. fossarum* in mg/gammarid/day after the 30-day exposure to the control, EINPs applied to the water phase (waterborne, EINP-W), EINPs adsorbed to the provided food (dietary, EINP-F), and the combination of both pathways (EINP-WxF). $nTiO_2$ exposure is represented in (A), whereas nAg exposure is illustrated in (B). Asterisks denote statistically significant difference to the respective control treatment.

## Lipid Content and Dry Weight

The results of the lipid analyses after the termination of the experiment showed no significant variations for gammarids exposed to EINPs, regardless of the exposure pathway when compared to the EINP-free control (Fig. 3 A-B). Given the high variability, we only observed a non-significantly increased lipid content (around 30%) in the organisms that were exposed to nAg exclusively via their diet (EINP-F; Fig. 3 A), relative to the control treatment. Final mean dry weight was also not affected among the different exposure scenarios relative to the control groups (Fig. 3 B).
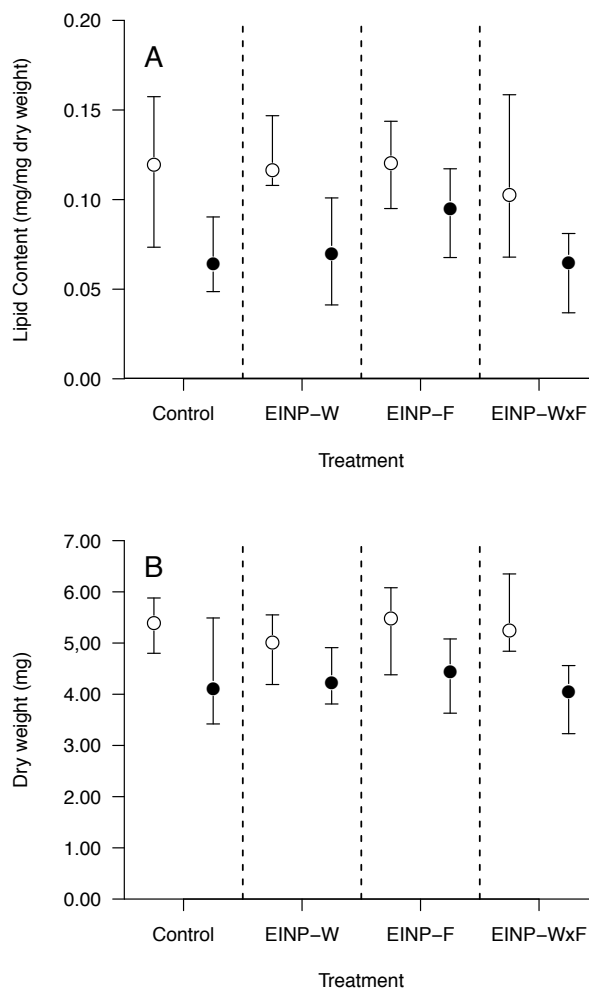
**Figure 3.** (A) Median lipid content, and (B) dry weight (±95% CI) of *G. fossarum* after the 30-day exposure to the control, EINPs applied to the water phase (waterborne, EINP-W), EINPs adsorbed to the provided food (dietary, EINP-F), and the combination of both pathways (EINP-WxF). White circles illustrate the $nTiO_2$ experiment, black circles the nAg experiment.

## DISCUSSION

During the $nTiO_2$ experiment gammarids' leaf consumption was not significantly affected via the waterborne exposure pathway when compared to the control (Fig. 2 A). These results are in accordance with former studies, where a waterborne exposure towards $nTiO_2$ (up to 5 mg/L) did not affect the leaf consumption of *G. fossarum* over 7-24 days of exposure (Kalčíková et al., 2014; Rosenfeldt et al., 2015; Seitz et al., 2014). Likewise, the dietary $nTiO_2$ exposure did not affect the feeding activity of *Gammarus*, relative to the control. The observation may be explained by the fact that the application of $nTiO_2$ to the water phase likely resulted in a higher exposure relative to the dietary route by increasing the possibility of EINPs to interact with, besides the

digestive system, other structures such as gills. More specifically, the preceding aging of the food resulted in an adsorption of the EINPs to the leaves, but compared to spiking the test medium, the exposure of *Gammarus* would likely be less pronounced in the dietary treatment explaining the studies outcome. Nonetheless, this meets our expectations of effects being more pronounced via the waterborne pathway.

The leaf consumption data of the $nTiO_2$ experiment match well with the organisms' cumulated feces production. Also, this variable is not significantly affected by either of the exposure pathways relative to the control (Fig. 2 A). However, a previous study by Rosenfeldt et al. (2015) observed a nearly significant increase in feces production of *G. fossarum* when exposed to $nTiO_2$ (2 mg/L) through the water phase. Similarly, we observed a trend of an increased feces production under waterborne exposure to $nTiO_2$ (EINP-W, EINP-WxF; Fig. 2 A). This is supported by an increase in the percentage of ingested food that was excreted from about 78% in the control and the dietary exposure pathway (EINP-F) to approximately 85% in treatments experiencing waterborne exposure (EINP-W, EINP-WxF), involving a significantly decreased energy assimilation (Fig. 2 A).

One explanation could be an increased ingestion of $TiO_2$ particles by the gammarids after applying the particles to the water phase, compared to the dietary exposure pathway. This hypothesis might be counterintuitive but is likely as not all $nTiO_2$ applied during the aging phase of this experiment were associated with the leaf discs, which inevitably reduces exposure relative to the waterborne exposure. Moreover, the increased NP ingestion may also be driven by the recurring exposure of the test organism towards 4 mg $nTiO_2$/L every 3rd day of the experiment triggered by the medium exchange. When considering the fast $nTiO_2$ agglomeration (Tab. 1) and dissipation from the water phase as visually confirmed by our study, as well as supported by literature (Dabrunz et al., 2011; Noss et al., 2013), $nTiO_2$ are transported into the gammarids' immediate environment, namely the sediment (Statzner and Bittner, 1983). These circumstances might have favored the increased uptake of $nTiO_2$ by the gammarids relative to the dietary pathway suggesting the assumed mechanisms as plausible. As a consequence, the organisms possibly prioritized the excretion of the ingested NPs, that finally resulted in a relatively higher mass of produced feces (Rosenfeldt et al., 2015), and therefore reduced energy assimilation (Schaller et al., 2011).

In contrast, nAg exposure of *G. fossarum* tendentially increased its leaf consumption by up to 20% relative to the control, though not statistically significant (Fig. 2 B). For nAg the ratio between leaf consumption and feces production decreased from about 85% for the control and the waterborne nAg exposure (EINP-W), to approximately 80% excretion of the consumed food under dietary exposure. Consequently, the energy assimilation was significantly increased compared to the control treatment (EINP-F: ~40%, EINP-WxF: ~30%; Fig. 2 B). This could be reasoned by the effect mechanism of nAg, supposedly being mainly driven by the release of Ag ions (Ag$^+$; Kennedy et al., 2010; Seitz et al., 2015), which along with its antimicrobial properties, makes nAg to one of the most toxic metals found in natural water systems (Ribeiro et al., 2014; Salomoni et al., 2017; Zhai et al., 2018). In our study the 6-day long preceding aging of the leaf material in the presence of nAg resulted in a visually observable adsorption of nAg onto the leaves. Subsequently, the dietary exposure pathway may have resulted in a higher Ag uptake in the gammarids than through the waterborne exposure. The discrepancy relative to nTiO$_2$ may be explained by the different mechanisms of toxic action of these two EINPs: nAg may have been taken up into cells with subsequent dissolution of Ag ions resulting in locally high concentrations of biologically active ions (Reidy et al., 2013).

Moreover, a study by Croteau et al. (2011) suggests that a dietary uptake of all forms of Ag, especially citrate coated nAg would result in high body levels of Ag in freshwater invertebrates. Further, they state that the ingestion of Ag adsorbed to particulate matter seems to be the most prominent path of uptake triggering adverse effects more pronounced than waterborne Ag exposures. Thereby, pivotal effects induced by nAg uptake include oxidative stress, apoptosis (e.g. through DNA damage or mitochondrial dysfunction), or disruptions of the gut microbiota (Fröhlich and Fröhlich, 2016; Völker et al., 2013). Consequently, it is possible that this triggered an energetic reallocation within *Gammarus* enhancing maintenance costs such as detoxification (Vellinger et al., 2012), finally causing the here observed effects. Zubrod et al. (2016) suggested that effects on the energy assimilation of *Gammarus* seem to be triggered by energetically costly responses to oxidative stress and principally can be attributed to an alteration in feeding behavior. These insights from literature finally suggest a higher energy demand to cope with the stress, which could explain the observed increase in feeding rate as an attempt to compensate for this higher energy demand (Andreï et al., 2016).

All in all, the exposure of benthic organisms towards EINPs will most likely be determined by agglomerated and sedimented EINPs. In this context, it seems also relevant to consider the ingestion of EINPs settled on or bound to sediment, leaves, biofilms or food sources (Selck et al., 2016). However, when looking at the partly contradicting outcome for the two EINP tested in our study, the relative importance of the exposure pathway seems attributable to the physical and chemical characteristics of the respective EINP (Sukhanova et al., 2018), i.e. chemically stable vs. release of toxic ions. Thus, it seems sensible to categorize EINPs based on their characteristics (e.g. morphology, shape, reactivity, persistency, solubility; Lamon et al., 2018), which should include the ecotoxicological relevance of exposure pathways (Selck et al., 2016) to enable a more accurate risk assessment for aquatic ecosystems. This suggestion is already partly covered through a stepwise grouping approach supporting the hazard and fate identification of nanoforms (ECHA, 2017). This grouping approach involves key physiochemical (size, shape and surface area), behavioral (e.g. solubility, hydrophobicity, zeta potential) parameters, as well as EINP reactivity (biological- and photoreactivity; ECHA, 2017), but lacks an estimation on the relevance of exposure pathways. A successful implementation of this strategy would ultimately facilitate a targeted risk assessment for species and groups of species likely experiencing the highest risks in the field.

**CONCLUSION**

Our study revealed energy assimilation as promising response for chronic EINP exposure aside from frequently used endpoints such as leaf consumption, feces production, growth, or lipid content. In the long run, alterations in the energy processing of *G. fossarum* could lead to impairments on a population or even community scale. Since gammarids play a crucial role in the decomposition of leaf litter and can be considered as key species with regards to this function, impairments like the ones observed in our study could inevitably lead to alterations in the energy allocation for the corresponding food web. However, when considering expected environmental concentrations for the most frequently used nanoparticles in the low ng and µg/L range (Gottschalk et al., 2013), benthic organisms like *G. fossarum* might not be currently threatened by EINP exposure.

**REFERENCES**

Adam, V., Loyaux-Lawniczak, S., Labille, J., Galindo, C., del Nero, M., Gangloff, S., Weber, T., Quaranta, G., 2016. Aggregation behaviour of $TiO_2$ nanoparticles in natural river water. J Nanapart. Res. 18, 13.

Aitken, R.J., Chaudhry, M.Q., Boxall, A.B.A., Hull, M., 2006. Manufacture and use of nanomaterials: current status in the UK and global trends. Occup. Med-C. 56, 300-306.

Andreï, J., Pain-Devin, S., Felten, V., Devin, S., Giambérini, L., Mehennaoui, K., Cambier, S., Gutleb, A.C., Guérold, F., 2016. Silver nanoparticles impact the functional role of *Gammarus roeseli* (Crustacea Amphipoda). Environ. Pollut. 208, 608-618.

Baun, A., Hartmann, N.B., Grieger, K., Kusk, K.O., 2008. Ecotoxicity of engineered nanoparticles to aquatic invertebrates: a brief review and recommendations for future toxicity testing. Ecotoxicology 17, 387-395.

Borgmann, U., 1996. Systematic analysis of aqueous ion requirements of *Hyalella azteca*: a standard artificial medium including the essential bromide ion. Arch. Environ. Contam. Toxicol. 30, 356-363.

Bundschuh, M., Filser, J., Lüderwald, S., McKee, M.S., Metreveli, G., Schaumann, G.E., Schulz, R., Wagner, S., 2018. Nanoparticles in the environment: where do we come from, where do we go to? Environ. Sci. Eur. 30, 6.

Croteau, M.-N., Misra, S.K., Luoma, S.N., Valsami-Jones, E., 2011. Silver bioaccumulation dynamics in a freshwater invertebrate after aqueous and dietary exposures to nanosized and ionic Ag. Environ. Sci. Technol. 45, 6600-6607.

Croteau, M.-N., Misra, S.K., Luoma, S.N., Valsami-Jones, E., 2011. Bioaccumulation and toxicity of CuO nanoparticles by a freshwater invertebrate after waterborne and dietborne exposures. Environ. Sci. Technol. 48, 10929-10937.

Dabrunz, A., Duester, L., Prasse, C., Seitz, F., Rosenfeldt, R., Schilde, C., Schaumann, G.E., Schulz, R., 2011. Biological surface coating and molting inhibition as mechanisms of TiO$_2$ nanoparticle toxicity in *Daphnia magna*. PLoS ONE 6, e20112. Dang, C.K., Chauvet, E., Gessner, M.O., 2005. Magnitude and variability of process rates in fungal diversity-litter decomposition relationships. Ecol. Lett. 8, 1129-1137.

ECHA, 2017. Appendix R.6-1 for nanomaterials applicable to the guidance on QSARs and grouping of chemicals [Online]. Available: https://echa.europa.eu/documents /10162/23036412/appendix_r6_nanomaterials_en.pdf.

Feckler, A., Goedkoop, W., Zubrod, J.P., Schulz, R., Bundschuh, M., 2016. Exposure pathway-dependent effects of the fungicide epoxiconazole on a decomposer-detritivore system. Sci. Total Environ. 571, 992-1000.

Feckler, A., Zubrod, J.P., Thielsch, A., Schwenk, K., Schulz, R., Bundschuh, M., 2014. Cryptic species diversity: an overlooked factor in environmental management? J. Appl. Ecol. 51, 958-967.

Forster, S.P., Olveira, S., Seeger, S., 2011. Nanotechnology in the market: promises and realities. Int. J. Nanotechnol. 8, 592-613.

Fröhlich, E.E., Fröhlich, E., 2016. Cytotoxicity of nanoparticles contained in food on intestinal cells and the gut microbiota. Int. J. Mol. Sci. 17, 509-509.

Gottschalk, F., Sun, T., Nowack, B., 2013. Environmental concentrations of engineered nanomaterials: review of modeling and analytical studies. Environ. Pollut. 181, 287-300.

Kaegi, R., Ulrich, A., Sinnet, B., Vonbank, R., Wichser, A., Zuleeg, S., Simmler, H., Brunner, S., Vonmont, H., Burkhardt, M., Boller, M., 2008. Synthetic $TiO_2$ nanoparticle emission from exterior facades into the aquatic environment. Environ. Pollut. 156, 233-239.

Kalčíková, G., Englert, D., Rosenfeldt, R.R., Seitz, F., Schulz, R., Bundschuh, M., 2014. Combined effect of UV-irradiation and $TiO_2$-nanoparticles on the predator–prey interaction of gammarids and mayfly nymphs. Environ. Pollut. 186, 136-140.

Keller, A.A., Lazareva, A., 2014. Predicted releases of engineered nanomaterials: from global to regional to local. Environ. Sci. Tech. Let. 1, 65-70.

Kennedy, A.J., Hull, M.S., Bednar, A.J., Goss, J.D., Gunter, J.C., Bouldin, J.L., Vikesland, P.J., Steevens, J.A., 2010. Fractionating nanosilver: importance for determining toxicity to aquatic test organisms. Environ. Sci. Technol. 44, 9571-9577.

Kiser, M.A., Westerhoff, P., Benn, T., Wang, Y., Perez-Rivera, J., Hristovski, K., 2009. Titanium nanomaterial removal and release from wastewater treatment plants. Environ. Sci. Technol. 43, 6757-6763.

Klaine, S.J., Alvarez, P.J.J., Batley, G.E., Fernandes, T.F., Handy, R.D., Lyon, D.Y., Mahendra, S., McLaughlin, M.J., Lead, J.R., 2008. Nanomaterials in the environment: behavior, fate, bioavailability, and effects. Environ. Toxicol. Chem. 27, 1825-1851.

Knight, J.A., Anderson, S., Rawle, J.M., 1972. Chemical basis of the sulfo-phospho-vanillin reaction for estimating total serum lipids. Clin. Chem. 18, 199.

Lamon, L., Aschberger, K., Asturiol, D., Richarz, A., Worth, A., 2018. Grouping of nanomaterials to read-across hazard endpoints: a review. Nanotoxicology, 1-19.

Lovern, S.B., Klaper, R., 2006. *Daphnia magna* mortality when exposed to titanium dioxide and fullerene ($C_{60}$) nanoparticles. Environ. Toxicol. Chem. 25, 1132-1137.

Maltby, L., Clayton, S.A., Wood, R.M., McLoughlin, N., 2002. Evaluation of the *Gammarus pulex* in situ feeding assay as a biomonitor of water quality: robustness, responsiveness, and relevance. Environ. Toxicol. Chem. 21, 361-368.

Markus, S., Tiina-Mari, P., Pirjo, S., 2011. Aggregation and deposition of engineered $TiO_2$ nanoparticles in natural fresh and brackish waters. J Phys.: Conf. Ser. 304, 012018.

Mehennaoui, K., Georgantzopoulou, A., Felten, V., Andreï, J., Garaud, M., Cambier, S., Serchi, T., Pain-Devin, S., Guérold, F., Audinot, J.-N., Giambérini, L., Gutleb, A.C., 2016. *Gammarus fossarum* (Crustacea, Amphipoda) as a model organism to study the effects of silver nanoparticles. Sci. Total Environ. 566-567, 1649-1659.

Metreveli, G., Frombold, B., Seitz, F., Grun, A., Philippe, A., Rosenfeldt, R.R., Bundschuh, M., Schulz, R., Manz, W., Schaumann, G.E., 2016. Impact of chemical composition of ecotoxicological test media on the stability and aggregation status of silver nanoparticles. Environ. Sci. Nano. 3, 418-433.

Metreveli, G., Philippe, A., Schaumann, G. E., 2015 Disaggregation of silver nanoparticle homoaggregates in a river water matrix. Sci. Total Environ. 535, 35-44.

Naylor, C., Maltby, L., Calow, P., 1989. Scope for growth in *Gammarus pulex*, a freshwater benthic detritivore. Hydrobiologia 188, 517-523.

Noss, C., Dabrunz, A., Rosenfeldt, R.R., Lorke, A., Schulz, R., 2013. Three-dimensional analysis of the swimming behavior of *Daphnia magna* exposed to nanosized titanium dioxide. PLoS ONE 8, e80960.

Petosa, A.R., Jaisi, D.P., Quevedo, I.R., Elimelech, M., Tufenkji, N., 2010. Aggregation and deposition of engineered nanomaterials in aquatic environments: role of physicochemical interactions. Environ. Sci. Technol. 44, 6532-6549.

Piccinno, F., Gottschalk, F., Seeger, S., Nowack, B., 2012. Industrial production quantities and uses of ten engineered nanomaterials in Europe and the world. J. Nanopart. Res. 14, 1-11.

Rajala, J.E., Vehniäinen, E.-R., Väisänen, A., Kukkonen, J.V.K., 2018. Toxicity of silver nanoparticles to *Lumbriculus variegatus* is a function of dissolved silver and promoted by low sediment pH. Environ. Toxicol. Chem. 37, 1889-1897.

Rao, N.V., Rajasekhar, M., Vijayalakshmi, K., Vamshykrishna, M., 2015. The future of civil engineering with the influence and impact of nanotechnology on properties of materials. Proc. Mat. Sci. 10, 111-115.

Reidy, B., Haase, A., Luch, A., Dawson, K.A., Lynch, I., 2013. Mechanisms of silver nanoparticle release, transformation and toxicity: a critical review of current knowledge and recommendations for future studies and applications. Materials (Basel) 6, 2295-2350.

Ribeiro, F., Gallego-Urrea, J.A., Jurkschat, K., Crossley, A., Hassellöv, M., Taylor, C., Soares, A.M.V.M., Loureiro, S., 2014. Silver nanoparticles and silver nitrate induce high toxicity to *Pseudokirchneriella subcapitata*, *Daphnia magna* and *Danio rerio*. Sci. Total Environ. 466-467, 232-241.

Ribeiro, F., Van Gestel, C.A.M., Pavlaki, M.D., Azevedo, S., Soares, A.M.V.M., Loureiro, S., 2017. Bioaccumulation of silver in *Daphnia magna*: waterborne and dietary exposure to nanoparticles and dissolved silver. Sci. Total Environ. 574, 1633-1639.

Rosenfeldt, R.R., Seitz, F., Zubrod, J.P., Feckler, A., Merkel, T., Lüderwald, S., Bundschuh, R., Schulz, R., Bundschuh, M., 2015. Does the presence of titanium dioxide nanoparticles reduce copper toxicity? A factorial approach with the benthic amphipod *Gammarus fossarum*. Aquat. Toxicol. 165, 154-159.

Rosenfeldt, R. R., Seitz, F., Haigis, A., Höger, J., Zubrod, J. P., Schulz, R., Bundschuh, M., 2016. Nanosized titanium dioxide influences copper-induced toxicity during aging as a function of environmental conditions. Environ. Toxicol. Chem. 35, 1766-1774.

Rosenkranz, P., Chaudhry, Q., Stone, V., Fernandes, T.F., 2009. A comparison of nanoparticle and fine particle uptake by *Daphnia magna*. Environ. Toxicol. Chem. 28, 2142-2149.

Salomoni, R., Léo, P., Montemor, A.F., Rinaldi, B.G., Rodrigues, M., 2017. Antibacterial effect of silver nanoparticles in *Pseudomonas aeruginosa*. Nanotechnol. Sci. Appl. 10, 115-121.

Schaller, J., Brackhage, C., Mkandawire, M., Dudel, E.G., 2011. Metal/metalloid accumulation/remobilization during aquatic litter decomposition in freshwater: a review. Sci. Total Environ. 409, 4891-4898.

Seitz, F., Bundschuh, M., Rosenfeldt, R.R., Schulz, R., 2013. Nanoparticle toxicity in *Daphnia magna* reproduction studies: the importance of test design. Aquat. Toxicol. 126, 163-168.

Seitz, F., Rosenfeldt, R.R., Schneider, S., Schulz, R., Bundschuh, M., 2014. Size-, surface- and crystalline structure composition-related effects of titanium dioxide nanoparticles during their aquatic life cycle. Sci. Total Environ. 493, 891-897.

Seitz, F., Rosenfeldt, R.R., Storm, K., Metreveli, G., Schaumann, G.E., Schulz, R., Bundschuh, M., 2015. Effects of silver nanoparticle properties, media pH and dissolved organic matter on toxicity to *Daphnia magna*. Ecotoxicol. Environ. Saf. 111, 263-270.

Selck, H., Handy, R.D., Fernandes, T.F., Klaine, S.J., Petersen, E.J., 2016. Nanomaterials in the aquatic environment: a European Union–United States perspective on the status of ecotoxicity testing, research priorities, and challenges ahead. Environ. Toxicol. Chem. 35, 1055-1067.

Stark, W.J., Stoessel, P.R., Wohlleben, W., Hafner, A., 2015. Industrial applications of nanoparticles. Chem. Soc. Rev. 44, 5793-5805.

Statzner, B., Bittner, A., 1983. Nature and causes of migrations of *Gammarus fossarum* Koch (Amphipoda): a field study using a light intensifier for the detection of nocturnal activities. Crustaceana, 271-291.

Sukhanova, A., Bozrova, S., Sokolov, P., Berestovoy, M., Karaulov, A., Nabiev, I., 2018. Dependence of nanoparticle toxicity on their physical and chemical properties. Nanoscale Res. Lett. 13, 44.

Core Team, R., 2013. R: A Language and environment for statistical computing. R Foundation for Statistical Computing, Vienna, Austria. Available: https://www.R-project.org/.

Turkevich, J., Stevenson, P.C., Hillier, J., 1951. A study of the nucleation and growth processes in the synthesis of colloidal gold. Faraday Discuss. Chem. Soc. 11, 55-75.

Van Handel, E., 1985. Rapid determination of total lipids in mosquitoes. J. Am. Mosq. Control Assoc. 1, 302-304.

Vellinger, C., Felten, V., Sornom, P., Rousselle, P., Beisel, J.-N., Usseglio-Polatera, P., 2012. Behavioural and physiological responses of gammarus pulex exposed to cadmium and arsenate at three temperatures: individual and combined effects. PLOS ONE 7, e39153.

Velzeboer, I., Quik, J.T.K., van de Meent, D., Koelmans, A.A., 2014. Rapid settling of nanoparticles due to heteroaggregation with suspended sediment. Environ. Toxicol. Chem. 33, 1766-1773.

Völker, C., Boedicker, C., Daubenthaler, J., Oetken, M., Oehlmann, J., 2013. Comparative toxicity assessment of nanosilver on three *Daphnia* species in acute, chronic and multi-generation experiments. PLOS ONE 8, e75026.

Von der Kammer, F., Ottofuelling, S., Hofmann, T., 2010. Assessment of the physico-chemical behavior of titanium dioxide nanoparticles in aquatic environments using multi-dimensional parameter testing. Environ. Pollut. 158, 3472-3481.

Westerhoff, P., Song, G., Hristovski, K., Kiser, M.A., 2011. Occurrence and removal of titanium at full scale wastewater treatment plants: implications for $TiO_2$ nanomaterials. J. Environ. Monitor. 13, 1195-1203.

Zhai, Y., Brun, N.R., Bundschuh, M., Schrama, M., Hin, E., Vijver, M.G., Hunting, E.R., 2018. Microbially-mediated indirect effects of silver nanoparticles on aquatic invertebrates. Aquat. Sci. 80, 44.

Zubrod, J.P., Bundschuh, M., Schulz, R., 2010. Effects of subchronic fungicide exposure on the energy processing of *Gammarus fossarum* (Crustacea; Amphipoda). Ecotoxicol. Environ. Saf. 73, 1674-1680.

Zubrod, J.P., Bundschuh, M., Feckler, A., Englert, D., Schulz, R., 2011. Ecotoxicological impact of the fungicide tebuconazole on an aquatic decomposer-detritivore system. Environ. Toxicol. Chem. 30, 2718-2724.

Zubrod, J.P., Englert, D., Wolfram, J., Wallace, D., Schnetzer, N., Baudy, P., Konschak, M., Schulz, R., Bundschuh, M., 2015. Waterborne toxicity and diet-related effects of fungicides in the key leaf shredder *Gammarus fossarum* (Crustacea: Amphipoda). Aquatic Toxicology 169, 105-112.

# Exposure pathway dependent effects of titanium dioxide and silver nanoparticles on the benthic amphipod *Gammarus fossarum*

Lüderwald, S., Schell, T., Newton, K., Salau, R., Seitz, F., Rosenfeldt, R., Dackermann, V., Metreveli, G., Schulz, R., Bundschuh, M.

**Table S1.** Outcome of the two-factor ANOVAs for $nTiO_2$ (A) and nAg (B) for the observed response variables food consumption, feces production, assimilation, and lipid content. Statistical significance ($p$-value<0.05) is printed in bold.

| (A) | Df | Sum Sq | Mean Sq | $F$-value | $p$-value |
|---|---|---|---|---|---|
| *Food consumption:* | | | | | |
| $nTiO_2$-W | 1 | 0.00 | 0.00 | 0.04 | 0.8482 |
| $nTiO_2$ F | 1 | 0.03 | 0.03 | 0.28 | 0.5972 |
| $nTiO_2$-WxF | 1 | 0.11 | 0.11 | 1.18 | 0.2807 |
| Residuals | 109 | 10.58 | 0.10 | | |
| | | | | | |
| *Feces production:* | | | | | |
| $nTiO_2$-W | 1 | 0.15 | 0.15 | 2.13 | 0.1474 |
| $nTiO_2$-F | 1 | 0.08 | 0.08 | 1.15 | 0.2862 |
| $nTiO_2$-WxF | 1 | 0.14 | 0.14 | 1.99 | 0.1609 |
| Residuals | 108 | 7.72 | 0.07 | | |
| | | | | | |
| *Assimilation:* | | | | | |
| $nTiO_2$-W | 1 | 0.11 | 0.11 | 14.03 | **0.0003** |
| $nTiO_2$-F | 1 | 0.01 | 0.01 | 1.64 | 0.2033 |
| $nTiO_2$-WxF | 1 | 0.00 | 0.00 | 0.12 | 0.7296 |
| Residuals | 108 | 0.87 | 0.01 | | |
| | | | | | |
| *Lipid content:* | | | | | |
| $nTiO_2$-W | 1 | 801.00 | 800.80 | 0.43 | 0.5137 |
| $nTiO_2$-F | 1 | 643.00 | 642.88 | 0.35 | 0.5583 |
| $nTiO_2$-WxF | 1 | 2908.00 | 2908.11 | 1.57 | 0.2156 |
| Residuals | 55 | 101920.00 | 1853.09 | | |

| (B) | Df | Sum Sq | Mean Sq | *F*-value | *p*-value |
|---|---|---|---|---|---|
| *Food consumption:* | | | | | |
| nAg-W | 1 | 0.19 | 0.19 | 1.79 | 0.1843 |
| nAg-F | 1 | 0.19 | 0.19 | 1.77 | 0.1861 |
| nAg-WxF | 1 | 0.12 | 0.12 | 1.15 | 0.2864 |
| Residuals | 106 | 11.17 | 0.10 | | |
| | | | | | |
| *Feces production:* | | | | | |
| nAg-W | 1 | 0.12 | 0.12 | 1.61 | 0.2068 |
| nAg-F | 1 | 0.00 | 0.00 | 0.01 | 0.9054 |
| nAg-WxF | 1 | 0.27 | 0.03 | 0.35 | 0.5537 |
| Residuals | 104 | 8.04 | 0.08 | | |
| | | | | | |
| *Assimilation:* | | | | | |
| nAg-W | 1 | 0.01 | 0.01 | 1.78 | 0.1856 |
| nAg-F | 1 | 0.13 | 0.13 | 17.31 | **0.0001** |
| nAg-WxF | 1 | 0.02 | 0.02 | 3.12 | 0.0804 |
| Residuals | 104 | 0.77 | 0.01 | | |
| | | | | | |
| *Lipid content:* | | | | | |
| nAg-W | 1 | 0.00 | 0.00 | 2.21 | 0.1454 |
| nAg-F | 1 | 0.00 | 0.00 | 0.92 | 0.3437 |
| nAg-WxF | 1 | 0.00 | 0.00 | 2.82 | 0.1016 |
| Residuals | 36 | 0.03 | 0.00 | | |

Df: Degrees of freedom

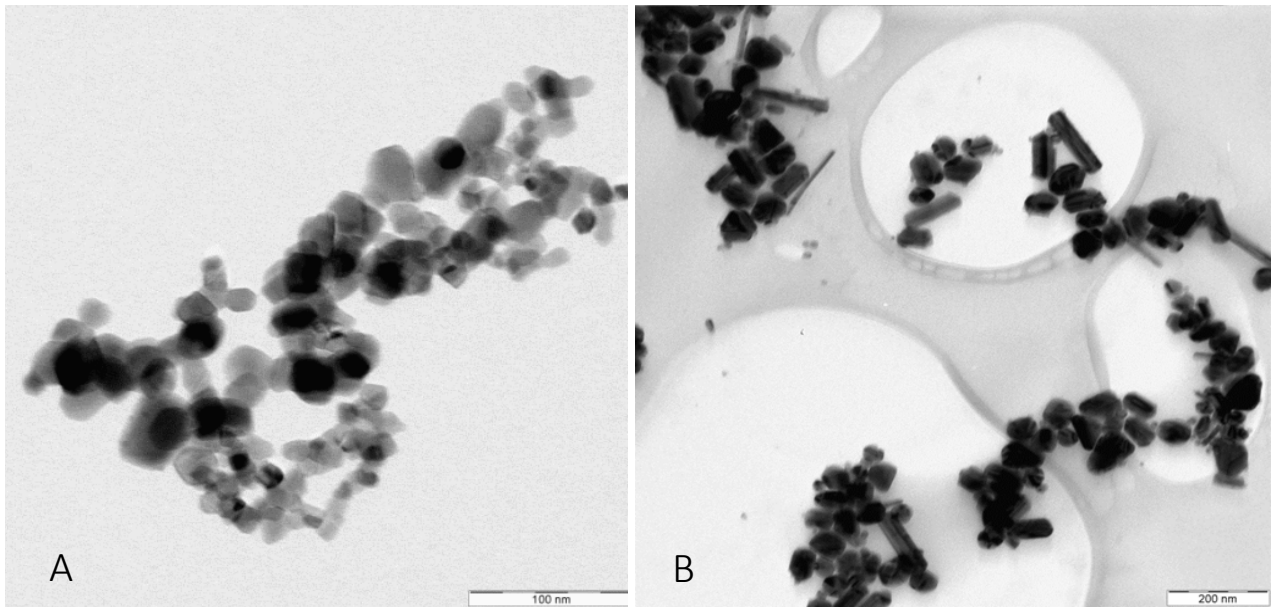Sum Sq: Sum of squares

Mean Sq: Mean squares

**Figure S1.** Transmission electron microscopy image of the applied $nTiO_2$ (A) and nAg stock dispersions (200 keV Zeiss 922 Omega; scale bar A: 100 nm; scale bar B: 200 nm), as detailed in Rosenfeldt et al. (2016), and Metreveli et al. (2015).

# Nanoparticles transported from aquatic to terrestrial ecosystems via emerging aquatic insects comprise subsidy quality

Bundschuh, M., Englert, D., Rosenfeldt, R.R., Bundschuh, R., Feckler, A., Lüderwald, S., Seitz, F., Zubrod, J.P., Schulz, R.

## ABSTRACT

Nanoparticle contaminants enter aquatic ecosystems and are transported along the stream network. Here, we demonstrate a novel pathway for the return of nanoparticles from aquatic to terrestrial ecosystems via cross-boundary subsidies. During their emergence, trichopteran caddisflies carried titanium dioxide and gold nanoparticles into their terrestrial life stages. Moreover, their emergence was delayed by ≤30 days, and their energy reserves were depleted by ≤25%. Based on worst case estimates, it is suggested that terrestrial predators, such as bats feeding on aquatic prey, may ingest up to three orders of magnitude higher gold levels than anticipated for humans. Additionally, terrestrial predator species may suffer from alterations in the temporal availability and nutritional quality of their prey. Considering the substantial transfer of insect biomass to terrestrial ecosystems, nanoparticles may decouple aquatic and terrestrial food webs with important (meta-)ecosystem level consequences.

## KEYWORDS

## INTRODUCTION

Over 1,000 products, including sunscreens, textiles, and self-cleaning surfaces, contain engineered nanoparticles or are produced utilizing nanotechnology. As a result, the unintentional introduction of engineered nanoparticles into freshwater environments, mainly via wastewater treatment plant effluents [1], is increasing [2] and represents a significant share of the manufacturing production volume [3]. The nanoparticles are transported downstream until their ultimate release into the marine ecosystem. However, the potential for nanoparticle transport from the aquatic environment back to terrestrial ecosystems has been neglected thus far. In this context, the transfer of nanoparticles via merolimnic aquatic insects represents a possible pathway directly into terrestrial food webs. Because nanoparticles are consumed within the insect aquatic life stages, this process likely results in a higher nanoparticle bioavailability for terrestrial species than if they were associated with the soil matrix. Although studies have shown that nanoparticles can be transmitted along the aquatic [4,5] and terrestrial [6] food chains, cross-ecosystem dietary exposure has not yet been examined. Additionally, it is unknown whether the temporal availability and

quality of these subsidies, namely the emergence pattern and nutritional value (e.g., energy reserves) of aquatic insects, are affected by nanoparticles. Both the trophic transfer of nanoparticles via aquatic subsidies and changes in the availability and quality of this subsidy may be of serious concern for the well-being of terrestrial predators and their offspring, including endangered species of amphibians, lizards, birds, bats and spiders [7-9]. Indeed, a contamination of aquatic systems by chemicals of anthropogenic origin such as metals, pharmaceuticals and others suggest alterations in the aquatic-terrestrial coupling [10-16] warranting for further studies [17].

To investigate the transfer of nanoparticles from an aquatic to a terrestrial ecosystem, this study employed laboratory flow-through stream microcosms (n=24; Fig. 1a) over a period of 140 days. In this system, the transfer of 62.3-nm titanium dioxide (4 and 400 µg $nTiO_2$/L; Fig. 1b) and 15.1-nm gold (6.5 µg nAu/L; Fig. 1c, see also Tab. S3) nanoparticles via the caddisfly *Chaetopteryx villosa* developing from aquatic larvae into a terrestrial adult stage was investigated. Nanoparticles were assumed to be taken up by *C. villosa* from the water phase or from consumed leaf material that adsorb nanoparticles during exposure (Tab. S1). In parallel, the temporal emergence pattern and the energy reserves (i.e., lipid stores) of this species, which can be found in large quantities in slow flowing streams [18], were monitored. In addition, the photocatalytic effects of nanoparticles on the responses of *Chaetopteryx* were assessed by exposure to ultraviolet (UV) irradiation at ambient intensities UV-A: 9.7 W/m2, UV-B: 0.35 W/m2, [19] in the presence and absence of $nTiO_2$/L [20].

## RESULTS AND DISCUSSION

Although none of the treatments affected the overall leaf consumption, survival and emergence rate of caddisfly larvae relative to the controls (Tab. S2), the temporal emergence pattern (Fig. 2a; Fig. S1), the energy reserves of (Fig. 2b) and the concentration of nanoparticles in the adult organisms (Tab. 1) deviated considerably among the treatments. The presence of nAu, for example, delayed the emergence (defined as the study duration at which 50% of *Chaetopteryx* individuals have emerged) by up to one month (Fig. 2a). In addition, the energy reserves, measured as total lipid concentration in emerged adults, were reduced by up to 25% (Fig. 2b). UV-irradiation alone delayed emergence by eleven days; in combination with 4 and 400 µg $nTiO_2$ per liter, this effect was significantly extended to 16 and 20 days, respectively, presumably due to the formation of reactive oxygen species [21]. Moreover, lipid

concentrations of these adults were significantly decreased (Fig. 2b). Because the lower experimental concentration of nTiO$_2$ (i.e., 4 µg/L) is at least seven times less than nTiO$_2$ concentrations measured in a recreational lake in central Europe and wastewater treatment plant effluents [22,23], the delay in emergence caused by the combination of nTiO$_2$ and ambient UV-irradiation can (despite the fact that the study was performed under controlled environmental conditions) be considered environmentally relevant with potentially strong implications for aquatic and terrestrial ecosystems. As outlined above, nAu exposure resulted in an even more severe delay in emergence and depletion of energy reserves at a concentration considered to be environmentally safe for Au ions – not nanoparticles, which are usually deemed to be less toxic – based on European regulations [24]. Although the concentration assessed in the present study is an order of magnitude above the nAu concentrations currently predicted for aquatic ecosystems [25], the data presented here raise concerns for unanticipated effects at the ecosystem level. This concern is underpinned by the substantial effect that shifts in the temporal emergence pattern and the nutritional value (i.e., energy reserves) of emerging adult insects may have on terrestrial predators, such as spiders and adult amphibians, lizards, bats and birds [26], that may ultimately influence their reproductive success [27,28]. In particular, migratory bird species must fill their energy reserves prior to or following seasonal movements, and changes in the temporal emergence pattern and lipid concentrations of merolimnic prey insects may have serious implications for the birds' life cycles [8].

Most importantly, emerging aquatic insects carried substantially elevated concentrations of either TiO$_2$ or Au following exposure to nanoparticles (Tab. 1). Environmental scanning electron microscopy coupled to energy dispersive X-ray spectroscopy images of thin image sections support the uptake of nanoparticles into abdominal tissue of the adult insects (Fig. 3). A potential adhesion of nanoparticles from the medium to the outer surface of the adults following pupation, as simulated by submersing control flies into the respective media, does not account for the measured TiO$_2$ and Au concentrations in the body (Tab. S1). This finding demonstrates the potential for nanoparticles to be transferred from the aquatic ecosystem into the terrestrial food web – a novel pathway for nanoparticles in the environment. In the gut of a terrestrial predator, nanoparticles may affect the digestive system [29] and thus the physiological constitution. Moreover, we calculated theoretical intake rates based on the estimated daily consumption of approximately 6 g of insects during pregnancy and

lactation of little brown bats (*Myotis lucifugus*) [30] assuming that their Au concentration equals the median concentrations detected in adults of the present study. These extrapolations suggest a theoretical ingestion of nAu with the aquatic prey at levels that are a factor of 1000 above those considered as maximum intake for humans as a consequence of gold being used as food additives [31]. At the same time, it was indicated that dietary ingestion of gold at levels comparable to this maximum intake can cause skin rash in humans [32].

Although these insights are worrying for aquatic-terrestrial meta ecosystems [17], predicting the implications of this exposure for terrestrial food webs remains difficult [33], particularly as the present study followed a relatively simplistic experimental setting involving one species under relatively well controlled environmental conditions. Nonetheless, based on simplistic assumptions that (i) the concentration of nAu and $nTiO_2$ is comparable among merolimnic insect species and (ii) environmental concentrations reach the levels tested here, nAu and $nTiO_2$ fluxes from the aquatic to the terrestrial environment can be as high as 1.4-31.8 mg and 2.4-56.5 mg each per square meter of water surface and year, respectively. This estimate is based on the median nanoparticle concentrations measured in the present study and the total annual biomass of emerging merolimnic insects from streams as reviewed by Raitif et al. [34].

These data therefore may raise concerns about the consequences for higher trophic levels in riparian systems, including endangered species, associated with the transfer of contaminants such as nanoparticles from the aquatic back to the terrestrial food web. Although recent explorations of the movement and impact of contaminants, such as microplastics [10], metals [11-14], polychlorinated biphenyls [15], pharmaceuticals [16] and in the present study nanoparticles, highlight impairments in the aquatic-to-terrestrial subsidy, research addressing this question is still in its infancy warranting further studies [17].

## MATERIALS AND METHODS

### Nanoparticles

$nTiO_2$ and nAu have been selected as model nanoparticles for the following reasons: Titanium dioxide is one of the most frequently applied nanoparticles worldwide used in personal care products, coatings, paints, and pigments [35,36], entering the natural environment for instance via wastewater treatment plant effluents and landfill leachates. Gold-nanoparticles, in contrast, have a low background concentration in environmental matrices, increasing the sensitivity of the chemical analyses and thus the possibility to quantify any potential transfer of nAu across ecosystem boundaries as part of the emerging insect.

The titanium dioxide product used in this study was purchased as a powder from Evonik (P 25; Germany) featuring an advertised primary particle size of 21 nm and crystalline composition of approximately 70% of anatase and 30% of rutile. Its advertised surface area was approximately 50 $m^2/g$. The powder was transferred into a dispersant additive-free, size-homogenized, charge-stabilized suspension by stirred media milling (PML 2, Bühler AG, Switzerland [37]) at a concentration of 83.87 g/L $nTiO_2$ in deionized water.

Gold nanoparticles (nAu) were synthesized by reducing $Au^{3+}$ with tri-sodium citrate, essentially following the protocol published by McFarland et al. [38]. Briefly, a 1 mM hydrogen tetrachloraurate ($HAuCl_4*3H_2O$; Sigma-Aldrich, Germany) solution in sterile deionized water was stirred and heated until boiling. When the solution reached boiling, tri-sodium citrate ($Na_3C_6H_5O_7$; 38.8 mM; 15% of the volume of the diluted hydrogen tetrachloraurate solution) was quickly added. Heating and stirring were ceased after the solution turned a deep red color, resulting in a 79.95 mg/L nAu stock suspension. The particle size distributions of both stock suspensions were determined by dynamic light scattering (DLS; DelsaNano C, Beckman Coulter, Germany), and their development in the test medium (SAM-S5) over a 24 h period (the time of one water exchange) is described in Table S3.

## Test organisms

The test species *Chaetopteryx villosa* (4th instar) was sampled from the Sauerbach, a near natural stream negligibly impacted by settlement or agricultural activity (49°05' N; 7°37' E). In the laboratory, the animals were acclimatized to experimental conditions in stainless-steel artificial streams (120x30x20 cm; water volume 50 liters) filled with SAM-5S medium [39] at 14±1°C for 14 days. Within each artificial stream microcosm, *Chaetopteryx* larvae (length greater than 10 mm) were kept in groups of 40 in stainless steel cages (70x14x20 cm) covered at the in-flow and out-flow with a 0.5 mm mesh screen. Each cage was equipped with artificial sediment comprised of 1.2 kg glass spheres of two size classes (1.0 and 0.2 kg with diameters of 105-210 μm and 800-1200 μm, respectively; Worf Glaskugeln GmbH, Germany). Glass spheres were used instead of natural sediment to minimize cross contamination with titanium from sources other than the water. Cages were deployed directly in front of the paddle wheel, which simulated running water conditions at a velocity of 0.1 m/s within the cages.

## Experimental set-up

In total, the experiment involved 24 independent stainless-steel artificial streams, while each of the six independent technical control units (Pequitec, Switzerland) supplied four streams with the respective test medium (i.e., SAM-5S; water quality parameters are detailed in Table S4). Thus, a continuous medium exchange in the experimental units was ensured (one complete water exchange per 24 h), as well as dosing with the respective nanoparticles (see below). Dosing was initiated following the 14-day acclimatization phase. The artificial stream system was coupled with a light system simulating daylight and emitting UV-A and UV-B (Magic Sun 23/160 R 160W, Heraeus, Germany) light at intensities of 9.7 and 0.35 W/m$^2$, respectively, at the water surface (measured with a RM12 radiometer; Dr. Gröbel UV-Elektronic GmbH, Germany). These intensities are less than 25% of the peak UV-intensities measured during summer in Central Europe [19] and represent values measured on a cloudy summer day near the test species sampling site [40]. Thus, the UV-intensities employed in the present study can be considered environmentally relevant, especially during the summer period. The day/night rhythm was set at 12/12 hours. Depending on the treatment, a UV-transparent or -filtering film (LLumar® UV CL-SR PS, SUNPOINT, Germany) covered the artificial stream. This film also served as a barrier to emerging insects.

The experimental system was used to establish six different treatments: (i) a control without the addition of nanoparticles or direct exposure to UV-irradiation, (ii) one treatment assessing the implication of UV-irradiation in the absence of nanoparticles, (iii) one assessing for the implications of 4 µg $nTiO_2$/L in the absence of UV, (iv) one using the same concentration of $nTiO_2$ in presence of UV, (v) a treatment investigating the combined effects of 400 µg $nTiO_2$/L and UV-irradiation, and (vi) a treatment that evaluated the effect of 6.5 µg nAu/L in the absence of UV. Each of these treatments was replicated four times and assessed over the course of 140 days. During the study, caddisfly larvae received approximately 10 g (dry weight) of preconditioned black alder leaves see for details [41] every other week, while all leaf material remaining from the former addition was removed, dried (at 60°C for 48 h) and weighed to calculate the consumed leaf mass. Subsequently, the leaves were stored frozen for chemical analysis. At the same time, dead larvae were removed from the system. In addition, each artificial stream system was checked for emerging aquatic insects daily, which were frozen until further use.

## Lipid analysis

The lipid content of 10-15 lyophilized and weighed (to the nearest 0.01 mg) adult insects per treatment was analyzed following the method described by Van Handel [42]: Lipids were extracted in a 1:1 chloroform:methanol (v:v) solution and reacted with sulfuric acid and vanillin-phosphoric acid reagent. For quantification, absorbance at 490 nm was measured and read against a standard curve prepared from commercially available soybean oil (Sojola Soja-Öl, Vandemoortele, Germany).

## Chemical analysis

To monitor nanoparticle concentrations in the test medium, water samples were taken prior to the start and once a month during the experiment and were immediately analyzed using inductively coupled plasma quadrupole mass spectrometry ICP-MS, cp. [43]. Briefly, the ICP-MS (XSeriesII, Thermo Fisher Scientific, Germany) was equipped with a FAST autosampler (ESI, Thermo Fischer Scientific, Germany), a peek spray chamber (Thermo Fischer Scientific, Germany) and a robust Mira Mist peek nebulizer (Burgener, England). The respective elements were analyzed for the following masses: $^{197}$Au and $^{46/47/49}$Ti. Additionally, the concentration of freeze-dried adult caddisflies (including any nanoparticles potentially adsorbed to the exterior of the

organisms) and adult control organisms submersed in either the 400 µg $nTiO_2$/L or the 6.5 µg nAu/L treatment to control for the feasible external adhesion of nanoparticles, as well as composite samples of the leaf material offered as a food source during the experiment, were analyzed via ICP-MS. The nAu samples were analyzed after digestion with aqua regia for 96 h in darkness while the temperature was increased from 30 to 80°C. All digested samples were diluted in 1% HCl and centrifuged (3000 rpm for 15 min) to remove indigestible residues. Finally, the supernatants were analyzed by ICP-MS as described for water samples. For $nTiO_2$ samples, the device was coupled with electrothermal vaporization (ETV 4000 System, Spectral Systems, Germany) for sample introduction to overcome the poor solubility of $TiO_2$ [44]. Prior to vaporization, the samples were incinerated (300°C) to lower the introduction of organics. Furthermore, the instrument was run in collision cell mode with -2.5 V and 4 mL He/$H_2$ cell gas in order to avoid polyatomic interference. In addition, 25 mL Ar/$O_2$ gas was applied to oxidize the introduced carbon.

**TEM analyses**

Each nanoparticle stock suspension ($nTiO_2$ and nAu) was diluted and transferred onto a copper grid coated with carbon by ultrasonic nebulization and investigated with the 200 keV Zeiss 922 Omega transmission electron microscope. The caddisflies, in contrast, were fixed in a mixture of 2.5% glutaraldehyde, 1.25% formaldehyde, 0.03% picric acid and 0.003% $CaCl_2$ in 0.1 M cacodylatbuffer (pH 7.4) for 24-h at 4°C. Subsequently the samples were washed three times with 0.1 M cacodylatbuffer and secondary fixed using 1% $OsO_4$ in 0.1 M cacodylatbuffer for 24-h at 4°C. Samples were dehydrated by undenatured ethyl alcohol and embedded in epoxy resin (intermediate medium: 1,2-epoxypropane). The abdomen of each fly was cut crosswise with a microtome and each slice was put on a single slot copper grid (oval hole), while leaving out any type of contrasting. The specimens were investigated with the transmission electron microscope and the Quanta 325 environmental scanning electron microscope in wet scanning transmission electron microscopy mode (dark and bright field) taking advantage of the energy dispersive X-ray spectroscopy.

## Data evaluation

Emergence over time was expressed as a percent relative to the total number of emerging insects at the end of the experiment (i.e., after 140 days). On the basis of the cumulative emergence data, non-linear regression analysis was performed to identify the time by which 50% of the *Chaetopteryx* larvae had emerged [with 95% confidence interval (CI)]. For this purpose, several 2-parameter models (generally Weibull or log-normal model) were fitted to the data using the "R" extension package "drc" [45]. The model fitting the data best was selected on the basis of Akaike's Information Criterion (i.e., lowest score; drc-function "mselect") and visual inspection. The time until median emergence was derived using the drc-function "ED". Obtained values were assessed for statistically significant differences between treatments using CI-testing (drc-function "comped") [46]. The concentrations of $TiO_2$, Au and lipids in emerged *Chaetopteryx* were compared based on their median or mean and (non-)parametric CI-testing methods, as detailed in Altman et al. [47]. CI-testing is basically a formalized approached to assess for the overlap of variability between treatments [48]. R version 3.0.3 for Mac was used for statistics and figures [49].

## Author contributions

M.B. and R.S. conceived and designed the experiment and initiated the analysis. M.B. and D.E. directed the experiment. R.R.R performed the ICP-MS measurements. R.R.R. and F.S. performed the nanoparticle analysis. D.E., R.R.R., R.B., A.F., S.L., F.S. and J.Z. jointly performed the experiment. M.B., D.E., J.Z. and R.S. conducted the statistical analyses. M.B. and R.S. prepared the first version of the manuscript and

handled its submission. D.E. and R.R.R. contributed parts of the methods section. All authors discussed the manuscript and contributed to the editing.

**COMPETING INTERESTS**

Some of the authors (R.R.R., F.S., R.S.) are managing directors of small consultancies working in the field of ecotoxicology and environmental risk assessment or are now employed as consultant (D.E.). The authors, however, do not feel a conflict of interest as a consequence of this situation.

**DATA AVAILABILITY**

Data are available from the corresponding authors upon request, if required by the journal the data will be made available at an appropriate data repository.

**REFERENCES**

1       Gottschalk, F., Sun, T. Y. & Nowack, B. Environmental concentrations of engineered nanomaterials: Review of modeling and analytical studies. *Environ. Pollut.* **181**, 287-300 (2013).

2       Klaine, S. J. *et al.* Nanomaterials in the Environment: Behavior, Fate, Bioavailability, and Effects. *Environ. Toxicol. Chem.* **27**, 1825-1851 (2008).

3       Mueller, N. C. & Nowack, B. Exposure modeling of engineered nanoparticles in the environment. *Environ. Sci. Technol.* **42**, 4447-4453 (2008).

4       Ferry, J. L. *et al.* Transfer of gold nanoparticles from the water column to the estuarine food web. *Nature Nanotechnology* **4**, 441-444 (2009).

5       Werlin, R. *et al.* Biomagnification of cadmium selenide quantum dots in a simple experimental microbial food chain. *Nature Nanotechnology* **6**, 65-71 (2011).

6       Judy, J. D., Unrine, J. M. & Bertsch, P. M. Evidence for biomagnification of gold nanoparticles within a terrestrial food chain. *Environ. Sci. Technol.* **45**, 776-781 (2011).

7       Epanchin, P. N., Knapp, R. A. & Lawler, S. P. Nonnative trout impact an alpine-nesting bird by altering aquatic-insect subsidies. *Ecology* **91**, 2406-2415 (2010).

8       Uesugi, A. & Murakami, M. Do seasonally fluctuating aquatic subsidies influence the distribution pattern of birds between riparian and upland forests? *Ecol. Res.* **22**, 274-281 (2007).

9       Pace, M. L. *et al.* Whole-lake carbon-13 additions reveal terrestrial support of aquatic food webs. *Nature* **427**, 240-243 (2004).

10      Al-Jaibachi, R., Cuthbert, R. N. & Callaghan, A. Up and away: ontogenic transference as a pathway for aerial dispersal of microplastics. *Biology Letters* **14,** 20180479 (2018).

11      Kraus, J. M. *et al.* Cross-ecosystem impacts of stream pollution reduce resource and contaminant flux to riparian food webs. *Ecol. Appl.* **24**, 235-243 (2014).

12      Kraus, J. M. *et al.* Metamorphosis alters contaminants and chemical tracers in insects: implications for food webs. *Environ. Sci. Technol.* **48**, 10957-10965 (2014).

13      Paetzold, A., Smith, M., Warren, P. H. & Maltby, L. Environmental impact propagated by cross-system subsidy: chronic stream pollution controls riparian spider populations. *Ecology* **92**, 1711-1716 (2011).

14      Cristol, D. A. *et al.* The movement of aquatic mercury through terrestrial food webs. *Science* **320**, 335-335 (2008).

15      Kraus, J. M., Gibson, P. P., Walters, D. M. & Mills, M. A. Riparian spiders as sentinels of polychlorinated biphenyl contamination across heterogeneous aquatic ecosystems. *Environ. Toxicol. Chem.* **36**, 1278-1286 (2017).

16      Richmond, E. K. *et al.* A diverse suite of pharmaceuticals contaminates stream and riparian food webs. *Nat Commun* **9**, 4491 (2018).

17      Schulz, R. *et al.* Review on environmental alterations propagating from aquatic to terrestrial ecosystems. *Sci. Total Environ.* **538**, 246-261 (2015).

18      Ulmer, G. in *Die Tierwelt Mitteleuropas VI.: XV 1 - XV*   (eds P. Brohmer, P. Ehrmann, & G. Ulmer)  (1929).

19      Häder, D. P. *et al.* ELDONET - a decade of monitoring solar radiation on five continents. *Photochem. Photobiol.* **83**, 1348-1357 (2007).

20      Fujishima, A., Rao, T. N. & Tryk, D. A. Titanium dioxide photocatalysis. *Journal of Photochemistry and Photobiology C: Photochemistry Reviews* **1**, 1-21 (2000).

21      Feckler, A., Rosenfeldt, R. R., Seitz, F., Schulz, R. & Bundschuh, M. Photocatalytic properties of titanium dioxide nanoparticles affect habitat selection of and food quality for a key species in the leaf litter decomposition process. *Environ. Pollut.* **196**, 276-283 (2015).

22      Gondikas, A. P. *et al.* Release of TiO2 nanoparticles from sunscreens into surface waters: a one-year survey at the old Danube recreational lake. *Environ. Sci. Technol.* **48**, 5415–5422 (2014).

23      Kiser, M. A. *et al.* Titanium nanomaterial removal and release from wastewater treatment plants. *Environ. Sci. Technol.* **43**, 6757-6763 (2009).

24      Nam, S. H. *et al.* Derivation of guideline values for gold (III) ion toxicity limits to protect aquatic ecosystems. *Water Res.* **48**, 126-136 (2014).

25      Tiede, K., Hassellov, M., Breitbarth, E., Chaudhry, Q. & Boxall, A. B. A. Considerations for environmental fate and ecotoxicity testing to support environmental risk assessments for engineered nanoparticles. *J. Chromatogr. A* **1216**, 503-509 (2009).

26      Baxter, C. V., Fausch, K. D. & Saunders, C. Tangled webs: reciprocal flows of invertebrate prey link streams and riparian zone. *Freshw. Biol.* **50**, 201-220 (2005).

27      Jackson, J. K. & Fisher, S. G. Secondary production, emergence, and export of aquatic insects of a sonoran desert stream. *Ecology* **67**, 629-638 (1986).

28      Strasevicius, D., Jonsson, M., Nyholm, N. E. I. & Malmqvist, B. Reduced breeding success of Pied Flycatchers *Ficedula hypoleuca* along regulated rivers. *Ibis* **155**, 348-356 (2013).

29      Mahler, G. J. *et al.* Oral exposure to polystyrene nanoparticles affects iron absorption. *Natuer Nanotechnology* **7**, 264-271 (2012).

30      Kurta, A., Bell, G. P., Nagy, K. A. & Kunz, T. H. Energetics of pregnancy and lactation in free- ranging little brown bats *Myotis lucifugus*. *Physiol. Zool.* **62**, 804-818 (1989).

31    Aguilar, F. *et al.* Scientific Opinion on the re-evaluation of gold (E 175) as a food additive. *Efsa Journal* **14** (2016).

32    Hadrup, N., Sharma, A. K., Poulsen, M. & Nielsen, E. Toxicological risk assessment of elemental gold following oral exposure to sheets and nanoparticles - A review. *Regul. Toxicol. Pharmacol.* **72**, 216-221 (2015).

33    Bundschuh, M., Seitz, F., Rosenfeldt, R. R. & Schulz, R. Effects of nanoparticles in fresh waters – risks, mechanisms and interactions. *Freshw. Biol.* **61**, 2185–2196 (2016).

34    Raitif, J., Plantegenest, M., Agator, O., Piscart, C. & Roussel, J.-M. Seasonal and spatial variations of stream insect emergence in an intensive agricultural landscape. *Sci. Total Environ.* **644**, 594-601 (2018).

35    Piccinno, F., Gottschalk, F., Seeger, S. & Nowack, B. Industrial production quantities and uses of ten engineered nanomaterials in Europe and the world. *Journal of Nanoparticle Research* **14**, 1109 (2012).

36    Keller, A. A. & Lazareva, A. Predicted Releases of Engineered Nanomaterials: From Global to Regional to Local. *Environmental Science & Technology Letters* **1**, 65-70 (2014).

37    Dabrunz, A. *et al.* Biological surface coating and molting inhibition as mechanisms of TiO2 nanoparticle toxicity in *Daphnia magna PLoS One* **6**, e20112 (2011).

38    McFarland, A. D., Haynes, C. L., Mirkin, C. A., Van Duyne, R. P. & Godwin, H. A. Color my nanoworld. *Journal of Chemical Education* **81**, 544-545 (2004).

39    Borgmann, U. Systematic analysis of aqueous ion requirements of Hyalella azteca: A standard artificial medium including the essential bromide ion. *Arch. Environ. Contam. Toxicol.* **30**, 356-363 (1996).

40    Kalčíková, G. *et al.* Combined effect of UV-irradiation and TiO2-nanoparticles on the predator-prey interaction of gammarids and mayfly nymphs. *Environ. Pollut.* **186**, 136-140 (2014).

41      Bundschuh, M. & Schulz, R. Population response to ozone application in wastewater: an on-site microcosm study with *Gammarus fossarum* (Crustacea: Amphipoda) *Ecotoxicology* **20**, 466-473 (2011).

42      Van Handel, E. Rapid determination of total lipids in mosquitoes. *J. Am. Mosq. Control Assoc.* **1**, 302-304 (1985).

43      Rosenfeldt, R. R., Seitz, F., Schulz, R. & Bundschuh, M. Heavy metal uptake and toxicity in the presence of titanium dioxide nanoparticles: A factorial approach using *Daphnia magna*. *Environ. Sci. Technol.* **48**, 6965-6972 (2014).

44      Duester, L., Prasse, C., Vogel, J. V., Vink, J. P. M. & Schaumann, G. E. Translocation of Sb and Ti in an undisturbed floodplain soil after application of Sb2O3 and TiO2 nanoparticles to the surface. *Journal of Environmental Monitoring* **13**, 1204-1211 (2011).

45      Ritz, C. & Streibig, J. C. Bioassay analysis using R. *Journal of Statistical Software* **12**, 1-22 (2005).

46      Wheeler, M. W., Park, R. M. & Bailer, A. J. Comparing median lethal concentration values using confidence interval overlap or ratio tests. *Environ. Toxicol. Chem.* **25**, 1441-1444 (2006).

47      Altman, D. G., Machin, D., Bryant, T. N. & Gardner, M. J. *Statistics with confidence - 2nd edition*.  (British Medical Journal, 2000).

48      Newman, M. C. "What exactly are you inferring?" A closer look at hypothesis testing. *Environ. Toxicol. Chem.* **27**, 1013-1019 (2008).

49      R Developmental Core Team, *R Foundation  for Statistical Computing* (2015).

50      Rosenfeldt, R. R., Seitz, F., Schulz, R. & Bundschuh, M. Heavy metal uptake and toxicity in the presence of titanium dioxide nanoparticles: A factorial approach using *Daphnia magna*. *Environ. Sci. Technol.* **48**, 6965-6972 (2014).
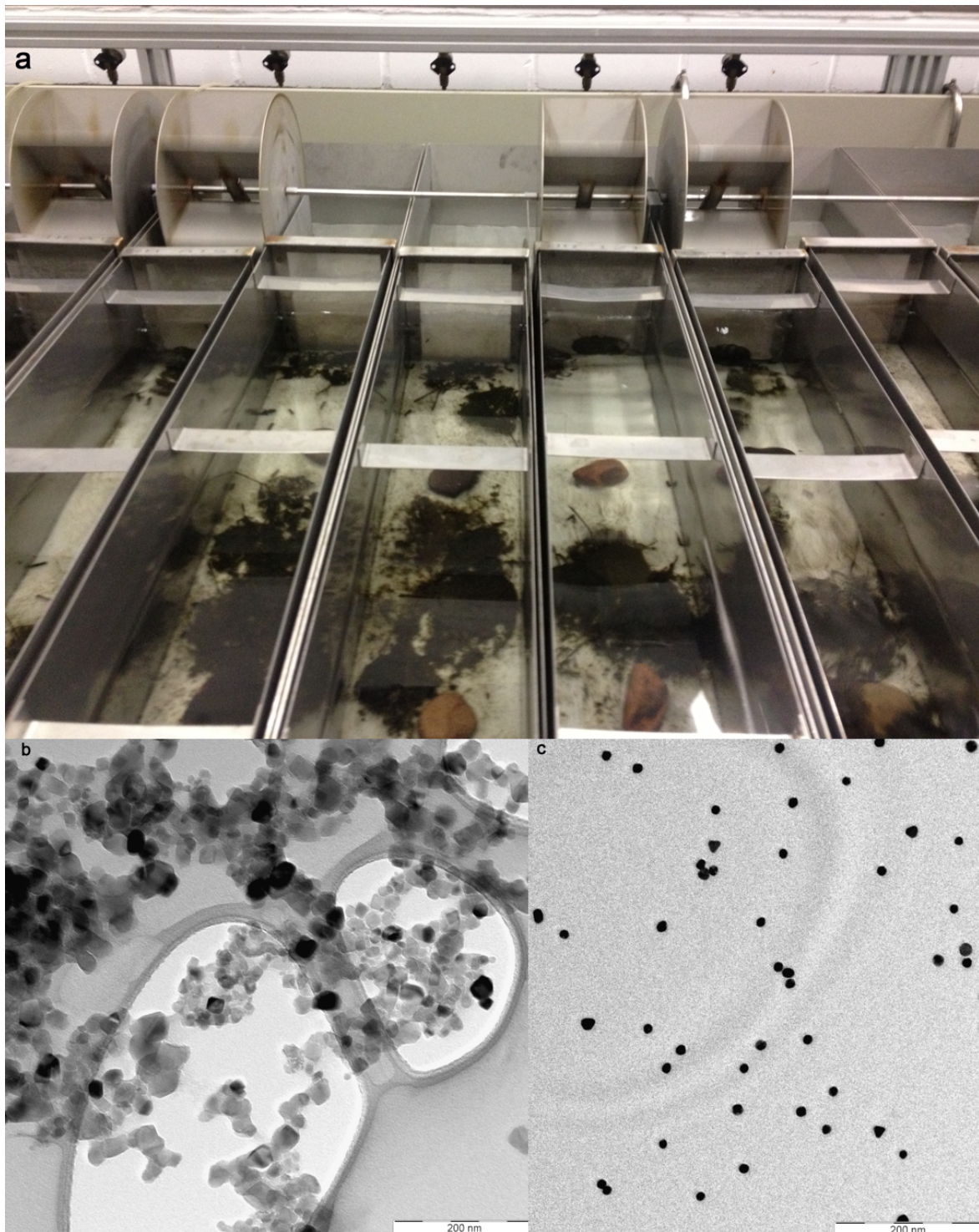
**Figure 1. Experimental set-up. a**, 24 stainless steel streams (n=24; volume: 40 L each) simulated freshwater stream habitats in the laboratory. Each stream was equipped with artificial sediment (i.e., glass spheres), leaves and caddisfly larvae. The units were run in flow-through mode, ensuring a constant concentration of nanoparticles over the 140-day duration of the study. **b**, Transmission electron microscopy (TEM) image of $nTiO_2$. **c**, TEM image of nAu.
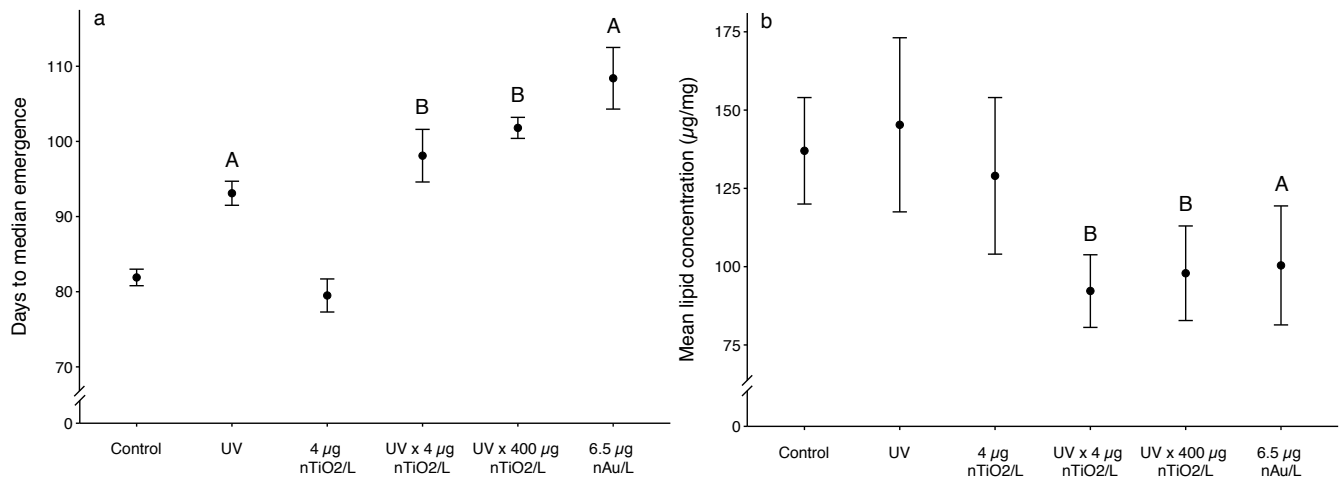
**Figure 2. Effects of nanoparticles on caddisflies.** Emergence pattern and mean lipid concentrations in adult caddisflies exposed as larvae for 140 days in stream microcosms to nanoparticles. A and B above the error bars refer to a statistically significant difference relative to the control or the UV treatment, respectively.
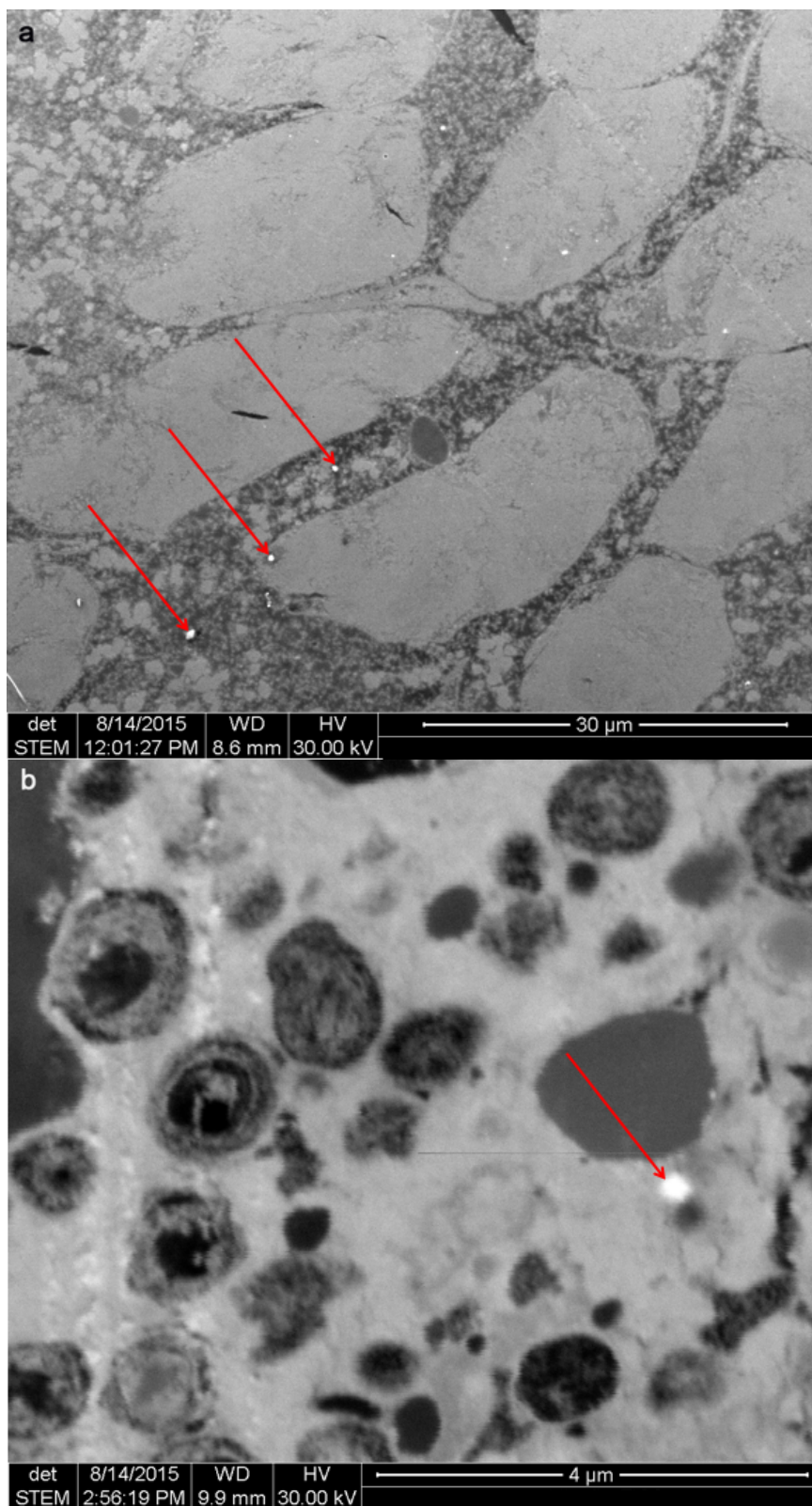
**Figure 3. Nanoparticles in adult caddisflies. (a)** Environmental scanning electron microscopy (ESEM) images, diagrams of the energy dispersive X-ray spectroscopy confirming that the particles are Au can be found in Fig. S2 and **(b)** ESEM image of $nTiO_2$ in adult caddisflies. Arrows point to nanoparticles in the organisms' abdominal tissue.

**Table 1. Concentration of nanoparticles in caddisflies.** Concentration of gold and titanium dioxide in adult caddisflies exposed as larvae for 140 days in stream microcosms to nanoparticles.

| Treatment | Median Au concentration (ng/mg; range) | Median TiO$_2$ concentration (ng/mg; range) |
| --- | --- | --- |
| Control | | |
| | <LOQ | 0.43 (0.25–1.09)[a] |
| UV | | |
| 4 µg nTiO$_2$/L | NA | |
| | | 0.93 (0.54–18.40)* |
| UVx4 µg nTiO$_2$/L | NA | |
| UVx400 µg nTiO$_2$/L | NA | 2.68 (0.47–9.44)* |
| 6.5 µg nAu/L | 1.51 (<LOQ–15.33)* | NA |

*Statistically significant compared to the control ($p < 0.05$)

[a]As titanium is among the ten most common elements of the earth crust, the detection of trace levels in organisms are expected even when they were not exposed to nTiO$_2$, e.g. shown by (Rosenfeldt et al., 2014).

NA=not assessed

LOQ=Limit of quantification (3.6 ng for Au)

**Nanoparticles transported from aquatic to terrestrial ecosystems via emerging aquatic insects comprise subsidy quality**

Bundschuh, M., Englert, D., Rosenfeldt, R.R., Bundschuh, R., Feckler, A., Lüderwald, S., Seitz, F., Zubrod, J.P., Schulz, R.,
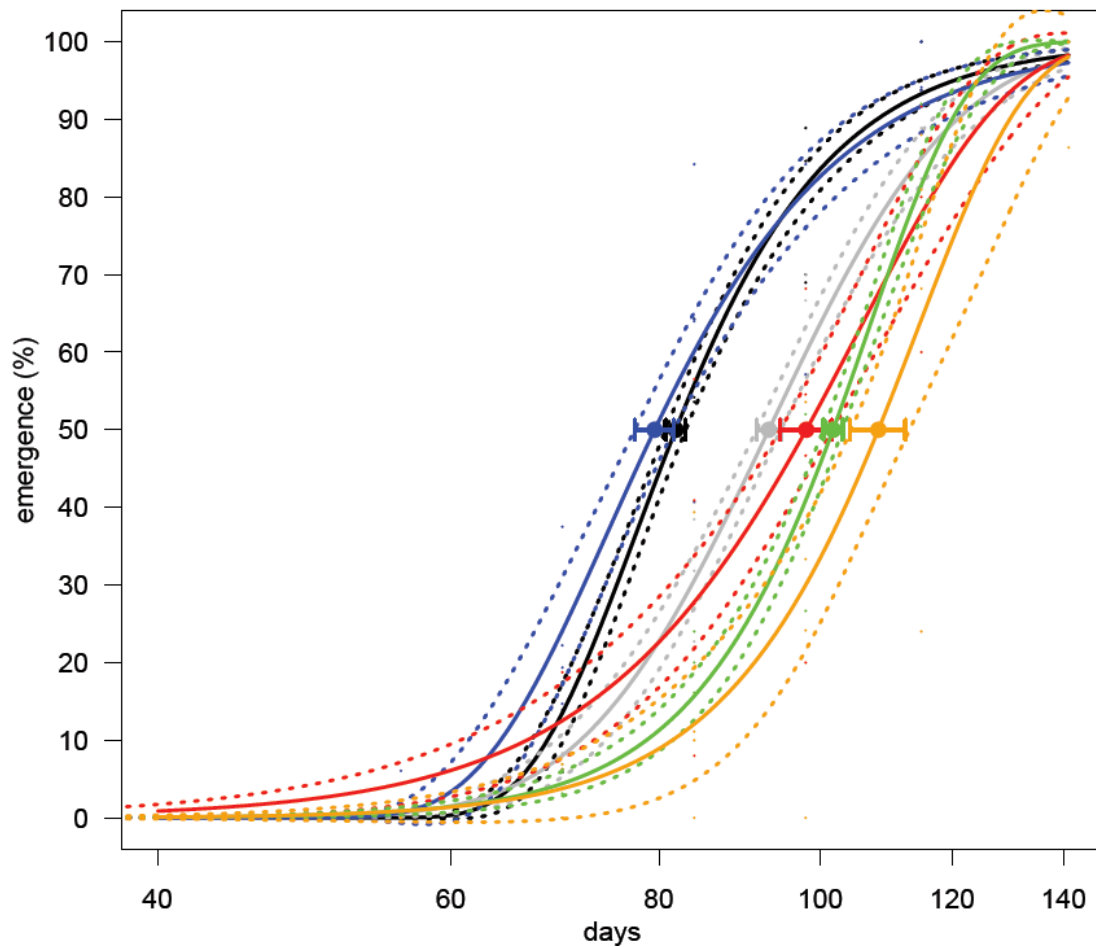
**Figure S1. Emergence of caddisfly larvae**. The emergence (solid lines with confidence interval dashed line) of *C. villosa* under control conditions (black) and in the presence of 4 µg/L $nTiO_2$ (blue), UV-irradiation (grey), 4 µg/L $nTiO_2$ and UV-irradiation (red), 400 µg/L $nTiO_2$ and UV-irradiation (green), or nAu (orange). Bold dots represent the median time until 50% of the larvae emerged together with the respective 95% confidence interval.
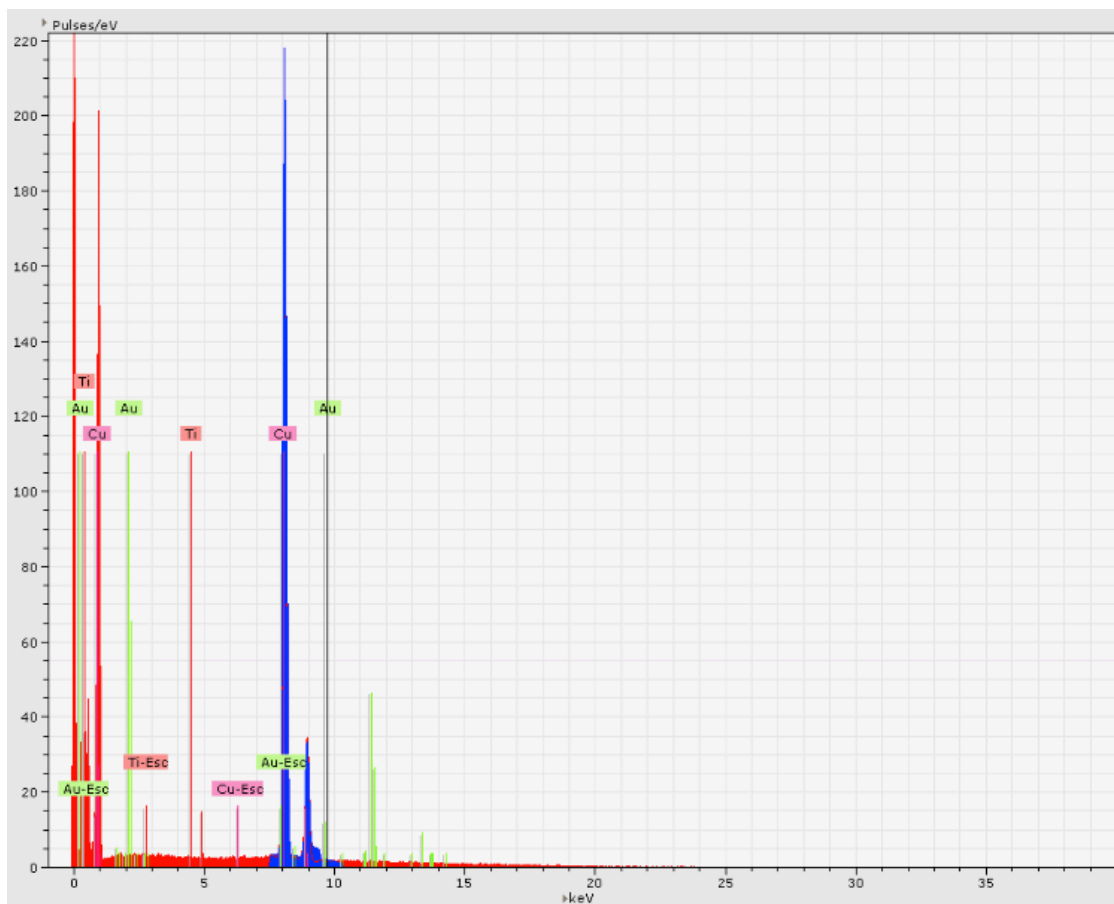
**Figure S2. EDX-diagram confirming the presence of Au.** The EDX analysis confirmed that tissue surrounding the nanoparticles detected in Fig. 2a is containing Au suggesting that these particles are indeed nAu.

**Table S1. Concentration of nanoparticles in the water phase, leaves and experimentally submersed adults**. Mean (±standard deviation) concentration of $TiO_2$ and Au in the water phase (µg/L; n=9) in leaf material at the time of food renewal (i.e., after 14 days; ng/mg; n=3) under treatment conditions, and in adult *Chaetopteryx villoss* (ng/mg; n=3) emerged from control larvae but briefly submersed in medium containing either 400 µg $TiO_2$/L or 6.5 µg nAu/L.

|  | $TiO_2$ (µg/L or ng/mg) | Au (µg/L or ng/mg) |
|---|---|---|
| Water phase |  |  |
| Control | <LOD | <LOD |
| 4 µg nTiO$_2$/L | 3.94 (±0.75) | NA |
| 400 µg nTiO$_2$/L | 373.52 (±61.23) | NA |
| 6.5 µg nAu/L | NA | 6.48 (±1.15) |
|  |  |  |
| Leaf material |  |  |
| Control | 27.30 (±3.52) | <LOD |
| 4 µg nTiO$_2$/L | 20.69 (±11.59) | <LOD |
| 400 µg nTiO$_2$/L | 276.00 (±128.28) | <LOD |
| 6.5 µg nAu/L | NA | 577.34 (±55.70) |
|  |  |  |
| Submersed control flies |  |  |
| 4 µg nTiO$_2$/L | NA | NA |
| 400 µg nTiO$_2$/L | 0.50 (±0.64) | NA |
| 6.5 µg nAu/L | NA | <LOD |

NA = not assessed

LOQ = absolute limit of quantification (3.6 ng for Au)

**Table S2. Implications of nanoparticles in caddisfly emergence, survival and feeding**. Mean (±standard deviation) number of emerged and dead *C. villosa* larvae together with cumulative leaf mass loss over the study duration of 140 days (n=4).

| Treatment | Mean emergence (No.) | Mean death (No.) | Cumulative leaf mass loss (mg) |
|---|---|---|---|
| Control | 19.0 (±6.6) | 21.0 (±6.6) | 773.4 (±36.5) |
| UV | 18.8 (±4.9) | 21.2 (±4.9) | 754.0 (±30.7) |
| 4 µg nTiO$_2$/L | 17.8 (±4.2) | 22.2 (±4.2) | 710.8 (±89.9) |
| UV x 4 µg nTiO$_2$/L | 16.3 (±4.3) | 23.7 (±4.3) | 716.1 (±24.5) |
| UV x 400 µg nTiO$_2$/L | 19.5 (±3.1) | 20.5 (±3.1) | 738.0 (±74.0) |
| 6.5 µg nAu/L | 21.0 (±1.8) | 19.0 (±1.8) | 783.8 (±73.1) |

**Table S3. Nanoparticle size characteristics**. Median, 10th and 90th percentiles of nTiO$_2$ and nAu size distributions at test initiation (0 h) and after 24 h in the stock suspension as well as in the test medium. In addition, the polydispersity index (PI) is reported (n=3).

| Time | Nanoparticle | Medium | 10th percentile (nm) | Median (nm) | 90th percentile (nm) | PI |
|---|---|---|---|---|---|---|
| 0 h | nTiO$_2$ | Stock | 37.4 | 62.3 | 104.1 | 0.1 |
| | | SAM-5S | 182.8 | 343.2 | 697.5 | 0.2 |
| | nAu | Stock | 10.3 | 15.1 | 22.3 | 0.2 |
| | | SAM-5S | 46.4 | 114.8 | 277.8 | 0.3 |
| 24 h | nTiO$_2$ | Stock | 37.2 | 61.0 | 100.5 | 0.1 |
| | | SAM-5S | 392.6 | 1583.5 | 8280.9 | 0.6 |
| | nAu | Stock | 9.8 | 16.3 | 27.8 | 0.2 |
| | | SAM-5S | 280.3 | 1412.0 | 29436.0 | 0.7 |

**Table S4. Water quality parameters**. Mean (±standard deviation) of water quality parameters over the duration of the study, measured weekly in one randomly selected control and any treatment (n=14; TOC n=4).

| Water quality parameter | Control | Treatment |
| --- | --- | --- |
| Ammonium (mg/L) | <0.02 | <0.02 |
| Phosphate (mg/L) | 0.19 (±0.28) | 0.28 (±0.80) |
| Nitrite (µg/L) | 7.58 (±8.01) | 6.34 (±6.07) |
| Nitrate (mg/L) | <1.00 | <1.00 |
| Chloride (mg/L) | 35.07 (±23.63) | 35.07 (±23.63) |
| Oxygen (mg/L) | 9.36 (±1.21) | 9.61 (±1.29) |
| Temperature (°C) | 14.07 (±0.19) | 13.94 (±0.30) |
| pH | 8.22 (±0.25) | 8.18 (±0.26) |
| Conductivity (µS/cm) | 361 (±139) | 378 (±116) |
| Hardness (°d) | 7.86 (±0.58) | 7.86 (±0.49) |
| Total organic carbon (mg/L) | 11.54 (±0.68) | 10.12 (±1.13) |

**Appendix A. 6**


**Curriculum Vitae**


**Name:**          Simon Lüderwald

**Date of birth:**     06.10.1986

**Nationality:**      German


**Education and Career:**

**Since 01/2016**

Scientist at the iES Landau, Institute for Environmental Sciences, University of Koblenz-Landau, Campus Landau, Germany


**10/2013 – 12/2015**

Studies in Ecotoxicology at the University of Koblenz-Landau, Campus Landau, Germany

**M.Sc. Ecotoxicology** (Thesis: Exposure pathway dependent effects of nanoparticulate $TiO_2$ on *Gammarus fossarum*)


**10/2009 – 12/2013**

Studies in Environmental Sciences at the University of Koblenz-Landau, Campus Landau, Germany

**B.Sc. Environmental Sciences** (Thesis: Acute and chronic effects of aged $TiO_2$ nanomaterials – A case study with *Daphnia magna*)


**06/2007**

Final secondary-school examination (Abitur) at the Wilhelm-Röpke-Schule, Ettlingen, Germany

**Publication list:**

*Peer-reviewed*

**Lüderwald, S.**, Meyer, F., Gerstle, V., Friedrichs, L., Rolfing, K., Bakanov, N., Schulz, R., Bundschuh, M., submitted. Reduction of pesticide toxicity under field relevant conditions? The interaction of titanium dioxide nanoparticles, UV, and NOM. Aquatic Toxicology.

Bundschuh, M., Englert, D., Rosenfeldt, R.R., Bundschuh, R., Feckler, A., **Lüderwald, S.**, Seitz, F., Zubrod, J.P., Schulz, R., 2019. Nanoparticles transported from aquatic to terrestrial ecosystems via emerging aquatic insects compromise subsidy quality. Scientific Reports 9, 15676.

Degenkolb, L., Leuther, F., **Lüderwald, S.**, Philippe, A., Metreveli, G., Amininejad, S., Vogel, H.J., Kaupenjohann, M., Klitzke, S., 2019. The fate of silver nanoparticles in riverbank filtration systems — The role of biological components and flow velocity. Science of the Total Environment 699, 134287.

**Lüderwald, S.**, Schell, T., Newton, K., Salau, R., Seitz, F., Rosenfeldt, R., Dackermann, V., Metereveli, G., Schulz, R., Bundschuh, M., 2019. Exposure pathway dependent effects of titanium dioxide and silver nanoparticles on the benthic amphipod *Gammarus fossarum*. Aquatic Toxicology 212, 47-53.

**Lüderwald, S.**, Dackermann, V., Seitz, F., Adams, E., Feckler, A., Schilde, C., Schulz, R., Bundschuh, M., 2019. A blessing in disguise? Natural organic matter reduces the UV light-induced toxicity of nanoparticulate titanium dioxide. Science of the Total Environment 663, 518-526.

Schell, T., Goedkoop, W., Zubrod, J. P., Feckler, A., **Lüderwald, S.**, Schulz, R., Bundschuh, M., 2018. Assessing the effects of field-relevant pesticide mixtures for their compliance with the concentration addition model - an experimental approach with *Daphnia magna.* Science of the Total Environment 644, 342-349.

Newton, K., Zubrod, J.P., Englert, D., **Lüderwald, S.**, Schell, T., Baudy, P., Konschak, M., Feckler, A., Schulz, R., Bundschuh, M., 2018. The evil within? systemic fungicide application in trees enhances litter quality for an aquatic decomposer-detritivore system. Environmental Pollution 241, 549-556.

Bundschuh, M., Filser, J., **Lüderwald, S.**, McKee, M. S., Metreveli, G., Schaumann, G. E., Schulz, R., Wagmer, S., 2018. Nanoparticles in the environment: where do we come from, where do we go to? 30: 6.

Zubrod, J.P., Englert, D., Poganiuch, S., **Lüderwald, S.**, Schulz, R., Bundschuh, M., 2017. History matters: pre-exposure to wastewater enhances pesticide toxicity. Environmental Science & Technology 51, 9280-9287.

Zubrod, J.P., Englert, D., Wolfram, J., Rosenfeldt, R.R., Feckler, A., Bundschuh, R., Seitz, F., Konschak, M., Baudy, P., **Lüderwald, S**., Fink, P., Lorke, A., Schulz, R., Bundschuh, M., 2017. Long-term effects of fungicides on leaf-associated microorganisms and shredder populations – An artificial stream study. Environmental Toxicology and Chemistry 36, 2178-2189.

**Lüderwald, S.**, Seitz, S., Seisenbaeva, G.A., Kessler, V.G., Schulz, R., Bundschuh, M., 2016. Palladium nanoparticles: is there a risk for aquatic ecosystems? Bulletin of Environmental Contamination and Toxicology 97, 153-158.

Seitz F., Rosenfeldt R. R., Müller M., **Lüderwald S.**, Schulz R., Bundschuh M., 2016. Quantity and quality of natural organic matter influence the ecotoxicity of titanium dioxide nanoparticles. Nanotoxicology 10, 1415-1421.

Zubrod, J.P., Englert, D., Rosenfeldt, R. R., Wolfram, J., **Lüderwald, S.**, Wallace, D., Schnetzer, N., Schulz, R., Bundschuh, M., 2015. The relative importance of diet-related and waterborne effects of copper for a leaf-shredding invertebrate. Environmental Pollution 205, 16-22.

Rosenfeldt, R.R., Seitz, F., Zubrod, J.P., Feckler, A., Merkel, T., **Lüderwald, S.**, Bundschuh, R., Schulz, R., Bundschuh, M., 2015. Does the presence of titanium dioxide nanoparticles reduce copper toxicity? a factorial approach with the benthic amphipod *Gammarus fossarum*. Aquatic Toxicology 165, 154-159.

Seitz, F., **Lüderwald, S.**, Rosenfeldt, R.R., Schulz, R., Bundschuh, M. 2015. Aging of $TiO_2$ nanoparticles transiently increases their toxicity to the pelagic micro-crustacean *Daphnia magna*. PLoS One, 10, e0126021.